



Volume 3

No. 1, 2008

# CHEMISTRY

## JOURNAL OF MOLDOVA

General, Industrial and Ecological Chemistry

Editor-in-chief: Gheorghe DUCA

Academy of Sciences of Moldova  
Institute of Chemistry  
State University of Moldova

Volume 3

No. 1, 2008

# CHEMISTRY

## JOURNAL OF MOLDOVA

General, Industrial and Ecological Chemistry  
A journal for all fields of Chemistry, including Industrial and Ecological Chemistry

**Editor-in-chief: Gheorghe DUCA**

Academy of Sciences of Moldova  
Institute of Chemistry  
State University of Moldova

# CHEMISTRY JOURNAL OF MOLDOVA

## General, Industrial and Ecological Chemistry

**Editor-in chief:** Academician Gheorghe DUCA, Academy of Sciences of Moldova  
**Editor:** Professor Tudor LUPAȘCU, Academy of Sciences of Moldova

### Local Editorial Board:

**Dr. A. ARICU**  
Academy of Sciences of Moldova

**Professor P. CHETRUȘ**  
State University of Moldova

**Dr. Galina DRAGALINA**, State University of Moldova

**Dr. M. GONTA**  
State University of Moldova

**Professor A. GULEA**  
State University of Moldova

**Dr. V. KULCIȚKI**, scientific secretary of the editorial board,  
Institute of Chemistry, Academy of Sciences of Moldova

**Dr.Hab. F. MACAEV**  
Institute of Chemistry, Moldova Academy of Sciences

**Professor I. OGURTSOV**  
Institute of Chemistry, Moldova Academy of Sciences

**Professor M. REVENCO**  
State University of Moldova

**N. SECARA**, scientific secretary of the editorial board, Institute of  
Chemistry, Academy of Sciences of Moldova

**Dr. R. STURZA**  
Technical University of Moldova

**Corr. Member of ASM C. TURTA**  
Institute of Chemistry, Moldova Academy of Sciences

**Academician P. VLAD**  
Institute of Chemistry, Moldova Academy of Sciences

### International Editorial Board:

**Academician S. ANDRONATI**  
Bogatsky Physico-Chemical Institute, Odessa, Ukraine

**Professor M. BAHADIR**  
Institute of Ecological Chemistry, Braunschweig, Germany

**Academician I. BERSUKER**  
University of Texas at Austin, USA

**Professor I. BERTINI**  
University of Florence, Italy

**Academician Yu. BUBNOV**  
INEOS, Russian Academy of Sciences, Moscow, Russia

**Academician V. GONCHEARUK**  
Dumansky Institute of Colloid and Water Chemistry, National  
Academy of Sciences, Kiev, Ukraine

**Academician I. HAIDUC**  
Romanian Academy, București, Romania

**Academician M. JURINOV**  
National Academy of Sciences, Astana, Kazakhstan

**Academician F. LAKHVICH**  
Institute of Bioorganic Chemistry, Minsk, Bielarusi

**Academician J. LIPKOWSKI**  
Institute of Physical Chemistry, Warszawa, Poland

**Academician V.LUNIN**  
State University of Moscow, Russia

**Professor M. MACOVEANU**  
"Gh. Asachi" Technical University, Iasi, Romania

**Professor J. MALIN**  
American Chemical Society, Washington, USA

---

### Editorial office address:

Institute of Chemistry, Academy of Sciences of Moldova, Str. Academiei, 3, MD-2028, Chisinau, Republic of Moldova  
Tel: + 373 22 725490; Fax: +373 22 739954; e-mail: chemjm@cc.acad.md

## ISSUE CONTENTS LIST WITH GRAPHICAL ABSTRACTS

## NEWS AND EVENTS

8

**The IX-th SYMPOSIUM ON COLLOID AND SURFACE CHEMISTRY with international participation, 29 –31 Mai 2008, Galați, România**

## NEWS AND EVENTS

9

**The VII-th International Scientifico-Practical Conference “CARPATIAN REGION NATURAL WATER RESOURCES. PROTECTION AND RATIONAL USING PROBLEMS”, 29-30 May 2008, Lvov, Ukraine**

## REVIEW

## ECOLOGICAL CHEMISTRY

10

**ESTIMATION OF THE NATURAL WATER SELF-PURIFICATION CAPACITY FROM THE KINETIC STANDPOINT**

Gheorghe Duca, Elena Bunduchi, Viorica Gladchi, Lidia Romanciuc, Nelli Goreaceva

The chemical composition of the abiotic component of natural waters:

$S - A - O_{2,aq} - H_2O_2 - \{R_x\} - Me^{n+}/Me^{(n-1)+} - L - Sed$

where  $O_{2,aq} - H_2O_2 - \{R_x\}$  – dissolved molecular oxygen and its activation products; S – substrates of chemical transformations, including anthropogenic pollutants; A – active particles acceptors, which form secondary, less active radicals;  $Me^{n+}/Me^{(n-1)+}$  – ions and complexes of transition metals in oxidized/reduced form; L – components with ligand properties; Sed – suspensions with various dispersion rate, which form the heterogeneous phase.

## REVIEW

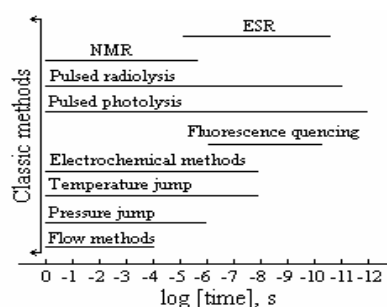
## PHYSICAL CHEMISTRY AND CHEMICAL PHYSICS

22

**PHYSICAL METHODS OF FAST REACTIONS INVESTIGATION**

Gheorghe Duca, Natalia Secara, Daniela Duca

The review offers a brief description of fast reactions commonly encountered in chemical systems, providing an insight into the possibilities of performing kinetic investigations of such reaction systems. The basic concepts of the methods used for investigation of fast reactions kinetics are presented in this article, such as: flow methods, with particular emphasis on the stopped-flow approach, NMR, ESR, electrochemical methods, spectroscopy, flash photolysis, and several others.



## FULL PAPER

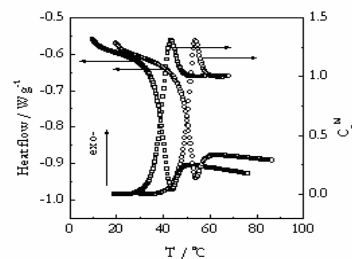
## PHYSICAL CHEMISTRY AND CHEMICAL PHYSICS

31

**VARIATION IN ACTIVATION ENERGY AND NANOSCALE CHARACTERISTIC LENGTH AT THE GLASS TRANSITION**

Ion Dranca

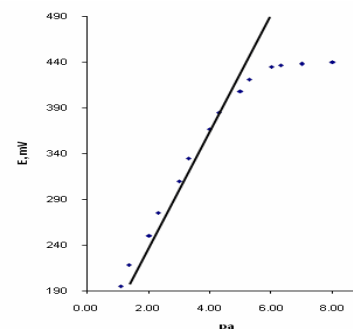
Differential scanning calorimetry has been used to study the  $\alpha$ -relaxation (glass transition) in virgin polystyrene (PS), PS-clay nanocomposite, amorphous indomethacin (IM), maltitol (Mt) and glucose (Gl). Variation of the effective activation energy ( $E$ ) throughout the glass transition has been determined by applying an advanced isoconversional method to DSC data on the glass transition. The relaxations have been characterized by determining the effective activation energies ( $E$ ) and evaluating the sizes of cooperatively rearranging regions at the glass transition ( $V_g$ ). The values of  $V_g$  have been determined from the heat capacity data.



**NITRATE-SELECTIVE ELECTRODES BASED ON THE TRINUCLEAR CHROMIUM(III) PIVALATES**

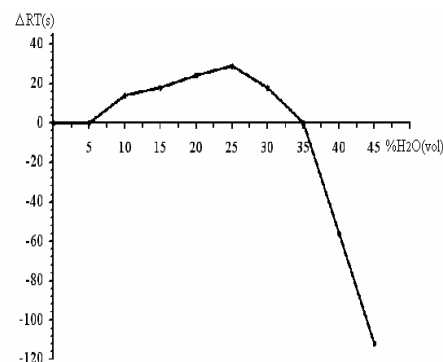
Mihail Revenco, Mariana Martin, Waell A.A. Dayyih

The paper describes the analytical potentialities of the trinuclear chromium(III) complexes as potentiometric ionophores for the construction of electrodes sensitive to the presence of nitrate anion. The electroactive material was prepared by interaction *in situ* of trinuclear chromium(III) pivalate with 4,4'-bipyridil. The electrodes presented a slope of 56 mV/decade, a low limit of detection ( $3,2 \cdot 10^{-6}$  mol/l), an adequate lifetime (4 months), and suitable selectivity characteristics when compared with other nitrate electrodes. The good parameters of this electrode made possible its application to the determination of nitrate in different types of fertilizers.

**CONSIDERATIONS ON LIQUID-CHROMATOGRAPHIC SEPARATION FOR AN EQUIMOLAR MIXTURE OF 2,4-DINITROPHENYLHYDRAZONES OF ACETALDEHYDE AND DIACETYL**

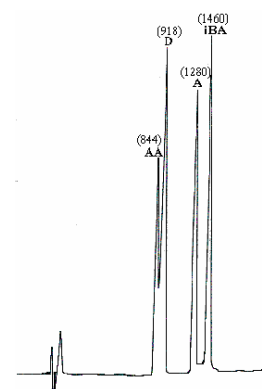
Gheorghe Zgherea

An equimolar mixture of 2,4-dinitrophenylhydrazones (2,4DNPH-ones) providing by acetaldehyde and diacetyl must be analyzed by liquid-chromatographic separation, using the mechanism of repartition with reverse phase; that full papers is for identification the optimal analytical conditions. As mobile phase are utilized various binary mixtures eluent, containing water and methanol, with 0-45% water. By the experimental studies were identified four domains of behavior and two optimal binary mixtures, with 25% and 45% water, thus this is a study on the behavior of binary mixtures mobile phases. The peaks are characterized by values of retention times and by position. The separation processes were appreciated by difference between the retention times of peaks; if the percent of water increase, the values of retention times is higher. When the percent of water is 45%, the difference between the retention times is maxim, associated

**THE MIXTURES OF 2,4-DINITROPHENYLHYDRAZONES OF INFERIOR CARBONYL COMPOUNDS AND THEIR HPLC SEPARATION WITH GRADIENT BINARY MIXTURES PHASES**

Gheorghe Zgherea

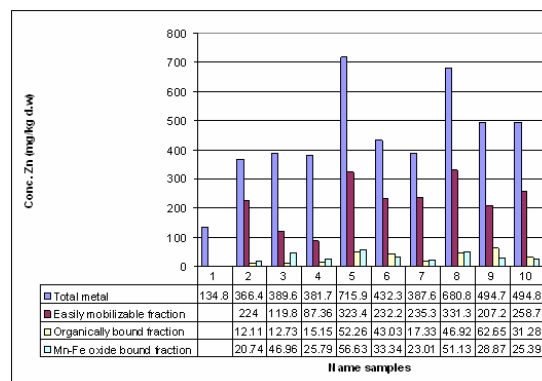
Mixtures of small quantities of carbonyl compounds are presents in foods, concerning sensorial qualities. The inferior carbonyl compounds ( $C_2-C_4$ , boiling point  $<100^\circ C$ ) – mono and dicarbonyl – can be identified and measured their concentrations, after a separation by distillation on the water bath. They are transferred in a strongly acid solution of 2,4-dinitrophenylhydrazine (2,4-DNPH), generating a mixture of insoluble 2,4-dinitrophenylhydrazones (2,4-DNPH-ones). The 2,4-DNPH-ones are organic compounds with weak polarity, solids, crystallized, yellows and water insoluble, soluble in organic solvents. The mixture of 2,4dinitrophenylhydrazones may be separated by liquid chromatography, using the reverse phase mechanism [1-3]. This paper contains experimental and theoretical considerations to the means of separation through liquid chromatography of two synthetically and a natural mixtures that contain 2,4-DNPH-ones provided by inferior carbonyl compounds; to obtain conclude results, in the synthetically mixtures was introduce and 2,4-DNPH-ones provided by carbonyl compounds having three (acetone and propanal) and four (isobutyl aldehyde) atoms of carbon.



### STUDY ON QUANTITATIVE SPECIATION, BY BCR METHOD, OF ZINC CONTENT FROM RIVER SEDIMENTS

Georgiana Vasile, Stanescu Bogdan, Tudor Claudia, Elena Mihaila

The present work presents the results obtained during investigation of the zinc content of the water and river sediments in an area polluted by mining activities, to provide information on the mobility and availability of this element. Sediment and water samples have been collected from significant sites in a former mining area in which with some sterile pits, which represent a major environmental hazard.



### THE ROLE OF ACTIVATED CARBON IN SOLVING ECOLOGICAL PROBLEMS

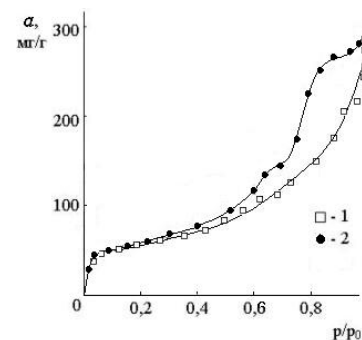
V. M. Mukhin, T. G. Lupascu

The authors present a brief analysis of the current global situation concerning the utilization of activated carbon in various fields. The article presents data concerning the synthesis and adsorption and structure properties of new activated carbons, used for solving ecological problems. The authors investigated the newly obtained activated carbons in comparison with several AC marks known in the world. It has been shown that currently synthesized AC are competitive with foreign marks.

### THE INFLUENCE OF BINDING MATERIAL ON POROUS STRUCTURE OF SHAPED HOPCALITE

N.K. Kulikov, S.G. Kireev, A.O. Shevchenko, V.M. Mukhin, S.N. Tkachenko, T.G. Lupascu

The authors have investigated the equilibrated adsorption of water vapors on GFG hopcalite, which was obtained using the extrusion shaping method, with bentonite clay as the binding compound. In the frames of the BET model, the values of the monolayer capacity and the size of medium area occupied by the water molecule in the filled monolayer have been determined. The distribution of pores according to their sizes has been evaluated.



### THE STUDY OF REDOX CONDITIONS IN THE DNIESTER RIVER

Viorica Gladchi, Nelli Goreaceva, Gheorghe Duca, Elena Bunduchi, Lidia Romanciuc, Igor Mardari, Ruslan Borodae

The work presented in the paper discusses the contribution of the Dniestrovsk water system to the formation of redox conditions in the lower Dniester. The conclusions were drawn on the basis of a long-term protocol of analyses that included the analysis of the oxygen regime, evaluation of the content of hydrogen peroxide,  $rH_2$ , biological oxygen demand as well as other additional parameters.

### INFLUENCE OF IODINATED OIL AND MARGARINE ON THE THYROID SYSTEM OF RATS

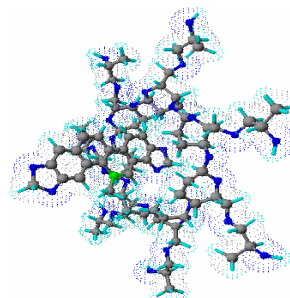
Rodica A. Sturza, Olga I. Deseatnicov, Cristina M. Popovici, Valentin S. Gudumac, Ion Nastas

The present work examines morphological changes in the thyroid system of rats at the experimental mercatholile-induced hypothyroidism. As well it determines the influence of iodinated oil and margarine on the thyroid system of rats. It specifies the safe value of iodinated oil and margarine for rats. In-vivo study demonstrated the efficacy of fortification of lipid products with iodine under iodine deficiency status.

**SPECTROPHOTOMETRIC STUDIES OF SANGUINARINE- $\beta$ -CYCLODEXTRIN COMPLEX FORMATION**

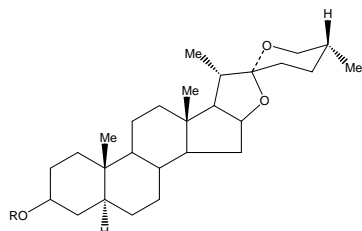
Veaceslav Boldescu, Irina Kacso, Ioan Bratu and Gheorghe Duca

The influence of pH and the presence of hydrophilic polymer polyvinylpyrrolidone on the formation of sanguinarine- $\beta$ -cyclodextrin (SANG- $\beta$ -CD) inclusion complex was investigated. Spectrophotometric studies of the SANG- $\beta$ -CD systems in the presence and without 0.1 % PVP at the pH 5.0 did not show any evidence of the complex formation. However, the same systems showed several obvious evidences at the pH 8.0: the hyperchromic and the hypochromic effects and the presence of the isosbestic point in the region of 200 – 210 nm.

**STEROIDAL SAPONINS FROM THE SEEDS OF *HYOSCYAMUS NIGER L.***

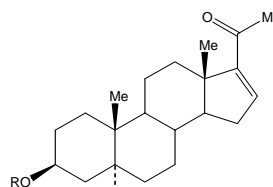
Irina Lunga, Pavel Kintia, Stepan Shvets, Carla Bassarelo, Sonia Piacente and Cosimo Pizza

The paper reports on the isolation of steroidal glycosides from the seeds of *Hyoscyamus niger L.* for the first time. Hyoscyamosides **B** (1), **C**(2) and **C**<sub>2</sub>(3) represent new compounds, their structures being determined by physico-chemical methods.



1: R=Glc(1-3)Gal

2: R=[Glc(1-3)][Glc(1-2)]Gal



3: R=Glc(1-2)Glc(1-4)Gal

**TOXICOPHORES AND QUANTITATIVE STRUCTURE -TOXICITY RELATIONSHIPS FOR SOME ENVIRONMENTAL POLLUTANTS**

N. N. Gorinchoy, I. Ya. Ogurtsov, A. Tihonovschij, I. Balan, I. B. Bersuker, A. Marenich and J. Boggs

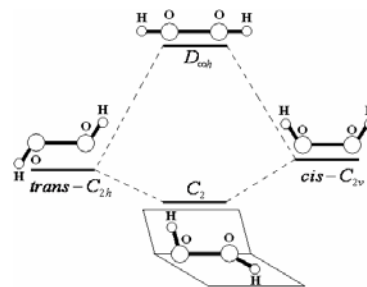
The electron-conformational (EC) method is employed to reveal the toxicophore and to predict aquatic toxicity quantitatively using as a training set a series of 51 compounds that have aquatic toxicity to fish. By performing conformational analysis (optimization of geometries of the low-energy conformers by the PM3 method) and electronic structure calculations (by *ab initio* method corrected within the SM54/PM3 solvation model), the Electron-Conformational Matrix of Congruity (ECMC) was constructed for each conformation of these compounds.

	C1	C2	C3	C4	C5	C6	C7	Br	N1	N2	O1	O2	O3	O4
C1	0,22	1,42	2,43	2,81	2,43	1,41	0,94	2,72	4,31	2,55	3,48	3,04	5,01	5,01
C2		0,19	1,40	2,42	2,79	2,41	2,54	3,52	3,80	0,73	2,34	2,35	4,19	4,76
C3			0,29	1,43	2,41	2,78	3,81	4,65	2,51	2,48	2,91	3,41	2,80	3,59
C4				0,20	1,41	2,40	4,28	5,11	0,77	3,77	4,26	4,63	2,34	2,34
C5					0,20	1,44	3,75	4,60	2,51	4,30	4,98	5,01	3,59	2,30
C6						0,32	2,46	3,45	3,78	3,82	4,66	4,36	4,75	4,18
C7							0,41	0,96	5,79	3,04	3,97	3,11	6,48	6,44
Br								0,42	6,52	3,84	4,28	4,22	7,22	7,11
N1									0,14	4,99	5,28	5,87	1,50	1,50
N2										0,14	1,52	1,48	5,10	6,06
O1											0,44	2,12	5,22	6,40
O2												0,45	5,98	6,93
O3													0,45	2,12
O4														0,45

**VIBRONIC ORIGIN OF THE "SKEWED" ANTICLINE CONFIGURATION OF THE HYDROGEN PEROXIDE MOLECULE**

N. N. Gorinchoy, I. Ya. Ogurtsov and Ion Arsene

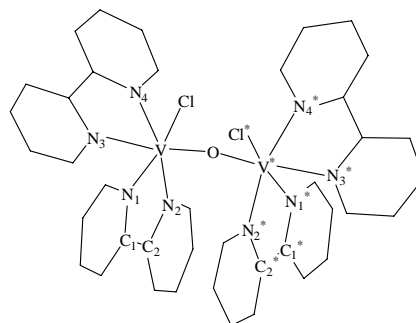
The vibronic origin of the instability of the symmetrical forms ( $D_{\infty h}$ ,  $C_{2h}$  and  $C_{2v}$ ) of the hydrogen peroxide molecule  $H_2O_2$  was revealed using *ab initio* calculations of the electronic structure and the adiabatic potential energy curves. The vibronic constants in this approach were estimated by fitting of the *ab initio* calculated adiabatic potential in the vicinity of the high-symmetry nuclear configurations to its analytical expression. It was shown that the equilibrium "skewed" anticline shape of the  $C_2$  symmetry can be realized in two ways:  $D_{\infty h} \rightarrow C_{2v} \rightarrow C_2$  or  $D_{\infty h} \rightarrow C_{2v} \rightarrow C_2$  with the decreasing of the adiabatic potential energy at every step.



**AB INITIO ANALYSIS OF EXCHANGE INTERACTIONS IN  $[V_2O(bipy)_4Cl_2]^{2+}$  COMPLEX**

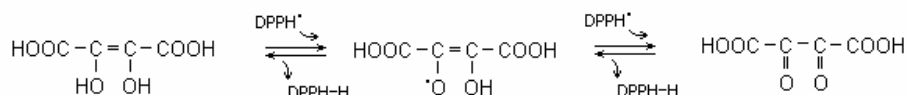
Ivan Ogurtsov, Andrei Tihonovschi

... The ground state was calculated to be a quintet, which means a ferromagnetic interaction between centers. The orbitals participating in exchange interaction according to ROHF+CI calculations are two molecular orbitals consisting of vanadium d-orbitals and two molecular orbitals with main contributions from p-orbitals of bipyridine ligands perpendicular to V-V axis, vanadium d- and p-orbitals and  $\mu$ -oxygen p-orbital. Calculated energy values of the multielectronic states are placed in accordance with Lande rule. The obtained value of magnetic moment at 293K calculated taking into consideration the Boltzmann distribution and the energies of the excited states is 3.95BM which is in accordance with experimental value of 3.99BM (for complex in acetone) and 4.48MB (in powder form).

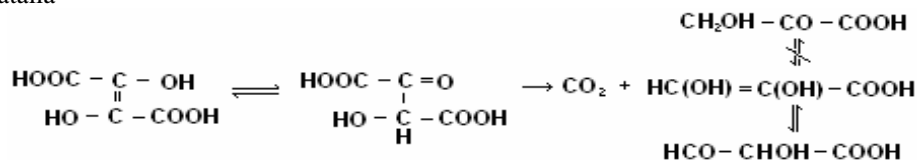
**ESTABLISHMENT OF THE ANTIOXIDANT/ANTIRADICAL ACTIVITY OF THE INHIBITORS USING THE DPPH – RADICAL**

Maria Gonta, Gheorghe Duca, Diana Porubin

This research paper presents the results of the investigation of antioxidant activities of various inhibitors, which are constituents of winery products: quercetin, rezveratrol, dihydroxyfumaric acid, sodium dihydroxyfumarate, dimethyl ester of DFH<sub>4</sub> and dimethyl ester of tartaric acid, the unoxidized enotannin extract *Eneox* and the oxidized one *-Enoxil*

**DIHYDROXYFUMARIC ACID TRANSFORMATION**

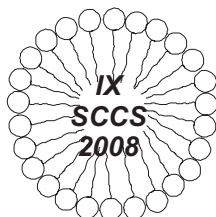
Secara Natalia

**HIS LIFE WAS A LEGEND**

Dumitru Batâr

**GUIDE FOR AUTHORS**

„DUNĂREA DE JOS” UNIVERSITY, GALAȚI  
Department of Science, Chair of Chemistry  
**BUCHAREST UNIVERSITY**  
Department of Science, Chair of Physical Chemistry  
**ROMANIEN CHEMICAL SOCIETY**  
**ROMANIEN SOCIETY OF COLLOID AND SURPHACE CHEMISTRY**



The IX-th SYMPOSIUM ON COLLOID AND SURFACE  
CHEMISTRY  
with international participation

29 –31 Mai 2008  
GALAȚI, ROMÂNIA  
www.ugal.ro

**S Y M P O S I U M   S E C T I O N S**

1. **Disperse systems and physical chemistry of surfaces** (*colloid stability, surfactants, films*)
2. **Biocoloids** (*food products, cosmetics, pharmaceuticals*)
3. **Functional surface modification** (*composites, coatings, treatments*)

**Workshop 1:** *Stimulation of Romanian research access to international funds*

**Workshop 2:** *Chemical and biochemical processes on the solid-liquid interface.*

**S C I E N T I F I C   C O M I T E E**

Prof. dr. Mihaela OLTEANU  
oltni@gw-chimie.math.unibuc.ro  
Acad. prof. dr. Bogdan SIMIONESCU  
Prof. dr. Olga MITOSERIU  
Prof. dr. Constantin GHEORGHIȘ  
Prof. dr. Viorica MUȘAT  
Conf. dr. Ștefan DIMA  
Prof. dr. Traian FLOREA  
Prof. dr. Gheorghe NECHIFOR  
Prof. dr. Teodor VISAN  
Prof. dr. Claudio PETTINARI  
Prof. dr. Lucia ODOCHIAN  
Prof. dr. Andreas BUND  
Prof. dr. Thomas LAMPKE  
Prof. dr. ing. Petre ALEXE  
Prof. dr. ing. Anca NICOLAU  
Dr. Dan Florin ANGHEL  
Dr. Viorica TRANDAFIR

**Contacts:** **Dr. Constantin APETREI**  
constantin.apetrei@ugal.ro

**L O C A L   O R G A N I Z I N G  
C O M I T E E**

Chairman: Prof. dr. Traian FLOREA  
Prof. dr. Geta CĂRAC  
Prof. dr. ing. Lucian Puiu GEORGESCU  
Dr. Gheorghe ZGHEREA  
Dr. Maria CIOROL  
Dr. Rodica DINICĂ  
Dr. ing. Doruleț RESMERIȚĂ  
Dr. Paula POPA  
Dr. Dumitru DIMA  
Dr. Cătălina ITICESCU  
Dr. Bianca FURDUI  
Cristina STOIAN  
Romică CRETU  
Mihaela TIMOȘTE  
Monica MURĂRESCU  
Vasile GRECU

**Dr. Manuela FLOREA-SPIROIU**  
manuela@gw-chimie.math.unibuc.ro

**NATIONAL ACADEMY OF SCIENCES OF UKRAINE  
THE MINISTRY OF ECOLOGY AND NATURAL RESOURCES OF UKRAINE  
LVOV REGIONAL STATE ADMINISTRATION  
DEPARTMENT OF ECOLOGY AND ENVIRONMENTAL PROTECTION OF LVOV REGION  
ENTERPRISE “ЗАХИДУКРГЕОЛОГИЯ” (“НЕДРА УКРАИНЫ”)  
INSTITUTE OF GEOLOGY AND GEOCHEMISTRY OF FOSSILE FUELS, NAS OF UKRAINE  
ASSOCIATION “UKRHYDROENERGO”  
THE NATIONAL “LVOV POLITECHNICAL” UNIVERSITY  
LVOV CENTER OF TECHNICO-SCIENTIFIC AND ECONOMIC INFORMATION**

**VII-th INTERNATIONAL SCIENTIFICO-PRACTICAL CONFERENCE  
Carpatian Region Natural Water Resources  
/Protection and rational using problems/**

**29-30 May 2008  
Lvov, Ukraine**

The Conference aims to review the problems of rational using and protection of Carpathian region natural waters and intellectual-professional potential cooperation.

**Conference issues**

- Natural waters resources and their ecological state;
- Hydro-thermal and hydro-energetic resources;
- Balneological potential of Carpathian region;
- Water supply and problems of rational using of drinking waters;
- Modern methods and technologies for purification and utilization of wastewaters;
- Problems of protection of trans-boundary water basins;
- Integration of the water resources research in the EU priorities.

**Organizing Committee**

**Organizing Committee co-Chairmen**

Prof. Dr. V. Kolodii, Lvov, Ukraine  
Prof. Dr. T. Lupascu, Chisinau, Moldova  
B. Matolicz, Lvov, Ukraine  
Prof. Dr. M. Pawliuk, Ukraine  
S. Potashnik, “Ukrhydroenergo”, Ukraine  
Prof. Dr. A. Sadurski, Poland  
Acad. V. Shestopalow, Ukraine  
Dr. M. Jaworski, Lvov, Ukraine

**Organizing Committee members**

Prof. Dr. O. Adamenko, Iv. Frankovsk, Ukraine  
Dr. B. Aksentiichiuk, Truskavets, Ukraine  
O. Gwozdevicz, Lvov, Ukraine  
Prof. Dr. L. Griniv, Lvov, Ukraine  
Dr. S. Ivasivka, Truskavets, Ukraine  
O. Kahnovets, Lvov, Ukraine  
A. Kovalczuk, Lvov, Ukraine  
Dr. O. Romaniuk, Ukraine  
P. Tchalii, Ukraine  
O. Mucha, Ukraine  
V. Skripitchaiko, Lvov, Ukraine  
Dr. M. Sprinski, Torun, Poland  
Dr. Yu. StafanikIO., Ukraine  
S. Tatuch, Lvov, Ukraine  
Dr. J. Chowanec, Poland

**Contacts:**

Mucha Orest

Tel: (0322) 52-30-23; 52-27-41; tel/fax 52-33-42, Cell. +380 95 83 33 462; E-mail: muha@cstei.lviv.ua

## ESTIMATION OF THE NATURAL WATER SELF-PURIFICATION CAPACITY FROM THE KINETIC STANDPOINT

Gheorghe Duca<sup>a</sup>, Elena Bunduchi<sup>\*b</sup>, Viorica Gladchi<sup>b</sup>, Lidia Romanciuc<sup>b</sup>, Nelli Goreaceva<sup>b</sup>

<sup>a</sup>Academy of Sciences of Moldova, Ștefan cel Mare 1, Moldova

<sup>b</sup> Moldova State University, 60 A.Mateevici str. MD 2009, Moldova

\* ebunduchi@mail.md, phone: 577796, fax: 577557

**Abstract:** The current paper contains a synthesis of the processes of chemical auto-purification that take place in natural waters; examples of mechanisms of such processes occurring with participation of dissolved organic matter, oxidants of the biogeochemical cycle of oxygen and of transition metals including copper and iron are presented. The kinetic indicators of natural water quality are presented as well.

**Keywords:** self-purification capacity, hydrogen peroxide, free radicals, kinetic indicators, redox state, inhibition capacity.

The global cycle of water, together with its property of dissolving gases, organic and mineral compounds determine the various and multicomponent composition of water. At the same time, water represents a natural life environment for living organisms; therefore it is always in a dynamic equilibrated state due to the continuous substances exchange with the aquatic biocenosis.

The various physical, chemical and biological processes in the water reservoirs determine the circuit of chemical substances and living organisms, and the establishment of the quasi-equilibrated state which constitute the basis of biota evolution. The natural self-purification processes were capable to fight the negative changes of water quality just until the anthropogenic action became significant. The excessive anthropogenic pollution damaged this equilibrium, leading to eutrophication of water reservoirs, changes in biocenoses, appearance of toxic effects.

One of the most important priorities of modern science lies in understanding and explaining of the self-purification capacity of natural waters, i.e. the capacity of diminishing the concentrations of various pollutants to a harmless concentration for ecosystems, as a result of various processes.

**The self-purification of surface waters** is defined as *the totality of biological, physical and chemical processes which take place within the water reservoir and which lead to the diminution of pollutants concentration to a level that is harmless for ecosystems functionality.*

Besides chemical compounds that infiltrate into surface waters with waste waters, or atmospheric precipitations, the processes of physical-chemical and chemical-biological transformations include those resulted during the vital activity of living organisms from water reservoirs.

Self-purification of the natural water environment implies physical-chemical processes of mass transfer (**physical self-purification**), **biological self-purification** during the metabolic and co-metabolic processes and chemical processes of substances transformation (**chemical self-purification**).

In fact, physical processes, such as dilution, vaporization or adsorption, lead only to a redistribution of pollutants in the aqueous environment, either amongst the other components of the water reservoir (suspensions, organisms, etc), or by their evacuation in the near-by systems (aquatic basins, bottom depositions, atmosphere).

The involvement of living organisms that are present in water, especially of those autotrophic (algae, bacteria), in the transformation of compounds, leads to the decrease of pollutants concentration due to metabolic and co-metabolic processes. The rate of the microbiological processes in decomposing the substances that don't participate in metabolism is rather small [1, 2]. This kind of self-purification is significant only for easily assimilable compounds, such as biogenic substances.

It is known that substances that don't participate in the biologic cycle of biota can undergo transformations due to co-metabolic processes. Still, the efficiency of such processes depends on a multitude of related factors; in case of the majority of compounds, chemical transformations are the most important. As opposed to microbiological processes, chemical and photochemical transformations can unfold in dissolved substances, as well as in those absorbed/adsorbed. Generally, organic pollutants participate only in few chemical transformations [3]:

- **hydrolysis**, when water is not only a solvent, but a reagent;
- **direct, induced and sensitization photolysis**, transformations under the influence of sunlight;
- **oxidation**, when transition metal ions or free  $\cdot\text{OH}$  radicals act as oxidants;

- a) *catalytic*, in the presence of  $O_2$ ,  $H_2O_2$  and transition metals ions;  
 b) *radical*, in the presence of free  $\cdot OH$  radicals.

### Hydrochemical indicators for surface waters quality estimation

As a system of surveillance and control of the environmental state, the monitoring has the tasks of evaluation of the real state and prognostication of possible modifications. The central element of monitoring is the estimation of the state of the environment.

Considering the range of substances which penetrate into and are formed within surface waters, it seems to be difficult and quite useless to control each component in part. There have been elaborated complex indicators which provide the information regarding the content of smaller or larger groups of substances, defined as hydrochemical indicators for the estimation of water quality.

Initially, the monitoring of water quality was based on indexes such as temperature, organoleptic properties, presence of suspensions (turbidity), hydrogen index (pH), redox potential (Eh), hardness, mineralization (content of main ions), content of dissolved oxygen, the chemical (CDO) and biochemical (BDO) doze of oxygen, content of mineral forms of nitrogen ( $NH_4^+$ ,  $NO_2^-$ ,  $NO_3^-$ ) and phosphorus ( $PO_4^{3-}$ ), content of heavy metals, organic pollutants (oil products, phenols, pesticides, surface active compounds, etc.). Afterwards, this group of hydrochemical indexes was enlarged with such indicator as: content of  $H_2O_2$ , redox state, inhibition capacity, named *kinetic indicators* [4]. Hydrochemical indexes are criteria that allow the correct establishing of the water source quality, its biologic value and utility for specific objectives (drinking, recreation, fish-growing).

In order to quantify and control the content of compounds in waters, the values of field measurements is compared with the admissible concentrations or with fon concentrations. In time it has been demonstrated that these indexes are not informative enough and can't explain the causes of changes that take place in water ecosystems, such as biocenoses change, appearance of toxicity for organisms living in waters and even for man. For example, the admissible limit concentration established for copper ions in hard water using the concentrations of aqua-forms can't be used with certainty in real conditions. In the natural water environment, living organisms can be submitted to a certain deficit of biologically accessible forms even in case of concentrations larger than the admissible limit concentration, due to certain specific properties of ions, such as: small charge, high capacity of copper (II) ions to form complexes, formation of stable compounds of copper (I) and several natural ligands. Also, the concentrations of organic pollutants and biogenic elements are not sufficient for the characterization of surface water quality. Thus, depending on the qualitative composition of organic compounds which determine the chemical doze of oxygen, surface waters can be biologically valuable at high CDO values and, in contrast, toxic at low CDO values. The method of comparison of the determined concentration with the admissible limit can, certainly, be applied only in case of compounds, such as the main ions ( $Ca^{2+}$ ,  $Mg^{2+}$ ,  $Na^+$ ,  $K^+$ ,  $CO_3^{2-}$ ,  $HCO_3^-$ ,  $SO_4^{2-}$ ,  $Cl^-$ ) which form the so-called *mineralization of natural waters*, as for the remaining components, their quantity is permanently changing, due to the variation of several factors.

*Kinetic indicators of surface water quality* characterize the content and dynamics of products of mono-electron activation of oxygen, such as highly reactive redox agents: hydroxyl radicals ( $\dot{O}H$ ), singlet oxygen ( $^1O_2$ ), superoxide anions ( $H\dot{O}_2$ ) and the product of bi-electron activation – hydrogen peroxide ( $H_2O_2$ ). The value and the dynamics of these indexes are of significant importance in establishing the quality class of the water object, its biological value and the self-purification capacity of the natural water [3-6].

One of the properties of surface waters is the *redox state*. It has been considered for a long time that the main indicator of the oxidative state is the presence of molecular oxygen in the water, and the reducing state is characterized by its absence and the presence of iron (II). However, as a result of numerous field measurements and observations, it has been demonstrated that the state of surface waters can be considered normal (oxidative) only in cases when besides the dissolved  $O_2$  the waters contain hydrogen peroxide ( $H_2O_2$ ) in physiological quantities, set as favorable for living organisms:  $9 \cdot 10^{-9} M < H_2O_2 < 9 \cdot 10^{-6} M$  ( $0,3 \mu g/l < H_2O_2 < 300 \mu g/l$ ) [6-9].

These observations lead to the conclusion that hydrogen peroxide is an indispensable component of the water environment.

Evolution made it natural that organisms live in oxidative conditions and die in reducing media. For example, daphnia and infusorians, juvenile fish, die shortly in case the hydrogen peroxide is absent in the environment. The juvenile fish needs the  $H_2O_2$  as exogenic oxidant until the formation of its own oxidation systems. The lack  $H_2O_2$  is characterized by the domination of reducing compounds which can act through blocking the oxidation-reduction centers f enzymes, damaging the redox equilibrium within the cell. Another impact of the domination of reducing conditions is the burst of pathogenic microflora, which eliminates toxins that can affect even man [3, 7-9].

Field measurements have shown cases when  $H_2O_2$  was absent in surface waters, but other significantly oxidative

compounds were observed [23]. Therefore, dynamic redox state can be created in the natural water environment, depending on the  $H_2O_2$  concentration in water, of reducing agents and highly oxidative compounds [4,6,9]:

- **oxidative**, the  $H_2O_2$  is present in concentrations of  $10^{-6}$ - $10^{-5}$  mol/l;
- **quasi-reducing ( $Red_{ep}$ )**,  $H_2O_2$  is absent and compounds with significant reducing properties are identified, which are titrated by  $H_2O_2$  (phenols, dienols, sulfur compounds etc.);
- **super-oxidative ( $Ox_{ep}$ )** – products and half-products of technological cycles are detected (active chlorine, Cr(VI),  $KMnO_4$ ).

The moment of appearance and the duration of instable states can change from season to season, but the qualitative aspect remains the same. It has been observed that in the case of redox state change, the classical hydrochemical and hydrobiological indexes remain almost the same.

*The biologically valuable state of surface waters is considered to be its oxidative state, when besides the dissolved  $O_2$  the water contains  $H_2O_2$  in physiologically favorable concentrations for living organisms -  $10^{-6}$ - $10^{-5}$  mol/l.*

The process of formation and decomposition of  $H_2O_2$  in natural waters is accompanied by the formation of free radicals. Amongst all intermediate products of oxygen reduction, the OH radical is considered the most powerful oxidant, due to its high redox potential (2,8 V). It interacts with most of organic substances with rate constants practically equal to the diffusion constant  $k_{OH+P} = 10^8 - 10^{10}$  mol<sup>-1</sup>s<sup>-1</sup> [11].

The stationary concentration of  $\dot{O}H$  radicals in natural waters is quite low, of the  $10^{-17}$ - $10^{-15}$  M order [9, 12-15]. Considering the reactivity towards  $\dot{O}H$  radicals, the components of natural waters form two groups [3]:

- substances whose radicals react either with  $O_2$ , or with transition metals ions, generating  $\dot{O}H$  in the end.

The rate of oxidation of each component from this chain is determined by the stationary concentration of  $\dot{O}H$ .

- substances whose radicals possess a low reactivity or, after undergoing transformations, become unreactive.

These compounds, at their turn, can become  $\dot{O}H$  traps or compounds which react with this radical and then form with  $O_2$  a peroxide radical, with low reactivity. Afterwards, these radical disappear due to recombination, disproportionation or the reaction with the reducing form of the metal. As a result, radical chains are destroyed.

The effective rate constant which characterizes the interaction of  $\dot{O}H$  with all components of this group makes the second category a parameter which characterizes the capacity of natural waters to *inhibit radical self-purification processes* through  $\dot{O}H$  radicals. *The inhibition capacity is the effective constant of the rate of destruction of  $\dot{O}H$  radicals.*

Considering the criterion *capacity to inhibit radical self-purification processes* of natural waters, they can be divided into three categories [3, 4, 6]:

- 1) if  $\Sigma k_i[S_i] < 3 \cdot 10^4$  s<sup>-1</sup> – very clean waters
- 2) if  $\Sigma k_i[S_i] 3 \cdot 10^4 - 3 \cdot 10^5$  s<sup>-1</sup> – normal state of natural waters
- 3) if  $\Sigma k_i[S_i] > 3 \cdot 10^5$  s<sup>-1</sup> – highly polluted waters.

The dynamics of the content of redox agents in natural waters is an index of the biocenosis state: homeostasis, reversible and irreversible perturbation. Excessively high or low values of indices, accompanied by an unclear dynamics correspond to an ecosystem with irreversibly disturbed ecological welfare. In a normal aquatic ecosystem, the range of variation of the rate of formation and lifetime of redox agents doesn't exceed with  $\pm 50\%$  any mean value, which formed under the influence of meteorological, hydro-physical, hydrochemical etc. factors.

The quality of natural waters must be defined not by its content of specific substances, but by its *biological value*. Waters with adequate biological value represent a good environment where vital processes unfold normally at various trophic levels, so that the cycle of chemical compounds is closed.

### Redox components of surface waters

The chemical circuit of water in nature is tightly correlated with redox processes which involve molecular oxygen, hydrogen peroxide and other active particle from the biogeochemical cycle of oxygen.

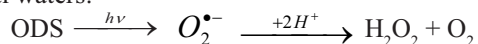
The vital activity of aquatic organisms is based on the biogeochemical cycle of oxygen which, in its turn, is correlated with other biogeochemical cycles (of nitrogen, sulfur, variable valence metals). The concentration of dissolved oxygen in surface waters ranges between 0 and 14 mg/l and is determined by two processes – photosynthesis and the biotic and abiotic consumption. Due to photosynthesis, there is enough oxygen in the atmosphere to oxidize all organic compounds on Earth. After fluorine, it is the next most powerful oxidant; it eliminates 491 kJ/mol of free

energy during its reduction to water. However, in spite of it being a strong oxidant from the thermodynamic point of view, oxygen is quite inert from the kinetic standpoint. This is due to its specific electronic structure, which determines the triplet state of oxygen as its ground state [10, 39].

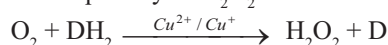
As to the chemistry of natural waters, the products of oxygen activation are the most important in the oxidation and reduction processes within the basin, as they are considered the most reactive elements of the biogeochemical cycle of oxygen. In fact, oxygen reactivity is not determined by its molecular form, but by the intermediates of its biogeochemical cycle ( $^1\text{O}_2$ ,  $\dot{\text{O}}\text{H}$ ,  $\text{O}_2^{\bullet-}$ ,  $\text{H}_2\text{O}_2$ ). Numerous field measurements allowed establishing the stationary concentrations of these particles:  $[\text{O}_2] = 10^{-14}$ - $10^{-12}$  M,  $[\dot{\text{O}}\text{H}] = 10^{-18}$ - $10^{-15}$  M,  $[\text{H}\dot{\text{O}}_2] = 10^{-8}$ - $10^{-9}$  M,  $[\text{H}_2\text{O}_2] = 10^{-6}$ - $10^{-5}$  M (Zepp R.G., 1977; Hoigne Z., 1979; Mill T., 1980; Zafiriou O.C., 1983; Скурлатов Ю.И., 1983, Duca Gh., 1983, 1988, 2000, 2006; Штамм Е.В., 1991; Эрнестова Л.С., 1995; Grannas A. M., 2006) [9, 14-19].

According to thermodynamic data of redox ( $\varphi_{\text{HO}_2/\text{H}_2\text{O}_2} = 1,44$  V) and acid-base ( $\text{pK}_a = 11,75$ ) transformations of oxygen, the most stable intermediate product of  $\text{O}_2$  reduction is hydrogen peroxide ( $\text{H}_2\text{O}_2$ ) [10].

The majority of  $\text{H}_2\text{O}_2$  in surface waters comes from photochemical generating processes. During the action of sunlight on organic dissolved substances (ODS), the superoxide anion radical results, being the precursor of  $\text{H}_2\text{O}_2$  in natural waters:



Some quantity of  $\text{H}_2\text{O}_2$  results in redox-catalytic processes:



Biologic emissions form another source of  $\text{H}_2\text{O}_2$ . Many species of algae are known, which eliminate in the environment the over-produced  $\text{H}_2\text{O}_2$ , formed in cells during photosynthesis. Also, on the exterior surface of several algae there are ferments, such as diaminases, which can oxidize organic compounds of nitrogen:

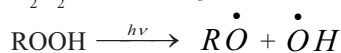
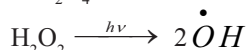
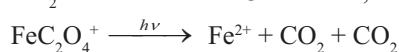
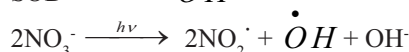
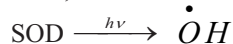


The amount of  $\text{H}_2\text{O}_2$  can increase due to hydro-peroxides:



In stationary conditions, mean concentrations of hydrogen peroxide range between  $10^{-6}$ – $10^{-5}$  M. The decomposition of  $\text{H}_2\text{O}_2$  in natural waters is triggered by biotic and abiotic processes. On the basis of numerous researches, it has been established that among potential catalysts of decomposition processes, the most active in natural waters are ions and complexes of copper and iron. Biotic destruction is determined by microalgae content.

Considering the mentioned above thermodynamic data, we can deduce that the most reactive particle from the oxygen cycle is  $\dot{\text{O}}\text{H}$  [10]. According to the specialty literature, the main mechanism of these radicals initiation is the photochemical one, namely the photolysis of organic compounds dissolved in water and of several inorganic components, such as: nitrates, nitrites, peroxides, complexes of variable valence metals (Fe, Cu, Mn, Cr):



The hydroxyl radical is the most reactive intermediate, non-selective and electrophilic. The second order constant of this oxidant with numerous organic compounds has values close to the diffusion constant ( $10^7$ – $10^{10}$  M $\cdot$ s $^{-1}$ ) [11]. Although it is present in natural waters in concentrations around  $10^{-14}$ – $10^{-18}$  M (Brezonik, 1998; Russi, 1982; Скурлатов Ю.И., 1983; Duca Gh., 1983, 1988, 2000, 2006; Штамм Е.В., 1991; Эрнестова Л.С., 1995; Grannas A. M., 2006) this photo-oxidant significantly contributes to reactions of limitation of organic contaminants in natural waters [9, 14-19]. The reactions with  $\dot{\text{O}}\text{H}$  participation are the hydrogen atom abstraction and its addition to the double bond [10].

Measurements regarding the influence of the wavelength on the rate of  $\dot{\text{O}}\text{H}$  generation by the ODS solutions contained in arctic waters have indicated that the highest amount of  $\dot{\text{O}}\text{H}$  is obtained at the wavelength of  $\approx 300$  nm [15]. Another drawn conclusion is that the quantity generated is function of the applied wavelength and isn't influenced almost at all by the geographical place of the water reservoir from which the ODS have been preloaded. This conclusion



One very important specific of natural waters is the presence of micro-quantities of transition metals in it. These components can participate in reactions with intermediate free radicals, hydrogen peroxide, and molecular oxygen. Metals can form various complexes with natural waters components which possess ligand properties, catalytic properties in redox transformations or which participate in photochemical processes [10, 35, 36].

The results obtained in model and natural conditions have demonstrated that in the natural aquatic environment and a pH value between 5 and 9 (characteristic for surface waters), almost all metals with variable valence are found predominantly as colloids of oxide or hydroxide or as soluble complexes, with natural ligands [35, 36]. Given that surface waters are oxidative environments in normal conditions, transition metals ions are found mainly in oxidized form ( $M^{2+}$ ). Only a small quantity of metals is in reduced form ( $M^+$ ), and it participates in the activation of  $O_2$  and  $H_2O_2$ . Among all transition metals in surface waters, especially important for redox transformations are copper, iron and manganese. Only copper ions exist in neutral environment in homogenic form, both in oxidized ( $[Cu^{2+} = 3 \cdot 10^{-7}$  mol/l]), and in reduced form ( $[Cu^+ = 10^{-8}$  mol/l]). Iron ions are found in aerobic conditions mainly in oxidized form, as micro-colloids of hydroxide ( $\equiv FeOOH$ ), at concentrations of  $10^{-5}$  mol/l. The highest concentration of the solvated form of the compound  $\equiv FeOOH$  is of  $2 \cdot 10^{-7}$  mol/l [24]. The soluble forms of iron (III) are represented especially by anionic hydroxy-fulvic complexes [35, 36]. Manganese ions are found either as free ions  $Mn^{2+}$ , or as micro-colloids of Mn (IV) hydroxide, which is formed in natural conditions at biological oxidation of Mn (II) [25].

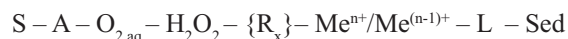
A characteristic of copper ions is their participation in reactions of one- or two-electrons transfer, leading to the formation of free  $\dot{O}H$  radicals and superoxide radical  $O_2^{\bullet -}$ . As to iron and manganese ions, they participate in catalytic reactions of  $H_2O_2$  decomposition with a two-electrons transfer [26].

Besides oxidants and catalysts (transition metals), in the oxidation-reduction processes also participate various reducing compounds, which can be formed directly in the aquatic environment (autochthonous compounds, metabolic products and those of biochemical destruction) or infiltrate in it with precipitations, floods or waste waters (allochthonous substances). Organic compounds are present in surface waters in relatively small concentrations, especially  $< 0,1$  mg/l or  $< 10^{-5}$  M [36].

### Modeling of redox transformations in the natural aquatic environment

From the chemical-kinetic point of view, natural waters form an open oxidation-reduction system; oxidizing and reducing compounds continuously infiltrate in it.

According to the database accumulated by various researchers, the chemical composition of the abiotic component of natural waters can be represented as follows:



where  $O_{2, \text{aq}} - H_2O_2 - \{R_x\}$  – dissolved molecular oxygen and its activation products; S – substrates of chemical transformations, including anthropogenic pollutants, A – active particles acceptors, which form secondary, less active radicals,  $Me^{n+}/Me^{(n-1)+}$  – ions and complexes of transition metals in oxidized/reduced form; L – components with ligand properties; Sed – suspensions with various dispersion rate, which form the heterogeneous phase.

The oxidation-reduction processes exist in natural waters only due to the presence of oxidative equivalents ( $M^{n+}$ ,  $O_2$ ,  $H_2O_2$ ,  $\dot{O}H$ ), reducing agents ( $DH_2$ ) and catalysts ( $M^{(n-1)+}/M^{n+}$ ). It should be mentioned that the redox model of natural waters doesn't include analysis of redox reactions that take place due to other oxidants that can infiltrate into waters as a result of anthropogenic pollution or chemical-biological transformations, but molecular oxygen and hydrogen peroxide. It is considered that these processes can be described by the laws established for catalytic oxygen-peroxide systems.

In order to involve  $O_2$  in oxidation processes chemical energy is necessary to activate it. This can happen on the account of sunlight absorption or interaction with compounds with significant reducing properties (metal ions in reducing forms, free radicals).

Hydrogen peroxide, the product of bi-electronic reduction of  $O_2$ , is considered the carrier of oxidative equivalents of oxygen in natural waters. As opposed to  $O_2$ ,  $H_2O_2$  can exhibit reducing and oxidizing properties in neutral environment, depending on its redox partner; thus it can interact with reduced and oxidized metal ions.

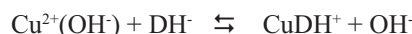
Among the transition metals present in natural waters, the most important for redox transformations are copper, iron and manganese ions.

Qualitative kinetic characteristics allow the prognostication of possible concentrations of compounds in waters with various loads, the estimation of maximal quantity of substance which can be discharged in water without disturbing the self-purification processes within the reservoir. The kinetic characteristic of processes is the effective rate constant, which is a function of the environment's parameters.

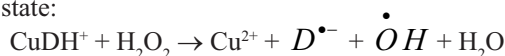
Much data exist nowadays regarding the chemical composition of natural waters, but very little is known about the kinetic laws that describe the interactions between these compounds [10, 39, 40]. A number of systems, such as  $M^{2+}/M^+ - L - S - O_2/H_2O_2$  (where,  $M^{2+}/M^+$  variable valence metal in oxidized/reduced form, L – ligand, S – substrate) have been studied. There is a lot of data on thermodynamic properties of metal complexes, reactivity of intermediate free radicals, mechanisms of activation of  $O_2$  and  $H_2O_2$ ; however very little is known about catalytic oxidation of several compounds of significant ecological importance.

Among all reducing agents which model the most successfully natural reducing compounds, most extensively studied are the ascorbic acid [20], thiolic compounds [27, 28], hydroquinone [27, 29], oxy and hydroxyacids [21, 22]. The ascorbic acid is a compound that regulates the intracellular redox state, having a significant medical-biological role. Oxy- and hydroxyl acids form the metabolic cycle of dicarboxylic acids and take part in the exchange of substances of living organisms with the environment. Hydroquinone is one of the poliphenols very often encountered in surface waters, being the precursors of natural humus. Thiolic compounds participate in metabolic processes of microorganisms, are used in the leather industry, in fertilizers technology etc.

On the basis of ascorbic acid the redox mechanism of processes within the aquatic environment has been established, with the participation of ions and complexes of copper when the pollutant (P) possesses ligand properties or significant reducing properties [20]. During the interaction between the metal and P, a compound with partial charge transfer is formed ( $CuDH^+$ ):

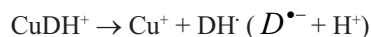


This complex plays the role of a one-electron donator, reducing the peroxide to  $\dot{O}H$  radicals, whereas the metal ion doesn't change its oxidation state:

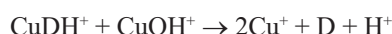


And this lead to the initiation of processes of conjugated oxidation of pollutants in natural water.

In the case of small copper ions concentrations, the complex can decompose in products with one-electron transfer:

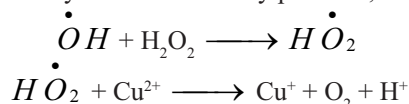


And in the case of high metal ions concentrations, it can interact with the second copper ion, thus oxidizing the donor by the two-electron pathway:



Given the copper ions concentration in natural waters, which is around  $\approx 10^{-7}$  M, the one-electron mechanism prevails in these conditions.

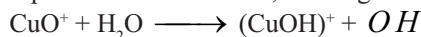
The discussed system is characterized by a specificity regarding the formation of OH radicals. As opposed to the Phenton system, the generation of  $\dot{O}H$  radicals doesn't interfere with the valence of the metal, this one remaining in its oxidized form. Copper (I) ions appear in this system as secondary particles, formed as a result of  $H_2O_2$  destruction:



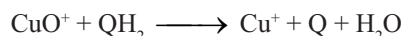
The impact of compounds with don't exhibit ligand properties in the natural aquatic environment (such as hydroquinone, glyoxalic acid) [28, 44] can be positive or negative, depending on the substrate's concentration. During the interaction of copper (I) ions with  $H_2O_2$ , the particle  $CuO^+$  results (which can be treated as the hydrolyzed  $Cu^{3+}$  ion), being the precursor of the  $\dot{O}H$  radical [34]:



In the absence of reactive substrates, this particle oxidizes water, forming OH radicals:



Given the fact that it is a two-electrons acceptor towards substrates, in the presence of H donors it oxidizes the donor according to the two-electrons pathway:

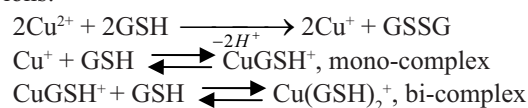


Thus, depending on the donors concentration in the environment, processes of inhibition or generation of OH radicals can take place.

Considering all stated above, the presence of reducing agents with no ligand properties has two roles: at small concentrations, substrates will nor essentially interfere the process of OH radicals generation, as a result of water oxidation by  $CuO^+$  (i.e.  $CuO^+$  will oxidize intensely the waters molecules and will be less consumed for the  $QH_2$  oxidation), at high concentrations, these substances will act as inhibitors, trapping the  $CuO^+$  particle, which is the precursor of OH radicals. This is of significant importance for the realization of chemical self-purification processes of natural waters, due to the possibility of conjugated oxidation.

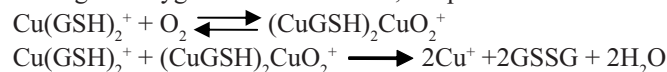
Sulfur compounds possess significant reducing and ligand properties (such as glutathione, thiourea, cysteine), but these compounds form stable complexes with low reactivity on interaction with copper ions (II) [27, 44].

The mechanism describing the processes of catalytic oxidation of cysteine, thiourea and glutathione are very much alike. The redox process unfolds with the formation of the intermediate complex of the thiol with the transition metal ions:

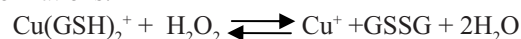


which can subsequently react with the dissolved oxygen or hydrogen peroxide.

During the oxygen driven oxidation, the process includes two metal ions:

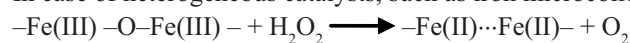


whilst in the case of hydrogen peroxide driven oxidation, only one metal ion participates in the transformations:



The mechanism of these processes is ion-molecular of activated type. The oxidation of thiols by hydrogen peroxide is a very rare case, when no free radicals are formed.

In case of heterogeneous catalysts, such as iron microcolloids, peroxide decomposition:



and compounds oxidation:



are not accompanied by free radicals formation.

The comparison of transition metals catalytic activities, it has been noted that iron microcolloids possess higher catalytic activity than copper ions. The phenomenon of the catalytic activity of these metals can be explained by the oxidation-reduction potentials of the pairs  $\text{Fe}_{\text{aq}}^{3+}/\text{Fe}_{\text{aq}}^{2+}$  ( $\varphi = 0,771$  V),  $\text{Cu}_{\text{aq}}^{2+}/\text{Cu}_{\text{aq}}^+$  ( $\varphi = 0,153$  V),  $\text{O}_2/\text{H}_2\text{O}_2$  ( $\varphi = 0,68$  V),  $\text{H}_2\text{O}_2/\text{O}_2$  ( $\varphi = 1,02$  V). The activation of oxygen or hydrogen peroxide can only take place when the metal redox potential has lower values than the redox potential of the pairs  $\text{O}_2/\text{H}_2\text{O}_2$  and  $\text{H}_2\text{O}_2/\text{O}_2$  [10].

The rate of substrate transformation can be influenced by various compounds present in natural waters. This influence can be observed through the variation of metals soluble forms and their reactivity capacities, by the formation of donor-acceptor complexes with the substrate and interaction with free radicals. As to the waters of our country, the most frequently encountered violations of the admissible limiting concentration are related to nitrogen compounds:  $\text{NO}_3^-$ ,  $\text{NO}_2^-$ ,  $\text{NH}_4^+$ .

The modification of the redox potential of the couple  $\text{Me}^{n+}/\text{Me}^{(n-1)+}$  due to complexing has a significant impact on the reaction velocity for systems such as  $\text{Me-Lig-H}_2\text{O}_2\text{-S}$ . It has been demonstrated that the more the ligand decreases the redox potential, the more effectively molecular oxygen and hydrogen peroxide are activated, and the more important is the catalytic activity of those compounds and the reaction velocity increases. In the case of increase of the redox potential of the couple, the role of the metal as an oxidant increases in the systems.

Addition of  $\text{NH}_4^+$  ions in systems which contained copper ions as catalysts leads to the increase of the reaction velocity, proportionally to the metal concentration. The  $\text{NH}_4^+$  and  $\text{Cl}^-$  ions are ligands that increase the potential of the pair  $\text{Cu}^{2+}/\text{Cu}^+$ , thus stabilizing the reduced form of the metal.

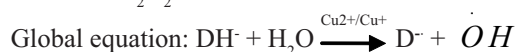
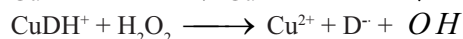
Investigations regarding the catalytic activity of iron microcolloids showed that iron complexes with humic compounds don't possess catalytic activity. Although measurements regarding the influence of iron complexing with these ligands show that the potential of the pair  $\text{Fe}^{3+}/\text{Fe}^{2+}$  decreases, which should have led to a higher catalytic activity of these complexes, it is not confirmed in the case of evaluation of oxidation involving iron microcolloids in the presence of humic compounds. In this case, the reaction is inhibited, which can be explained by the formation of chelated complexes. Addition of these compounds into the copper-containing system doesn't imply any influences. The lack of any impact in the case of these ions can be explained by the fact that the redox potential of the pair  $\text{Cu}^{2+}/\text{Cu}^+$  is not at all changed or only slightly varied in the structure of these complexes.

The generalization of all stated above allows concluding the following.

In the natural aquatic environment, reducing agents are only oxidized catalytically by the dissolved oxygen and hydrogen peroxide. The process of catalytic oxidation involving hydrogen peroxide, which is the carrier of oxidative equivalents in surface waters, is more effective.

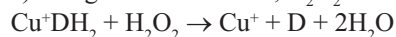
Depending on the donor's properties of being a ligand or not, the  $\text{H}_2\text{O}_2$  reduction can be accompanied or not by the OH radicals formation.

If redox ligands infiltrate into surface waters which contain  $\text{H}_2\text{O}_2$  and copper ions, formation of OH radicals can be initiated, without the change of the metal's oxidation state, according to the reactions:

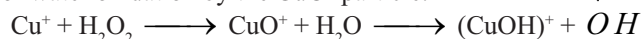


In the case of infiltration of reducers that don't exhibit ligand properties, two situations can appear, depending on the substrate concentration:

a) at high concentrations,  $\text{H}_2\text{O}_2$  is consumed without free radicals formation:



b) at small concentrations, substrates will not interfere significantly the process of OH radicals initiation, as a result of water oxidation by the  $\text{CuO}^+$  particle:



These cases show the main difference between the two redox states which can exist in natural waters: *oxidative* and *quasi-reducing*. In the first case, reducers initiate the decomposing of  $\text{H}_2\text{O}_2$  with the formation of free radicals, in the second case,  $\text{H}_2\text{O}_2$  is only consumed at the reducers oxidation.

Thiol-containing compounds exclude the copper ions from other redox processes, by transforming them into a biologically inaccessible form within the intermediate complex compounds. The presence of thiol substrates in natural waters can lead to the inhibition of chemical self-purification processes due to, on one hand, elimination of transition metals ions from the environment through their complexing, and, on the other, to the diminution or elimination of  $\text{H}_2\text{O}_2$ , which plays a very important part in the regulation of the natural waters redox state. All these contribute to the formation of the reducing state, toxic for living organism.

Comparing the catalysts activities, it can be confirmed that the oxidation process unfolds more intensely in the presence of copper, than iron.

The researches show that the velocity of substrates oxidation in natural waters is determined by the presence of copper ions, iron microcolloids, the content of  $\text{O}_2$  and  $\text{H}_2\text{O}_2$ . The influence of other water components is exhibited, as a rule, through the change of metals states in the solution.

### Photochemical transformations

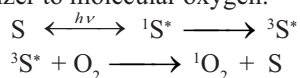
The majority of UV beams of the solar radiation are retained in the upper atmospheric layers (by the ozone layer) and only near-UV and VIS rays of the solar radiation spectrum ( $\lambda \geq 300$  nm) reaches the Earth surface. In the range of wavelengths 300-350 nm the solar intensity significantly increases. Under the action of this radiation, various photochemical transformations take place in natural waters, greatly determining the self-purification capacity of surface waters [3, 39, 40].

In the irradiated surface waters, two types of photodestruction can occur: *direct photolysis* and *indirect (sensitization and induced) photolysis*.

Organic compounds which absorb the actinic radiation ( $\lambda = 290$ -800 nm), become instable and subsequently decompose. The direct transformation of a compound under the action of solar radiation can occur when the region of the solar spectrum radiation overlaps the absorption spectrum of the compound; this region is named "the spectrum of action". For the wide majority of compounds, the maximum of the spectrum of action is situated in the range 310-330 nm. Most of the surface waters components absorb the near-UV radiation ( $\lambda \leq 350$  nm), making this part of the solar radiation the most effective in the self-purification processes.

In the case of sensitization photolysis, the solar radiation is absorbed by the sensitizer and the excitation is then transmitted to another compound which undergoes changes. Humus substances have the greatest importance in these reactions. Humus substances (HS) can be divided in two groups: fulvic acids (FA), which are predominant and humus acids (HA). Fulvic acids serve as sensitizers, as their maximum of the spectrum of action is situated at 365 nm. The absorption spectrum in the near-UV and far-UV regions (UVA and UVB) of humus acids is characterized by a maximum of high intensity at  $\lambda = 270$  nm, and for  $\lambda > 270$  nm the absorbance decreases drastically, and is almost zero for  $\lambda > 300$  nm.

As a result of sensitization photolysis, intermediate non-radical active particles are formed: the electronically excited particles of the sensitizer ( $^3\text{S}^*$ ) and singlet oxygen ( $^1\text{O}_2$ ), resulted during the passing of the excitation from the sensitizer to molecular oxygen:



Induced photolysis takes place in the presence of such active intermediates as the hydroxyl radicals ( $\dot{O}H$ ), carbonate (which results during the hydroxyl radicals interaction with the carbonate/bicarbonate ions), alkyl peroxide ( $RO_2$ ), solvated electrons ( $\bar{e}_{aq}$ ), which are generated by the natural waters' constituents. The absorption of actinic radiation by the ODS and nitrates leads to the highest production of these species.

Several researchers point the fact that indirect photolysis is important for compounds which absorb in the far UV region, while direct photolysis – for compounds with absorption maxima at wavelengths  $\geq 300$  nm [30, 31].

Monica et al. studied the direct and indirect photochemical reactions in surface waters submitted to irradiation with the implication of several pharmaceutical compounds (atorvastatin (ATR), carbamazepine (CAR), levofloxacin (LEVO), sulfamethoxazole (SMX)). They deduced that direct photolysis is important for the elimination of LEVO and SMX, while the presence of humus materials reduces the degradation velocity. In contrast, indirect photodestruction is the most important one for the limitation of ATR and CAR persistence, due to the fact that the destruction velocity increases in solutions which contain photo-producers of oxidants, humus acids. The explanation of the specific behaviour of these pharmaceutical products is given by their absorption spectra, for LEVO and SMX the absorption maxima are situated in the near UV region, while those for ATR and CAR – in the far UV [30].

Kępczyński M. et al. have studied the photooxidation of phenol, sensitized by humic acids Aldrich (AHA), in aqueous solutions at neutral and alkaline pH. Solutions containing phenol and various AHA concentrations were irradiated with monochromatic light at  $\lambda = 253,7$  nm and polychromatic light in the wavelength range of 310-420 nm. The results showed that addition of AHA to phenol solutions have different impact on its photooxidation. Thus, depending on the wavelength of the radiation and the AHA concentration, the process can be intensified or inhibited. For  $\lambda = 253,7$  nm direct photolysis is the main pathway of phenol oxidation, while at  $\lambda = 310-420$  nm the process is effectively sensitized by AHA [31].

In other works [32, 33] it has been deduced that the efficiency of direct photo-transformation depends not only on the presence of the benzoic ring and the chromophore group in the structure of aromatic compounds, which make possible the absorption of light in the UV-VIS range, but also on the type and position of the substituent in the benzoic ring. Prya M. et al studied the photocatalytic degradation at  $\lambda = 365$  nm of 7 derivatives of phenol which contained 2 substituents from the range Cl,  $NO_2$ ,  $CH_3$  in the presence of  $TiO_2$ . The results indicated that chloromethyl derivatives are destructed faster than chloronitrophenols [32]. Ksibi M. et al. have investigated the catalytic photodestruction in  $TiO_2$  suspension with UV radiation ( $\lambda = 280$  nm), at the pH of natural waters of 2 hydroxyphenols (hydroquinone and resorcinol) and 3 nitrophenols (4-nitrophenol, 4-NF; 2,4-dinitrophenol, 2,4-DNF; 2,4,6-trinitrophenol, 2,4,6-TNF). According the initial velocity of destruction, nitrophenols placed in the range: 4 NF > 2,4 DNF > 2,4,6 TNF, and hydroxyphenols: resorcinol > hydroquinone [33]. In order to explain the results, we appealed to the Hammett ( $\sigma$ ) constant, which represents the relationship between structure and reactivity in the range of aromatic compounds. The results showed that the lowest the positive Hammett constant is, the highest the destruction constant. Thus, knowing this constant allows deducing the compound's susceptibility towards photocatalytic transformations.

Hydrogen peroxide, nitrates and nitrites are the most important photo inducers of processes of induced photolysis [40]. Under the action of the solar radiation on these compounds, the OH radicals are generated, and subsequently oxidize the pollutant.

Although nitrates are characterized by pronounced absorption at  $\lambda < 250$  nm, in the case of natural waters, which are irradiated by light of  $\lambda \geq 300$  nm, their absorbance is quite low (for example for  $\lambda = 310$  nm,  $\epsilon_{310} = 7,4 \text{ M}^{-1}\cdot\text{cm}^{-1}$ ). Despite this, nitrates can't be neglected when it comes to discussing induced photolysis in natural waters. The role of nitrates in eliminating such contaminants as pesticides has been evaluated [41]. Frequently, this type of photolysis is applied in waste waters treatment procedures.

Usually, the thickness of the water layer where photochemical transformations take place is quite low and it doesn't exceed several meters; therefore, they are characteristic for surface layers of aquatic basins.

The variation of physical-chemical parameters of the aqueous environment influence the velocity of the self-purification processes, as follows [29, 39]: the variation of the pH value leads to the decrease of the extent of hydrolysis in hydrolytic pollutants transformations; the increase of turbidity leads to the diminution of the extent of photochemical processes for the compounds with photochemical activity, but, at the same time, sensitized photolytic processes are intensified, leading to the increase of the velocity of photochemical processes of free radicals initiation; contamination with compounds which possess ligand properties leads to the distribution of metal forms, which, at its turn, will influence the mass transfer processes and will change the catalytic activity of metals; temperature increase will intensify the temperature-depending processes, such as catalytic hydrolysis and oxidation; radioactive pollution will increase the velocity of OH radicals initiation and their stationary concentrations, which could have an impact on the biogenic elements cycles; pollution with S-containing compounds will reduce the  $Cu^{2+}$  ions, forming stable complexes which

are biologically inaccessible to living organisms. As a result, free radical oxidation is inhibited, accompanied by the appearance of toxicity effects for the organisms which are involved in an intense exchange of water with the environment.

There is a continuous unfolding of biotic and abiotic processes of formation of interacting reducing and oxidizing equivalents in natural waters. The result of this interaction is determined by the ratio between the oxidation equivalents fluxes – hydrogen peroxide ( $\omega_o$ ) and reducing equivalents – reducing compounds ( $DH_r$ ) which interact with it ( $\omega_r$ ) effectively. Reducers which infiltrate into the aquatic environment are oxidized by hydrogen peroxide, accompanied or not by the conjugated radical oxidation processes. If oxidation equivalents fluxes predominate ( $\omega_o > \omega_r$ ), the environment is in an oxidative state. By contrast, in case that reducing fluxes are superior to the  $H_2O_2$  flux ( $\omega_r > \omega_o$ ) the quasi-reducing state appears (reducers will be slowly oxidized by the dissolved oxygen).

The monitoring of free radical processes in natural waters is necessary for estimating the self-purification capacity of waters, as well as for preventing the phenomenon of toxicity towards mature living organisms in waters.

Regarding the efficiency of radical self purification, the increase of the stationary  $\dot{OH}$  radicals concentration is a positive factor. However, along with the increase of radicals concentrations, increases the danger of involving into the radical processes not only polluting compounds, but also the components of the environment which determine the structure and stability of hydro-biocenoses, or the perturbation of the manganese ions biogeochemical cycle can occur.

The increase of the stationary  $\dot{OH}$  radicals concentrations is the result of the increase of the initiating processes velocities, or the decrease of the constant which describes the radical's interaction with various "traps". The velocity of initiation increases with the pollution of the environment, especially with nitrates and nitrites (particularly at abundant rains) or due to the radioactive pollution.

## References

- [1] Каплин, В.Т.; Панченко, С.Е.; Шлычкова, В.В., Ж. Гидрохим. матер. Гидрометеиздат: Обнинск 1968, Т. XLIV; с. 183.
- [2] Головлёва, Л.А.; Филькинштейн, З.И.; Перцова Р.Н. Тез. докл. сов.-амер. симп.: Прогнозирование поведения пестицидов в окружающей среде, Ереван, 1981, с. 6-7.
- [3] Скурлатов, Ю.И.; Дука, Г.Г.; Эрнестова, Л.С. Ж. Изв. АН Молд.ССР, сер. биол.-хим. наук, Штиинца: Кишинёв, 1983, 5; с.3-20.
- [4] Семеняк, Л.В.; Штамм, Е.В.; Скурлатов, Ю.И.; Швыдский, В.О. и др. Мат. III Межд. Симпоз: Критерии самоочищ. способ. и качества природ. водной среды. Комплекс. глобал. мониторинг состояния окруж. природ. водной среды, Гидрометеиздат: Ленинград, 1986, с. 209-216.
- [5] Эрнестова, Л.С.; Скурлатов, Ю.И. Ж. Физ. Хим. Наука: Москва, 1995, 69, 7; с. 1159-1166.
- [6] РД 52.18.24.83-89. Методические указания. Методика определения кинетических показателей качества поверхностных (пресных) вод; Гидрометеиздат: Москва, 1990; 36 с.
- [7] Скурлатов, Ю.И.; Эрнестова, Л.С.; Штамм, Е.В.; Шпотова, Т.В.; Калинин Б.Б. Ж. Докл. Акад. Наук СССР. Наука: Москва, 1984, 276, 4; с. 1014-1016.
- [8] Штамм, Е.В. В сб.: Эколог. Химия водной среды. Мат. I Всес. школы, Кишинёв, 1988, с. 278-294.
- [9] Штамм, Е.В.; Пурмаль, А.П.; Скурлатов, Ю.И. Журн. Успехи химии. Наука: Москва, 1991, 60, 11; с. 2373-24062.
- [10] Сычёв, А.Я.; Травин, С.О.; Дука, Г.Г.; Скурлатов, Ю.И. Калитические реакции и охрана окружающей среды; Штиинца: Кишинёв, 1983; с.88.
- [11] Buxton, B.V.; Greenstock, C.L.; Helman, W.P.; Ross, A.B. J.Phys. Chem. 1988, 17, 513-886.
- [12] Mopper, K.; Zhou, X., J. Science. 1990, 250, 661.
- [13] Vaughan, P.; Blough, N., J. Environ. Sci. Technol. 1998, 32, 2947.
- [14] Bunduchi, E.; Duca, Gh.; Gladchi, V.; Goreaceva, N.; Mardari, I. Chemistry Journal of Moldova. General, Industrial and Ecological Chemistry. Ed. ASM: Chisinau, 2006, 1, 1; pp. 68.
- [15] Grannas, A. M.; Martin, Ch. B.; Chin, Yu-Ping, Platz, M., Biogeochemistry. 2006, 78. p.51.
- [16] Zepp, R.G.; Cline, D.M., J. Envir.Sci.Technol. 1977,11, 359.
- [17] Hoigné, J.; Bader, H., J. Ozone: Science and Engineering. 1979, 1, 357.
- [18] Mill, T.; Hendry, D.E.; Richardson, H., J. Sci. 1980, 207, 286.
- [19] Zafiriou, O.C., J. Chem. Oceanography. 1983, 8, p.339.
- [20] Штамм, Е.В. Автореф.: Кислородозависимые окислительно-восстановительные и фотохимические процессы в природных водах, Москва, 1992.

- [21] Дука, Г.Г. Автореф.: Механизмы экокхимических процессов в водной среде, Одесса, 1988.
- [22] Романчук, Л.С. Автореф.: Окислительно-восстановительный катализ и фотолиз некоторых оксо- и оксикислот, Кишинёв, 1990.
- [23] Эрнестова, Л.С. Автореф.: Методология и методика изучения состояния водных экосистем на основе кинетического подхода, Обнинск, 1995.
- [24] Пурмаль, А.П.; Скурлатов, Ю.И., Ж. Природа. Наука: Москва, 1984, 10, с. 94-102.
- [25] Emerson, S.; Kalthorn, S.; Jacobs, L. et al. J. Geochim.Cosmochim Acta.1982, 46, 1073-1079.
- [26] Эрнестова, Л.С.; Скурлатов, Ю.И.; Фурсина, А. Ж. Физ. Хим.1984, 58; с.914-918.
- [27] Duca, Gh.; Gladchi, V.; Romanciuc, L. Procese de poluare și autoepurare a apelor naturale; CE USM: Chișinău, 2002, p.3-140.
- [28] Gladchi, V.; Bunduchi, E. In Abstracts: Ecological chemistry, october 11-12, 2002, Chisinau, p. 42.
- [29] Скурлатов, Ю.И.; Дука Г.Г., Mediul ambinat. Ministry of Ecology: Chisinau, 2003,3; pp. 4-11.
- [30] Monica, W. Lam and Scott A. Mabury. Aquatic Sciences. Vol. 67, Nr.2, 2005, p. 177-188.
- [31] Kępczyński, M.; Czosnyka, A.; Nowakowska, M., J. Photochemistry and Photobiology. 2004, 79(3), 259-264.
- [32] Prys, M.; Giridnar, M. J. of Photoch. and Photob. A: Chemistry. 2006, 179, 256-262.
- [33] Ksibi, M.; Zemzemi, A.; Bouqchina, R. J. of Photoch. and Photob. A: Chemistry. 2003, 159, 61-70.
- [34] Штамм, Е.В.; Скурлатов, Ю.И.; Пурмаль, Ю.П. Ж. Физ. Хим.1987, 51, 12; сс. 3136-3139.
- [35] Лапин, И.А.; Красюков, В.Н. Водные ресурсы. №1, 1988, сс. 134-145.
- [36] Линник, П.М.; Набиванец, Б.И.; Брагинский Л.П. IV Межд. симпоз. по гомог. катал.: Формы существования, основные закономерности превращений и биологическая роль соединений тяжёлых металлов в природных водах. 1994; с. 237-238.
- [37] Секи Хумитаке. Органические вещества в водных экосистемах; Гидрометеиздат: Ленинград, 1986; с. 55-58.
- [38] Xiani Liu, Dong Xu, Feng Wu, Zhenhaun Lia, Jiantong Liu, Nansheng Deng., J. Photoch. and Photob., 2004, 79(3), 259-264.
- [39] Duca, Gh.; Scurlatov, Yu. Ecological chemistry; Publishing Center MSU: Chisinau, 2002; pp. 154-196.
- [40] Сычѐв, А.Я.; Дука Г.Г. Фундаментальные и прикладные аспекты гомогенного катализа металлокомплексами; Изд. центр Молд. Гос. Унив.: Кишинѐв, 2002, Ч. I и II.
- [41] Sharpless Charles, Seibold Deborah, Linden K., J. Aquat. Sci. 2003, 65, 359-366.
- [42] Borodaev, R., Anal. Științ. ale USM, seria „Științe chimico-biologice”. CE USM: Chișinău, 2002; p.401-407.
- [43] Duca, Gh.; Goreaceva, N.; Romanciuc, L.; Gladchi, V., J. Intellectus., Știința: Chișinău, 1999, 4; p.62-68.
- [44] Семянк, Л.В. Автореф.: Эколого-химические закономерности формирования биологической полноценности водной среды, Москва, 1996.

# PHYSICAL METHODS OF FAST REACTIONS INVESTIGATION

Gheorghe Duca<sup>a</sup>, Natalia Secara<sup>b\*</sup>, Daniela Duca<sup>c</sup>

<sup>a</sup>Academy of Science of Moldova, 1 Stefan cel Mare str., MD-2001, Chisinau, Republic of Moldova;

<sup>b</sup>Institute of Chemistry, 3 Academy str., MD-2028, Republic of Moldova, Tel: (0373-22)7297;

<sup>c</sup>Lafayette College, Easton, PA, USA

\*Corresponding author: E-mail: natalia\_secara@yahoo.com

**Abstract.** This review presents the basic concepts of the methods used for investigation of fast reactions kinetics, such as: flow methods, with particular emphasis on the stopped-flow approach, NMR, ESR, electrochemical methods, with particular emphasis on the time resolved Fourier Transform electrochemical impedance spectroscopy, flash photolysis, and several others. It offers a brief description of fast reactions commonly encountered in chemical systems, providing an insight into the possibilities of performing kinetic investigations of such reaction systems.

**Keywords:** fast reactions kinetics, spectroscopy, relaxation, flow methods.

## Introduction

The outstanding interest in investigating rapid reactions that burst out in the last decades of the last century is nowadays greatly supported by the development of new approaches and methodologies. Modern methods, formed on the basis of classical ones, allow the discovery of precious information about elementary processes in various systems: chemical, biological, environmental, biochemical, real systems or models.

A wide range of physical methods can be applied in order to perform kinetic investigations of rapid reactions, depending on the specificities of the reacting system. Further we will shortly present some of the basic concepts of physical methods of fast reactions investigation and new directions in the field of rapid reactions study.

## Fundamental aspects of rapid reactions' research

Usually, fast reactions are divided into three categories, depicted in the figure below:

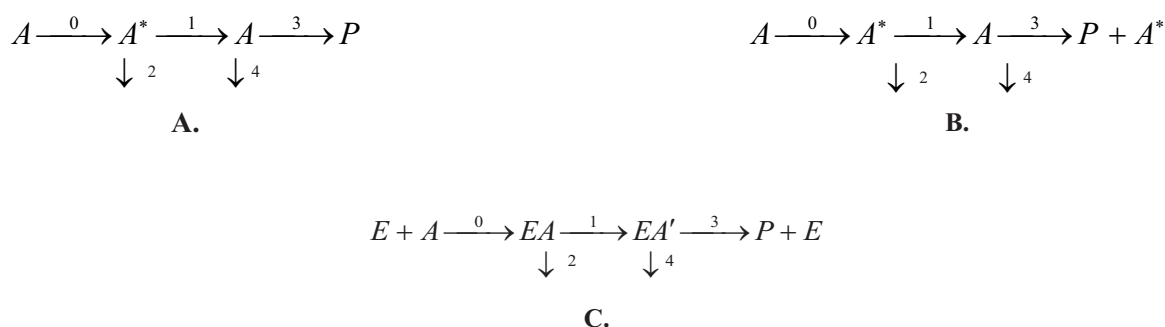
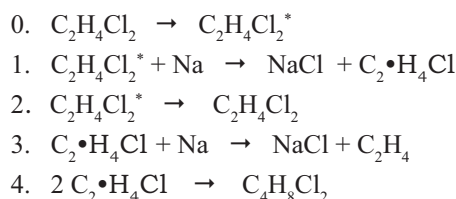


Fig. 1. Multi-stage fast reactions.

**A.** Type I complex reaction – a “simple” multi-stage reaction. **B.** Type II multi-stage reaction – cyclic, chain reaction. **C.** Type III multi-stage reaction – cyclic, catalytic reaction. Where: A\* - active particle; X - intermediate substance; P - reaction product; E – catalyst; (0) – reaction of reactants activation; (1, 3) – reactions that involve an active particle, intermediate substance on the formation of P; (2, 4) – reactions of A\*, X, not yielding P.

An example of type I complex reaction is the following transformation:  $2\text{Na} + \text{C}_2\text{H}_4\text{Cl}_2 \rightarrow 2\text{NaCl} + \text{C}_2\text{H}_4$ , which involves one-stage reactions steps:



The reaction rate can be expressed as follows:  $w = d[C_2H_4] / dt = w_0 - w_2 - 2w_4$ .

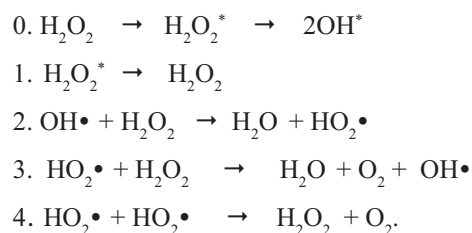
A wide variety of consecutive and consecutive-parallel reactions as such are known. For instance, photochemical reactions are a significant group of reaction that can be related to this mechanism. No more than one particle of reaction product is formed per one adsorbed light quantum during these reactions.

Cyclic reactions proceed according to type II and type III mechanisms. A particular feature of such reactions is the formation of a particle in addition to the products. This particle then participates in one of the reactions that lead to the formation of the product. There are two types of cyclic transformations: chain and catalytic. It is important that reaction rates of chain transformations are higher than the rate of active particles formation:

$$w = dP/dt = w_0 v,$$

where  $v$  is the chain length, shows how many particles of P product are formed per active particle which are formed during the activation stage (0). Reactions are known with  $v \approx 10^5$ , but usually  $v \approx 10 - 10^3$ .

The photolysis of  $H_2O_2$  in aqueous solutions is one of the many examples of chain transformations:



For the wide majority of the studied chain processes, the active particles are atoms and free radicals, and the processes are called radical-chain. The lifetime of active particles such as  $OH\cdot$ ,  $CH_3\cdot$ , etc. is short due to their high reactivity, and low concentrations, compared to the typical reaction time and reagents' concentrations. The non-stationary period, where the concentrations of active particles increase from zero to stationary values, is usually around milliseconds. The method of quasi-stationary concentrations can be applied for most reactions, with regard to active particles.

The second type of cyclic reactions is represented by catalytic reactions, when the activation of the reagent proceeds not as a result of thermal, photochemical or other influence, but as a result of its interaction with the introduced substance-catalyst [1]. Due to the fact that the cycle is closed on the link preceding the activation stage, the rate of a catalytic reaction cannot be higher than the activation rate of the interaction between A and E.

Catalytic reactions are similar to chain reactions, considering their cyclic mechanism, and are similar to "simple" fast-reactions of type I for the reaction rate does not exceed the rate of the reagents activation on their interaction with the catalyst.

The limiting stage for catalytic cycle reactions is the share of the catalyst present in the (EA)' complex; the initial activation of the reagent – EA complex formation – is seldom a limiting stage, in contrast to radical-chain reactions, where the rate of the process depends on the initial formation of atoms or radicals from the reagent molecules.

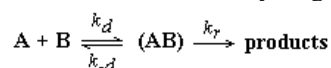
Taking into account that the most important fast reactions with relevance to chemical and biological systems take place in liquid media, there are three general factors that are to be considered in case of investigating the reaction rates in solution [2,3]:

- The rate at which initially separated reactant molecules come together and become neighbours, i.e. the *rate of encounters*.
- The time that two reactants spend as neighbours before moving away from each other, i.e. the *duration of an encounter*. During this time, the reactants may collide with each other hundreds of times.
- The requirement of energy and orientation which two neighbouring reactant molecules must satisfy in order to react.

Any one of these three factors may dominate in governing the reaction rate.

Many chemical reactions occur as soon as the reactant molecules come together and thus, for these fast reactions, the activation energy and orientation requirements are negligible. The reaction rate is limited only by the first factor (i.e., the rate at which encounters occur), which makes it diffusion-controlled.

A simple mechanism for these diffusion controlled reactions may be given by the following kinetic scheme:



where  $k_d$  is the rate constant for diffusion of A and B towards each other,  $k_{-d}$  is the rate constant for diffusion of A and B away from each other, and  $k_c$  is the rate constant for the conversion of the complex (AB) to product R (i.e., the rate constant with out diffusive effects).

Using the Steady-State Approximation on (AB):

$$\frac{d[(AB)]}{dt} = 0 = k_d[A][B] - k_{-d}[(AB)] - k_c[(AB)] \Rightarrow [(AB)](k_{-d} + k_c) = k_d[A][B]; [(AB)] = \frac{k_d[A][B]}{k_{-d} + k_c}$$

Thus, the reaction velocity is given by the equation:  $r = k_r[(AB)] = \frac{k_r k_d[A][B]}{k_{-d} + k_r}$

Thus, the rate constant of the bimolecular reaction  $A + B \xrightarrow{k_2} \text{products}$ , is given by:  $k_2 = \frac{r}{[A][B]} = \frac{k_r k_d}{k_{-d} + k_r}$

In this case, two limiting cases should be considered:

(i) *diffusion-controlled reaction*:  $k_r \gg k_{-d}$ , separation of A and B is relatively difficult, e.g., the solvent has a large viscosity  $\eta$ , or the reaction has a small activation energy, so the rate-determining step is the diffusive approach of the reactants; once they are in the solvent reaction cage, reaction is assured,  $k_2 = k_d$  (where for aqueous solutions at room temperature,  $k_d \approx 10^9 - 10^{10} \text{ M}^{-1}\text{s}^{-1}$ , and a value of  $k_d > 10^9 \text{ M}^{-1}\text{s}^{-1}$  usually indicates that the aqueous solution reaction is diffusion controlled).

(ii) *activation-controlled reaction*:  $k_r \ll k_{-d}$ , reactions with large activation energies,  $E_a \geq 20 \text{ kJ mol}^{-1}$  for reactions in water  $k_2 = k_r \frac{k_d}{k_{-d}}$

where the second factor is the equilibrium constant  $K_{AB}$  for the formation of the encounter pair; thus  $k_2 = k_r K_{AB}$ , and the reaction rate is determined by the equilibrium concentration of encounter pairs and the rate of passage over the activation energy barrier.

One way to assess the validity of the assumption of fast chemistry is to estimate the Damkohler number [3], an important dimensionless parameter that quantifies whether a process is kinetically or diffusion controlled. Damkohler number is defined as  $Da \equiv \tau_{\text{mix}} / \tau_{\text{react}}$ . Here,  $\tau_{\text{mix}}$  is a characteristic mixing time for the system, while  $\tau_{\text{react}}$  is a characteristic time for the chemical reaction. If the Damkohler number has a value much larger than unity, the process is diffusionally controlled, while a value much lower than unity indicates a kinetically controlled process.

Another factor which affects the rate of reactions in solution involves the effects of solvent molecules on the motions of reactant molecules.

Once two reactant molecules diffuse together, their first collision may not satisfy the energy and orientation requirements for reaction. The surrounding solvent molecules create a "solvent cage" which inhibits the separation of the reactant molecules.

This solvent "cage effect" provides the opportunity for the molecules to undergo many more collisions before finally either reacting or diffusing away from each other.

The duration of such an encounter may be  $10^{-10} \text{ s}$ , during which the reactant molecules may collide hundreds of times. The cage effect tends to increase the reaction rate by increasing the opportunity for reactant molecules to find the required energy and/or orientation to react during the caged encounter.

However, there are a large number of reactions that are initiated by the formation of a reactive species in the investigated solution, rather than by mixing the reagents. In the case of such chemical reactions it has to be taken into consideration that the duration of the initiation process has to be a lot shorter than the reaction time and it has to be performed by techniques that would not alter the solution's homogeneity.

The main physical methods that are currently used in the investigation of rapid reactions are reviewed below.

## Basic concepts of the methods that are used to study fast reactions

### Flow-based Methods

Flow analysis comprises all analytical methods that are based on the introduction and processing of test samples in flowing media. A primary classification can be based on two aspects [4]:

- the way the test portion is introduced, *i. e.* continuously or intermittently/discretely,
- the basic character of the flowing media, *i. e.* either segmented, unsegmented or monosegmented where segmentation is primarily considered as being applied for the purpose of preventing intermixing of successive analyte zones.

However, among all the flow methods used for the study of fast reactions the most popular seems to be the stopped-flow method. Due to the short analysis time and feasibility, flow based systems have become one of the most powerful analytical tools used for studying fast reactions. This can also be explained by the possibility of employing most various detection systems.

The apparatus [5] is made of 2 reservoir syringes that are loaded with the desired species. A pneumatic syringe push

will drive the reactant species to the mixing tube or jet. The syringe drive could be positioned either horizontally or vertically. The mixed solutions then pass to the measuring cell or the observation chamber where the data is collected. If the reaction involves three reactants, a modification to have 3 drive syringes and two mixing tubes is required (KinTek Corporation, 2007). The optical path can be either along this tube or perpendicular to it. Finally, the reaction mixture fills the stopping syringe which triggers the start of data acquisition. The lifetime of the reactions that can be analyzed using the stopped-flow apparatus is limited by the time it takes the solution to fill in the measuring cell, also known as the "dead time".

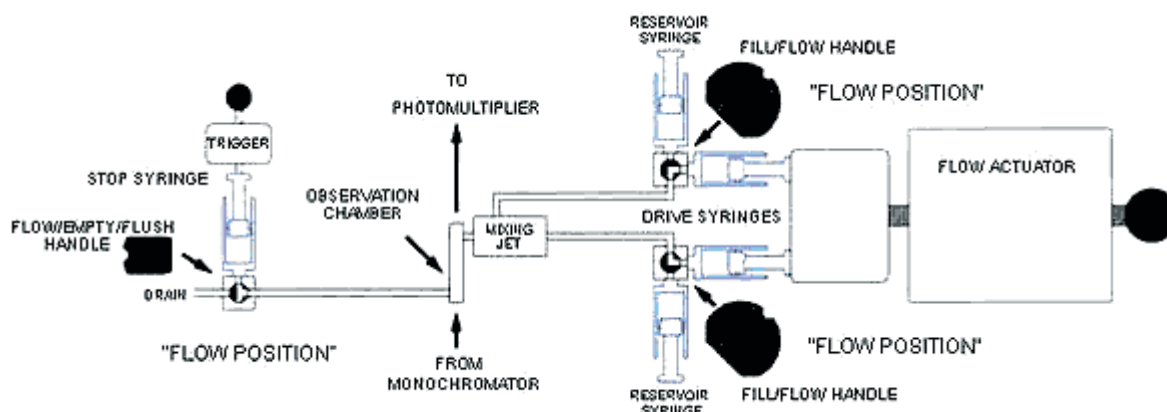


Fig. 2. Diagram of a stopped-flow apparatus

There are three main ways to compute the kinetic parameters via the stopped-flow: steady-state approach, taking the concentration gradient into account, and standard second order treatment assuming the conditions mentioned earlier. Dunn and Rorabacher [6] determined that all three are reliable in the analysis of second order reactions. The standard treatment can be used when the rate constant is on the order of  $(1-4) \times 10^6 \text{ M}^{-1} \text{ s}^{-1}$ . However, if the second order reaction half-life is less than the dead time, then the steady state approach should be used to check the viability of results. In the case when the values of the rate constant obtained by the standard approach and that obtained when considering the concentration gradient are significantly different, the steady state should be considered as the better approach to determining the parameter. In order to assess the validity of this result, different initial concentrations of the reactants can be used via an iterative approach until a consistency in the rate constant is obtained [6].

The stopped-flow method has been extensively applied in scientific investigations, such as: studying the dimer-tetramer equilibria of oxyhemoglobins and the kinetics of association of unligated dimers [7], determination of nitrite in natural and drinking-water [8], fluorimetric determination of uric acid in serum and urine samples [9], study of the mechanism of bacteriophage T7 RNA polymerase binding to its promoter DNA [10], spectroscopic detection and kinetic analysis of aromatic amine cation radicals [11], activation of  $\alpha$ -chymotrypsin [12], complex formation processes [13,14], redox catalytic processes [15,16], and many others.

Stopped-flow mixing coupled with time-resolved Fourier transform infrared (FT-IR) spectroscopy represents a new experimental approach to explore protein folding events, with one specific advantage - the ability to monitor directly the kinetics of processes involving  $\beta$ -sheet structures [17], which is exceptionally difficult to do with other techniques. The *temperature-jump/stopped-flow* method combined with the application of structure specific fluorescence signals provides novel opportunities to study the stability of certain regions of enzymes and identify the unfolding-initiating regions of proteins.

### NMR methods

NMR methods have a significant advantage over other methods used for the investigation of fast processes that are not accompanied by veritable chemical reactions.

The NMR methods are largely used for investigation of equilibrated chemical transformations and of exchange processes, which are accompanied by periodic structure modifications, i.e. modifications of nuclei electronic surroundings and nuclei spin-spin interactions. These processes refer to intramolecular transformations (tautomerism [18], racemization [19], delayed internal rotation, cycle inversion [20]), as well as to intermolecular exchange chemical reactions and other equilibrated reactions (protons exchange in aqueous solutions of carbonic acids, ammonia, ligand exchange [21], ions recombination, biochemical enzyme-substrate interactions).

### ESR methods

It is almost impossible to observe the reactive free radicals using direct methods, due to their low stationary

concentration. Such methods as photometry, UV-, IR- spectroscopy, radiospectroscopy, allow the registration of the less reactive, rather stable radicals of secondary origin [22]. The electronic spin resonance technique is extremely used in the investigation of mechanisms and kinetic laws of chemical reactions unfolding. This is mainly due to the role played by paramagnetic particles in chemical processes, and by the high sensitivity of the method, as well.

The utilization of ESR coupled with flow methods is very widespread: the reaction mixture is moved rapidly through the cell in the resonator, making possible to maintain concentrations of unstable radical species, high enough and for a time long enough to allow spectra registration. This offers the possibility to monitor intermediate compounds formed during the reaction, as well as the determination of rate constants of individual elementary stages of the process.

### **IR spectroscopy**

In general, IR spectroscopy is difficult to implement in fast reactions researches [23], but good results can be obtained when using this method in addition to the others (temperature-jump technique, stopped-flow method etc.).

A widespread technique largely applied in the study of rapid reactions is the *IR spectroscopy coupled with Fourier-transform* (FTIR), which is an interferometric method, as opposed to classic spectrometry where the spectral absorption is scanned. FTIR spectrometers have high sensitivity, but the time-resolved performance is limited by the scan rate, unless step-scan or stroboscopic methods are used for the study of events that can be repetitively photoactivated [24].

Time-resolved infrared absorption spectroscopy is widely used to probe the kinetics of short-lived (down to  $\sim 1$  ms) coordinatively unsaturated organometallic species, thus allowing scientists to deepen their understanding of organometallic reaction mechanisms. IR spectroscopy has the twin advantages that many organometallic complexes have strong absorptions in the infrared, making detection relatively straightforward, and that the IR spectrum of an organometallic complex frequently reveals information about its electronic structure. Also, time-resolved FT-IR difference spectroscopy in combination with molecular biological methods allows a detailed analysis of the molecular reaction mechanism of proteins from the nanosecond time range up to several minutes [25].

### **UV-VIS spectroscopy**

UV-visible spectroscopic methods are well suited for timeresolved measurements, and these can be made in the subpicosecond range if lasers are used. They suffer from the disadvantage that little structural information is provided [26], although in favourable cases, such as in studies of bacteriorhodopsin, where the intermediates of the photocycle show distinct and accurately interpretable spectral characteristics, these methods have proved very valuable [27]. Among the UV-VIS spectrometric methods, photolorimetry is currently very popular, especially due to its very sensitive detection limit ( $10^{-5} - 10^{-6}$  M) and a relative error value of 1 – 2% for the majority of experiments. Thus, the possibilities of electronic spectra application emerge from their tight correlation with the molecular structure and the character of the interaction of these molecules with the surroundings.

### **Flash photolysis**

This technique is commonly used for studying fast photochemical reactions. Generally, the pulse width of the light source must be much shorter than the half-time of the chemical reaction. Thus, depending on the rate of the process under investigation, several lamps are available. In the case of moderate rates of reactions (microsecond time scale) flash lamps can be used; a typical flash lamp is the xenon lamp in a standard camera. For very fast reactions, however, the slow decay time of the light emission from a flash lamp covers the progress of the reaction. For faster reactions, specially designed lasers must be used that have pulse widths in the nanosecond range. Using ultra-fast pulsed lasers allows processes in the sub-femtosecond time scale to be studied.

**Pulse radiolysis** is a radiochemical analogy of the flash photolysis technique, where the sample is excited by a short pulse ( $10^{-9}$ – $10^{-6}$  s) of ionizing radiation (usually high energy electrons). Instruments used in pulsed radiolysis can be classified according to their characteristic time, which can be micro-, nano- or picoseconds.

Pulse radiolysis method offers important information on the spectra and reactivities of electrons solvated in polar liquids, reactivities of hydroxyl radicals in aqueous solutions, spectra and kinetic behaviour of free radicals in solutions (organic and inorganic), optic spectra of the singlet states of the anion-radicals of aromatic compounds etc.

### **Relaxation techniques**

In the methods that use *relaxation phenomena*, a system in equilibrium is perturbed by a sudden change of external parameters, such as temperature, pressure or the electric field intensity. The kinetic study of the instauration of the new equilibrium delivers information about the chemical reactions that take place in the system. Due to the fact that relaxation methods don't require rapid mixing of reagents, the characteristic time is determined only by the rate at which the equilibrium is perturbed. This allows performing kinetic investigations of reactions that take place in seconds

to  $10^{-10}$ s. Besides the large time interval, relaxation methods facilitate the analysis of complex reaction systems [28]. As the variations of external parameters are always quite small, the equations that describe the kinetic behaviour of the system can be easily linearized. The process of relaxation of the system to the new equilibrium is described by a set of relaxation times, related to the mechanism of the reaction.

Methods of equilibrium perturbation, used for the estimation of relaxation times comprise:

– methods of discrete perturbation: temperature-jump technique, pressure-jump technique and electric field jump technique. The methods used for monitoring and registration of concentration variations have to possess high specificity and sensibility (spectrophotometry, fluorimetry, polarimetry, conductometry).

– methods of periodic perturbation: sound wave absorption technique, dielectric losses technique. In these methods, the chemical relaxation processes lead to a phase shift between the external parameters variations and parameters that describe the relaxing system. The amplitude of this shift, or the energy dissipation that accompanies it, are determined by the reaction mechanism.

### **Electrochemical methods**

Major electroanalytical techniques that can be successfully applied if the investigated compound possesses a certain electroactivity, are *conductometry*, *voltammetry* (including polarography, triangular wave voltammetry, AC voltammetry, differential pulse voltammetry, and pulse voltammetry), *potentiometry* and *amperometry*. The choice depends on the species under investigation.

A powerful tool for investigating electrochemical reactions is the electrochemical impedance spectroscopy. Still, its application is generally limited to certain experimental systems where the applied D.C. voltage must be kept fixed during the time (at least several minutes in most cases) when an impedance spectrum is recorded, and this makes it quite difficult to study transient systems. Apart from this limitation, it is also difficult in traditional EIS to distinguish between adsorption and desorption (or anodic and cathodic) processes. The *time resolved* technique of FT-EIS expands the capabilities of EIS beyond these constraints [29]. FT-EIS can provide detailed kinetic information about surface reactions at solid-liquid interfaces and thus, can considerably help to understand the mechanisms of multi-step reactions in multi-component solutions [30]. FT-EIS is particularly useful for studying kinetically controlled time dependent electrochemical systems. These include: oxidation of organic molecules (for fuel cell studies), electrocatalysis, double layer characterization, electrodeposition studies, characterization of bio-electrochemical reactions, metal dissolution reactions (relevant for chemical mechanical and electrochemical mechanical planarization), electrochemistry of ionic liquids, real time monitoring of corrosion reactions.

There is a wide variety of methods available for those who deal with fast reactions kinetics, and new possibilities arise every day for the study of chemical and biochemical processes that have been a mystery until not so long ago.

### **New directions and approaches in the investigation of fast reactions: DNA related reactions**

Oxygen is essential for life. However, active forms of oxygen such as hydroxyl and superoxide radicals, hydrogen peroxide and singlet oxygen arise as by-products and intermediates of aerobic metabolism and during oxidative stress [31]. Directly or indirectly, these chemical species of oxygen, as well as reactive species of nitrogen, can transiently or permanently damage nucleic acids, lipids, and proteins [32].

Aerobic organisms are normally protected by a defence system against oxidative damage, which comprises various compounds with different functions, including enzymes (e.g. catalase, glutathione peroxidase, glutathione transferase, superoxide dismutase) and the sequestration of metals (e.g. iron, copper) by chelating agents. In addition, there are several hydrophilic and lipophilic compounds, such as vitamin C and vitamin E, which can act by scavenging or suppressing the generation of free radicals. These are the reasons for the impressive number of papers that deal with the investigation of fast reaction related to the factors that decrease the defence against reactive damaging species.

A number of investigations have revealed that vitamin C and E levels are decreased by exposure to ethanol. Recent research has suggested that ethanol may exert its cell toxicity via DNA damage, possibly via the generation of ROS arising from microsomal NADPH-dependent electron transfer and the oxidation of the ethanol metabolite, acetaldehyde [33]. There was a significant increase in the number of *in vivo* single-strand breaks in the DNA of rat brain cells after an acute dose of ethanol [34]; ethanol combined with acetaldehyde induced cleavage of DNA in rat hepatocytes [35] and ethanol-induced DNA fragmentation and cell death was also observed in mouse thymocytes [36]. Ethanol alone, however, did not induce *in vitro* DNA strand breaks in human lymphocytes, whereas acetaldehyde induced both single- and double-strand breaks (30), indicating that ethanol may induce DNA strand breaks via its primary metabolite. The spin trapping technique has been used to demonstrate the increased generation of 1-hydroxyethyl radical both *in vitro* and *in vivo* [37]. P.Navasumrit and co-workers have used these procedures to follow the effects of acute and chronic doses of ethanol on the generation of free radicals and we have further attempted to correlate free radical generation with the evolution of DNA strand breaks using single electrophoresis. Results of these studies indicate that ethanol-induced DNA damage is mediated by free radicals and that both can be significantly inhibited by prior treatment with antioxidants.

Cellular DNA is subjected to the action of reactive oxygen species during the entire lifecycle of the cell.

The most common purine base redox lesions *in vivo* are 8-oxoguanine (8-oxoG), 8-oxoadenine, 4,5-diamino-5-formamidopyrimidine (FapyAde) (derived from adenine) and 2,6-diamino-4-hydroxy-5-formamidopyrimidine (FapyGua) (derived from guanine) [38].

A large number of scientific work [39,40,41] is related to the investigation of the process of incorporation of inappropriate nucleotides by DNA polymerases opposite these lesions, which results in a considerable mutagenicity. However, there are enzymatic systems that counteract this damage.

For example, it is known that human 8-oxoguanine-DNA glycosylase (hOgg1) excises 8-oxo-7,8-dihydroguanine from damaged DNA. Recently, Kuznetsov et al. [42] have performed a kinetic analysis of hOgg1 mechanism using stopped-flow and enzyme fluorescence monitoring, and proposed a kinetic scheme for hOgg1 processing an 8-oxoG:C-containing substrate. The authors report that the mechanism consists of at least three fast equilibrium steps followed by two slow, irreversible steps and another equilibrium step. The second irreversible step was rate-limiting overall. By comparing data from Ogg1 intrinsic fluorescence traces and from accumulation of products of different types, the irreversible steps were attributed to two main chemical steps of the Ogg1-catalyzed reaction: cleavage of the N-glycosidic bond of the damaged nucleotide and  $\beta$ -elimination of its 3'-phosphate. The fast equilibrium steps were attributed to enzyme conformational changes during the recognition of 8-oxoG, and the final equilibrium, to binding of the reaction product by the enzyme.

Analogically, uracil DNA glycosylase (UNG) is responsible for the removal of uracil from DNA by hydrolysis of the N-glycosidic bond that links the base to the deoxyribose backbone [43]. Despite the significant number of scientific papers discussing the possible mechanisms employed at the protein/DNA interface, there are considerable differences in interpretation and there remains a lack of information regarding the dynamics of interactions at the protein-DNA interface, which are the key to understanding the biophysical basis of base flipping. Bellamy et al. [44] have performed a rapid kinetic analysis with DNA substrates of different sequence in order to examine the dynamics of the protein-DNA interface in base flipping by UNG. The stopped-flow analysis (fluorescence and anisotropy) was used to obtain an insight into the binding of substrate and the formation of the activated complex, and quench-flow analysis allowed the investigation of the chemical cleavage step.

Lately, ESR methods have gained a huge popularity in the investigation of radicals formed during the oxidation of DNA, which has implications in mutations, strand breaks and cell death [45, 46]. The interactions among radical species largely depend on both the amount and location of radicals generated. Therefore, the detection and simultaneous mapping of individual radical species generated *in vivo* are both essential for understanding the function of radical formation *in vivo* [47].

Thus, *in vivo* ESR spectroscopy allows studying and understanding the redox reactions in physiological phenomena [48,49] and in oxidative injuries, such as hypoxia-hyperoxia [50], iron overload [51], and selenium deficiency [52]. The combination of *in vivo* ESR spectroscopy with an imaging technique allows 2D or 3D imaging of radicals in living organisms [53]. However, biological systems are very complex and multiple radical species coexist within an organ; therefore, it is critical that the individual radical species be visualized separately. Ken-ichiro Matsumoto and Hideo Utsumi have developed a method of separable ESR-CT (electron spin resonance-computed tomography) imaging for multiple radical species, and applied it to imaging of  $\cdot\text{OH}$  and  $\cdot\text{NO}$ . The algorithm was improved by combining filtered back-projection with a modified algebraic reconstruction technique to enhance accuracy and shorten calculation time. This ESR-CT technique was combined with L-band ESR spectroscopy and applied to the separate imaging of  $\cdot\text{OH}$  and  $\cdot\text{NO}$ , which were spin trapped with 5,5-dimethyl-1-pyrroline-N-oxide (DMPO) and  $\text{Fe}^{2+}$ -N-methyl-D-glucamine dithiocarbamate complex, respectively. The present results strongly suggest that this technique would be further applicable to *in vivo* investigation of other free radical reactions. This separable ESR-CT imaging technique might become one of the most powerful diagnosis techniques [53].

## Closing notes

In this review, it has been shown that various techniques exist that can be applied for studying fast chemical reactions, which can be correlated to the specificity of the reaction under investigation. Whether the reaction is equilibrated or irreversible, whether the species investigated are unstable radicals, or possesses electroactivity, or display luminescence, there is always a possibility to perform scientific investigations by coupling several physical methods.

This article offers a brief review of physical methods commonly used to study rapid reactions. The truly vertiginous development of various techniques (mostly hyphenated methods) for investigating fast reactions has enabled scientists to reveal complex laws of many chemical reactions, and this progress is so unequivocal that it seems only to be limited by scientists' creativity and ingenuity.

## References

- [1] Sychev A., Duca, Gh. Fundamental and Applied Aspects of Homogeneous Catalysis with Metal Complexes. Chisinau, Moldova State University Publ., 2002.
- [2] Isac V., Onu A., Tudoreanu C., Nemtoi G., Physical chemistry, Chisinau, Stiinta Publ., 1995, Robert J. Kee, Chemically reacting flow. Theory and practice, New Jersey: John Wiley & Sons, 2003.
- [3] Robert J. Kee, Chemically reacting flow. Theory and practice, New Jersey: John Wiley & Sons, 2003.
- [4] Pure & Appl. Chem., Vol.66, No 12, 1994, pp. 2493-2500.
- [5] "U.S.A. Stopped-Flow: Block Diagrams". Retrieved from <http://olisweb.com>.
- [6] Dunn B. C, Meagher N. E., Rorabacher D. (1996) J. Phys. Chem., 100, 16925-16933.
- [7] Berjis M, Sharma VS, Double mixing stopped-flow method for the study of equilibria and kinetics of dimer-tetramer association of hemoglobins: studies on Hb Carp, Hb A, and Hb Rothschild, Anal Biochem. 1991 Aug 1;196(2):223-8.
- [8] Rui-Yong WANG, Xiang GAO and Ying-Tang LU, Anal. Sci., Vol. 22, 2006, p.299.
- [9] D. Perez-Bendito, A. Gomez-Hens, M.C. Gutierrez and S. Anton, Nonenzymatic stopped-flow fluorimetric method for direct determination of uric acid in serum and urine, Clinical Chemistry 35: 1989, p. 230-233.
- [10] Yiping Jia, Amarendra Kumar and Smita S. Patel, Equilibrium and Stopped-flow Kinetic Studies of Interaction between T7 RNA Polymerase and Its Promoters Measured by Protein and 2-Aminopurine Fluorescence Changes, J. Biol. Chem., vol.271, No. 48, 1996, pp. 30451-30458.
- [11] Oyama Munetaka, Spectroscopic Detection and Kinetic Analysis of Aromatic Amine Cation Radicals Using an Electron Transfer Stopped-Flow Method, Erekutoro Oganikku Kemisutori Toronkai Koen Yoshishu, V.25, 2001, pp.71-72.
- [12] Gert Verheyden, Janka Matrai, Guido Volckaert and Yves Engelborghs, A fluorescence stopped-flow kinetic study of the conformational activation of  $\alpha$ -chymotrypsin and several mutants, Protein Science, 2004, vol 13, p. 2533-2540.
- [13] Duca, Gh., Scutaru, Yu., Sychev A. Kinetics of Interaction of Iodine with Dihydroxyfumaric Acid, J. of Physical Chem., vol.61, 1987, no 8, p.2266-2268.
- [14] Duca, Gh., Travin, S., Purmali, A. Catalytic Condensation of Epycatechol in the Presence of Iron Ion, J. of Physical Chem., 1989, vol.63, no 12, p.3214-3220.
- [15] Duca, Gh., Scurlatov, Yu., Sychev, A. Redox Catalysis and Ecological Chemistry. – Chisinau, Moldova: CEUSM, 2002, p. 316.
- [16] Sychev A., Duca Gh., Scurlatov Yu., Travin S, The investigation of the process of DFH<sub>4</sub> oxidation by the stopped-flow method, Phys. and mathem. methods in coord. chem. Abstracts of the 7<sup>th</sup> congress, Chisinau, 1980, p. 32-33.
- [17] Heinz Fabian and Dieter Naumann, Methods to study protein folding by stopped-flow FT-IR, Methods, 2004, Vol. 34, issue 1, p. 28-40.
- [18] Dieckmann H., Kreuzig R., Bahadir M., Significance of keto-enol-tautomerism in the analysis of 1,2,4-triazinone metabolites, Fresenius' j. anal. chem., vol. 348, n°11, pp. 749-753, 1994.
- [19] Philip J. Bailey et al., Barriers to Racemization in C<sub>3</sub>-Symmetric Complexes Containing the Hydrotris(2-mercapto-1-ethylimidazolyl)borate (Tm<sup>Et</sup>) Ligand, Inorg. Chem., 44 (24), 8884 -8898, 2005.
- [20] Georgii E. Salnikov, Alexander M. Genaev and Victor I. Mamatyuk, Unusually strong temperature dependence of <sup>13</sup>C chemical shifts and degenerate conformational exchange in cyclobutenyl carbocations, Mendeleev Commun., 2003, 13, 48 – 49.
- [21] von Ahsen B, Bach C, Balzer G, Bley B, Bodenbinder M, Hägele G, Willner H, Aubke F., Dynamic <sup>13</sup>C NMR studies of ligand exchange in linear (d10) silver(I) and gold(I) and square-planar (d8) rhodium(I) homoleptic metal carbonyl cations in superacidic media, Magn Reson Chem. 2005 Jul;43(7):520-7.
- [22] Gh. Duca, Free radicals in natural water, in Free radicals in biology and Environment, edited by F. Minisci, Vol.27, p. 475.
- [23] Andrew J. White, Kevin Drabble and Christopher W. Wharton, A stopped-flow apparatus for infrared spectroscopy of aqueous solutions, Biochem. J., 1995, vol. 306, p. 843-849.
- [24] Gerwert, K. (1993) Curr. Opin. Struct. Biol. 3, 769-773.
- [25] Klaus Gerwert, Molecular Reaction Mechanisms of Proteins Monitored by Time-resolved FT-IR Difference Spectroscopy, John Wiley & Sons Ltd, Chichester, 2002.
- [26] Andrew J. White, Kevin Drabble and Christopher W. Wharton, A stopped-flow apparatus for infrared spectroscopy of aqueous solutions, Biochem. J., 1995, vol. 306, p. 843-849.
- [27] Doig, S. J., Reid, P. J. and Mathies, R. A. (1991) J. Phys. Chem. 95, 6372-6379.
- [28] G. Hammes, Investigation of rates and mechanisms of reactions, "Mir", Moscow, 1977.
- [29] J. E. Garland, C. M. Pettit and D. Roy, Analysis of experimental constraints and variables for time resolved detection of Fourier transform electrochemical impedance spectra, Electrochimica Acta 49 (2004) 2623-2635.

- [30] J.E. Garland, K. A. Assiongbon, C.M. Pettit, S.B. Emery and D. Roy, "Kinetic analysis of Electrosorption using Fast Fourier Transform Electrochemical Impedance spectroscopy: Underpotential Deposition of  $\text{Bi}^{3+}$  In The Presence of Coadsorbing  $\text{ClO}_4^-$  on Gold", *Electrochimica Acta* 47 (2002) 4113-4124.
- [31] Halliwell, B. & Gutteridge, J.M.C. (1999) *Free Radical in Biology and Medicine*. Oxford Science Publications, New York, NY.
- [32] Henry J. Thompson, DNA Oxidation Products, Antioxidant Status, and Cancer Prevention, *J. Nutr.* 134: 3186S-3187S, 2004.
- [33] Fridovich, I. (1989) Oxygen radicals from acetaldehyde. *Free Radic. Biol. Med.*, 7, 557-558.
- [34] Singh, N.P., Lai, H. and Khan, A. (1995) Ethanol-induced single strand DNA breaks in rat brain cells. *Mutat. Res.*, 345, 191-196.
- [35] Rajasingh, H., Jayatilleke, E. and Shaw, S. (1990) DNA cleavage during ethanol metabolism: role of superoxide radicals and catalytic iron. *Life Sci.*, 47, 807-814.
- [36] Ewald, S.J. and Shao, H. (1993) Ethanol increases apoptotic cell death of thymocytes in vitro. *Alcohol. Clin. Exp. Res.*, 17, 359-365.
- [37] Moore, D.R., Reinke, L.A. and McCay, P.B. (1995) Metabolism of ethanol to 1-hydroxyethyl radicals in vivo: detection with intravenous administration of  $\mu$ -(4-pyridyl-1-oxide)-N-t-butyl nitron. *Mol. Pharmacol.*, 47, 1224-1230.
- [38] Gajewski, E., Rao, G., Nackerdien, Z., Dizdaroglu, M. (1990) Modification of DNA bases in mammalian chromatin by radiation-generated free radicals *Biochemistry*, 29, 7876-7882.
- [39] Shibutani, S., Bodepudi, V., Johnson, F., Grollman, A.P. (1993) Translesional synthesis on DNA templates containing 8-oxo-7, 8-dihydrodeoxyadenosine *Biochemistry*, 32, 4615-4621.
- [40] Wiederholt, C.J. and Greenberg, M.M. (2002) Fapy dG instructs Klenow exo(-) to misincorporate deoxyadenosine *J. Am. Chem. Soc.*, 124, 7278-7279.
- [41] Delaney, M.O., Wiederholt, C.J., Greenberg, M.M. (2002) Fapy•dA induces nucleotide misincorporation translesionally by a DNA polymerase *Angew. Chem. Int. Ed. Engl.*, 41, 771-773.
- [42] Nikita A. Kuznetsov, Vladimir V. Koval, Dmitry O. Zharkov, Georgy A. Nevinsky, Kenneth T. Douglas, and Olga S. Fedorova, Kinetics of substrate recognition and cleavage by human 8-oxoguanine-DNA glycosylase, *Nucleic Acids Res.*, Jul 2005; 33: 3919 - 3931.
- [43] Lindahl, T. (1974) An N-glycosidase from *Escherichia coli* that releases free uracil from DNA containing deaminated cytosine residues *Proc. Natl. Acad. Sci. U.S.A.*, 71, 3649-3653.
- [44] Stuart R.W. Bellamy, Kuakarun Krusong, and Geoff S. Baldwin, A rapid reaction analysis of uracil DNA glycosylase indicates an active mechanism of base flipping, *Nucleic Acids Res.*, March 2007; 35: 1478 - 1487.
- [45] Sandau, K., J. Pfeilschifter, and B. Brune. 1997. The balance between nitric oxide and superoxide determines apoptotic and necrotic death of rat mesangial cells. *J. Immunol.* 158:4938-4946.
- [46] Yoshie, Y., and H. Ohshima. 1997. Nitric oxide synergistically enhances DNA strand breakage induced by polyhydroxyaromatic compounds, but inhibits that induced by the Fenton reaction. *Arch. Biochem. Biophys.* 342:13-21.
- [47] Ken-ichiro Matsumoto and Hideo Utsumi, Development of Separable Electron Spin Resonance-Computed Tomography Imaging for Multiple Radical Species: An Application to  $\cdot\text{OH}$  and  $\cdot\text{NO}$ , *Biophys J*, December 2000, p. 3341-3349, Vol. 79, No. 6.
- [48] Takeshita, K., H. Utsumi, and A. Hamada. 1993. Whole mouse measurement of paramagnetism-loss of nitroxide free radical in lung with an L-band ESR spectrometer. *Biochem. Mol. Biol. Int.* 29:17-24.
- [49] Takeshita, K., A. Hamada, and H. Utsumi. 1999. Mechanisms related to reduction of radical in mouse lung using an L-band ESR spectrometer. *Free Radic. Biol. Med.* 26:951-960.
- [50] Miura, Y., A. Hamada, and H. Utsumi. 1995. In vivo ESR studies of antioxidant activity on free radical reaction in living mice under oxidative stress. *Free Radic. Res.* 22:209-214.
- [51] Phumala, N., T. Ide, and H. Utsumi. 1999. Noninvasive evaluation of in vivo free radical reactions catalyzed by iron using in vivo ESR spectroscopy. *Free Radic. Biol. Med.* 26:1209-1217.
- [52] Matsumoto, K., K. Endo, and H. Utsumi. 2000. In vivo electron spin resonance assessment of decay constant of nitroxyl radical in selenium-deficient rat. *Biol. Pharm. Bull.* 23:641-644.
- [53] Sano, H., M. Naruse, K. Matsumoto, T. Oi, and H. Utsumi. 2000. A new nitroxyl-probe with high retentivity in brain and its application to brain imaging. *Free Radic. Biol. Med.* 28:959-969.

# VARIATION IN ACTIVATION ENERGY AND NANOSCALE CHARACTERISTIC LENGTH AT THE GLASS TRANSITION

Ion Dranca

Chemistry Institute, Moldova Academy of Sciences

3 Academiei Str., Chisinau MD2028, Moldova

drancai@yahoo.com; Tel. 37322 72 54 90 Fax.37322 73 98 54

Current address: Department of Pharmaceutics, University of Minnesota, 55455, USA

**Abstract:** Differential scanning calorimetry has been used to study the  $\alpha$ -relaxation (glass transition) in virgin polystyrene (PS), PS-clay nanocomposite, amorphous indomethacin (IM), maltitol (Mt) and glucose (Gl). Variation of the effective activation energy ( $E$ ) throughout the glass transition has been determined by applying an advanced isoconversional method to DSC data on the glass transition. The relaxations have been characterized by determining the effective activation energies ( $E$ ) and evaluating the sizes of cooperatively rearranging regions at the glass transition ( $V_g$ ). The values of  $V_g$  have been determined from the heat capacity data. The  $\alpha$ -relaxation demonstrates markedly larger values of  $E$  ( $\sim 340$  vs  $\sim 270$  kJ mol $^{-1}$ ) for the PS-clay system than for virgin PS. For IM in the glass transition region, the effective activation energy of relaxation decreases with increasing temperature from 320 to 160 kJ mol $^{-1}$ . In the  $T_g$  region  $E$  decreases (from  $\sim 250$  to  $\sim 150$  kJ mol $^{-1}$  in maltitol and from  $\sim 220$  to  $\sim 170$  kJ mol $^{-1}$  in glucose) with increasing  $T$  as typically found for the  $\alpha$ -relaxation. It has been found that in the sub- $T_g$  region  $E$  decreases with decreasing  $T$  reaching the values  $\sim 60$  (glucose) and  $\sim 70$  (maltitol) kJ mol $^{-1}$  that are comparable to the literature values of the activation energies for the  $\beta$ -relaxation. Heat capacity measurements have allowed for the evaluation of the cooperatively rearranging region in terms of the linear size. The PS-clay system has also been found to have a significantly larger value of  $V_g$ , 36.7 nm $^3$  as compared to 20.9 nm $^3$  for PS. Heat capacity measurements of IM have allowed for the evaluation of the cooperatively rearranging region (CRR) in term of linear size (3.4 nm) and the number of molecules (90). The size of CRR have been determined as 3.1 (maltitol) and 3.3 (glucose) nm.

**Keywords:** activation energy; differential scanning calorimetry (DSC);  $\alpha$ - and  $\beta$ -relaxation; advanced isoconversional method; kinetics (polym. and pharm.).

## Introduction

Differential scanning calorimetry (DSC) is a major tool for measuring the glass transition or, so-called,  $\alpha$ -relaxations in polymer systems [1]. In particular, it has been successfully employed to explore glass transition in various nanostructured polymer systems, including thin films [2,3] and polymers confined to nanopores [4,5]. In DSC, the glass transition shows up as a heat capacity step. An increase in the heating rate  $q$  causes this step to shift to a higher temperature. This effect is used in the popular method by Moynihan et al [6], for evaluating the effective activation energy,  $E$ , from the slope of the  $q$  versus  $T_g^{-1}$  plots.

The glass transition kinetics are commonly treated in the frameworks of the Tool [7]-Narayanaswamy [8]-Moynihan [9] (TNM) model that assumes the activation energy of the process to be constant. As fairly noted [10,11], the assumed Arrhenius temperature dependence disagrees with the typically observed Vogel [12]-Tamman [13]-Fulcher [14] (VTF) and/or Williams-Landel-Ferry [15] (WLF) dependencies. In particular, Kovacs et al. [10], stressed that the applications of the TNM model should be limited "to systems in which viscosity obeys an Arrhenius dependence within and above the glass transition range". According to Angell [16], such systems are termed as strong glass-forming liquids, whereas the systems that obey the VTF/WLF behavior are called fragile liquids. The departure from the Arrhenius behavior is characterized by the dynamic fragility,  $m$ . In general, this parameter is the smallest for inorganic oxide glasses and the largest for polymeric glasses. Needless to say, the VTF/WLF behavior typically observed for polymers gives rise to an effective activation energy that varies with temperature [17]. In our previous communication [18], we proposed to use an isoconversional method to detect the variation in the activation energy throughout the glass transition. The application of the method was demonstrated for two polymers: polystyrene (PS) and poly(ethylene terephthalate) (PET). *Why variation?* Constant activation energy is usually the anticipated outcome of kinetic evaluations. This expectation appears to be supported by theoretical reasoning. The Arrhenius equation, eq (1),

$$k = A \exp(-E / RT) \quad (1)$$

where  $E$  is the activation energy (the heat of activation),  $A$  the preexponential factor,  $T$  the temperature,  $R$  the gas constant, materializes Arrhenius hypothesis [19] that normal (i.e. inactive) molecules are in an endothermic equilibrium with active ones, which take part in the reaction. According to Arrhenius,  $E$  is the heat absorbed in the process of

transformation of inactive molecules into active ones, or, in other words, the heat (or energy) of activation. Owing to its thermodynamic meaning,  $E$  was treated [19,20] as a constant that is independent of the pathway taken by a system from an initial to a final state. Van't Hoff [20] expected only a minor temperature dependence of the activation energy as a result of the temperature dependence of the heat capacity.

Later, collision theory [21, 22] and activated-complex theory [23] introduced the idea of an energy barrier that has to be crossed over for a reaction to occur. From the standpoint of these theories, Arrhenius' activation is a parameter that is directly related to the height of the energy barrier. Unlike the Arrhenius theory, collision theory and activated complex treat the activation energy as a truly kinetic (dynamic) parameter, which is associated with reaction act itself. However, similar to Arrhenius theory, these theories treat the activation energy as an essentially constant parameter of a reaction system [24]. These theoretical considerations led to the formation of the concept of constant activation energy, which seems to be a very reasonable approximation for the gas phase where chemical transformations take place by a series of isolated binary collisions of molecules [25]. The temperature variation of the activation energy has always been a topic of considerable interest among kineticists. Hulett [26] published a short review, which appears to be the first attempt to systematize the effects causing deviations from the Arrhenius law. Although thermal analysis is not really concerned with the kinetics of gas phase reactions, it is worthy of note that even for these reactions the activation energy should show a temperature dependence because of the temperature dependence of the heat capacity of activation [26, 27].

There is a strong but rather unjustified tendency in the thermal analysis community to directly interpret the effective activation energy in terms of a free energy barrier. Also, there are many flawed methods (the Coats-Redfern method definitely being the champion in popularity) that use a single heating rate and directly deliver a single and constant value of the activation energy as well as a preexponential factor for any reactions, no matter how complex it might be [27]. By accepting the concept of variable activation energy as a practical compromise, people abandon the methods that invariably produce a single value of the activation energy and start using multiple run (isothermal and/or nonisothermal) methods that allow for detecting reaction complexity [28-30]. Since this phenomenon is obviously inconsistent with the concept of constant activation energy, it seems reasonable to introduce a concept of variable activation energy. This is not only more practical, but also universal because it permits a constant activation energy as a special case of a variable activation energy [25].

*PS and PS-clay nanocomposites.* Implanting layered silicates into polymers is known [31] to modify dramatically various physical properties including thermal stability and fire resistance [32]. It has been found that compared to virgin PS the clay nanocomposites have a somewhat higher glass transition temperature [33,34] and mechanical modulus, [34, 35] decompose at significantly greater temperatures, [33,36] and demonstrate a substantial decrease in the maximum heat release rate of on combustion [36-38].

It should be stressed that even when clay content is as little as 0.1%, the initial decomposition temperature is increased by 40°C and the heat peak release rate is decreased by about 40% relative to virgin PS [36]. The mechanism of such remarkable effect is not yet well understood. Although the thermal behavior of polymer-clay nanocomposites has been studied extensively, the kinetic aspects of degradation and relaxation remain practically unknown. The importance of reliable kinetic analysis cannot be overestimated as it may provide information on the energy barriers of the process as well as offer mechanistic clues.

*Indomethacin (IM).* Obtaining crystalline pharmaceuticals in an amorphous form in certain cases leads to a significant increase in the bioavailability. A fundamental problem associated with solid amorphous drugs is that they

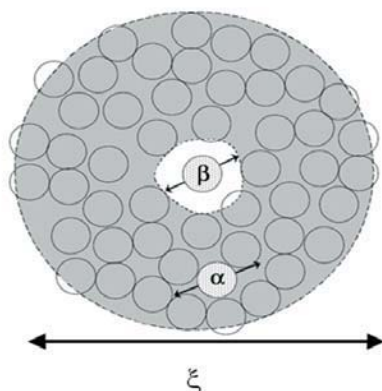


Fig. 1. Schematic presentation of the cooperative  $\alpha$ -process and noncooperative  $\beta$ -process occurring in a cooperatively rearranging region of size  $\xi$ . The open area in the middle represents a mobility island

are inherently unstable because of a strong thermodynamic drive toward crystallization. A great deal of studies has been concerned with evaluating the physical stability of amorphous drugs. Most of these studies have been focused on the dynamics of the glass transition ( $\alpha$ -relaxation), because this is the process that on its heating transforms an amorphous system from a low- to high-mobility state, in which crystallization occurs very quickly. It is known that the molecular mobility associated with the  $\alpha$ -relaxation fades away rapidly as the temperature drops below the glass transition temperature,  $T_g$ . Nevertheless, slow crystallization of indomethacin has been reported by several workers [39, 40] at temperature as low as 20 °C, which is about 25 °C below the respective  $T_g$  value. On the other hand, relaxation in amorphous indomethacin is still detectable as much as 47 °C below  $T_g$  [41]. It seems to be generally thought that at temperature 50 °C below  $T_g$ , the molecular mobility should be too negligible to cause any significant relaxation and, therefore, crystallization. This is certainly true for the  $\alpha$ -relaxation that requires a cooperative motion of multiple molecules and therefore has a huge energy to it. However, local noncooperative motion has a significantly smaller energy barrier and continues to occur at lower temperatures, giving rise to the  $\beta$ -process [46]. Although the  $\beta$ -relaxations (Fig. 1) had been well known for polymers, Johari and Goldstein [42] discovered similar processes in simple inorganic glasses, and suggested these to be universal feature of the glassy state.

*1.3 Glucose (Gl) and Maltitol (Mt).* Sugar and sugar alcohols find a wide application in various pharmaceutical systems as sweeteners and/or binding matrices for drug components. As such they are frequently used in the glassy state, which is thermodynamically unstable and unavoidably tends to relax toward the liquid state [43]. Understanding the dynamics of this process is of a great practical importance for designing physically stable formulations of amorphous drugs.

In this work, we apply DSC to measure the  $\alpha$ -relaxation in a PS-clay system, in virgin PS, in amorphous indomethacin, and also in amorphous glucose and maltitol. The objective of this study is to obtain comparative information on the relaxation dynamics of these systems by estimating the effective activation energies of the relaxation as well as the sizes of cooperatively rearranging regions at the glass transition. This paper is intended to initiate systematic kinetic studies of polymer nanocomposites and pharmaceutical materials, therefore, to fill the presently existing void in the understanding of the thermal behavior of these exciting materials.

## Experimental Section

*A sample of the PS-clay composite* was provided by Dr. Xiaowu Fan (Northwestern University). The composite was prepared by intercalating a monocationic free radical initiator into montmorillonite clay and the subsequent solution surface-initiated polymerization (SIP), where the chain growth was initiated in situ from clay surfaces. The montmorillonite clay was Cloisite® Na<sup>+</sup> (Southern Clay Product Inc.) with the cation exchange capacity 92 mequiv per 100g and the specific surface area 750 m<sup>2</sup>g<sup>-1</sup>. The initiator was an azobisisobutyronitrile (AIBN)-analogue molecule with a quaternized amine group at one end. The intercalation process was realized by cation exchange reaction in which the cationic end of the initiator was ionically attached to the negatively charged clay surfaces. The details regarding the preparation and characterization of the intercalated clay can be found elsewhere [44]. The subsequent SIP was performed in THF solvent with styrene as the monomer, resulting in a PS-clay nanocomposite by the in situ polymerization. Details of the initiator synthesis, the SIP process and product analysis can be found in previous publication, which shows that this free radical SIP strategy can achieve exfoliated PS-clay nanocomposites of high clay loading. According to our previous TGA [45] measurements the resulting composite contains about 1% of clay by weight. The molecular weight (~90,000) and polydispersity (~2.3) of the product were measured by size exclusion chromatography (SEC) using PS standards. The obtained material will be referred to as nPS90. For comparison purposes, we have used radically polymerized PS that was purchased from Alfa Aesar and used as received. Its Mw value is 100,000 (polydispersity is around 2.1) and it will be referred to as PS100.

The  $\alpha$ -relaxation measurements were performed on ~10 mg samples placed in 40 $\mu$ L Al pans. The glass transition was measured by heating a sample ~40°C above its glass transition temperature and holding it at this temperature for 10 min to erase thermal history. The samples were then cooled down to ~40°C below the glass transition temperature at the rates from 5, 7.5, 10, 12.5, 15, 17.5, 20, 22.5 and 25 °C min<sup>-1</sup>. Immediately after completion of the cooling segment, the samples were heated at a rate whose absolute value was equal to the rate of preceding cooling. TGA data [45] indicate that no detectable degradation of PS100 and nPS90 occurs in air below 240°C.

*Indomethacin (1-(p-chlorobenzoil)-5-methoxy-2-methylindole-3-acetic acid)* was obtained from MPBiomedicals, LLC (catalogue number 190217, lot number 9331E), with a melting point at 160°C obtained by DSC, and it was used without further purification.

The  $\alpha$ -relaxation measurements were performed on ~10.0 mg samples placed in 40 $\mu$ L Al sealed pans without holes. TGA data [46] indicate that no detectable degradation of Indomethacin occurs in air atmosphere below 180°C. The glass transition was measured by heating a sample ~40°C above its glass transition temperature (90°C) and holding it at this temperature for 10 min to erase thermal history. The samples were then cooled down to ~40°C below the glass transition temperature (-10°C) at the rates from (10, 15, 20, 25 and 30°C min<sup>-1</sup>). Immediately after completion of the

cooling segment, the samples were heated at a rate whose absolute value was equal to the rate of preceding cooling. The heat capacity was measured on ~27 mg sample by using a standard procedure that is precise to 1%. A sapphire sample of 41.48 mg was used as the calibrant. The temperature program used for the heat capacity measurement involved 5 min isothermal hold at 0°C followed by heating at 10°C min<sup>-1</sup> to 90°C and another 5 min isothermal hold at the final temperature.

*Anhydrous glucose (Dextrose) and maltitol* were, respectively, purchased from Fisher and MP Biomedicals and used without purification. In order to produce amorphous (glassy) samples, ~15 mg of samples was placed in 40 µl closed Al pans and heated to ~10°C above their respective melting points, 161°C (glucose) and 149°C (maltitol). Shortly after heating the samples were quenched into liquid nitrogen. The glass transition temperatures of amorphous samples were estimated as midpoint temperatures of the DSC glass transition steps measured at 10°C min<sup>-1</sup>.

*Sub- $T_g$  measurements*, freshly quenched samples were quickly placed into the DSC cell that was maintained at -40°C. From -40°C the samples were heated to an annealing temperature,  $T_a$ , and held at it for 30 min. After completion of the annealing segment, the samples were cooled down to -40°C and immediately heated above  $T_g$ . The heating rates were 15, 20, 25, and 30°C min<sup>-1</sup>.

All the aforementioned measurements we conducted by using a Mettler-Toledo heat flux DSC 822e in the atmosphere of nitrogen flow (80 ml min<sup>-1</sup>) at University of Alabama, USA. The temperature and heat flow calibration were performed by using an Indium standard.

## Results and Discussion

*Glass transition or  $\alpha$ -relaxation in PS100 and nPS90.* DSC data for both materials demonstrate (Fig. 1) typical glass transition steps, the midpoint of which has been used as an estimate of the  $T_g$  value. It is seen that in nPS90 the glass transition occurs at about 10 °C greater temperature than PS100.

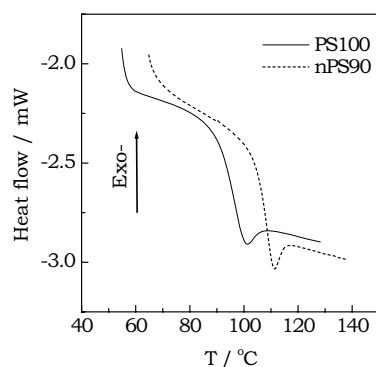


Fig. 2. DSC curves for the glass transition ( $\alpha$ -relaxation) in PS100 and nPS90 measured at 10 °C min<sup>-1</sup>

The values of  $T_g$  have been determined at nine heating rates (two times at each heating rate). The heating rate dependence of  $T_g$  can be used to evaluate the effective activation energy of the glass transition from eq 1.

$$E = -R \frac{d \ln \beta}{dT_g} \quad (2)$$

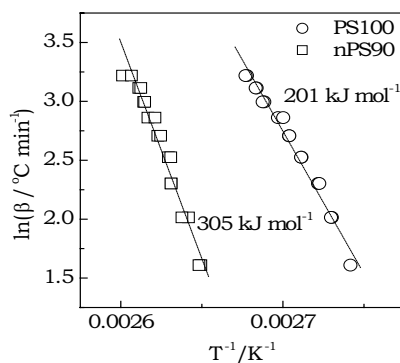


Fig. 3. Evaluating activation energies (eq 2) for  $\alpha$ -relaxation in PS100 and nPS90 as proposed by Moynihan et al. [6, 47]

A necessary constraint of eq 2, is that the sample must be heated at a rate whose absolute value is equal to the rate of preceding cooling [6, 47]. The resulting dependence of  $\ln \beta$  versus  $T_g^{-1}$  are shown in Fig. 3. The plots are nonlinear, which is typically observed for the  $\alpha$ -relaxations [11, 48]. The effective activation energy decreases with temperature, which is consistent with the general tendency predicted by the WLF equation [15, 17]:

$$E = 2.303R \frac{c_1 c_2 T^2}{(c_2 + T - T_g)^2} \quad (3)$$

where  $c_1$  and  $c_2$  are the constants. Forcing data to an Arrhenius plot yields averaged values of the effective activation energy for PS100 and nPS90 that respectively are 201 and 305 kJ mol<sup>-1</sup>. To determine a variation of  $E$  with the extent of conversion from the glassy to rubbery state,  $\alpha$ , we have used an advanced isoconversional method [49, 50]. The method offers two major advantages over the frequently used methods of Flynn and Wall [51] and Ozawa [52]. First, it has been designed to treat the kinetics that occur under arbitrary variation in temperature,  $T(t)$ , which allows one to account for self-heating/cooling detectable by the thermal sensor of the instrument. For a series of  $n$  experiments carried out under different temperature programs,  $T(t)$ , the activation energy is determined at any particular value of  $\alpha$  by finding  $E_\alpha$ , which minimizes the function

$$\Phi(E_\alpha) = \sum_{i=1}^n \sum_{j \neq i}^n \frac{J[E_\alpha, T_i(t_\alpha)]}{J[E_\alpha, T_j(t_\alpha)]} \quad (4)$$

where

$$J[E_\alpha, T_i(t_\alpha)] \equiv \int_{\alpha - \Delta\alpha}^{\alpha} \exp\left[\frac{-E_\alpha}{RT_i(t)}\right] dt \quad (5)$$

The second advantage is associated with performing integration over small time segments (eq 4), which allows for eliminating a systematic error [50] occurring in the Flynn and Wall and Ozawa methods when  $E_\alpha$  varies significantly with  $\alpha$ . In eq 5,  $\alpha$  is varied from  $\Delta\alpha$  to  $1 - \Delta\alpha$  with a step  $\Delta\alpha = m^{-1}$ , where  $m$  is the number of intervals chosen for analysis. The integral,  $J$  in eq 4, is evaluated numerically by using the trapezoid rule. The minimization procedure is repeated for each value of  $\alpha$  to find the dependence  $E_\alpha$  on  $\alpha$ . Isoconversional methods determine the  $E_\alpha$  values independently of the preexponential factors, which are not produced directly by these methods. It allows one to eliminate the bias in the value of the activation energy caused by its strong correlation with the exponential factor that is generally found when both parameters are fit simultaneously [53]. The conversion,  $\alpha$ , can be evaluated from DSC data (Fig. 2) as the normalized heat capacity [54] as follows:

$$C_p^N = \frac{(C_p - C_{pg})}{(C_{pl} - C_{pg})} \Big|_T \equiv \alpha \quad (6)$$

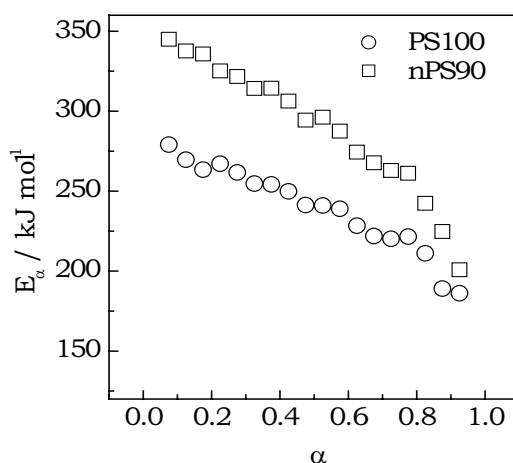


Fig. 4. Variation of the activation energy for  $\alpha$ -relaxation with the extent of conversion

where  $C_p$  is the observed heat capacity, and  $C_{pg}$  and  $C_{pl}$  are respectively the glassy and equilibrium (liquid) heat capacity. Because the values  $C_{pg}$  and  $C_{pl}$  are temperature dependent, they must be extrapolated into the glass transition region.

According to Hodge, [54] the  $C_p^N$  value provides a precise approximation to the temperature derivative of the fictive temperature. The application of the isoconversional method to the resulting  $\alpha$  versus  $T$  data obtained at different heating rates yields the  $E_a$  dependencies shown in Figure 4. The activation energies decrease from 280 to 140 kJ mol<sup>-1</sup> for PS100 and from 350 to 160 kJ mol<sup>-1</sup> for nPS90. Note that the values obtained for PS100 fall within the large interval, 160-900 kJ mol<sup>-1</sup>, reported in the literature [54-59].

*Volume of Cooperatively Rearranging Regions in PS100 and nPS90.* On the basis of the result discussed in the previous section, the polymer-clay system should have a larger region of cooperative rearrangement. Donth has demonstrated that the volume of the cooperatively rearranging region at the glass transition can be estimated from calorimetric data by using the following equation [48, 60]:

$$V_g = \frac{k_B T_g^2 \Delta(C_v^{-1})}{\rho (\delta T)^2} \quad (7)$$

$k_B$  is the Boltzman constant,  $T_g$  is an apparent glass transition temperature,  $\rho$  is the density (1.05 g cm<sup>-3</sup> for PS [61]), and  $C_v$  is the isohoric heat capacity. The value of  $\Delta(C_v^{-1})$  is determined as

$$\Delta(C_v^{-1}) = (C_{vg}^{-1} - C_{vl}^{-1}) \quad (8)$$

where  $C_{vg}$  and  $C_{vl}$  are respective values of the glassy and liquid heat capacity extrapolated to  $T_g$ . The difference between isohoric and isobaric heat capacities is usually neglected [60] so that  $C_v$  can be replaced with  $C_p$  which is readily obtainable from calorimetric measurements. More recently, Hempel et al. [62] demonstrated that the difference can be accounted via the following correction:

$$\Delta(C_v^{-1}) = (0.74 \pm 0.22) \Delta(C_p^{-1}) \quad (9)$$

If the glass transition is measured on heating, the mean temperature fluctuation,  $\delta T = \frac{\Delta T}{2.5}$  (10)

where  $\Delta T$  is the temperature interval within which  $C_p$  varies between 16 and 84% of the total  $\Delta C_p$  at  $T_g$  [60 62].

Figure 5, shows the results of our  $C_p$  measurements for PS100 and nPS90.

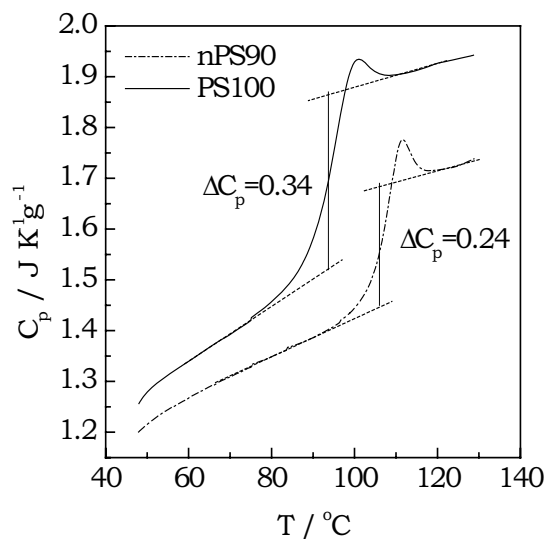


Fig. 5. Temperature dependence of the heat capacity for PS100 and nPS90

The values of  $C_p$  for PS are in very good agreement with earlier measurements [63, 64].

Size of Cooperatively Rearranging Region and Experimental Parameters Used for Its Calculations

sample	$T_g, K$	$C_{pg}, J K^{-1}g^{-1}$	$C_{pp}, J K^{-1}g^{-1}$	$\delta T, K$	$V_g, nm^3$
PS100	366.9	1.53	1.87	2.6	20.9
nPS90	379.4	1.45	1.69	1.9	36.7

It is seen that the  $C_p$  values for the PS-clay system are noticeably smaller than for virgin PS. The decrease cannot be explained by the simply presence of clay because it is present in a very small amount (1%) and its heat capacity [65] is comparable to that of PS. On the other hand, the value of heat capacity is proportional to the number of internal degrees of freedom of molecular motion. By applying 7-10 to the heat capacity data (Fig. 5), we have evaluated the volume of cooperatively rearranging region PS100 and nPS90 (Table 1). The values  $\zeta = (V_g)^{1/3}$  gives the characteristic length of the cooperatively rearranging region [48, 60]. According to our data for PS100 (Table 1),  $\zeta$  is 2.8 nm, which agrees well with the value 3.0 nm recently reported by Hempel et al. [62].

*Glass transition or  $\alpha$ -relaxation in Indomethacin.* By applying the isoconversional method [49, 50] to the  $\alpha$  versus  $T$  data for different heating rates, [46] we obtained the  $E_\alpha$  dependence shown in Fig. 6.

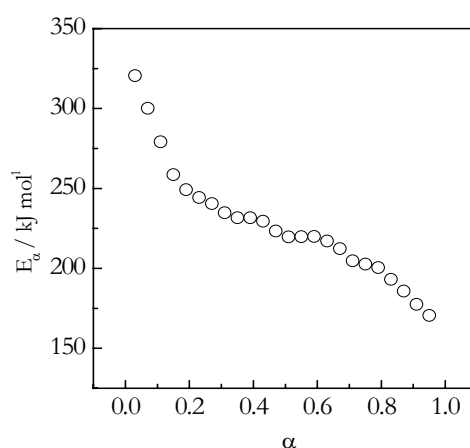


Fig. 6. Variation of the activation energy for the  $\alpha$ -relaxation with the extent of relaxation for the glass transition in indomethacin

The effective activation energy decreases from 320 to 160 kJ mol<sup>-1</sup>. A decrease in  $E$  with the transition from the glassy to liquid state has also been reported by Hancock et al. [66], who estimated  $E$  for the onset, midpoint, and offset of the transition, and obtained respective values of 385, 263, and 190 kJ mol<sup>-1</sup>.

The decrease in  $E$  can be explained in terms of cooperative molecular motion. The glassy state has a small amount of free volume that permits only the local motion (i.e., the  $\beta$ -process) (Fig. 1) that persists well below the glass transition temperature. As the temperature increases and approaches the region of the glass transition, the molecular motion becomes more intense, and the free volume rises, initiating the  $\alpha$ -process. This process needs a great degree of cooperativity between the molecules, which gives rise to a large energy barrier represented by a large value of  $E$  at the initial stage of transition. As the free volume grows with increasing temperature, the molecular packing becomes looser, allowing molecules to relax more independently (i.e., with a smaller degree of cooperativity). As a result, the energetic constraints relax, and the effective activation energy drops. Note that a fall of  $E$  is consistent with both the WLF and VTF equations [12-15]. A decrease is also predicted by the Adam-Gibbs equation [67].

$$\tau = A \exp\left(\frac{z^* \Delta\mu}{k_B T}\right) \quad (11)$$

where  $k_B$  is the Boltzman constant,  $\Delta\mu$  is the activation energy per particle, and  $z^*$  is the number of particles that rearrange cooperatively. In eq 11,  $z^*$  is inversely proportional to the configurational entropy that rises with  $T$ , so that both  $z^*$  and the effective activation energy (i.e.,  $z^*\Delta\mu$ ) decrease with increasing  $T$ .

*Size of Cooperatively Rearranging Regions in Indomethacin.* Figure 7 shows a  $C_p$  versus  $T$  curve that is an average of three independent measurements.

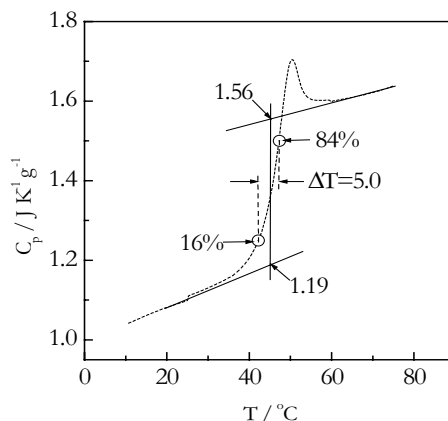


Fig. 7. Temperature dependence of the heat capacity for indomethacin. The heat capacity at the glass transition (319 K) changes from 1.19 to 1.56  $\text{K}^{-1} \text{g}^{-1}$ .  $\Delta T$  is determined as the temperature interval in which  $C_p$  changes from 16 to 84% of the total  $\Delta C_p$

The obtained  $C_p$  data agree very well with the earlier measurements [68]. The application of eqs 7-10 to the  $C_p$  data (Figure 6) yields the volume of the cooperatively rearranging region of  $40.5 \text{ nm}^3$ . The characteristic length of the cooperatively rearranging region (Figure 1) or the average distance between the mobility islands [42] estimated as  $\xi = (V_a)^{1/3}$  is 3.4 nm. The value is comparable to that estimated for sorbitol, 3.6 nm [62]. The numbers of molecules involved in the cooperatively rearranging region is determined as

$$N_\alpha = \frac{RT_g^2 \Delta(C_p^{-1})}{M(\Delta T)^2} \quad (12)$$

where  $R$  is the gas constant and  $M = 357.8 \text{ g mol}^{-1}$  is the molecular weight of indomethacin. The resulting value is  $\sim 90$  molecules.

*Glass transition or  $\alpha$ -relaxation in Glucose and Maltitol.* Heating glassy maltitol and glucose throughout the temperature region of the glass transition results in obtaining typical step-like DSC traces (Fig.8).

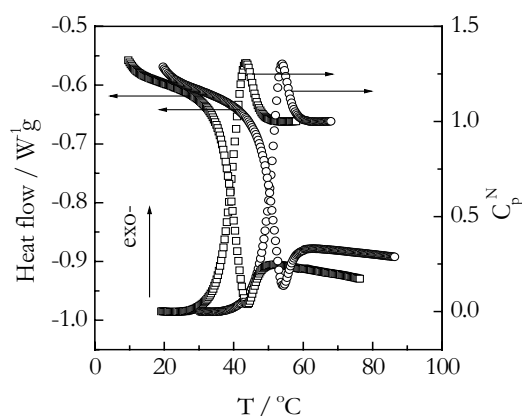


Fig. 8. DSC curves and normalized heat capacities for the glass transition of maltitol (circles) and glucose (squares) at  $20^\circ\text{C min}^{-1}$ . Prior to heating the samples were heated  $\sim 40^\circ\text{C}$  above their  $T_g$ , held at this temperature for 10 min, and cooled down to  $\sim 40^\circ\text{C}$  below  $T_g$  without aging

The steps shift to higher temperature with increasing the heating rate. The application of the isoconversional method to several systems demonstrated [18] that the variability in  $E$  correlates with the dynamic fragility. For maltitol and glucose the reported values of the dynamic fragility, respectively, are 75 [69] and 70 [70]. As these values are not very large, we may expect a moderate variability in  $E$  throughout the glass transition. The actual dependencies of the effective activation energy on conversion are shown in Fig. 10. As expected, we observe a moderate decrease for both systems. For maltitol the activation energy decreases from  $\sim 250$  to  $\sim 150$  kJ mol $^{-1}$  whereas for glucose from  $\sim 220$  to  $\sim 170$  kJ mol $^{-1}$ .

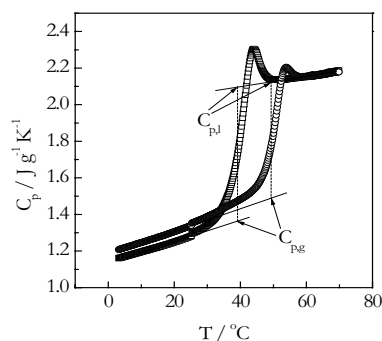


Fig. 9. Temperature dependence of the heat capacity for maltitol (*circles*) and glucose (*squares*).  $C_{p,l}$  and  $C_{p,g}$  show the values extrapolated to the  $T_g$  values (*dashed lines*) that are used in evaluating  $\xi$  by eq. 7

The  $E_a$  vs  $\alpha$  plots (Fig. 10) were converted into  $E_a$  vs  $T$  plots by replacing  $\alpha$  with temperature which is estimated as an average of the temperatures corresponding to this  $\alpha$  at different heating rates.

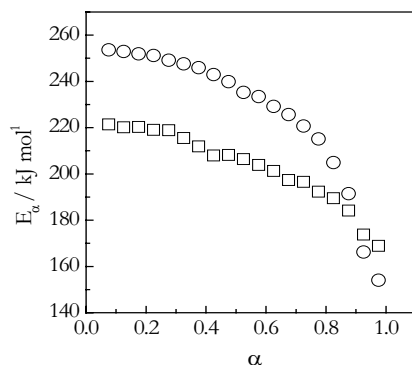


Fig. 10. Variation of the activation energy with the extent of relaxation for the glass transition in maltitol (*circles*) and glucose (*squares*)

The resulting dependencies are shown in Fig. 11 and 12. As mentioned earlier, a decrease in the effective activation energy with temperature is typical for the glass transition ( $\alpha$ -relaxation). We observed similar effects for polystyrene and polystyrene composite [71] as well as for poly(ethylene terephthalate) and boron oxide [18]. For the most fragile system studied [18], poly(ethylene terephthalate) ( $m=166$ ), the value of  $E$  decreased more than 2 times per 7°C, whereas for boron oxide ( $m=32$ ) it decreased less than 1.5 times per 57°C.

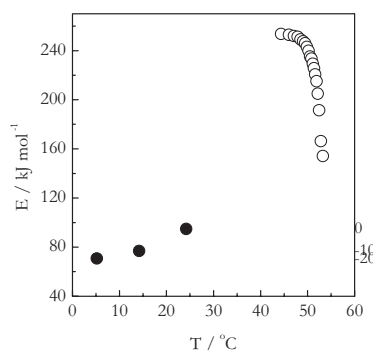


Fig. 11. Variation of the activation energies for the sub- $T_g$  (*solid symbols*) and  $T_g$  (*open symbols*) relaxation of maltitol with average temperature of the process. Numbers by the points represent annealing temperatures

Maltitol and glucose have intermediate fragilities of about the same value so that they demonstrate similar variability in  $E$  that amounts to 1.7 times  $10^\circ\text{C}$  for maltitol and 1.3 times per  $8^\circ\text{C}$  for glucose. Therefore, the correlation of the variability in  $E$  with the fragility appear to hold for these two systems as well.

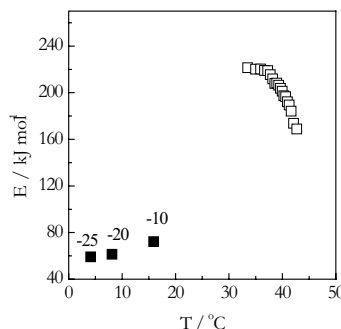


Fig. 12. Variation of the activation energies for the sub- $T_g$  (solid symbols) and  $T_g$  (open symbols) relaxation of *glucose* with average temperature of process. Numbers by the points represent annealing temperatures

The Arrhenius activation energies reported for the  $\alpha$ -relaxation in maltitol and in glucose span a rather wide range which is not surprising as their values depend on the temperature and, therefore, on the temperature region used their determination. For this reason, single value of  $E$  (440 [72] and 460 [69]  $\text{kJ mol}^{-1}$ ) reported for maltitol are difficult to compare with our variable values. On the other hand, our dependence fits well within the reported [73] decrease in  $E$  from 560 to 50  $\text{kJ mol}^{-1}$  with increasing temperature. Single values of  $E$  for the  $\alpha$ -relaxation in glucose are 180, [74] 320 [75], and 420  $\text{kJ mol}^{-1}$  [70].

It should be stressed that the effective activation energy landscapes presented in Figs. 11 and 12 are remarkably similar to the temperature dependence of the effective activation energy for stress relaxation as well as for viscous flow in polymers. These latter also show a significant increase in  $E$  on approaching the glass transition region from the glassy state, followed by a significant decrease in  $E$  while further relaxing toward the liquid state. This effect was originally predicted by Fox and Flory [76] and observed experimentally by McLoughlin and Tobolsky [77]. Passing of the  $E$  value through a maximum can be understood in terms of molecular cooperativity that is very low significantly below  $T_g$  where relaxation occurs via a noncooperative local process that has a small activation energy. As the temperature rises, the molecular mobility intensifies increasing cooperativity and the activation energy that reach their maximum in the region of  $T_g$ . Above  $T_g$ , the free volume starts to quickly increase with temperature so that cooperativity decreases, and the effective activation energy drops down to the values characteristic of the viscous flow.

**3.5. Sizes of Cooperatively Rearranging Regions in maltitol and glucose.** Figure 9 displays  $C_p$  vs  $T$  data for maltitol and glucose. The data agree well with the earlier measurements [69, 78]. By applying Eqs. 7, 8, 9, 10 to the  $C_p$  data (Fig. 9) we determined the values of  $V_a$  to be 30.6 (*maltitol*) and 36.4 (*glucose*)  $\text{nm}^3$ . The values of the characteristic length were determined as  $\xi = (V_a)^{1/3}$  yielding, respectively, 3.1 and 3.3 nm. The values are very close to each other and comparable to the value reported [62] for sorbitol, 3.6 nm. By its meaning the value of  $\xi$  provides an estimate of the average distance between the mobility islands in the heterogeneous glassy system [48]. The closeness of the  $\xi$  values suggests similarity of the heterogeneous structures of the maltitol and glucose glasses. The  $C_p$  data can also be used to estimate the number of molecules involved in the cooperatively rearranging region as [48].

The resulting values are  $\sim 90$  for maltitol and 190 for glucose. The value for glucose is almost the same as for sorbitol ( $N_a = 195$  molecules [48]), whose molecular mass is similar to that of glucose.

**3.6. Sub- $T_g$  Region.** While reheating polyvinyl chloride samples annealed significantly below the glass transition temperature,  $T_g$ , Illers [79], detected small endothermic DSC peaks that appears before the main glass transition step. The effect was later studied more extensively for metallic glasses by Chen [80] and for various polymers by Bershtein and Egorov [81]. An interpretation of the effect was given by Chen as a partial enthalpy relaxation and recovery that occur at the expense of the faster part of a broad relaxation spectrum of the glassy state. It was suggested [80, 81] that effective activation energy,  $E$  of the underlying process can be determined from the shift in the annealing peak temperature,  $T_p$  with the heating rate,  $q$  as

$$E = -R \frac{\ln q}{dT_p^{-1}} \quad (13)$$

where  $R$  is the gas constant. The  $E$  values determined this way [80, 81] were found to be several times smaller than the activation energies of the  $\alpha$ -relaxations in the respective glassy systems. The annealing peaks are easily produced

by annealing a glassy material in the region around  $0.8 T_g$ . It has been pointed that the dielectric and mechanical loss peaks for  $\beta$ -relaxation in polymers are commonly found at temperature around  $0.75 T_g$  [82]. For maltitol, we were able to obtain good annealing peaks at  $T_a = -20, -10, \text{ and } 0^\circ\text{C}$ . A representative example of the annealing peaks obtained for maltitol is shown in Fig. 13.

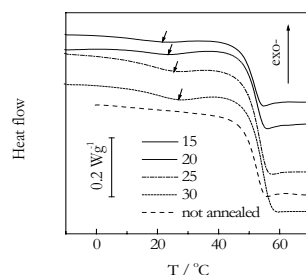


Fig. 13. DSC curves obtained on heating of *maltitol* at the heating rates  $15\text{--}30^\circ\text{C min}^{-1}$  (numbers by the lines represent the heating rates) after annealing at  $0^\circ\text{C}$  for 30 min. “Not annealed” curve obtained by heating a sample immediately after quenching. Arrows show the location of the annealing effect

The resulting peaks are very broad and shallow but readily noticeable especially when comparing DSC for annealed samples against those for not annealed samples. At a constant annealing temperature, the peak temperature increase with increasing the heating rate (Fig. 13) that allowed us to estimate the effective activation energies by Eq.13. The respective  $\ln q$  vs  $T^{-1}$  plots are shown in Fig. 14. It is seen the slopes of the plots increase with increasing the annealing temperature. This means that the effective value of  $E$  rises with  $T_a$ . For maltitol, the obtained values of  $E$  are 71, 77, and  $95 \text{ kJ mol}^{-1}$  (Fig. 11), for glucose,  $E$  rises from 59 to 61 and to  $72 \text{ kJ mol}^{-1}$  (Fig. 12). The values are obviously smaller than the activation energies of the  $\alpha$ -relaxation energies whose typical values for sugars lie in the region  $200\text{--}400 \text{ kJ mol}^{-1}$ . The smaller values of  $E$  suggest that the underlying relaxation process is either noncooperative or weakly cooperative (Fig. 1). Apparently, the observed increasing dependence of  $E$  with  $T_a$  reflects an increasing contribution of the cooperative molecular motion that starts to unfreeze as the annealing temperature approaches to the glass transition, ( $T_g$ ) region. For the  $\beta$ -relaxation in maltitol the reported values of the activation energy are as follow: 57 [72] and 61 [73] by using dielectric spectroscopy. For glucose, our best estimate is  $59 \text{ kJ mol}^{-1}$ . The literature reports the following values for the activation energy of the  $\beta$ -relaxation: 42 [75], 52 [83], and 62 [84]  $\text{kJ mol}^{-1}$ , all of which were determined by using dielectric spectroscopy. Clearly, our estimate falls within the region of the reported values that constitutes its good correlation with activation energies of the  $\beta$ -relaxation.

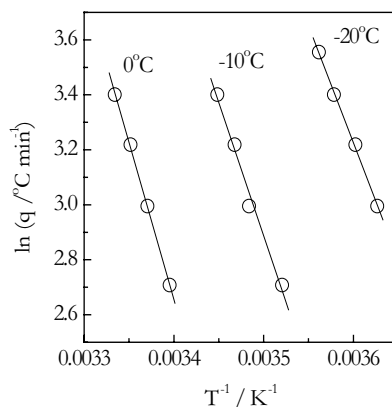


Fig. 14. Evaluating activation energies (Eq. 13) for sub- $T_g$  relaxation of *maltitol* annealed at different temperatures. The magnitudes of the annealing temperatures shown by the *straight lines*

Lastly, both estimates for maltitol and glucose, fit well into the empirical correlation,  $E_\beta = (24 \pm 3) RT_g$  reported by Kudilik *et al.* [85]. According to this, the activation energies of the  $\beta$ -relaxation in maltitol and glucose, should respectively, lie within  $\sim 8 \text{ kJ mol}^{-1}$  limits of 64 and  $62 \text{ kJ mol}^{-1}$ .

## Conclusions

DSC can be used to determine the activation energies of the  $\alpha$ - and  $\beta$ -relaxations and for evaluating the sizes of cooperatively rearranging regions at the glass transition in polymer-clay systems and pharmaceuticals.

A dramatic difference from virgin PS and PS-clay system has been observed for  $\alpha$ -relaxation, which demonstrates a significant increase in both effective activation energy and size of cooperatively rearranging region for the PS-clay system. Both values suggest that transitional motion in the PS-clay system require extra cooperativity.

For indomethacin, in the glass transition region, the effective activation energy of relaxation decreases with increasing temperature from 320 to 160 kJ mol<sup>-1</sup>.

The sub- $T_g$  relaxation data for maltitol and glucose suggest that with decreasing the annealing temperatures the effective activation energies decrease and tend to converge to the activation energies of the  $\beta$ -relaxation. In sub- $T_g$  and  $T_g$  regions the effective activation energies for maltitol are somewhat greater than for glucose that appears to be associated with the added impeding effect of the bulky substitute group in maltitol.

The comparable sizes of the cooperatively rearranging regions suggest a similarity of the heterogeneous glassy structures of the two compounds.

Therefore, DSC can be effectively used to determine the activation energy landscape for relaxation of non-polymer glasses in a wide temperature range covering both the  $\alpha$ - and  $\beta$ -relaxation. The resulting information on the effective activation energies and respective temperatures is of a great practical importance for evaluating the physical stability of amorphous polymers and pharmaceuticals. It allows one to detect the mobility and identify its type (cooperative vs noncooperative) in a given temperature region.

**Acknowledgment.** Thanks are due to Mettler-Toledo, Inc. for loan of the DSC and TGA instruments used in this work.

## References

- [1] Wunderlich, B. *Thermal Analysis*; Academic Press: Boston, 1990.
- [2] Bernazzani, P.; Simon, S. L.; Plazek, D. J.; Ngai, K. L. *Eur. Phys. J. E.* 2002, 8, 201.
- [3] Efremov, M. Y.; Olson, E.A.; Zhang, M.; Zhang, Z.; Allen, L. H. *Phys. Rev. Lett.* 2003, 91, 085703.
- [4] Park, J. Y.; McKenn, G. B.; *Phys. Rev. B* 2000, 61, 6667.
- [5] Schonhals, A.; Goering, H.; Schick, C.; Frick, B.; Zorn, R. *Eur. Phys. J. E.* 2003, 12, 173.
- [6] Moynihan, C.T.; Eastel, A.J.; Wilder, J.; Tucker, J. *J. Phys. Chem.* 1974, 78, 2673.
- [7] Tool, A. Q. *J. Am. Ceram. Soc.* 1946, 29, 240.
- [8] Narayanaswamy, O. S. *J. Am. Ceram. Soc.* 1971, 54, 491.
- [9] Moynihan, C.T.; Eastel, A.J.; DeBolt, M. A.; Tucker, J. *J. Am. Ceram. Soc.* 1976, 59, 12.
- [10] Kovacs, A. J.; Hutchinson, J.M.; Aklonis, J.J. *The Structure of Non-Crystalline Materials*; Gaskell, P.H. Ed: Taylor & Francis, 1977, p. 153.
- [11] Matsuoka, S. *Relaxation Phenomena in Polymers*; Hanser Publishers: Munich, 1992.
- [12] Vogel, H. *Phys. Z.* 1921, 22, 645.
- [13] Tamman, G.; Hesse, G. *Z. Anorg. Allg. Chem.* 1926, 156, 245.
- [14] Fulcher, G. S. *J. Am. Ceram. Soc.* 1925, 8, 339.
- [15] Williams, M. L.; Landel, R. F.; J. D. *J. Am. Chem. Soc.* 1955, 77, 3701.
- [16] Angell, C. A. *J. Non-Cryst. Solids* 1991, 13, 131.
- [17] Ferry, J. D. *Viscoelastic Properties of Polymers*, 3<sup>rd</sup> ed.; J. Wiley: New York, 1980.
- [18] Vyazovkin, S.; Sbirrazzuoli, N.; Dranca, I. *Macromol. Rapid Commun.* 2004, 25, 1708.
- [19] Arrhenius, A. *Phys. Chem.*, 1889, 4, 226.
- [20] Van't Hoff, J. H. *Studies in Chemical Dynamics*, Frederik Muller & Co., Amsterdam, 1894.
- [21] McC. Lewis, W. C. *J. Chem. Soc.*, 1918, 113, 471-492.
- [22] Hinshelwood, C. N. *The Kinetics of Chemical Change*, Oxford University Press, Oxford, 1940.
- [23] Glasstone, S.; Laidler, K. J.; and Eyring, H. *The theory of Rate Processes*, McGraw-Hill, New York, 1941.
- [24] Note that the two aforementioned theories have a temperature dependent preexponential factor, so that if this factor is assumed constant in computations the estimated activation energy may exhibit some small dependence as a computational artifact.
- [25] Vyazovkin, S. *New J. Chem.*, 2000, 24, 913.
- [26] Hulett, J. R. *Q. Rev. Chem. Soc.*, 1964, 18, 227.
- [27] Vyazovkin, S. *Thermochim. Acta*, 397, 2003, 269.
- [28] Brown, M. E.; Maciejewski, M.; Vyazovkin, S.; Nomen, R.; Sempere, J.; Burnham, A.; Opfermann, J. J.; Strey, R.; Anderson, H. L.; Kemmler, A.; Keuleers, R.; Janssens, J.; Desseyn, H.O.; Li, C. -R.; Tang, T.B.; Roduit, B.; Malek, J.; Mitsunashi, T. *Thermochim. Acta*, 2000, 355, 125.
- [29] Maciejewski, M. *Thermochim. Acta* 355, 2000, 145.
- [30] Burnham, A. *Thermochim. Acta* 2000, 355, 165.
- [31] Alexandre, M.; Dubois, P. *Mater. Sci. Eng., R* 2000, 28, 1.

- [32] Porter, D. E.; Metcalfe, E.; Thomas, M. J. K. *Fire Mater.* 2000, 24, 45.
- [33] Noh, M.W.; Lee, S. C. *Polym. Bull.* 1999, 42, 619.
- [34] Okamoto, M.; Morita, S.; Tafuchi, H.; Kim, Y. H.; Kotaka, T.; H. Tateyama, H. *Polymer*, 2000, 41, 3887.
- [35] Wang, J.; Zhu, J.; Yao, Q.; Wilkie, C. A. *Chem. Mater.*, 2002, 14, 3837.
- [36] Zhu, J.; Wilkie, C. A. *Polym. Int.* 2000, 49, 1158.
- [37] Gilman, J. W.; Jackson, C. L.; Morgan, A. B.; Harris, P.; Manias, E.; Giannelis, E. P.; Wuthenow, M.; Hilton, D.; Phillips S. H. *Chem. Mater.*, 2000, 12, 1866.
- [38] Morgan, A. B.; Harris, R. H.; Kashiwagi, T.; Chyall, L. J.; J. W. Gilman, J. W. *Fire Mater.*, 2002, 26, 247.
- [39] Yoshioka, M.; Hancock, B. C.; Zografi, G. *J. Pharm. Sci.*, 1994, 83, 1700.
- [40] Andronis, V.; Zografi, G. *J. Non-Cryst. Solids* 2000, 271, 236.
- [41] Hancock, B. C.; Shamblin, S. L.; Zografi, G. *Pharm. Res.*, 1995, 12, 799.
- [42] Johari, G. P.; Goldstein, M. J. *Chem. Phys.*, 1970, 53, 2372.
- [43] Vyazovkin, S.; Dranca, I. *Pharm. Res.*, 2006, 23, 2158.
- [44] Fan, X.; Xia, C.; Advincula, R. C. *Colloids Surfaces: A*, 2003, 219, 75.
- [45] Vyazovkin, S.; Dranca, I.; Fan, X.; Advincula, R. *Macromol. Rapid. Commun.* 25, 2004, 25, 498.
- [46] Vyazovkin, S.; Dranca, I. *J. Phys. Chem. B*, 2005, 109, 18637.
- [47] Moynihan, C. T.; Lee, S.-K.; Tatsumisago, M.; Minami, T. *Thermochim. Acta* 1996, 280/281, 153.
- [48] Donth, E. *The Glass Transition: Relaxation Dynamics in Liquids and Disordered Materials*; Springer: Berlin, 2001.
- [49] Vyazovkin, S. *J. Comput. Chem.* 1997, 18, 393.
- [50] Vyazovkin, S. *J. Comput. Chem.* 2001, 22, 178.
- [51] Flynn, H.; Wall, L. A. *J. Res. Nat. Bur. Stand.: A*, 1966, 70, 487.
- [52] Ozawa, T. *Bull. Chem. Soc. Jpn.*, 1965, 38, 1881.
- [53] Vyazovkin, S. *Int. Rev. Phys. Chem.* 2000, 19, 45.
- [54] Hodge, I. M. *J. Non-Cryst. Solids* 1994, 169, 211.
- [55] Gao, H.; Harmon, J. P. *Thermochim. Acta* 1996, 284, 85.
- [56] McCrum, N. G.; Read, B. E.; Williams, G. *Anelastic and Dielectric Effects in Polymeric Solids*; Dover: New York, 1991.
- [57] Boller, A.; Okazaki, I.; Wunderlich, B. *Thermochim. Acta*, 1996, 284, 1.
- [58] Schawe, J. E. K. *J. Polym. Sci. B* 1998, 36, 2165.
- [59] Simon, S. L.; Sobieski, J. W.; Plazek, D. J. *Polymer* 2001, 42, 2555.
- [60] Donth, E. *J. Polym. Sci. B* 1996, 34, 2881.
- [61] Van Krevelen, D. W. *Properties of Polymers*, 2<sup>nd</sup> ed.; Elsevier: Amsterdam, 1976.
- [62] Hempel, E.; Hempel, G.; Hensel, A.; Shick, C.; Donth, E. *J. Phys. Chem. B* 2000, 104, 2460.
- [63] Karasz, F. E.; Bair, H. E.; O'Reilly, J. M. *J. Phys. Chem.*, 1965, 69, 2657.
- [64] ATHAS Database available at <http://web.utk.edu/~athas/databank/intro.html>.
- [65] Abu-Hamdeh, N. H. *Biosyst. Eng.*, 2003, 86, 97.
- [66] Hancock, B. C.; Dalton, C. R.; Pikal, M. J.; Shamblin, S. L. *Pharm. Res.*, 1998, 15, 762.
- [67] Adams, G.; Gibbs, J. H. *J. Chem. Phys.*, 1965, 43, 139.
- [68] Shamblin, S. L.; Tang, X.; Chang, L.; Hancock, B. C.; Pikal, M. J. *J. Phys. Chem. B* 1999, 103, 4113.
- [69] Busstin, O.; Descamps, M. *J. Chem. Phys.*, 1999, 110, 10982.
- [70] Wungttanagorn, R.; Schmidt, S. J. *Thermochim. Acta* 2001, 369, 95.
- [71] Vyazovkin, S.; Dranca, I. *J. Phys. Chem. B*, 2004, 108, 11981.
- [72] Carpentier, L.; Descamps, M. *J. Phys. Chem. B*, 2003, 107, 271.
- [73] Faivre, A.; Niquet, G.; Maglione, M.; Fornazero, J.; Jal, J. F.; David, L. *Eur. Phys. J.* 1999, 10, 277.
- [74] Kawai, K.; Hagiwara, T.; Takai, R.; T. Suzuki, T. *Pharm Res.* 2005, 22, 490.
- [75] Noel, T. R.; Parker, R.; Ring, S. G. *Carbohydr. Res.* 2000, 329, 839.
- [76] Fox, T. G.; Flory, P.J. *J. Appl. Phys.* 1950, 21, 581.
- [77] McLoughlin, J. R.; Tobolsky, A. V. *J. Coll. Sci.* 1952, 7, 555.
- [78] Orford, P. D.; Parker, R.; Ring, S. G. *Carbohydr. Res.* 1990, 196, 11.
- [79] Illers, K. -H. *Makromol. Chem.*, 1969, 127, 1.
- [80] Chen, H. S. *J. Appl. Phys.* 1981, 52, 1868.
- [81] Bershtein, V. A.; Egorov, V. M. *Differential Scanning Calorimetry of Polymers*, Ellis Horwood, New York, 1994.
- [82] Boyer, R. F. *Polymer*, 1976, 17, 996.
- [83] Gangasharan; Murthy, S. S. N. *J. Phys. Chem.* 1995, 99, 12349.
- [84] Chan, R. K.; Pathmanathan, K.; Johari, G. P. *J. Phys. Chem.* 1986, 90, 6358.
- [85] Kudilik, A.; Benkof, S.; Blochowicz, T.; Tschirwitz, C.; Rössler, E. *J. Mol. Str.* 1999, 479, 201.

# NITRATE-SELECTIVE ELECTRODES BASED ON THE TRINUCLEAR CHROMIUM(III) PIVALATES

Mihail Revenco<sup>a\*</sup>, Mariana Martin<sup>a</sup>, Wael A.A. Dayyih<sup>b</sup>

<sup>a</sup>State University of Moldova, A.Mateevici street, 60 MD 2009, Chisinau, Republic of Moldova

<sup>b</sup>University Petra, Amman, Jordan

\*E-mail: revenco@usm.md; phone 373-22-57-74-94, 373-22-43-22-98, 373-69-19-48-91;  
fax 373-22-24-42-48

**Abstract:** The paper describes the analytical potentialities of the trinuclear chromium(III) complexes as potentiometric ionophores for the construction of electrodes sensitive to the presence of nitrate anion. The electroactive material containing 4,4'-bipyridil was synthesized *in situ*. The membrane was prepared using dioctylphthalate as a solvent mediator and poly (vinyl chloride) as a polymeric matrix. The electrodes presented a slope of 56 mV/decade, a low limit of detection ( $3,2 \cdot 10^{-6}$  mol/l), an adequate lifetime (4 months), and suitable selectivity characteristics when compared with other nitrate electrodes. The good parameters of this electrode made possible its application to the determination of nitrate in different types of fertilizers.

**Keywords:** Trinuclear chromium(III) pivalate, nitrate-sensors.

## Introduction

Nitrate is an anion of major importance in environmental and biological areas. The necessity for nitrate monitoring in drinking water and food products is recognized by most health authorities. This ion, after chemical transformation, could have a direct impact on health because of its reaction with amines to produce nitrosamines, which are known to be one of the most powerful carcinogens to mammals. This is why, a lot of various methods including spectrophotometry, electrochemical methods based on modified electrodes and nitrate-selective electrodes have been developed for the determination of nitrate in different samples. Among these methods, potentiometric detection using the ion-selective electrodes [1-5] provides a rapid, simple, reasonably selective and inexpensive way for determination the content of this ion.

Recently the trinuclear chromium(III) benzoates were investigated as ionophores in the membrane of the anionic sensors [7]. The lipophilic complex cation can be combined with some inorganic and organic anions, which are part of a number of pharmaceutical materials. Variation of the carboxylic acid anion and use of different amines offer a real possibility to elaborate new sensors of high performance level. Recently we have described an electrode, sensitive to the presence of the perchlorate anion, based on the trinuclear chromium(III) pivalates [8].

Therefore, using this type of chromium(III) complexes, we were prompted to study the response of a membrane to the presence of nitrate anions. One of these electrodes shows improved selectivity for some of the interferences when compared with those for the commercially available nitrate-selective electrodes.

## Experimental

### Reagents and solutions

Dioctylphthalate (DOP) and poly (vinyl chloride) (PVC) of relative high molecular weight were used. All the reagents and solvents were of analytical reagent grade.

A standard nitrate solution (0,1 mol/l) was prepared by carefully weighing solid sodium nitrate. Standard solutions of all other anions were prepared from their respective sodium or potassium salts as 0,1 mol/l stock solutions. The pH adjustments were made with dilute sulphuric acid or sodium hydroxide solutions, as required. All solutions were prepared with twice distilled water.

### Synthesis of ionophores

The initial compound -  $[\text{Cr}_3\text{O}(\text{C}_5\text{H}_9\text{O}_2)_6(\text{H}_2\text{O})_3]\text{NO}_3$  (**I**) - was prepared using the described previously procedure [9] by dissolving 2 g of  $[\text{Cr}_3\text{O}(\text{C}_5\text{H}_9\text{O}_2)_6(\text{H}_2\text{O})_3]\text{C}_5\text{H}_9\text{O}_2$  in 10 ml acetone, containing 0,5 ml of  $\text{HNO}_3$  solution (31%). The precipitated green crystals were filtered and washed with ether.

The compounds  $[\text{Cr}_3\text{O}(\text{C}_5\text{H}_9\text{O}_2)_6(\text{C}_9\text{H}_7\text{N})_3]\text{NO}_3$  (**II**) and  $[\text{Cr}_3\text{O}(\text{C}_5\text{H}_9\text{O}_2)_6(\text{C}_{10}\text{H}_8\text{N}_2)_3]\text{NO}_3$  (**III**) were prepared by dissolving **I** in acetone and addition of quinoline or 4,4'-bipyridil in stoichiometric ratio. The precipitated after a slow evaporation complexes were filtered, washed and dried at 105 °C. The composition of the complexes has been confirmed by the elemental analysis for C, H, N, and Cr.

The complexes **I** and **II** are soluble in ethanol, acetone, tetrahydrofuran (THF), nitrobenzene (NB), while the compound **III** is poorly soluble in this solvents. All pivalates are insoluble in water.

### Preparation of the electrodes

The PVC membrane electrodes were prepared using a procedure similar to those described in [10].

The mixture of PVC cocktail, prepared by dissolving 0,02 – 0,03 g ionophore, 0,3 g PVC, 0,3 g DOP, and 0,9 g nitrobenzene in 3 – 5 ml of tetrahydrofuran (THF), was poured onto a glass dish (ca. 5 cm diameter) and allowed to dry at room temperature. A membrane (ca. 16 mm diameter) was cut and glued to the polished end of a PVC tube by using a PVC (ca. 5 %) – THF solution. According to the number of complexes used for preparation of the membrane the ion selective electrodes (**ISE**) are noted as (**ISE1**, **ISE2** and **ISE3**). The Ag/AgCl electrode and  $10^{-1}$ M of  $\text{NO}_3^-$  +  $5 \cdot 10^{-3}$  M of KCl solution were used as reference electrode and the internal filling solution, respectively.

The assembled electrodes were conditioned by soaking into solution of sodium nitrate ( $10^{-1}$  M) for 12 h before the electrodes have been used.

### Measurement of electromotive force

A nitrate-selective PVC electrode and saturated Ag/AgCl electrode were used as the indicating and the reference electrode, respectively. All potential measurements were performed at an ambient temperature ( $25 \pm 1^\circ\text{C}$ ) using a galvanic cell of the following type:

Ag/AgCl, KCl ( $5 \cdot 10^{-3}$ M) | internal filling solution ( $10^{-1}$ M  $\text{NO}_3^-$ ) | PVC membrane || tested solution || KCl satd. AgCl/Ag.

The behavior of each electrode was investigated in the concentration range of  $1 \cdot 10^{-7}$  –  $1 \cdot 10^{-1}$  M at a constant pH. The data were plotted as the observed potential against the negative logarithm of the  $\text{NO}_3^-$  activity. The potentiometric coefficients ( $\text{KNO}_3/\text{X}^-$ ) were determined according to the fixed interference method.

## Results and discussion

### Influence of the nature of the ligand in the apical position of the trinuclear chromium(III) pivalates on the sensors parameters

The potentiometric response of the **ISE1** was linear Nernstian in the concentration range  $8 \cdot 10^{-5}$  –  $1 \cdot 10^{-1}$  M with a slope 50 mV/decade. The detection limit was  $3,2 \cdot 10^{-5}$  mol/l and the electrode lifetime – only one day. We explain this short lifetime, by the possible hydrolysis of the complex and loss of the charge by the complex species according to the scheme:



The substitution of the co-ordinated water by quinoline in **ISE2** gives rise to an increase of the lipophilic properties of the complex, extending his lifetime up to 7 day and diminishing the detection limit up to  $2 \cdot 10^{-5}$  M, similar to the behavior of the electrodes described in [7, 8].

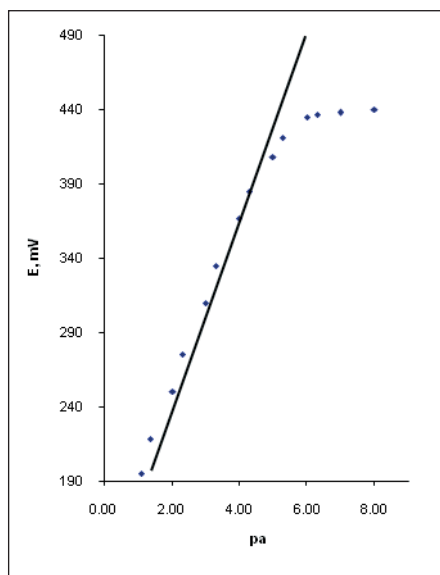


Fig. 1. Calibration curve of **ISE3**

Although the substitution of the water molecules by quinoline improves the parameters of the sensor, the lifetime is short enough. A possible washing-out of the electroactive material could be the cause of this relatively short lifetime. To stabilize the ionophore in membrane, we have tried the polymerisation of the trinuclear cores using bridging ligands.

The 4,4'-bipyridil was suitable for this purpose. The interaction of pivalate **I** with 4,4'-bipyridil in stoichiometric ration 2:3, leads to formation of a product **III**, which one is poorly soluble both in water and in the used for preparation the membrane solvents. Use of a saturate in nitrobenzene solution and incorporated in membrane, does not give rise to a nitrates sensitive electrode. This behavior demonstrates the formation of a polymer with very low solubility, which cannot assure a sufficient concentration to prepare a PVC membrane.

To achieve the objective we have tried the synthesis of the active material *in situ* [8], directly in membrane during its formation. The complex **I**, 4,4'-bipyridil and the other components used for preparation of the membrane of **ISE1**, all together, were mixed stirred and left for evaporation. During this time part of water molecules was substituted by 4,4'- bipyridil, and a new polymeric structure has appeared and plays the role of ionophore. We suppose, that the presence of the PVC does not allow the formation of the crystalline polymer, but it ensures the lacing of a number of trinuclear unities encapsulated by the solvent containing nitrate as counter ion.

Washing-out of this compound from membrane is surely hindered. The potentiometric response of **ISE3**, containing the ionophore synthesized *in situ*, was linear with a Nernstian slope of 56 mV/decade within the  $\text{NO}_3^-$  concentration range  $2 \cdot 10^{-5}$ - $1 \cdot 10^{-1}$  mol/l. Detection limit is  $3,2 \cdot 10^{-6}$  mol/l (Fig. 1).

The reponse time of the electrode was  $\leq 15$  s over the entire linear concentration range of the calibration plot. In order to study the effect of pH on the performance of **ISE3**, the responses of the sensor to  $\text{NO}_3^-$  ion at different concentrations of  $\text{H}^+$  ion were measured. It was observed that the sensor exhibit a stable behavior with a constant potential in the pH range 2 –11. The Fig. 2 shows the variation of the potential of the sensors immersed in a solution with the concentration 0,001 M. To achieve stable parameters the preconditioning time must be close to 12 h in a 0,1 mol/l solution of  $\text{NaNO}_3$ . The drift of the potential for a constant concentration is negligible. The electrodes prepared by this method show stable parameters during 4 months. During this period, the electrode was kept in a 0,1 mol/l  $\text{NaNO}_3$  solution and calibrated periodically. No significant change in the performance of the electrode was observed.

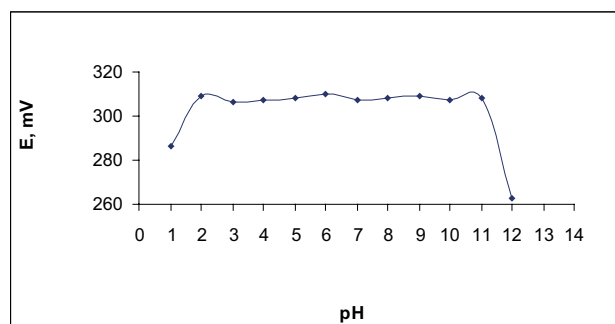


Fig. 2. Influence of pH on the response of the ISE3 immersed in a solution of  $\text{NaNO}_3$  (0,001 M)

The performances of a selection of different electrodes published in literature are shown in the Table 1. As it can be observed the parameters of the proposed electrode are comparable with of available nitrate-selective electrodes.

Table 1

Parameters of a selection of nitrate-selective electrodes

Concentration range, mol/l	Slope, mV/decade	Detection limit, mol/l	pH range	Lifetime	Reference
$1 \cdot 10^{-1} - 1 \cdot 10^{-6}$		$3,4 \cdot 10^{-7}$	2 - 8		[1]
$1 \cdot 10^{-1} - 2 \cdot 10^{-5}$	58		5 - 11		[2]
	60	$4,2 \cdot 10^{-6}$		1 year	[3]
	54-55	$5,0 \cdot 10^{-5}$			[4]
$1 \cdot 10^{-1} - 1 \cdot 10^{-5}$	54,7	$2,3 \cdot 10^{-6}$	2 - 12		[5]
$1 \cdot 10^{-1} - 2 \cdot 10^{-5}$	56	$3,2 \cdot 10^{-6}$	2 -11	4 months	<b>ISE3</b>

#### Selectivity of the electrode ISE3

The potentiometric selectivity coefficients were determined by fixed interference method [10]. The potentiometric selectivity coefficients of the proposed electrode are summarized in table 2.

Table 2

Selectivity coefficients ( $-\lg K_{\text{NO}_3^-/X^-}$ ) of ISE3 determined using fixed interference method

X	$\text{ClO}_4^-$	$\text{I}^-$	$\text{SCN}^-$	$\text{Br}^-$	$\text{BF}_4^-$	$\text{Cl}^-$	$\text{CH}_3\text{COO}^-$	$\text{SO}_4^{2-}$	$\text{F}^-$
$-\lg K_{\text{NO}_3^-,X}$	0,83	1,05	1,14	1,38	1,83	3,71	3,83	4,17	4,65

The reason for selecting these ions was their presence in the environment when (in drinking water, fertilizers, fountain waters, industrial effluents, soils, etc.). The proposed electrode doesn't demonstrate a significant deviation in the selectivity from the Hofmeister series  $\text{ClO}_4^- > \text{I}^- > \text{SCN}^- > \text{Br}^- > \text{BF}_4^- > \text{Cl}^- > \text{CH}_3\text{COO}^- > \text{SO}_4^{2-} > \text{F}^-$ . The main interfering anions were found to be perchlorate, iodide and thiocyanate and this selectivity is similar to commercial nitrate selective electrode [2].

#### Analytical application, table 3

To assess the applicability of the proposed electrode for the analysis of the real samples, an attempt was made to determine nitrate contents in fertilizer – ammonium nitrate.

**Direct potentiometry** – before use, **ISE3** was calibrated by measuring a series of known standard solutions (6) in the conditions of constant ionic strength ensured by sodium sulfate solution 0,1 M. The equation of the calibration  $E_x = 56,19(-\log C_x) + 139,33$ , where  $E_x$  is measured potential (mV),  $C_x$  – concentration (mol/l). A known mass of fertilizer was dissolved in a volumetric flask of 100 cm<sup>3</sup> and adjusted to the mark with distilled water. Using **ISE3** and the above mentioned galvanic cell, the potential  $E_x$  was measured. The concentration of the nitrate was calculated using the equation of the calibration curve. The values of  $E_x$  and the calculated concentration are given in the table 3.

Table 3

Determination of nitrate in fertilizer -  $\text{NH}_4\text{NO}_3$

m(fertilizer), g	$E_x$ , mV	Concentration, mol/l		$\omega(\text{NH}_4\text{NO}_3)$ , %	
		$\text{C}(\text{NO}_3^-)$ pot	$\text{C}(\text{NH}_4^+)$ tit	potentiometry	titrimetry
0,1524	237	0,01827	0,0182	95,92	95,60
	238	0,01756		92,19	
0,1770	234	0,02066	0,0211	93,38	95,37
0,1135	244	0,01372	0,0134	96,70	94,42
	245	0,01316		92,72	
average				94,2±1,7	95,1±0,4

For comparison and confirmation of the potentiometric data the determination of the using the titrimetric method. A aliquot of the solution containing  $\text{NH}_4^+$  was made basic, and the liberated  $\text{NH}_3$  was distilled into receiver containing a known amount of  $\text{H}_2\text{SO}_4$ . Unreacted acid was then titrated with standard NaOH solution [11]. The results recorded by the potentiometric method agree reasonably well with those obtained using titrimetry. The advantage of potentiometric method consists in the short time spent for analysis and reliable results.

#### Conclusion

The reaction of the triaqua-hexapivalato-tri- $\mu$ -oxo-trichromium(III) nitrate with 4,4'-bipyridyl *in situ* during the formation of the plastisized PVC membrane gives rise to a nitrate potentiometric sensor with good operating characteristics (sensitivity, stability, life time and response time), able to be used for potentiometric determination of this ion.

#### References

- [1] Braven J., Ebdon L., Scholefield D. High-performance nitrate-selective electrodes containing immobilized amino acid betaines as sensors. *Anal. Chem.*, 2002 Jun, V 74, p. 2596-2602.
- [2] Asgari A., Amini M., Mansour H. Nitrate-selective membrane electrode based on bis(2-hydroxyanil)acetylacetone lead(II) neutral carrier. *Analytical Sciences*, 2003 august, V 19, p. 1121-1125.
- [3] Kong Thoo L., Araujo A., Montenegro M. New PVC nitrate-selective electrode: application to vegetable and mineral waters. *Agric. Food Chem.*, 2005 Jan, V 26, p. 211-216.
- [4] Bendikov T., Harmon T. A sensitive nitrate ion-selective electrode from a pencil lead. *Journal of Chemical Education*, 2005 March, V 82, p. 439.
- [5] Ortuno J., Exposito R., Sanchez-Pedreno C. A nitrate-selective electrode based on a tris(2-aminoethyl)amine triamide derivative receptor. *Anal. Chim. Acta*, 2004 november, V 525, p. 231-237.
- [6] Revenco M., Martin M. Noi materiale electroactive pentru membranele senzorilor potențiometrice. *Analele științifice ale Universității de Stat din Moldova, Seria „Științe reale”*, Lucrări de sinteză 1996-2006, Chișinău, 2006, p.90-97.
- [7] Wael Ahmad Abu Dayyih. Potentiometric sensors based on polynuclear complex compounds for determination of some drug-substances. Ph.D. Thesis, State University of Moldova, Chisinau, 2002.
- [8] Revenco M., Martin M. Senzori potențiometrice pentru determinarea percloraților. *Analele științifice ale Universității de Stat din Moldova, Seria „Științe chimico-biologice”*, Chișinău, 2006, p.480-483.
- [9] Simonov Yu., Bouroush P., Timco G. Synthesis, structure and mass-spectrometric-investigation of chromium trinuclear  $\mu$ -oxo-carboxylates. *Chem. Bull., Romania* 1998, V 43, p. 128-136.
- [10] Камман К. Работа с ионселективными электродами, М., Мир 1980, 283 с.
- [11] Harris D. *Quantitative Chemical Analysis*, New York, Freeman and Company 1998, p.1025.

# CONSIDERATIONS ON LIQUID-CHROMATOGRAPHIC SEPARATION FOR AN EQUIMOLAR MIXTURE OF 2,4-DINITROPHENYLHYDRAZONES OF ACETALDEHYDE AND DIACETYL

Gheorghe Zgherea

*Department of Chemistry, Faculty of Sciences, University "Dunărea de Jos" of Galați  
111 Domnească street, 800.201 Galați, Romania, phone +40 236 414871, fax +40 236 461353  
gzgherea@chem.ugal.ro*

**Abstract:** An equimolar mixture of 2,4-dinitrophenylhydrazones (2,4DNPH-ones) providing by acetaldehyde and diacetyl must be analyzed by liquid-chromatographic separation, using the mechanism of repartition with reverse phase; that full papers is for identification the optimal analytical conditions. As mobile phase are utilized various binary mixtures eluent, containing water and methanol, with 0-45% water. By the experimental studies were identified four domains of behavior and two optimal binary mixtures, with 25% and 45% water, thus this is a study on the behavior of binary mixtures mobile phases. The peaks are characterized by values of retention times and by position. The separation processes were appreciated by difference between the retention times of peaks; if the percent of water increase, the values of retention times is higher. When the percent of water is 45%, the difference between the retention times is maxim, associated with a change of peaks position.

**Keywords:** acetaldehyde, diacetyl, reverses phase, polarity, percent of water, inversion of position.

## Introduction

Any foods obtained by fermentation have small quantities of carbonyl compounds. They have a very important contribution to the flavor and the fragrance; between these compounds there are acetaldehyde and diacetyl. On consider that the diacetyl is the vicinal dicetone with a very important contribution at the sensorial properties of beer. In addition, his concentration in beer ( $0.01-0.2 \text{ mg}\cdot\text{L}^{-1}$ ) is a reference values for the level of oxidative process during preparative process. That explains the major preoccupations on the physical-chemistry methods to identification and to dose beer's diacetyl. Between these methods there is the distillation of carbonyl compounds and transfer in a strong acid solution of 2,4-dinitrophenylhydrazine; the mixture of insoluble precipitates of 2,4-DNPH-ones is separated by filtration, washed with bidistilate water, dried and solved in organic solvent (methanol, acetonitrile, tetrahydrofuran), followed by an appropriate liquid-chromatographic separation.

The described analytical method may be use for any mixture of carbonyl compounds. The 2,4-DNPH-ones are solid substances, yellows, soluble in organic solvents [1]. The literature doesn't have specific reference about their polarity [2-3]; may be compared only the polarity values for carbonyl compounds providers.

After their behaviors, the mixtures of 2,4-DNPH-ones may be analyzed by HPLC, using the mechanism of repartition with reverse phase; may be used a slightly polar stationary phase (octadecysilan) and a mixture of mobile phase containing water (strongly polar solvent) with a slightly organic solvent [4-7]. The no polar stationary phase assures a strongly retaining of slightly polar molecules of 2,4DNPH-ones. The no polar mobile phases provides a better solubilisation of 2,4DNPH-ones, assuring a better mass transfer between the mobile and stationary phase; thus, the peak are symmetrically, narrows and with small values of retention times. The polar mobile phase provides a small solubilisation and a hard mass transfer between the phases; the peaks are asymmetrically and with higher values of retention times. Therefore, a higher resolution between peaks is assured only by optimal mixture of mobile phase, when the difference between retention time values is maxim, for the adjacent peaks.

In the upper case, analytical difficulties are generating by the similar behavior of 2,4DNPH-ones providing by diacetyl (2,4-DNPD) and acetaldehyde (2,4-DNPHAA). Must be established the optimal mixture of mobile phase (with water and methanol) to assure the best separation for an equimolar mixture (a model synthetic mixture) of the two 2,4-DNPH-ones.

## Results

Ten chromatograms were obtained. Each chromatogram has two chromatographic signals (peak); the identity of signals was verified by addition method.

The behavior of eluent (methanol or mixtures of mobile phase) was appreciate by difference between the values of retention times of 2,4DNPH-ones

$$\Delta RT = (RT_{2,4DNFHAA} - RT_{2,4DNFHD}) \quad (1)$$

The  $\Delta RT$  values are dependence by molecular structure of 2.4DNPH-ones and the phenomena that are produce during the liquid chromatographic separation process, being an expression of relation between their repartition coefficients values.

The  $\Delta RT$  (sec) values are represented graphic against the mobile phase polarity, defined by the percent of water value in the mixture of mobile phases. On obtain the diagram of figure 1, with delimitation of four especially domains behavior of eluent mixtures.

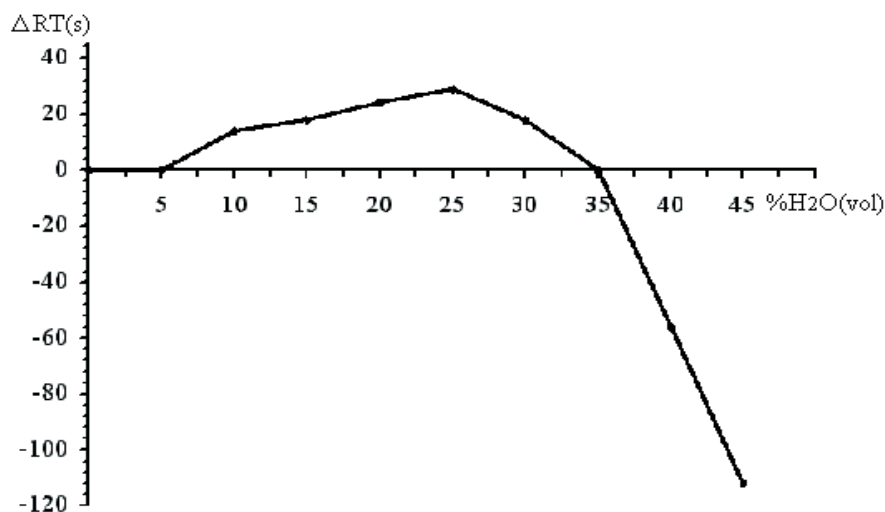


Figure 1. Diagram of  $\Delta RT$  values against the polarity of mobile phase mixture

## Discussion

Need to explain the structure and behavior of two 2.4DNPH-ones, beginning from the structure of provider's carbonyl compounds. To explain the difference between behaviors, need to consider physical behavior of two species of molecules: mass, volume and polarity. Can be considerate that the asymmetric molecules of 2.4DNPHAA ( $M_{2,4DNFHAA} = 224 \text{ g}\cdot\text{mol}^{-1}$ ) are slowly plus polar than the symmetric molecules of 2.4DNPHD ( $M_{2,4DNFHD} = 446 \text{ g}\cdot\text{mol}^{-1}$ ).

To explain the four distinct behaviors of the mobile phase mixtures, need to considerate the contributions of the essential process which there are on the stationary phase: the zone of concentration, for each 2.4DNPH-one, is in extension. This process affects the retention time values, thus and the  $\Delta RT$  values.

On the stationary phase there are, simultaneously, three distinct phenomena: the longitudinal diffusion, the turbulent diffusion and the no local equilibrium (resistance at the mass transfer process, between the two immiscible phases). On may be considered that only two distinct phenomena have the most important contribution at the concentrated zone extension. The stationary phase have only spherically and equal particles and the mobile phase flow at the high pressure ( $> 100 \text{ bar}$ ); in this instance, the contribution of turbulent diffusion is insignificant for the general process.

Follow-up are presented the behavior of mobile phase, against the water percent in the mixture.

### *The domain 0-5% water (the mobile and stationary phase are no polar too)*

The polarity of mixture is very slow, as the stationary phase as. The interaction between the 2.4DNPH-one's molecules and the stationary phase must be higher, but the most important part of molecules is dissolved in the no polar liquid mobile phase. No local equilibrium is completely absent, but is very weak the phenomenon of longitudinal diffusion, generating a simultaneously elution for the molecules of the two 2.4DNPH-ones. The two molecular species are characterized by identically and low coefficients of repartition and retention times values, thus  $\Delta RT = 0$  seconds.

### *The domain 5-25% water (the behavior's molecules is in accord with their dimensions)*

Increase the polarity of the eluent by water percent; this value produces an increase of interaction between the 2.4DNPH-one's molecules and no polar stationary phase. Simultaneously, increase the intensity of no local equilibrium.

The lower and asymmetrically molecules of 2.4DNPHAA, weak polar, are characterized by lower value of diffusion coefficient from the stationary phase to mobile phase, being intense retained. The lower diffusion process

in mobile phase produce an intense process of longitudinal diffusion, thus an extension of zone; the 2.4DNPHAA molecules generate large peaks, symmetrically, but with high values of retention time.

The big and symmetrically molecules of 2.4DNPHD, no polar or slightly polar, are characterized by higher value of diffusion coefficient from the stationary to mobile phase. Because their physical dimension, these molecules are slowly values of longitudinal diffusion in the mobile phase, generating narrow and symmetrically peak, but with low values of retention time. Like the different behavior, the relation between the coefficients of repartition is

$$k_{2,4DNPHAA} > k_{2,4DNPHD} \quad (2)$$

The retention time values there are in the same relation, thus the  $\Delta RT$  values are positive; the mobile phase with 25% water represent the binary eluent mixture who generate two chromatographic peaks with a maxim value of difference between retention time values,  $\Delta RT = 29$  seconds.

*The domain 25-35% water (the behavior's molecules is in accord with their slow polarity)*

For higher values of water percent, the polar eluent produce a higher interaction of molecules with the particle of stationary phase, increasing the values of retention times. The phenomenon of longitudinal diffusion becomes important. In addition, became very intense the process of no local equilibrium (resistance at mass transfer from the stationary phase to the mobile phase); the eluent mixture with a high percent of water undertake very hard the organic molecules of 2.4DNPH-ones. Conclusively, increase the dimension's zone of concentration and the values of retention times. The values of retention times have an unequal increasing, with the tendencies to become identically (at higher value of water percent), thus the molecular species have the same behavior; the  $\Delta RT$  values subside. If the mobile phase have 30% water, the corresponding value  $\Delta RT = 18$  seconds. For the superior limit of domain, 35% water, the two 2.4DNPH-ones are characterized by identical values of repartition coefficients, thus, equal values of retention times,  $\Delta RT = 0$  seconds

$$k_{2,4DNFHAA} = k_{2,4DNFHD} \quad (3)$$

All the mixture of mobile phase with 25-35% water (plus polar mixture) produce subside of peak's resolution.

*The domain 35-45% water*

The eluent mixtures become very polar and produce an intense interaction between the non polar molecules and the particle of stationary phase, non polar too; the behavior of molecules may be justified again by the slowly different values of polarity. In this case, the values of repartition coefficients increase very much; for the phenomenon of mass transfer from stationary phase to mobile phase there are a similarly evolution, extending the zones of concentration. Simultaneously, the retention time's values increase with proper rate. On observe that relation between the values of repartition coefficients become,

$$k_{2,4DNFHAA} < k_{2,4DNFHD} \quad (4)$$

A similar relation is between retention times values, thus  $\Delta RT$  values become negative.

Because the water percent is very higher, the 2.4DNPH-ones molecules transport is affected by no local equilibrium and by high values of coefficient of longitudinal diffusion.

The symmetric and no polar molecules of 2.4DNPHD are strongly retained on stationary phase particles. The asymmetric and weak polar molecules of 2.4DNPHAA pass soft from the particles of stationary phase in the liquid polar mobile phase.

The polar mixture mobile phase provides an inversion of zones position on stationary phase, thus a position's inversion of the peaks in chromatogram. The eluent mixture with 40% water assure a separation process characterized by a good resolution between peak,  $\Delta RT = -56$  seconds; if the percent of water is 45%, the process of chromatographic separation have a better resolution,  $\Delta RT = -112$  seconds.

## Conclusion

On the experimental results may be formulated the following conclusions:

1. Using binary isocratic mixture, containing methanol and water (0-45%, percent of volume), the equimolar mixture of 2.4DNPHAA and 2.4DNPHD may be separate by liquid-chromatography with reverse phase; the resolution of chromatographic signals depend by the polarity of mobile phase.

2. The similarly behavior of 2.4DNPH-ones may be described by structurally particularity of carbonyl compounds provider: dimension, symmetry, solubility in solvents and, especially, by polarity.

3. The succession of concentrated zones on the stationary phase, thus the positions of signals in chromatograms

is dependent of mobile phase polarity; the retention time values of two 2,4-DNPH-ones are too higher, for big values of mobile phase polarity.

4. Higher values of mobile phase polarity provide a change of chromatographic signal positions, thus the inversion of signals positions in chromatograms.

## Experimental

### *Etalons, solvents, equimolar mixture, mobile phase and liquid chromatographic separations*

The 2,4-DNPH-ones etalons, provided by acetaldehyde (2,4-DNPHAA) and diacetyl (2,4-DNPHD), was synthesized (by simply mixing at room temperature, with a better yield, being perfectly reproducible) and purified (by recrystallisation) in our laboratory, through: filtration, washing with water, drying and filtration.

In acetonitrile (Merck) was obtained solution  $10^{-4}$  M, for each 2,4-DNPH-one etalon. In figure 2 are presented the structures of two 2,4-DNPH-ones etalons. The equimolar mixture was obtained by mixing the two etalon solutions in ratio 1:1 (v:v); each 2,4-DNPH-one has  $5 \cdot 10^{-5}$  M concentration.

The bidistillate water ( $2 \mu\text{S} \cdot \text{cm}^{-1}$ ) is prepared in our laboratory, from distilled water, after a treatment with sulphuric acid and kalium permanganate. The mobile phases are methanol and nine binary mixtures containing bidistillate water and methanol (Merck, for liquid chromatography); the percent of water has the value 0-45%, controlled by LC gradient programmer module.

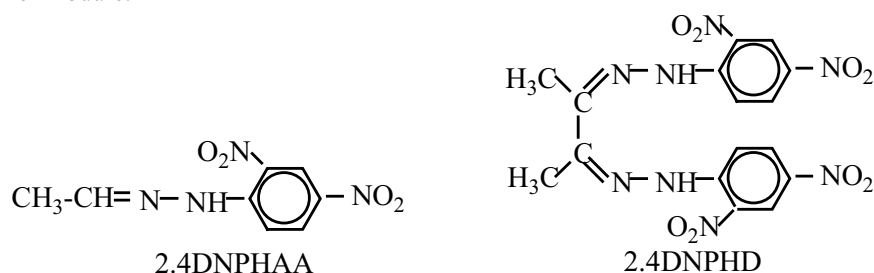


Figure 2. The chemical structures of 2,4-DNPH-ones etalons

### *Apparatus*

The separations was utilized LC-XPD Pye Unicam Philips liquid chromatograph who include: solvent metering system (two reservoir for mobile phases, the module of controlled mixing type LC gradient programmer, high pressure pump type Spectra Physics 100A), Rheodyne valve 7125 (for the mixture sample), liquid chromatographic column (Spherisorb 5ODS, 25 cm length and 4,6 mm internal diameter, with gradient of stationary phase), with a module of thermostatisation, LC-UV detector, electronic integrator for chromatographic signal (type DP101) and potentiometric recorder (type PM8251).

### *Experimental conditions*

The equimolar mixture was liquid-chromatographic separate, in the following conditions:

10  $\mu\text{L}$ , volume of mixture;

Temperature of separation column  $37,5^{\circ}\text{C}$  (at high temperature of mobile phase increase the solubility of compounds);

Detector: UV Absorbance ( $\lambda=355$  nm);

Flow rate= $1 \text{ mL} \cdot \text{min}^{-1}$ .

### *Liquid chromatographic separations*

Identical volumes of equimolar mixture were separate by HPLC, using the précised mobile phases.

## References

- [1] Gheorghe Zgherea, Synthesis and Comparative Characterization of Eight 2,4-dinitrophenylhydrazones, The Annals of „Dunărea de Jos” University of Galați, Fascicle VI, 1999, ISSN 1221-4574, pp 4-9.
- [2] David R. Lide, ed., CRC Handbook of Chemistry and Physics, Internet Version 2005, <<http://www.hbcnpnetbase.com>>, CRC Press, Boca Raton, FL, 2005.
- [3] Zahn C. T., The Dielectric Constant of Dichlorethane, Dibromethane, Chlorobromethane, and Diacetyl; and the Phenomenon of Free Rotation, 1932 The American Physical Society, <http://link.aps.org/abstract/PR/v40/p2>.
- [4] Candin Liteanu; Simion Gocan; T. Hodisan; H. Nascu, Cromatografia de Lichide, Editura Stiintifică, București, 1974, pp 156-157.
- [5] Douglas A. Skoog, Principles of Instrumental Analysis, Third edition, Saunders College Publishing, 1985, pp 801-815.
- [6] Simion Gocan, Cromatografie de Înaltă Performanță, Partea a II-a, Cromatografia de Lichide pe Coloane, Editura RISOPRINT, Cluj-Napoca, 2002, pp 173-183.
- [7] Raymond P.W. Scott, Liquid Chromatography, pag 55-62, <http://www.library4science.com/eula.html>.

# THE MIXTURES OF 2,4-DINITROPHENYLHIDRAZONES OF INFERIOR CARBONYL COMPOUNDS AND THEIR HPLC SEPARATION WITH GRADIENT BINARY MIXTURES PHASES

Gheorghe Zgherea

Department of Chemistry, Faculty of Sciences, University "Dunărea de Jos" of Galați  
111 Domnească street, 800.201 Galați, Romania, phone +40 236 414871, fax +40 236 461353  
gzgherea@chem.ugal.ro

**Abstract:** Mixtures of small quantities of carbonyl compounds are presents in foods, concerning sensorial qualities. The inferior carbonyl compounds ( $C_2$ - $C_4$ , boiling point  $<100^\circ C$ ) – mono and dicarbonyl – can be identified and measured their concentrations, after a separation by distillation on the water bath. They are transferred in a strongly acid solution of 2,4-dinitrophenylhydrazine (2,4-DNPH), generating a mixture of insoluble 2,4-dinitrophenylhydrazones (2,4-DNPH-ones). The 2,4-DNPH-ones are organic compounds with weak polarity, solids, crystallized, yellows and water insoluble, soluble in organic solvents. The mixture of 2,4-dinitrophenylhydrazones may be separated by liquid chromatography, using the reverse phase mechanism [1-3]. This paper contains experimental and theoretical considerations to the means of separation through liquid chromatography of two synthetically and a natural mixtures that contain 2,4-DNPH-ones provided by inferior carbonyl compounds; to obtain conclude results, in the synthetically mixtures was introduce and 2,4-DNPH-ones provided by carbonyl compounds having three (acetone and propanal) and four (isobutyl aldehyde) atoms of carbon.

**Keywords:** acetic aldehyde, diacetyl, 2,4-dinitrophenylhydrazone, reverse phase, low polarity, gradient of mobile phase

## Introduction

In many case, for the foods obtained by fermentation, it is very important to know the concentration of diacetyl and acetic aldehyde. Accordingly the literature, in beer there is diacetyl and acetic aldehyde in ratio 1:100. The interest on diacetyl concentration needs especially analytical conditions. It is possible to solve that problem by HPLC for the mixtures of 2,4-DNPH-ones provided by inferior carbonyl compounds. HPLC can be made a good separation only for the synthetics mixtures of 2,4-DNPH-ones; the molecules of inferior carbonyl compounds have the same physical and chemical behavior [4]. The difficult appears for the natural mixtures of carbonyl compounds. The difficult is greater if the ratio between quantities is too low. To have a good analytical performance, need to use liquid chromatography separation with gradient of mobile phase [5].

## Results and Discussion

The synthetic mixtures ( $SM_I$  and  $SM_{II}$ ) and a natural mixture from beer were separate by liquid-chromatography, using a mechanism of reverse phase.

### Conditions of chromatographic separation

Injection volume: 10  $\mu L$ ;

Column: Spherisorb 5 ODS with gradient of stationary phase ( $L=25$  cm,  $\Phi=4.6$  mm);

Temperature of separation column:  $37.5^\circ C$ ;

LC UV detector:  $\lambda=355$  nm;

Flow rate: 1 mL/min.

Eluent: a mixture of A-methanol and B-water, accordingly to two programs realized by the LC-XPD module.

### The liquid-chromatographic separations

Both categories of liquid-chromatographic separation were realized on the same column, at the same temperature, changing only the program on mixing of liquids in binary mixture of mobile phase.

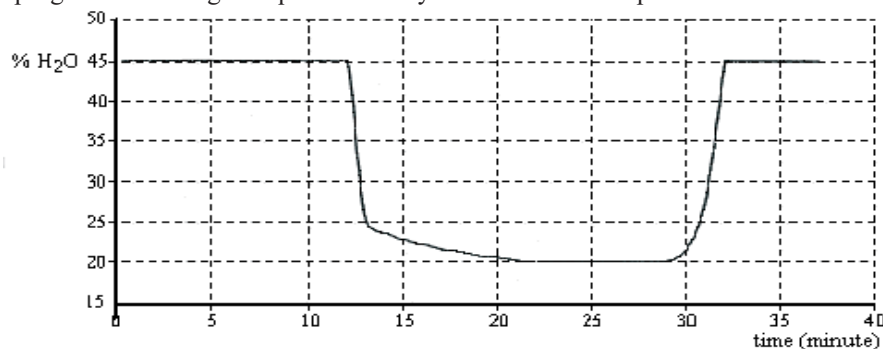


Figure 1. The program of GBMP<sub>1</sub>

The mixtures of mobile phase has the same initially composition, with 45% water. In this instance, the 2.4-DNPHAA will be eluted before the 2.4-DNPHD. This way is guaranteed the maximum difference between the values of retention times for the mentioned 2.4-DNPH-ones and a preliminary separation of the 2.4-DNPH-ones with three and four atoms of carbon. The synthetic mixture SM<sub>I</sub> contains four 2.4-DNPH-ones in the following ratio of volume:

2.4-DNPHAA: 2.4-DNPHD: 2.4-DNPHA: 2.4-DNPHiBA = 2:1:1:1.

The first program of binary mobile phase, BGMP<sub>I</sub> (32 minutes, figure 1), contains four time segments; in figure 2 there are the chromatogram of synthetic mixture SM<sub>I</sub>, obtained with BGMP<sub>I</sub>.

According BGMP<sub>I</sub>, the separation begins with a mobile phase having 45% water; the mixture of mobile phase has a higher polarity. This mixture is hold during the first time segment, g=1 (t=12 minutes), assuring a better resolution between the signal of 2.4-DNPHAA (844 s) and the signal of 2.4-DNPHD (918 s). The weak polar molecules of two 2.4-DNPH-ones are strongly retained on the no polar stationary phase. Therefore, the longitudinal diffusion of concentrated zone is lower. Simultaneously, on the stationary phase are strongly retained the 2.4-DNPH-ones provided by acetone and i-buthanal.

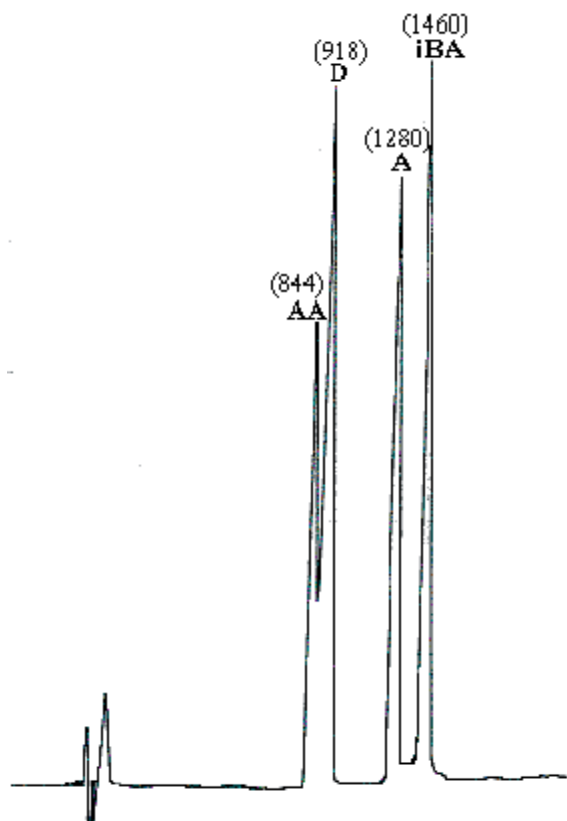


Figure 2.

The chromatogram of synthetic mixture abbreviate SM<sub>I</sub> AA is the chromatographic signal for the 2.4-DNPHAA and 844 is the retention time, in seconds;

D represents the chromatographic signal for the 2.4-DNPHD and 918 is the retention time (seconds);

A represents the chromatographic signal for the 2.4-DNPHA and 1280 is the retention time (seconds);

iBA represents the chromatographic signal for the 2.4-DNPHiBA and 1460 is the retention time (seconds).

On the second timing segment, g=2 (t=10 min, n=0.1), the percent of water will be reduce at 20%, thus the polarity of mobile phase subside; the 2.4-DNPHAA and 2.4-DNPHD (more soluble in organic solvent) diffuse in the mobile phase and will be transported to the end of separation column. On the third timing segment, g=3 (t=5 min, n=1), the percent of water is constant (20%), to assure the best separation of 2.4-DNPHA and 2.4-DNPHiBA. The last timing segment, g=9 (t=5 min, n=5.5), is destined to recondition stationary phase, for a new separation; all the timing segments g=4-8 are inactive.

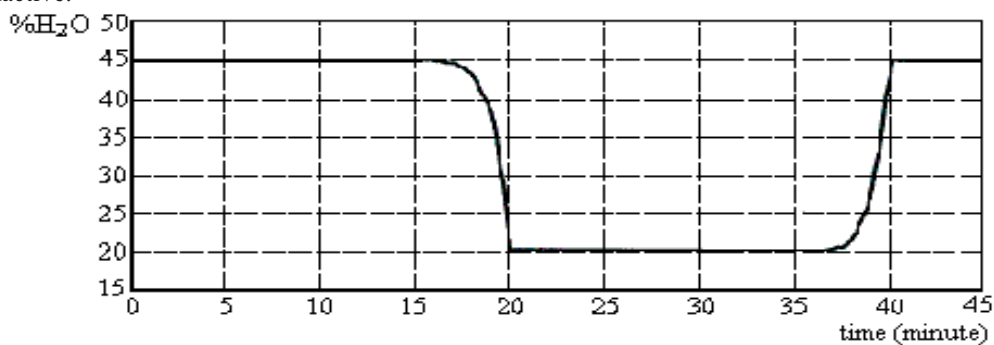


Figure 3. The program of GBMP<sub>II</sub>

The second program of binary mobile phase, BGMP<sub>II</sub> (40 minutes, figure 3), contains four time segments too; in figure 4 there are the chromatogram of synthetic mixture SM<sub>II</sub>, obtained with BGMP<sub>II</sub>. The synthetic mixture SM<sub>II</sub> contains the same 2.4-DNPH-ones as SM<sub>I</sub>, in the ratio of volume:

2.4-DNFHAA: 2.4-DNFHD: 2.4-DNFHA: 2.4-DNFHiBA = 4:1:5:5.

As in previous case, the first timing segment, g=1 (t=15 min), the mixing program assures an eluent with 45% water, for the best separation between 2.4-DNPHAA and 2.4-DNPHD; the polarity of mobile phase is higher (the molecules of 2.4-DNPH-ones are strongly retained on the stationary phase).

The second timing segment, g=2 (t=10min, n=9.9), the percent of water is reduced at 20%; this value is constant and during the third timing segment, g=3 (t=15min). Subside of mobile phase polarity produce a desorbitive process from the stationary phase. The timing segments, g=4-8 haven't got a specific content. In the last timing segment, g=9 (t=5min, n=0.1) quickly rebuilds the initial mixture of mobile phase; at the finish, the analytical system is completely ready to a new separation.

Comparing the chromatograms from figures 2 and 4, may be concluded that the BGMP<sub>I</sub> assure a better separation for the 2.4-DNPHAA and 2.4-DNPHD; for the 2.4-DNPHA and 2.4-DNPHiBA, the resolution is comparable.

The figure 5 is a chromatogram of a natural mixture of 2.4-DNPH-ones, for the inferior carbonyl compounds of beer. The liquid-chromatographic separation is on the same column and the eluting program GBMP<sub>I</sub>.

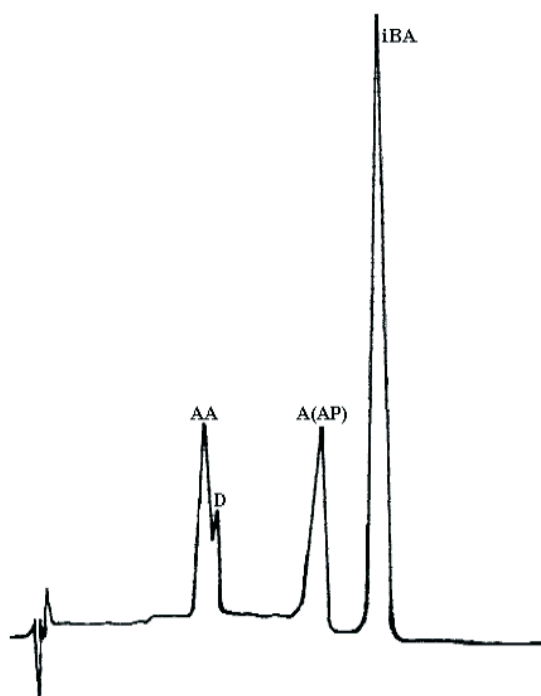


Figure 4.

The chromatogram of SM<sub>II</sub>

AA - chromatographic signal for the 2.4-DNPHAA;

D - chromatographic signal for the 2.4-DNPHD;

A - chromatographic signal for the 2.4-DNPHA  
(after the same retention time appear the signal for  
propanal);

iBA - chromatographic signal for the 2.4-DNPHiBA.

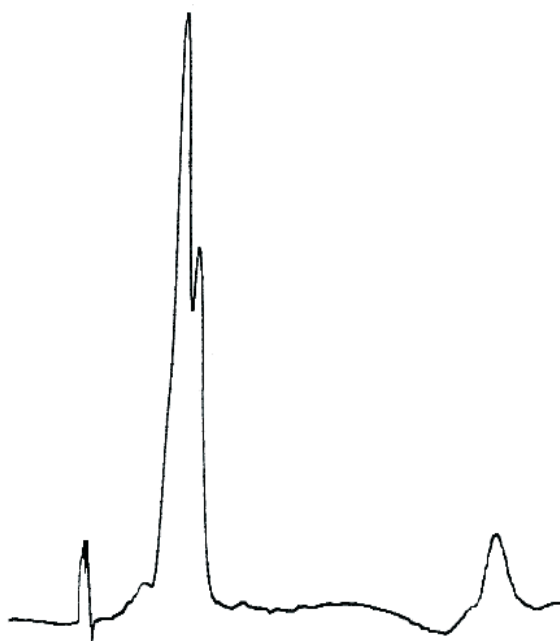


Figure 5.

The chromatogram of  
natural mixture of 2.4-DNPH-ones

Using the external standard method, for the chromatographic signal of 2.4-DNPHAA, obtain 14.75 mg·L<sup>-1</sup> as concentration of acetic aldehyde in beer; the value is in concordance with the literature. The surface of chromatographic signal of 2.4-DNPHD offer a value of 2.5 mg·L<sup>-1</sup> as concentration of diacetyl in beer; this value is higher. In beer, the normal values of diacetyl concentration is 0.01-0.2 mg·L<sup>-1</sup>; 0.15 mg·L<sup>-1</sup> is the threshold value.

## Conclusions

On the basis of these experiments may be formulating the following conclusions:

1. Was established two optimal programs for providing mixtures of binary eluent; according them, it is provided

two mixture of binary phase that assure liquid-chromatographic separation, with a good resolution, for the synthetically mixtures of 2.4-DNPH-ones provided by the carbonyl compounds with 2-4 atoms of carbon.

2. The binary mixtures of mobile phase, obtained by the programs GBMP<sub>I</sub> and GBMP<sub>II</sub>, assure a better separation of synthetic mixtures which contain the derivate compounds of inferior carbonyl compounds; in these synthetic mixtures the ratio between 2.4-DNPHAA and 2.4-DNPHD is higher than one, but very low.

3. In the case of natural mixtures of 2.4-DNPH-ones, similarly with synthetic mixtures, the binary mixtures of mobile phase offer only partially analytical satisfaction. Thus, the figure 5 contains evident the dominant peak of 2.4-DNPHAA. Using his surface value for quantitative appreciation by external standard method, obtain experimental values accordingly with the literature, namely 15 mg·L<sup>-1</sup> acetic aldehyde [6]. In the same chromatogram, the peak of 2.4-DNPHD there is the second, but the second one is on the tailing peak of the first one. On the natural mixture of 2.4-DNPH-ones one might make the following consideration: if the literature offer the real concentration values for the two carbonyl compounds, the accuracy of analytical system will be justified by the big value, ~100, of the ratio between the quantities of acetic aldehyde and diacetyl. In this instance, the little peak of 2.4-DNPHD appears as a tailing peak on the big peak of 2.4-DNPHAA, thus, his surface is higher than the normal one; the mistake value of surface chromatographic signal became a source of mistake value of concentration.

4. Each chromatogram – figures 2, 4, and 5 – contains any signals with lower values of retention time; it is the signals for solvent.

## Experimental

### *Solvents and mobile phases*

The acetonitrile was utilized to solve the pure 2.4-DNPH-ones. To liquid-chromatographic separations was utilized two binary gradient mixtures of mobile phase – GBMP<sub>I</sub> and GBMP<sub>II</sub> – with water (2 S·cm<sup>-1</sup>) and methanol (Merck).

### *The synthetic mixtures of 2.4-DNPH-ones*

The pure 2.4-DNPH-ones – yellow powders – are obtained in our laboratory, using 2.4-DNPH and chemical pure carbonyl compound; thus: 2.4-DNPHAA (acetic aldehyde), 2.4-DNPHD (diacetyl), 2.4-DNPHA (acetone), 2.4-DNPHP (propanal) and 2.4-DNPHiBA (isobutyl aldehyde). Their purity was verified by: elemental analysis, IR spectrophotometry and liquid-chromatographic separations. In acetonitrile (Merck, pro liquid chromatography) were obtained 5·10<sup>-4</sup> M solutions. By controlled mixing was obtained two synthetic mixtures, abbreviated SM<sub>I</sub> and SM<sub>II</sub>; the ratio between the quantities 2.4-DNPHAA and 2.4-DNPHD is higher to one, in each mixture.

### *The natural mixtures of 2.4-DNPH-ones*

The carbonyl compounds from beer were separate by distillation on the water bath and transferred in 2.4-DNPH, acid solution; the precipitates form a natural mixture of 2.4-DNPH-ones. They are isolated by filtration, washing with pure water, drying and solved in acetonitrile.

### *Apparatus*

For the separations was utilized Pye Unicam Philips liquid chromatograph, equipped with: an installation for degassing of mobile phase (by refluxation) [7], gradient programmer for mobile phase (type LC-XPD, able to mix two liquids), separation columns with gradient of stationary phase, installation for column thermostatisation, electronic integrator (type DP101) and potentiometric recorder (type PM8251). The mixing program of liquids has nine segments of time, g=1-9; each timing segment has independent dimension of 0-99 minutes. In every moment, the value of **B**, the percent of the second component in the mixture of mobile phase (**A** + **B**=100), is

$$\% B = k \cdot t^n \quad (1)$$

where, t – dimension of timing segment (minutes), k – slope of curve (describes the evolution of **B** value on the t segment), n – exponent, with values 0.0-9.9 (describes the geometry of mixing curve).

## References

- [1] Simion Gocan, Cromatografie de Înaltă Performanță, Partea a II-a, Cromatografia de Lichide pe Coloane, Editura RISOPRINT, Cluj-Napoca, 2002, pp 173-183.
- [2] Douglas A. Skoog, Principles of Instrumental Analysis, Third edition, Saunders College Publishing, 1985, pp 801-815.
- [3] Candin Liteanu; Simion Gocan; T. Hodisan; H. Nascu, Cromatografia de Lichide, Editura Stiintifica, Bucuresti, 1974, pp 156-157.
- [4] Radu Bacaloglu; Carol Csunderlik ; Livius Cotarcă; Hans-Horst Glatt, Structura și Proprietățile Compușilor Organici, volumul I, Editura Tehnică, București, 1985, pp 116-127.
- [5] Gort S.M., Hogendoorn E.A.; Dijkman E.; Van Zoonen P.; R. Hoogerbrugge, The Optimisation of Step-Gradient Elution Conditions in Liquid Chromatography, Chromatographia, vol. 42, No 1/2, ian 96, pp 17-24.
- [6] \*\*\* BIERANALYSE 9.11 Bestimmung der Gärungsnebenprodukte in Bier, pp 246-250.
- [7] Gheorghe Zgherea, Installation to Continuously Degassation by Refluxing of Mobile Phases for HPLC, Annals of West University of Timișoara, series Chemistry 12 (3) (2003) pp 1157-1160.

## STUDY ON QUANTITATIVE SPECIATION, BY BCR METHOD, OF ZINC CONTENT FROM RIVER SEDIMENTS

Georgiana Vasile\*, Stanescu Bogdan, Tudor Claudia, Elena Mihaila

National Research and Development Institute for Industrial Ecology – ECOIND 90-92 Panduri Road, 050663,  
Bucharest, sector 5, Romania

\*Corresponding author: phone: +40/21/4100377; fax: +40/21/4100575; e-mail: ecoind@incdecoind.ro

**Keywords:** sediment, sequential extraction, bioavailability, zinc mobility.

An unwanted consequence of human activity and of uncontrolled industrialization is the environment contamination with a lot of pollutants, among them heavy metal anthropogenic pollution having some most serious consequences. A reliable estimation of pollution level is made by studying heavy metal concentrations in the sediments.

In our study the zinc content of the water and river sediments has been investigated, in an area polluted by mining activities, to provide information on the mobility and availability of this element. Sediment and water samples have been collected from significant sites in a former mining area in which with some sterile pits, which represent a major environmental hazard.

The zinc mobility and bioavailability in the environment was investigated by the three-step sequential extraction procedure, a protocol proposed by the Standards, Measurements and Testing programme (SM & T—formerly BCR) of the European Union. The BCR sequential extraction scheme has the advantage that there are reference materials available with certified and indicative values for the concentrations of selected elements in the particular extraction steps. The BCR procedure enables fractionalization of metal content into the following fractions:

- EASILY MOBILIZABLE FRACTION: This fraction contains the specifically bound, surface occluded species (sometimes also CaCO<sub>3</sub> bound species and metallo-organic complexes with low bonding forces).
- ORGANICALLY BOUND FRACTION
- Mn-Fe-and Al-OXIDE BOUND FRACTION
- RESIDUAL FRACTION: This fraction mainly contains crystalline-bound trace metals and is most commonly dissolved with high concentrated acids and special digestion procedures.

Combination of data from sequential extraction procedures and normalisation approaches provides a good basis to estimate the proportions of the easily and sparingly soluble metal fractions in the samples investigated and to identify the anthropogenic input of metals into the environment.

### Introduction

From the pollution types that are to be found in our country, the most prevalent and having powerful effects for the quality of surface waters and of the sediments, is the heavy metals pollution that is to be found especially in the areas having a long ores extraction activity.

Understanding the importance of sediments role in contaminants transport and storage, conduced to an increasing preoccupation of the researchers and of the organisms responsible for the control and the prevention of water pollution, in the pollutant compounds knowledge field.

For an evaluation of heavy metals charge in the sediments, is not sufficient to determinate their total concentration. The establishment of the metals proportions in easy soluble fractions and in the hard soluble ones is very important.

These fractions evaluation allows the elucidation of their existing dangers and seriousness for the aquatic ecosystems [1].

The signification of speciation analyze as a method for estimating the environment risk was recognized by the Environment Conservation Council from Australia and New Zeeland (ANEZECC), who recomanded the examination of bioaccessible concentrations, where the metals total levels overpass the levels established into the Interimare Quality Criteria for Sediments[2].

For the estimation of the natural and the anthropogenic inputs of the heavy metals in the sediments, are used identification methods by sequential chemical extraction (BCR technique) and normalizations, based on the correlations between the concentrations of the elements present in the tracks, and an element that is naturally present in the investigated environment [3].

Further on are presented the results of the researches effectuated on sediments sampled from Certej River, which is affected by the long ore extraction activities. The papers that present the results in the thematic approach were directed towards zinc content knowledge and towards the quantification of its existing forms in sediments.

## Experimental part

### Study area

The studied Certej River sector is placed on the territory of Certej village, Hunedoara district almost 20 km to Deva, on north direction.

This river sector, named Baiaga Valley, is spreading on a 1 km distance between the confluence with Bocsă Mare (Coranda) River and the confluence with Bocsă Mica (Ciongani) River. This rivers tributary to Certej Valley bring a significant contribution of heavy metals pollution, taking into account the fact that in the area between the rivers, on their valleys and also in Baiaga Valley sector, are placed objectives belonging to some mining exploitations having the precious metals extraction activity field. These objectives are represented by open exploitations, underground exploitations and by wastes deposits afferent to them – dumps.

### Sampling

The investigations objective was to establish the quality of the sediments of Baiaga River (Certej) upstream and downstream the objectives that generate pollution as a consequence of the activity unrolled in the area, in order to put in bold line a possible accumulation of the pollutants from the water, in the sediments.

In order to effectuate the experiments the sediments were collected along Baiaga River sector (samples 1-7) and on its affluent (Coranda River, Nicodim gallery, Ciongani River and quarry water) (samples 8-10) presented in figure 1. The samples were collected from the upper layer of the sediment, along with the surrounding water, in order to estimate the natural substance of the studied analytes.

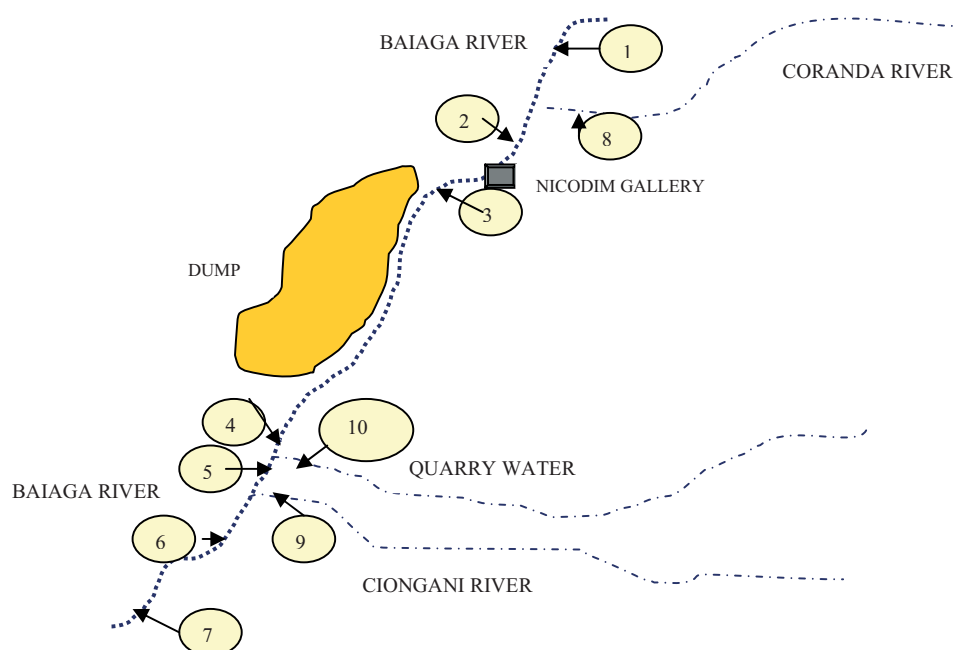


Fig. 1. Sampling sites of the investigated area

### Equipment

Metals concentrations were determined by atomic absorption spectrophotometer in flame, to a Nova A 300 instrument (Analytik Jena, Germany), in air-acetylene flame.

Zinc extraction from the sediment by the sequential extraction procedure was realized in 50 ml polyethylene tubes. A mechanical shaker was used for samples shaking. Sediment extracts were whizzed to a Rotofix 32 centrifuge (Hettich, Germany) to 2200 rpm for 20 min.

### Reagents

Zinc standard solution was used ( $1000 \pm 2 \text{ mg dm}^{-3}$ ) in 5%  $\text{HNO}_3$ . Work standardization solutions used for calibration in analyzing the samples from the sequential extraction, were daily prepared by diluting storage solution with extraction solution. The extractors used in the three extraction steps are: 0,11 M acetic acid; 0,5 M hydroxyl ammonium chloride; 1 M ammonium acetate.

The scheme of the sequential extraction method, as it was applied in the study is presented in fig.2.

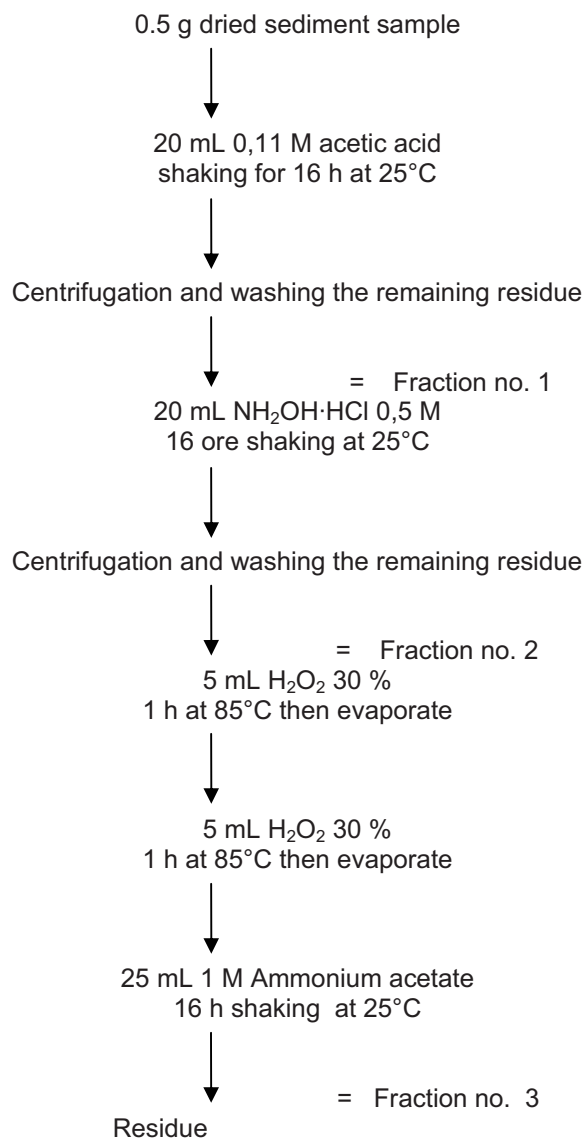


Fig. 2. BCR Sequential Extraction Scheme

Work method

In the first step of the scheme are set free the metals connected to carbonates and the ones from the changed fraction. In the second step, are leached the metals connected to iron and manganese amorphous oxides and hydroxides. In the third step ( $\text{H}_2\text{O}_2$  30% oxidation, stabilized with acid and 1 M ammonium acetate extraction, pH 2, adjusted with nitric acid) are separated the metals connected to the organic matter and the sulfates.

The sequential extraction of the heavy metals from the sediment was realized using 0,5 g sediment in which was added in a 20 ml whizzing tube, 0,11 M acetic acid. The tube was shaken by rotating it to 30 rpm for 16 hours with a shaker, and then they were whizzed to 2200 rpm for 20 minutes.

The supernatant was passed into 25 ml glass bottles. Then over the sediment in the tubes were added 10 ml bidistilled water. The tubes were shacked for 15 minutes, whizzed, and the supernatant was eliminated.

In each tube was added 20 ml 0,5 M hydroxylamine chlorine hydrate, pH = 2 repeating the shaking, whizzing and washing process.

In the third step in each tube was added 5 ml hydrogen peroxide, the tubes were closed untied on room temperature for an hour and then they were kept on the water bath to 85°C for another hour.

The tubes were opened and hydrogen peroxide was evaporated, the volume being reduced to almost 1 ml. a additional quantity of 5 ml hydrogen peroxide was added and the tubes wee closed and kept on the water bath for an

hour. Hydrogen peroxide was evaporated than almost close to dry. After cooling, 25 ml 1M ammonium acetate was added (acidulated to pH 2 with HNO<sub>3</sub>) repeating the shaking, whizzing and washing.

## Results and discussions

### *The determination of metal total concentration from sediments*

In order to evaluate zinc charge, total concentrations were determined and it was observed that in all the sediments except the first one, which is situated upstream the objectives that generates pollution as a consequence of the activity deruled in the area, zinc concentrations overpassed the limit value (150 mg kg<sup>-1</sup>d.w.) established by Romania's legislation for zinc in sediments [4].

Table 1

Total concentrations of zinc (mg/kg d.w.) in river sediments determined within FAAS

Sample name	Sample location	Zn Concentration (mg/kg d.w.)
1	Baiaga River	134,8
2	Baiaga River	366,38
3	Baiaga River	389,6
4	Baiaga River	381,74
5	Baiaga River	715,85
6	Baiaga River	432,3
7	Paraul Baiaga	387,6
8	Coranda River	680,8
9	Ciongani River	494,68
10	Quarry water	494,75

### *Zinc partitioning in sediments*

Because only a part of the total quantity of heavy metals from the sediments can be considered bioaccessible, labile, mobile and potentially toxic for the environment, the total concentrations of metals are not enough for the estimation of heavy metals pollution stat. This is the reason for which it was made the study of zinc partitioning in the sediments by applying BCR extraction procedure[5-7].

This procedure allows zinc concentrations partition into the following fractions:

- Easy soluble fraction: this fraction contains the metal connected to carbonates or absorbed to the surface and metallic-organic complexes in which the metal in weakly connected.
- The fraction connected to iron or manganese oxides.
- The fraction connected to organic combinations.

Zinc concentrations from 1-3 steps were summed and compared to the total concentration. The results referring to zinc partition in the sediments from the mining area are presented in figure 3.

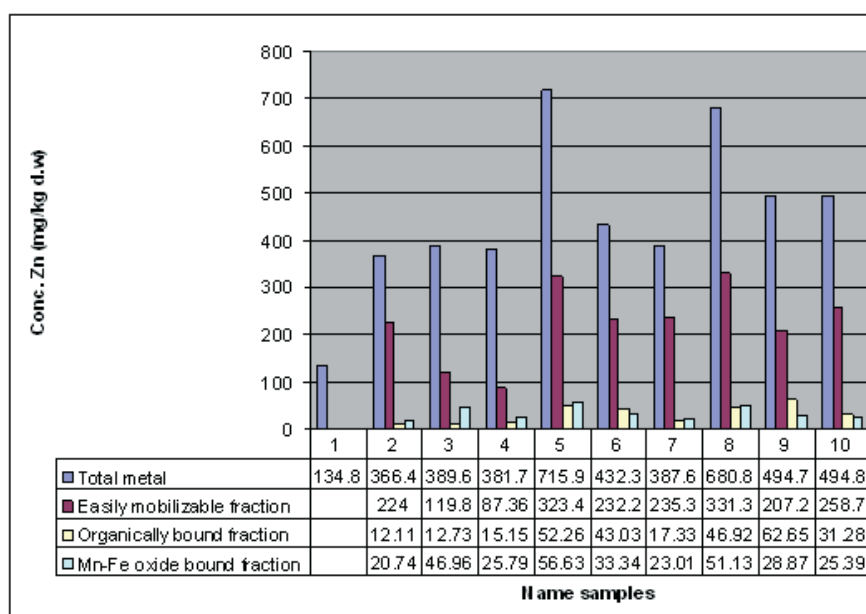


Fig. 3. Partitioning of Zn in river sediments

The dates from figure 3 indicate that in the analyzed samples 20-80% of zinc exists as easy soluble fractions, 5-20% of zinc is connected in organic combinations and 3-20% represents zinc fraction connected to the iron and manganese oxides and hydroxides.

#### Normalization process

This process allows aluminum use, a major constituent of aluminosilicates or iron use, a clay pointing constituent.

In order to evaluate iron and aluminum as candidates for establishing the normalization factors, were determined the total concentrations of these elements. The correlation between iron concentration and aluminum concentration should be linear if the two elements come from natural environment. Because of the mining activities, for iron content is very high for the analyzed samples (5-10 % d.w.) comparing to the aluminum content (0,1-0,3 % d.w.) which indicates the fact that it does not exist a linear dependence between the concentrations of these metals. Because of these reason it wasn't allowed iron use as a normalization factor, aluminum being choose in this scope, because it was considered that it comes from the natural environment.

In order to establish the natural and the anthropogenic inputs in zinc sediments, the total concentrations of this element were correlated with aluminum concentration in the same sediment sample.

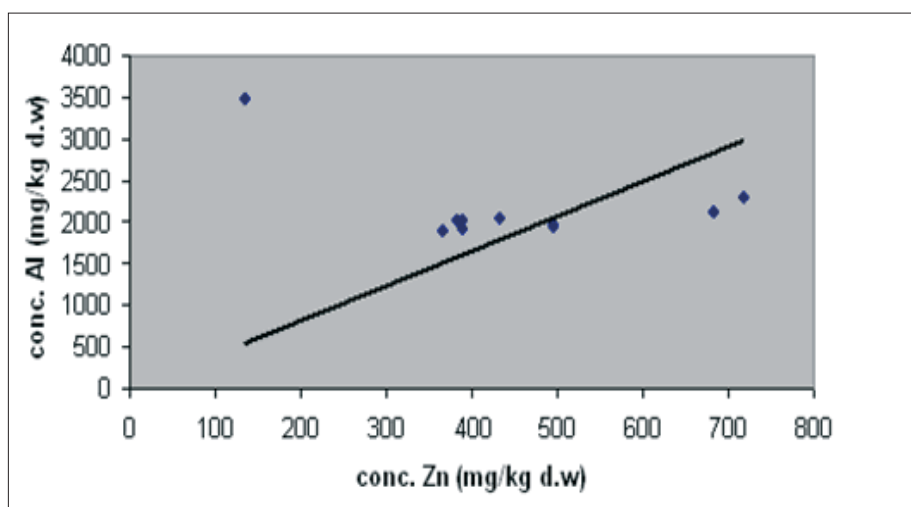


Fig.4. Relationships of Zn with Al in sediments

In figure 4 it can be seen that, in the investigated sediments case does not exist a linear dependence of zinc concentrations to aluminum concentration, which indicates the anthropogenic origin of this element because of the mining activities.

#### **Conclusions**

Within both methods it was putted into bold line the fact that zinc content induced in the system and accumulated in sediments from the pollution sources generated by mining activities unrolled in the area.

Sequential method allowed the quantification of accessible fraction and therefore able to generate impact to the aquatic ecosystems, and the aluminium normalization method confirmed the existence of a zinc content over passing the concentrations of the natural environment.

#### **References**

- [1] SVETE, P. R., MILAC, PIHLAR, B., Ann. Chim. (Rome), **90**, 2000, p. 323.
- [2] ANZECC, Guidelines for Fresh and Marine Water Quality, 2000.
- [3] DASKALAKIS, D.K., O'CONNOR, T.P., Environ. Sci. Technol., **29**, 1995, p. 470.
- [4] Ordin nr.161/2006 pentru aprobarea Normativului privind clasificarea calității apelor de suprafață în vederea stabilirii stării ecologice a corpurilor de apă.

- [5] QUEVAUVILLER, Ph., RAURET, G.J., LO'PEZ-SANCHEZ, F., RUBIO, R.A., URE, MUNTAU, H., *Sci. Total Environ.*, **205**,1997, p. 223.
- [6] RAURET, G.J., LO'PEZ-SANCHEZ, F.A., SAHIQUILLO, RUBIO, R.C., DAVIDSON, URE, A., QUEVAUVILLER, Ph., *J. Environ. Monit.*, **1**,1999, p. 57.
- [7] RAURET, G.J., LO'PEZ-SANCHEZ, F.A., SAHIQUILLO, BARAHONA, E.M., LACHICA, URE, A.M., DAVIDSON, C.M., GOMEZ, A.D., LU'CK, BACON, J.M., YLI-HALLA, MUNTAU, H., QUEVAUVILLER, Ph., *J. Environ. Monit.*, **2**, 2000, p. 228.

# THE ROLE OF ACTIVATED CARBON IN SOLVING ECOLOGICAL PROBLEMS

V. M. Mukhin<sup>a</sup>, T. G. Lupascu<sup>b</sup>

<sup>a</sup> OJSC "NPO "Neorganika", Electrostal, Moscow region.

<sup>b</sup> Institute of Chemistry of the Academy of Sciences of Moldova

**Abstract:** The authors present a brief analysis of the current global situation concerning the utilization of activated carbon in various fields. The article presents data concerning the synthesis and adsorption and structure properties of new activated carbons, used for solving ecological problems. The authors investigated the newly obtained activated carbons in comparison with several AC marks known in the world. It has been shown that currently synthesized AC are competitive with foreign marks.

**Keywords:** activated carbon, precious metals, environment.

The end of the so-called era of "cold war" was called forth significantly by the fact that the fear of an ecological bomb detonating overwhelmed the hearts of people. The sudden increase of the rate of environmental pollution began to bring such harm to mankind that it could be compared with the use of WMD including chemical weaponry.

According to the information provided by the WHO (2002) the state of health of an individual depends on: 51% of the way of life, 39% of the environment, and 10% of the quality of medical treatment.

The analysis initiated in 1945 showed that casualties of military conflicts during the period from 1945 till 1993 came to 23 million people of military personnel AND civilians. In the mean time, during the same period, approximately 150 million people became victims of malaria, tuberculosis, AIDS, and other diseases. This shows how vital a clean environment is, an environment where contagious diseases have no ability to spread.

Therefore, in the twenty first century mankind has entered a new age – age of environmental protection, where the key role in purification of industrial discharges is assigned to carbon-adsorbing technologies.

On the other hand, activated carbons allow us to perform a variety of tasks in industries, power engineering, agriculture, oil and gas refinement, etc.

At present, fields of application of adsorption technologies based on activated carbons (AC for short) are developing at a great pace. This is due to three main reasons: firstly, activated carbons allow solving the most burning issues of protecting the environment against industrial discharges, secondly - preserve high cleanness of substances, materials, and products, and thirdly - contribute to implementation of high technologies of production.

Table 1

Ecological activated carbon utilizing technologies of global importance

Component of biosphere	Carbon-adsorption technology
Atmosphere	Recuperation of solvents Purification of gases of combustion, including desulfurization Gas fumes trapping Chemical weaponry disposal Incoming air cleaning (air conditioning) [1,2]
Hydrosphere	Drinking water purification [3,4] Sewage sterilization Liquid radioactive waste processing Gold and non-ferrous metals mining
Lithosphere	Protection of soil from xenobiotics, i.e. pesticides Soil remediation Zones of sanitary protection of water sources
Human	Ecologically clean food production Pharmaceutical production Production of antibiotics, vitamins, remedies Entero-sorption and hemo-sorption [5,6]

In the USSR during the most favourable 1985-88 years 38k tons of AC were produced each year, comprising 85% coal based AC (AG and AR types), 2% peat based AC (SKT type), and 13% wood based AC (BAU type).

In Russia, the main source of raw materials for production of carbon sorbents remains to be rock carbon material of different stages of metamorphism (from lignite to anthracite), main deposits of which are concentrated in the Kuznetsk Basin.

In the Republic of Moldova, the main raw material for AC obtaining is represented by the secondary materials resulted after processing agricultural materials, such as: stones of peaches, prunes and apricots, grape seeds and nuts shells. According to data presented by the officials in this area, Moldova needs annually around 240 tons of AC, mainly for potabilization of surface and underground water (180 t), food industry (50 t) and for health protection (10t) [4].

In order to develop new technologies of producing AC, fulfilment of two major goals is required. These are: conversion of currently running developments and construction of new enterprises connected to sources of materials.

Let us discuss in detail the most vital directions of carbon-adsorption technologies' development.

Environment pollution created by motor transport is constantly growing, thus cars are to be equipped with gas-trapping systems (GTS) in accordance with the "EURO" standards. A GTS represents an adsorber filled with AC.

On the basis of coal half-coke of Leninsk-Kuznetskiy factory of coking, an adsorber for GTS with USK-DB mark rational pore structure has been developed. The adsorber had petrol fumes desorption value about 40% higher than its foreign analogues. It was later modified and reconstructed as annular cylindrical unit. At the moment, the full quantity of GTS developed is 800k pieces with worth estimated as 220 million rubles, as a result they have caught nearly 7k tons of petrol.

It is known that from 35 to 40% of the world's AC production are dedicated to drinking water supply; moreover, its deployment is essential in emergency situations (e.g. nitrophenol contamination of river Amur in December 2005).

SS coal mark of Belovskoy open-pit mine was used as a basis for the technology of producing "Hydrosorb" mark AC, which is used for ozone-sorption drinking water purification. It was successfully implemented in 2002 at Rublyovskaya waterworks (RW) in Moscow (the extent of implementation was 1500 tons).

The water quality control data, taken after three years of the fourth bloc being operational (240k m<sup>3</sup> per day), was compared to the original structures of the RW. According to the data the effectiveness of water purification from general organic pollution had an increase of 40 to 50%. Stable deodorization of water was achieved as well as absence of ozone treatment by-products (formaldehydes).

Open water sources in Western Europe suffer much greater technological assignment, thus AC must have a higher total organic carbon (DOC) adsorbing capability. Within the framework of Russian-German international project a new mark of AC named "Hydrosorb UK" was developed and tested at OJSC "Sorbent" (Perm). The AC has an adsorbing capability of 24 mg/l in accordance with DOC (C = 1.0 mg/l). Such results were achieved due to utilization of 100% SS rock carbon and lowering pellets' heating rate during pelletizing to 12 to 20° C/min.

"Hydrosorb UK" AC was loaded and tested at Hosterwiz waterworks (Dresden). It was clear that it absolutely complies with DIN-EN 12915 requirements and exceeds the sample ROW 08S (Netherlands) in multiple respects, which is shown in Table 2

Table 2

Iodine number, DOC adsorption ability and concentration in water of the studied AC

Active carbon	Iodine number, mg/g	DOC adsorption ability (C = 1,0 mg/l), ml/g	Concentration in water, micg/l	
			1,2-cis-dichloroethene	1,2- cis-dichloroethane
Hydrosorb-5	820	16,0	< 0,1	< 0,1
Hydrosorb -UK	850	24,0	< 0,1	< 0,1
ROW08S (sample)	1000	12,0	< 0,1	< 0,1
DIN-EN 12915	> 600	-	< 0,1	< 0,1

The part in life of a modern population centre played by household post-treatment water filters is of great importance and not only in Russia but, literally, in the whole world. Such devices allow to after-extract micro-amounts of toxic organics completely preventing it from entering human tissues. Therefore, individual, as well as collective filters can be used.

One of the major researches produced upon conversion of manufacture of AC for gas masks is the creation of adsorbers for gold hydrometallurgy. By optimizing the solutions of the basis (50-70% of rock carbon and 30-50% of half-coke) and of the binding agent (a mixture of coal and wood-chemical resins) the production technology for AG-90 mark AC was developed, and technology for producing AG-95 mark AC was developed by modifying the binding agent with phosphoric acid. Their performance meets OJSC "IRGIREDMET"'s requirements and reaches the level of foreign sorbents (see Table 3).

This research is both of ecological and economical importance. It is well known that old gravitational technologies of gold mining brought harm upon the nature, but new hydrometallurgy technologies that utilize AC represent closed systems. Carbon demand of this market in Russia is presumed to be in the range of 1500 to 3000 tons a year.

Table 3

Characteristics of domestically produced and foreign AC for precious metals extraction (the data is available from OJSC "IRGIREDMET")

AC mark	GOST hardness 16188-70,%	Gold activity, mg /g	Leftovers mg/l
FAS	98,4	17,6	1,3
AG-90	85-88	12,2	1,1
AG-95	88-90	18,0	1,1
VKS-500	87,6	17,5	1,1
Taiko GW 612 (Japan)	91,5	19,6	1,3
Chemviron FFW-A (USA)	88,6	14,4	1,3
Norit R-2520 (Holland)	88,0	25,8	1,3
Jx-102 (China)	89,0	13,5	1,3

Solid binding agent application (use of coal and wooden pitches) allows creating the most perspective technology of AC production, utilized by Chemviron Calgon (Belgium) and Calgon Carbon Corp. (USA). Such carbons are of wide spectrum of application in adsorbing technologies, first of all in water conditioning and treatment of waste and technological solutions.

One of the most progressive technologies is mixed activation, when carbon-containing material of low stage of metamorphism (peat, lignite or cannel coal) is used along with special chemical modifiers. These AC provide very high adsorption capabilities (see Table 4).

Table 4

Quality indices and structural parameters of carbon adsorbers

Indices	Lignite BKS	Peat TKS	Long flame carbon DKS
1. Apparent density, g/dm <sup>3</sup>	320	290	340
2. Hardness, %	70	65	75
3. Ash level, %	14	16	121
4. Interstice capacity, cm <sup>3</sup> /gr			
• V <sub>mi</sub>	0,75	0,65	0,80
• V <sub>me</sub>	0,25	0,25	0,22
• V <sub>ma</sub>	0,30	0,30	0,13
• V <sub>Σ</sub>	1,30	1,20	1,15
5. Adsorption activity			
Iodine, %	115	105	120
Methylene blue, mg/g	385	360	395

High technologies of the present century (circuit boards, electronics, life support systems, etc.) as well as endoecology of humankind will require especially pure carbons with ash admixture content below 0,1% of mass and ultrahigh durability. Thus there is no way of avoiding the usage of polymeric materials during the production of AC. The most preferable materials for AC production are phenol-formaldehyde resin (FTD mark), polyvinylidene chloride (PAU type carbons) and furfural copolymers (FAS).

Having no equals in this respect, FAS adsorbent is produced on the basis of furfural, using the simplest technological scheme comprising polymerization, gelatinization, and condensation. It's exploiting characteristics regarding industry (durability – 7000 kg/cm<sup>2</sup>) and medicine (ash admixture content – 0,01% of mass) speak of a great investment potential.

Hydrometallurgy processes of nonferrous and precious metals mining, for the most part of gold, using FAS might lead to a technological revolution in that strategic industry. It has no matches amongst other carbons used in hydrometallurgy (see Table 3).

Utilization of AC in pharmaceutical industry is extremely significant. I would willingly put stress on the simple

fact that gemo-sorption and entero-sorption based on AC literally protect people from lethal dangers. In 1814 in order to show marvellous properties of AC to full extent French monk Bertrand swallowed some arsenic oxide and an adequate portion of AC in series and remained alive. Another even more astonishing experiment was performed by apothecary Turey of Montpellier in 1834. He took a tenfold draught of the most lethal poison strychnine and an aliquot amount of AC. As in the previously mentioned example his experiment was a success. In 1948 German scientist Schmidt proved that active AC can absorb up to 100% of microbes from diluted culture of infectious bacteria in 10 minutes' time. At the present moment dozens of diseases from allergy to narcotism are cured thanks to gemo-sorption and entero-sorption (see "Entero-sorption" of professor N. Belaev).

One very special kind of food industry sorbents based upon shells and fruit pits is seen fulfilled at OJSC "NPO "Neorganika" experimental factory. Properties of AC domestically produced out of pits material, are shown in Tab. 5.

Table 5

Quality indices and structural parameters of active carbons made of pits material

Indices	Pit of fruit trees			coco		
	MeKS	AKU	MeKS enterosorbent	VSK	VSK-V	VSK-A
1. Apparent density, g/dm <sup>3</sup>	400	400-450	380-390	530	450	380
2. Hardness, %	91	93	86	92	90	85
3. Ash level, %	1,0	5,0	0,1	5,0	5,6	6,8
4. Interstice capacity, cm <sup>3</sup> /gr						
• V <sub>mi</sub>	0,510	0,390	0,620	0,325	0,420	0,580
• V <sub>me</sub>	0,110	0,120	0,240	0,120	0,140	0,200
• V <sub>ma</sub>	0,200	0,225	0,145	0,110	0,200	0,160
• V <sub>Σ</sub>	0,820	0,735	1,05	0,555	0,750	0,940
5. Adsorption activity:						
Iodine, %	120	80	126	60	85	110
Methylene blue, mg/g	315	225	350	140	185	340

Implementation of such AC produces outstanding results in production of vodka, especially when AC block filter systems are used.

In the future, large scale implementation of AC will be required by the modern field of sorption technologies (e.g. soil detoxication, production of ecologically clean food). This means that the demand for "Agrosorb" class AC will only rise. Treatment of pesticide polluted soil with "Agrosorb" AC, utilizing from 50 to 200 kg of AC per hectare, allows not only to lift crop capacity of various crops but to ensure the harvest that would guarantee the production of ecologically clean food (see Tables 6, 7).

Table 6

Harvest of crops on herbicidal background after using active carbon (50 kg/hectare norm)

Crop	Herbicidal background and doses (kg/hectare)	Harvest on herbicidal background (centner/hectare)	Harvest after using AC (centner/hectare)	Harvest increase (centner/hectare, %)
Maize	Treflan, 1,4	53	78	25(47)
Tomato	The same	333	652	319(96)
White beet	The same	343	416	73(21)
Rice	Ronstar, 2,0	60	72	12(20)
Bulb onion	Ramrod, 8,5	228	295	67(29)
Cucumber	Treflan, 1,0	85	202	117(138)
Soy	Dialen, 9,0	11	24	13(118)
Winter wheat	Unidentified remainder	43	49	6(14)
Maize*	The same	342	592	250(73)
Rice*	The same	63	85	22(35)

\* The normal amount of AC was 100 kg/hectare.

Table 7

## Assemblage of treflan and 2,4-D herbicides by crops

Herbicide and it's dose (kg/hectare)	Normal amount of AC (kg/hectare)	Test-crop	Herbicide content in harvest (mkg/kg)
Treflan, 1,0	-	tomato	28,0
-«-	100	-«-	0,6
Treflan, 1,0	-	carrot	95
-«-	100	-«-	not detected
2,4-D	-	barley	220
-«-	200	-«-	not detected
2,4-D	-	barley	670
-«-	200	-«-	not detected

Incidentally, after completion of works on “Agrosorb” in the Krasnodar Territory in 1989 regional agroindustry department of Kuban purchased annual supply of 25 thousand tons of “Agrosorb” per year.

The area of utilization of such sorbents is larger than just agricultural holdings. It's the protection of open sources of water that serve as water-supply for cities, blocking of sewage from dumps and military testing areas, preservation of biological resources of reservoirs etc.

One of the most significant areas of utilization of agricultural AC is the detoxication of fodder in broiler poultry keeping, cattle breeding, pig-breeding etc., as they rise the safety of livestock and lowers the cost in fodder of a unit of weight of produce. The results of utilization of “Ptitsesorb” AC in broiler poultry keeping are shown in Table 8.

Table 8

## The effectiveness of “Ptitsesorb” AC in detoxication of fodder in broiler poultry keeping

Groups	Safety of livestock (%)	Cost in fodder of a unit of weight of produce (kg)
OR + 8 mkg/kg of T-2 toxin	72	2,73
OR + 8 mkg/kg of T-2 toxin + 0,5 % mass of AC	92	2,57

Presently, about 500 thousand tons of AC is produced in the whole world but, the main showings are rates of production and of use of AC per each man a year. In the Soviet Union the norm was 0,15 kg/man, and in the Republic of Russian Federation it's only 0,02 to 0,05 kg/man. In the meantime in the USA, Japan, and Western Europe countries this showing is about 0,5 kg/man. And in Holland that is situated at mouth of the Rhine the rate is 2,5 kg/man.

Reasoning from these numbers, Holland produces 40 thousand tons of AC per year. The People's Republic of China requires 500 tons of AC per year, thus they are vigorously developing their production capacities. Therefore, Russia has to produce 75 thousand tons of AC a year.

Russia has always been at the forefront of developing high-quality active carbons, catalysts and chemical absorbers based on AC. And, although we occupy 7-8 position amongst the producers of AC, the superiority of Russian AC is internationally recognized.

The direction of developing the production of AC for ecology is quite plain for specialists. We, from our own part, are open towards cooperative activities with our investors who are to gain not only considerable profits but also the worldwide recognition and appreciation of their part in preserving ecological safety and defending our Earth from ecocide.

## References

- [1] Mukhin V.M., Tarasov A.V., Klushin V.I. Active Carbons of Russia – Metallurgy, 2000 – 352 p.
- [2] Kienle H., Bader E. Activated carbons and their industrial utilization. Ferdinand Enke Verlag Stuttgart, 1980, 316 p.
- [3] Kawamura S.: Integrated design of water treatment facilities. J. Wiley&sons, Inc., 1991, 658 p.
- [4] Lupascu T.: Activated carbons obtained from vegetal raw materials. “Stiinta”, Chisinau, 2004, 224 p.
- [5] Giordano C.: Sorbents and their clinical applications, Academic Press, 1980, 400 p.
- [6] Nikolaev V.: The method of hemoperfusion in experimental and clinical trials. “Naukova dumka”, Kiev, 1984, 360p.

## THE INFLUENCE OF BINDING MATERIAL ON POROUS STRUCTURE OF SHAPED HOPCALITE

N.K. Kulikov<sup>a</sup>, S.G. Kireev<sup>a</sup>, A.O. Shevchenko<sup>a</sup>, V.M. Mukhin<sup>a</sup>, S.N. Tkachenko<sup>b</sup>, T.G. Lupascu<sup>c</sup>

*JSC EHMZ, Elektrostal, Moscow region, 144001, K.Marks str., 1*

*<sup>a</sup>JSC ENPO "Neorganika", Elektrostal, Moscow region, 144001, K.Marks str.,4*

*<sup>b</sup>MSU by M.V. Lomonosov, Chemistry faculty, Moscow*

*<sup>c</sup>Institute of Chemistry of Academy of Sciences Moldova*

**Abstract:** The authors have investigated the equilibrated adsorption of water vapors on GFG hopcalite, which was obtained using the extrusion shaping method, with bentonite clay as the binding compound. In the frames of the BET model, the values of the monolayer capacity and the size of medium area occupied by the water molecule in the filled monolayer have been determined. The distribution of pores according to their sizes has been evaluated. It has been established that the modification of the bentonitic clay allows directed construction of the hopcalite porous structure, i.e. the formation of the mesoporous structure with a narrow distribution of the pores capacities by sizes, which was achieved varying the sizes of binding compound particles.

**Keywords:** bentonitic clay, hopcalite, adsorption, porosity, catalytic properties.

It is known that physical-chemical properties of manganese oxide catalysts (MOC) that are used for oxidation of carbon monoxide and ozone decomposition, greatly depend on the base phase structure – manganese dioxide and also on the method and conditions of the latter receiving [1,2]. Besides, catalyst properties may be also influenced by the binding material. For example, the use of different binding materials in shaped catalysts produced on the basis on MnO<sub>2</sub>/CuO determines different adsorption properties, in particular in connection with water vapors. So, in case of utilization of bentonitic clay (BC), talum and calcium oxide the value of monolayer capacity according to BET is correspondingly [3] 40, 38 and 24 mmole/g.

During the present work we investigated the influence of properties of one and the same binding material on adsorption properties of hopcalite, consisting of MnO<sub>2</sub>/CuO and 10% by weight of BC. The following samples were chosen as investigation objects: industrial hopcalite GFG as the a control and modified hopcalite GFG-M for a development type. The samples used as investigation objects differed in binding particles size: maximum distribution treatment was 12 μm for GFG, 4 μm for GFG-M.

Bentonitic clay (BC) used as binding material in hopcalite production has complicated chemical and mineralogical structure [4]. One of the main minerals is montmorillonite but also quartz, amorphous aluminum silicates, hydroxides and other compounds are present. Thus BC consists both of clayey components, providing binding properties, and clean components which are catalyst ballast. Clayey fraction separation was carried out in the following way: BC hinge was poured over with tenfold quantity of water and kept at room temperature with periodical mixing. After some astronomical days clayey fraction was separated from settled clean components. The final rate appeared to be ~40%, converted to dry substance. This was followed by the mixing of manganese dioxide and black copper oxide with modified binder in the ratio taken in active production. Subsequent operations were: forming of granules 1 mm in diameter by the extrusion method, drying, crushing, separation of principal fraction – cylindrical particles 2-5 mm in length and thermal treatment at operating practice characteristics similar to those taken in hopcalite industrial production.

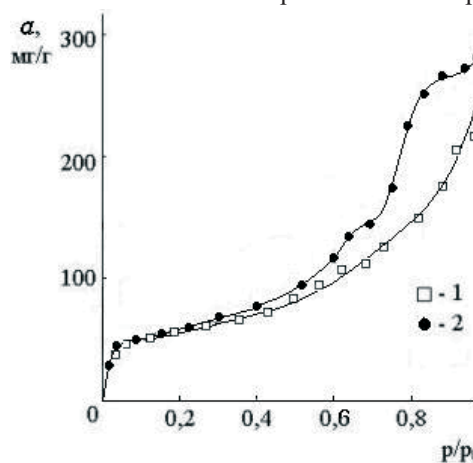


Fig. 1. Water vapors adsorption on GFG (1) and GFG-M (2) hopcalites

Adsorption investigation method, equipment, way and conditions of sample training before the metrology were analogous to those described in the work [5].

Samples specific surface was defined by means of nitrogen thermal desorption. Figure 1 shows isotherms of water vapors adsorption on GFG and GFG-M hopcalites, measured at room temperature.

Both isotherms are described satisfactorily in the context of BET model [6] with the help of the calculation device, which determined constant C, monolayer capacity ( $a_m$ ) and the size of medium area occupied by the water molecule in the filled monolayer ( $\omega$ ). All the values are given in table 1.

Samples adsorption properties in the monolayer area and closest monolayer area, situated next to it, are practically equal, because the beginning parts of isotherms coincide, and volumes of constant C,  $a_m$ , monolayer capacity and  $\omega$  differ slightly. But at the increase of equilibrium pressure of adsorbate beginning with  $\sim 0,4 p/p_0$ , the differences in adsorption behavior of GFG and GFG-M are evident. According to the classification of Brunauer, Deming and Teller isotherm of sample GFG may be ascribed to II type, however for sample GFG-M in the area of high relative pressures isotherm part is of the IV type with characteristic inflection [6] which gives the possibility to track the moment of mesopore infill.

Table 1

Hopcalite adsorption characteristics

Sample	C	$a_m$		$S_{sp}, m^2/g$	$\omega, \text{\AA}^2$	$S_{me}, m^2/g$ , in the interval		
		mg\g	mmole\g			3-5 nm	5-7 nm	7-16 nm
GFG	42	38.7	2.15	156	12.1	13.7	4.1	4.2
GFG-M	45	40/4	2.24	180	13.3	26.5	7.6	1.8

Information about pore structure of the solid, for example, pore distribution according to size, may be also obtained from experimental isotherms. Adsorption branches of isotherms have been chosen for the calculation. First, according to the modern point of view, it is more valid in the thermodynamic respect. Second, in real adsorption systems there is always interrelation pore influence (unlike ideal model of separate independent pores) and distribution, measured on adsorption branch, gives more correct information about pore structure.

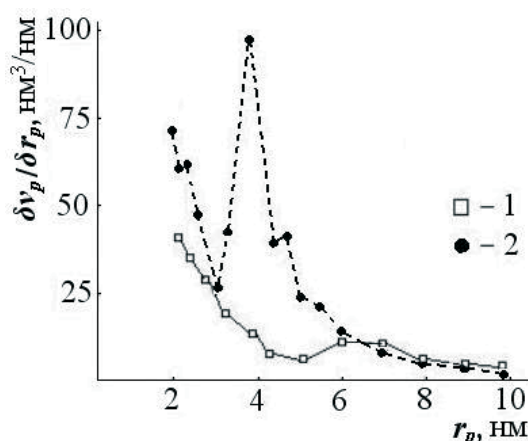


Fig. 2. Distribution of pore volume according to sizes for GFG (1) and GFG-M (2)

On Roberts method [6] we carried out the measurement of pore distribution according sizes with the use of cylindrical pores model (fig. 2) and also of pore surface area in the range of 3-16 nm (table 1). To calculate adsorption film thickness we used Hely equation [7]. The data given on fig. 2 and in the last three columns of table 1 are the evidence of great influence of binding material modification on GFG pore structure. If at 6-7 nm you can observe rather weak wave at distribution curve for initial hopcalite, then GFG-M at 3.8 nm is characterized by manifestly evident and rather intensive distribution maximum. Taking into account the form variety of making hopcalite particles and also the irregular nature of their arrangement, we can assume that the most likely reason of such effect is not only another binding material pore size but also the motive change of adsorbent gel-forming particles arrangement.

Actually, on one hand, the separation of clayey fraction from initial BC led to great decrease of binding material particle size as a result of swelling and aliquation. But on the other hand, for all that total quantity of binding material as in GFG, the use of modified BC in GFG-M provides 2.5 times more of clayey fraction which is just a binding component. This is confirmed by the fact that granules abrasion resistance is 77.8 and 85.2% for GFG and GFG-M

correspondingly. Besides, BC modification led to certain compacting of catalyst granules: it is confirmed by bulk density growth, which is 986 and 1037 g/dm<sup>3</sup> for GFG and GFG-M correspondingly.

The specific surface of GFG-M sample is greater by 24 m<sup>2</sup>/g than that of GFG. From the other hand, as the data of table 1 show, the difference between mesopores of mentioned samples is 13.9 m<sup>2</sup>/g. However taking into account the fact that there is a certain error at S<sub>sp</sub> determination and adsorption measurements, we have reasons to establish rather satisfactory coincidence of both calculation results and those received by the instrumental method. Hence, we can draw a conclusion about the correctness of application of chosen models for the description of equilibrium adsorption processes in the system "hopcalite – water". If initial hopcalite GFG is characterized with rather equal mesopore volume distribution according to their size, GFG-M is characterized with narrow distribution with maximum at 3.8 nm.

Thus, bentonitic clay modification allows to construct hopcalite porous structure purposively, to be exact: to form mesoporous structure with narrow distribution of pore volume on sizes by means of variation of binding material particle size.

## References

- [1] Golbraih Z.E. Manganese dioxide as an adsorbent // In the book: Active manganese dioxide.-L.:ONTI-Himteoret. 1937.-p.124-162.
- [2] Rode E.Y. Manganese oxygen compounds.-M.: PH AN SSSR. 1953.-478 p.
- [3] Kireev S.G., Mukhin V.M., Kireev A.S. and others. Theoretical problems of chemistry of surface, adsorption and chromatography: Thesis of rep. to X International conference. April, 24-28, 2006, Moscow-Klyazma.-M.: IFH RAN, 2006.-p.175.
- [4] Keltsev N.V. Principles of adsorption technique. 2<sup>nd</sup> edition, revised and complem.- M.:Chemistry. 1984.-592 p.
- [5] Kireev S.G., Mukhin V.M., Tchebykin V.V. Modern state and development perspectives of adsorption theory: Coll. of mater. of IX International conference on theoretical questions of adsorption and adsorption chromatography- Moscow, 2001, April,24-26.- M.: IFH RAN. 2001.-p. 225-228.
- [6] Greg S., Sing K. Adsorption, specific surface, porosity: Transl. from Engl. 2<sup>nd</sup> edition.-M.: Mir. 1984.-306 p.
- [7] Komarov V.S. Adsorbents and their properties.-Minsk: Science and technique. 1977.-248 p.

## THE STUDY OF REDOX CONDITIONS IN THE DNIESTER RIVER

Viorica Gladchi<sup>a\*</sup>, Nelli Goreaceva<sup>a</sup>, Gheorghe Duca<sup>b</sup>, Elena Bunduchi<sup>a</sup>, Lidia Romanciuc<sup>a</sup>,  
Igor Mardari<sup>a</sup>, Ruslan Borodaev<sup>a</sup>

<sup>a</sup>Moldova State Univeristy, 60 A.Mateevici str. MD 2009, Moldova

<sup>b</sup>Academy of Sciences of Moldova, Ștefan cel Mare 1, Moldova

\*E-mail: ggladchi@yahoo.com, phone: 577538, fax: 577557

**Abstract:** The work presented in the paper discusses the contribution of the Novodnestrovsc water system to the formation of redox conditions in the lower Dniester. The conclusions were drawn on the basis of a long-term protocol of analyses that included the analysis of the oxygen regime, evaluation of the content of hydrogen peroxide, rH<sub>2</sub>, biological oxygen demand as well as other additional parameters.

**Keywords:** kinetic indicators, hydrogen peroxide, redox state, free radicals, inhibition capacity.

### Introduction

The Dniester is a trans-boundary river crossing the countries of Moldova and Ukraine, discharging into the Black Sea. Its total length is 1352 km, with 636 km flowing through Moldova. The river is the largest one in Moldova and the chief source of drinking water for more than a million people. The Dniester River basin occupies 57% of the area of the Republic of Moldova, and run-off water, municipal effluents and industrial discharges contribute to the degradation in water quality [1-5].

In 1981 in the middle part of the river on the territory of Ukraine a barrage was constructed, creating the Hydropower Station. The newly formed storage pond is 194 km long; the capacity of the reservoir is 3.0 km<sup>3</sup>. The main purpose of the reservoir construction was for power supply and flood control. In 1985 another dam was constructed downstream of the Novodnestrovsc barrage in order to create a 20-km buffer reservoir. The second barrage also serves as a frontier between Moldova and Ukraine. The main purpose of the second barrage construction was to regulate the water discharge from the first barrage and also to generate electric power.

The Dniester reservoir is a canyon-type, deep-water lake with a 54 m maximum depth near the dam. Low water temperature, a deficiency in dissolved oxygen, and the presence of hydrogen sulfide and ammonium are typical for the hypolimnion of such reservoirs [6]. Once the reservoir was filled with water, organic-rich sediments have accumulated, and the decomposition of this organic material creates low red-ox conditions. In other similar reservoirs, elevated phosphate and transition metal concentrations have been measured that can be attributed to the reductive-dissolution of iron- and manganese- oxides, and the release of adsorbed phosphate [7]. All these chemical species can have an adverse impact on down-stream aquatic life [8].

Since the beginning of full-capacity operation of the Hydroelectric Power Plant, dramatic changes in the water quality occurred in the river emerging from the buffer reservoir. The temperature regime of the river has been changed as follows: the mean temperature value decreased by 8-10°C in summer time; when the average air temperature reached 30-32°C, the water temperature in the lower reach was 16-18°C. Severe changes in the aquatic ecosystem occurred: the diversity of hydrobiont species was decreased, fish stocks also decreased, and mass fish kills were often observed [9]. Ichthyologists have pointed out the negative effects of the dam on the ichthyo-fauna. Some fish species have stopped spawning, and fish stocks have been 18-fold reduced. Reproduction of some species has decreased 30-fold. Certain studies revealed that 80% of the sturgeon sampled showed signs of spawn reabsorption. The presence of reducing substances in the amounts exceeding quite often the contents in oxidizers (hydrogen peroxide), provoke the unbalance of these processes in water environment. It is known that the reductive, quasi-reducing and super oxidative conditions of natural waters are destructive for the development of hydro-bionts, including fish [10-12; 13-32]. Quasi-reducing conditions is toxic for certain bacteria, and fish larvae [13]. The red-ox state of surface natural waters is a parameter that characterizes the ecological state of the water body and its auto-purification capacity [8; 15-17; 30-32]. Biologically healthy fresh water is determined by the presence in it of hydrogen peroxide within the limits of 10<sup>-6</sup> mol/l [15-16]. In sea water the amount of hydrogen peroxide is substantially lower then in fresh waters [7,11,12; 22-25]. In the biogeochemical cycle of oxygen in fresh water ecosystems the stationary concentrations of oxidative equivalents such as OH radicals constitute 3-5·10<sup>-16</sup> mol/l. The range of variation of their concentration should not vary by more than a factor of 10 [23]. Redox processes in surface natural waters containing dissolved oxygen occur with the formation of intermediate active forms, namely, hydrogen peroxide, and hydroxide - and super-oxide radicals. Chemical processes of oxidation, which change the redox state of metal ions, depend on the rates of free radical formation and destruction, and their steady-state concentrations.

In order to perform investigations of the river there were selected 6 permanent sites located as follows: Site 1 – v.

Naslavcea, below the Dniestrovsk dam, 200 m from the buffer reservoir; site 2 – v. Mereseuca, 18 km from the dam, site 3 – v. Cosauti, 87 km from the dam and buffer reservoir; site 4 – v. Bosernita located at the distance of 145 km from Naslavcea; site 5 – c. Dubasari, above the dam of the Dubasari water reservoir, 309 km from Naslavcea; site 6 – 100 m below the dam of the Dubasari water reservoir (310 km from the site 1). During the summer of the year 2006 two more sites have been added between the first and second sites. One was located at the fourth km from Naslavcea and the other one was located at v. Verejeni, 6 km from Naslavcea. The sites located between Naslavcea and Cosauti were characteristic for the river-bed flow while the sites 4-6 were located very close to the Dubasari water reservoir.

The water samples were collected from the upper horizons (0,5 – 0,6 m). The measured hydrochemical indicators included hardness, mineralization and the content of major ions ( $\text{Ca}^{2+}$ ,  $\text{Mg}^{2+}$ ,  $\text{Na}^+ + \text{K}^+$ ,  $\text{HCO}_3^-$ ,  $\text{SO}_4^{2-}$ ,  $\text{Cl}^-$ ). The traditional hydrochemical parameters of the river waters has served as additional indicators of potential impact of the water reservoir on the river waters flowing from the barrage. Redox components measured included: the temperature, the dissolved oxygen, pH, Eh,  $r\text{H}_2$ , BOD, COD,  $\text{NH}_4^+$ ,  $\text{NO}_3^-$ ,  $\text{NO}_2^-$ ,  $\text{PO}_4^{3-}$ , Cu(II), Fe(III),  $\text{H}_2\text{O}_2$ , and OH radicals.

## Results

### Redox active components

The assessment of the components of the Dniester river waters determining the oxidation-reduction processes has identified a series of regularities in seasonal and spatial dynamics. The hydrogen indicator (pH) for the duration of the year cycle was varying within the investigated segment of the river from 7.3 till 9.1, its average values constituted respectively 7.8 at Naslavcea and 8.2 at Dubasari water reservoir (at the barrage). Practically at all the times the pH of the initial site was lower than in other investigation sites. The seasonal variations were manifested by the decrease of this indicator almost in all the sectional lines of the water flow.

The dissolved oxygen was present in the Dniester waters during the investigation continuously, however, in the water masses, coming into Naslavcea pool from Novodnestrovsc's water reservoir; its content was reaching normal saturation only in spring. In summer the saturation of water with oxygen constituted 70.5% and was decreasing in certain periods down to 52%; in autumn the average saturation was equal to 79.5%. The decrease of saturation of waters with oxygen by 83% was observed also in summer at the Bosernita site. The investigation of saturation with oxygen at Cosauti, Bosernita and Dubasari water reservoir has identified over saturation of Novodnestrovsc water with oxygen up to 158 – 177%.

Novodnestrovsc's waters have demonstrated during the investigation an instable oxidation – reduction state. According to the  $r\text{H}_2$ , at Naslavcea the ratio of reduction and oxidation processes was varying from the predominance of the reduction processes to neutral state and in average it can be characterized as close to neutral. In Mereseuca the waters most often was predominant the reduction processes. The domination of reduction processes over oxidation processes was observed in summer period at Dubasari water reservoir as well.

Table 1

The content of redox components in Dniester waters between 12.08.05 and 24.08.06 (Numerator- the average value of the period, denominator - the limits of variation of the indicators)

Site	Naslavcea	Mereseuca	Cosauti	Bosernita	Dubasari, above the barrage	Dubasari, below the barrage
pH	$\frac{7.8}{7.3-8.5}$	$\frac{8.11}{7.7-8.5}$	$\frac{8.24}{8.0-8.6}$	$\frac{8.0}{7.3-8.4}$	$\frac{8.2}{7.4-9.0}$	$\frac{8.15}{7.6-9.1}$
$r\text{H}_2$ , $r\text{H}_2$	$\frac{27.7}{26.9-28.6}$	$\frac{27.2}{25.5-28.0}$	$\frac{28.0}{27.6-28.4}$	$\frac{28.4}{27.2-30.5}$	$\frac{27.5}{25.3-29.0}$	$\frac{27.1}{22.1-29.2}$
[O <sub>2</sub> ]	$\frac{8.7}{4.8-12.0}$	$\frac{11.65}{8.2-14.7}$	$\frac{12.5}{8.9-17.0}$	$\frac{11.3}{7.5-14.6}$	$\frac{11.1}{7.8-14.7}$	$\frac{10.6}{8.1-15.2}$
	$\frac{80.6}{52-101}$	$\frac{109.9}{87.2-127.0}$	$\frac{118.8}{97-187}$	$\frac{107.2}{83-158}$	$\frac{113.3}{88-171}$	$\frac{107.6}{95-133}$
[NO <sub>3</sub> <sup>-</sup> ], mg/l	$\frac{5.84}{1.9-8.4}$	$\frac{7.42}{3.9-10.7}$	$\frac{5.68}{1.7-10.7}$	$\frac{6.6}{1.6-14.2}$	$\frac{5.5}{0.9-12.0}$	$\frac{6.94}{0.6-13.4}$
[NO <sub>2</sub> <sup>-</sup> ], mg/l	$\frac{0.027}{0.008-0.054}$	$\frac{0.037}{0.014-0.078}$	$\frac{0.027}{0.006-0.052}$	$\frac{0.027}{0.012-0.042}$	$\frac{0.058}{0.0-0.231}$	$\frac{0.03}{0.0-0.095}$
[NH <sub>4</sub> <sup>+</sup> ], mg/l	$\frac{0.021}{0.0-0.07}$	$\frac{0.015}{0.0-0.10}$	$\frac{0.044}{0.0-0.20}$	$\frac{0.06}{0.0-0.20}$	$\frac{0.071}{0.0-0.32}$	$\frac{0.136}{0.0-0.54}$
[PO <sub>4</sub> <sup>3-</sup> ], mg/l	$\frac{0.48}{0.21-0.77}$	$\frac{0.54}{0.16-0.92}$	$\frac{0.73}{0.11-3.22}$	$\frac{0.52}{0.21-1.37}$	$\frac{0.46}{0.12-0.67}$	$\frac{0.52}{0.22-0.82}$
CBO, mgO <sub>2</sub> /l	$\frac{3.3}{1.2-4.45}$	$\frac{3.13}{0.6-5.6}$	$\frac{3.21}{1.0-5.83}$	$\frac{3.6}{1.5-6.1}$	$\frac{3.9}{1.4-6.7}$	$\frac{3.7}{1.9-5.0}$
[H <sub>2</sub> O <sub>2</sub> ], 10 <sup>6</sup> M	$\frac{1.02}{0.0-4.8}$	$\frac{1.22}{0.0-5.44}$	$\frac{0.95}{0.0-1.9}$	$\frac{0.32}{0.0-1.44}$	$\frac{1.76}{0.0-9.52}$	$\frac{1.4}{0.0-8.48}$

The ammonia ions in the section line of Dniester were present in concentrations 0.015 – 0,136 ml  $\text{NH}_4^+$ /l. Starting from Cosauti towards the Dubasari hydroelectrical plant their content was steadily increasing. The maximal content was observed below the dam at Dubasari. The seasonal dynamics of ammonium nitrogen was manifested by the increase of its concentration in autumn. In spring the  $\text{NH}_4^+$  ions were not identified in any site but Bosernita.

In average for the year, the content of  $\text{NO}_3^-$  in the section lines constituted 5.5 – 7.4 mg  $\text{NO}_3^-$ /l, and the lowest values were detected in autumn; the highest concentrations of  $\text{NO}_3^-$  were observed in spring in all the sites but Naslavcea.

The nitrites, during the investigation period, were a permanent component of Dniester waters. Their absence was registered only once in May 2006 above and below the Dubasari barrage. The average content of nitrites throughout the year constituted between 0.027 and 0.058 mg  $\text{NO}_2^-$ /l. In summer the content of nitrites in Dniester waters was increasing, while in spring it was decreasing. The permanent presence of nitrites in the background of low content or complete absence of ammonium nitrogen can occur due to unfavorable oxidation state and slow oxidation of  $\text{NO}_2^-$  to  $\text{NO}_3^-$ .

The phosphates were present in the river in quantities 0.11 – 3.22 mg  $\text{PO}_4^{3-}$ /l. Their average concentrations in the sections lines varied in the range 0.48-0.73 mg  $\text{PO}_4^{3-}$ /l. The maximal pollution with phosphates was observed in the summer of 2006 at Cosauti and Bosernita sites, and constituted respectively 3.22 and 1.37 mg  $\text{PO}_4^{3-}$ /l. The seasonal dynamics have shown an increase of the phosphates content in the segment Naslavcea – Mereseuca in spring, another increase being detected in summer between Cosauti and Dubasari.

The average content of organic compounds according to the  $\text{BOD}_5$  in the section lines of the investigated sector of Dniester constituted 3.1 – 3.9 mg  $\text{O}_2$ /l. In summer this indicator was rising above the yearly average at Mereseuca and Cosauti sites and constituted respectively 4.6 and 3.7 mg  $\text{O}_2$ /l, in spring – at the Dubasari water reservoir (Bosernita – Dubasari, lower reach) and constituted respectively 6.1 – 5.0 mg  $\text{O}_2$ /l. At Naslavcea the maximal amount of organic compounds was 4.45 mg  $\text{O}_2$ /l that was detected in spring.

### The hydrogen peroxide and the redox state of waters

The analyses of the waters of the sector under investigation have never detected an oxidant state throughout the period of research (table 2). The most favorable state, according to this parameter, was registered in September 2005 when hydrogen peroxide was detected in the samples collected from all the sites (the range of concentrations:  $1.44 \cdot 10^{-6}\text{M}$  –  $9.52 \cdot 10^{-6}\text{M}$ ) except Naslavchea. At that site the waters were continuously in reducing state, the hydrogen peroxide was missing and only the organic substances of peroxidazic type that are easily titrated by hydrogen peroxide were present. The reducing state of water below the Naslavchea dam could be caused by a shift from the equilibrium state in the waters of the accumulation reservoir above the dam resulting from the inflow of substantial amounts of reducing peroxidazic substances. The negative impact of the resulted disequilibria has been attenuated along the investigation segment of the river, that was confirmed by the presence of hydrogen peroxide in the waters of the Mereseuca site, where its concentration was the lowest ( $1.19 \cdot 10^{-6}\text{M}$ ) in the hole investigated part of the river. The detection of hydrogen peroxide can be related to the occurrence in the segment Naslavcea – Mereseuca (18 km) of self-purification processes that lead to the total oxidation of peroxidazic substances and to the low excess of hydrogen peroxide.

The maximal content of  $\text{H}_2\text{O}_2$  in September 2005 was registered below and above the Dubasari dam ( $8.48 \cdot 10^{-6}\text{M}$  and  $9.52 \cdot 10^{-6}\text{M}$ ), that can be explained by the existence of large quantities of microflora that eliminates metabolic  $\text{H}_2\text{O}_2$  in the surrounding environment.

Table 2

The content of hydrogen peroxide and reducing substances ( $\text{H}_2\text{O}_2 \cdot 10^{-6}\text{M}/\text{Red} \cdot 10^{-6}\text{M}$ ) in the waters of Dniester River)

Month, year	Naslavcea	Mereseuca	Cosauti	Bosernita	Dubasari, above the dam	Dubasari, below the dam
09.2005	- 1,10	1,19	1,77	1,44	9,52	8,48
10.2005	1,24	1,05	1,90	-	1,52	-
11.2005	0,32	0,35	0,70	-	0,33	0,42
03.2006	-	-	-	-	-	-
05.2006	0,30	- 0,30	0,50	-	0,50	0,40
06.2006	4,80	5,44	1,26	- 0,50	- 0,46	- 0,64
08.2006	0,50	0,49	0,48	0,49	0,49	0,48

In October 2005 the waters of the Dniester River collected from the Naslavecea- Cosauti segment and above the Dubasari dam were in oxidant state and hydrogen peroxide was present in quantities  $1.05 \cdot 10^{-6} \text{M} - 1.52 \cdot 10^{-6} \text{M}$ . The maximal concentration values were registered, as well as in September 2005, above the Dubasari dam. At the sites located near Bosernica and below the Dubasari dam the state of the waters was characterized as instable since the samples did not contain either hydrogen peroxide or signs of organic substances that easily reacts with hydrogen peroxide.

In November 2005, March and May 2006 the quality of waters was characterized as being unfavorable for the occurrence of chemical self-purification with participation of hydrogen peroxide. In the other parts of the investigated segment the waters were in instable state as well, since the  $\text{H}_2\text{O}_2$  content was very low ( $3,2 \cdot 10^{-7} \text{M} - 7,0 \cdot 10^{-6} \text{M}$ ) while at Bosernita  $\text{H}_2\text{O}_2$  was not detected at all.

The obtained results have denoted that the worst situation was established in March 2006, when the instable state of the waters was extended throughout the total segment Naslavcea – Bosernita (neither hydrogen peroxide nor reducing peroxiacids were present), while above and below the barrage there were detected reducing substances in quantities  $9,0 \cdot 10^{-7} \text{M}$  and  $2 \cdot 10^{-7} \text{M}$  respectively.

In May 2006 the instable state of waters was similar to the state detected in November 2005. Insignificant concentrations of  $\text{H}_2\text{O}_2$  were registered at Naslavcea ( $3,7 \cdot 10^{-7}$ ), Cosauti ( $5,0 \cdot 10^{-7} \text{M}$ ), above ( $5,0 \cdot 10^{-7} \text{M}$ ) and below ( $4,0 \cdot 10^{-7} \text{M}$ ) the barrage at Dubasari. At the Mereseuca site the waters were in the reducing state (the content of reducers was  $3,0 \cdot 10^{-7} \text{M}$ ), while at Cosauti and Bosernita neither  $\text{H}_2\text{O}_2$  nor reducers were detected.

In June 2006 the redox state of waters was different in various segments of the river. Thus, in the segment Naslavcea – Cosauti (the part of the river with most intense flow) the waters were in oxidized state, and the content of hydrogen peroxide constituted  $1,26 \cdot 10^{-6} \text{M} - 5,44 \cdot 10^{-6} \text{M}$ , that can assure the realization of the chemical self-purification processes with participation of effective oxidizers. The segment of the river Bosernita – upper side of Dubasari barrage did not contain  $\text{H}_2\text{O}_2$  while in the content of peroxidazic reducers in the water samples constituted  $4,6 \cdot 10^{-7} \text{M} - 6,4 \cdot 10^{-7} \text{M}$ . This variation of the redox state in this part of the river can be explained by the decrease of the water flow, the accumulation of organic substances of reducing nature, mass development of microflora and related discharge of peroxidazic nature. Besides, it must be taken into account that in the warm part of the year, especially during summer, the hydrogen peroxide cycle in the natural water media is influenced both by the anthropogenic factors such as discharge of biologically treated residual waters, enriched with reducing substances and by the abundant development of blue-green algae that disseminate toxic metabolites that have reducing properties.

In August 2006 the state of water was again instable from the point of view of redox equivalents equilibrium. In the total segment under investigation there were identified insignificant quantities of  $\text{H}_2\text{O}_2$  ( $4,8 \cdot 10^{-7} \text{M} - 5,0 \cdot 10^{-7} \text{M}$ ), a fact that impedes the occurrence of self-purification processes. This fact is related to the intense anthropogenic pollution of the river with organic substances.

During May – August 2006, when the solar irradiation was more intense, in the investigated segment there were evaluated kinetic parameters characterizing the self-purification processes occurring with participation of free radicals. The evaluated parameters included the capacity of inhibition of waters ( $\Sigma k_i[S_i]$ ) and stationary concentration of OH free radicals. The value of the capacity of inhibition and its physical sense allows the consideration of this parameter as being the effective constant of rate of the reaction of OH free radicals “disappearance” in water medium, therefore it can be regarded as an indicator of the state of the water. The smaller the parameter  $\Sigma k_i[S_i]$ , the bigger is the contribution of the source of free radicals to the self-purification by radicals. When the  $\Sigma k_i[S_i]$  is less than  $10^4 \text{ s}^{-1}$  the water is pure, at values of  $\Sigma k_i[S_i]$  bigger than  $10^6 \text{ s}^{-1}$  the water is more polluted. For the majority of natural waters the typical values of  $\Sigma k_i[S_i]$  equals  $10^5 \text{ s}^{-1}$ .

Table 3

Values of the capacity of inhibition of Dniester waters ( $\Sigma k_i[S_i]$ ,  $\text{s}^{-1}$ ) and the stationary concentration OH free radicals

$\text{OH}, \text{M}([\Sigma k_i[S_i]/[\text{OH}]])$  during May – August 2006

Month, year	Naslavcea	Mereseuca	Cosauti	Bosernita	Dubasari, above the barrage	Dubasari, below the barrage
05.2006	$5,80 \cdot 10^5$ $1,72 \cdot 10^{-17}$	$7,60 \cdot 10^5$ $1,30 \cdot 10^{-17}$	$8,10 \cdot 10^5$ $1,23 \cdot 10^{-17}$		$3,0 \cdot 10^5$ $1,75 \cdot 10^{-17}$	$5,70 \cdot 10^5$ $3,4 \cdot 10^{-17}$
06.2006	$5,40 \cdot 10^4$ $7,60 \cdot 10^{-16}$	$6,70 \cdot 10^4$ $8,40 \cdot 10^{-16}$	$3,20 \cdot 10^4$ $6,70 \cdot 10^{-16}$	$5,60 \cdot 10^5$ $9,70 \cdot 10^{-17}$	$5,30 \cdot 10^5$ $8,30 \cdot 10^{-17}$	$4,20 \cdot 10^5$ $7,20 \cdot 10^{-17}$
08.2006	$1,85 \cdot 10^5$ $5,50 \cdot 10^{-17}$	$1,90 \cdot 10^5$ $5,20 \cdot 10^{-17}$	$1,50 \cdot 10^5$ $6,70 \cdot 10^{-17}$	$2,30 \cdot 10^5$ $4,40 \cdot 10^{-17}$	$1,90 \cdot 10^5$ $5,30 \cdot 10^{-17}$	$1,90 \cdot 10^5$ $5,30 \cdot 10^{-17}$

In May 2006 the Dniester water were in normal state from the point of view of chemical self-purification by free radicals (see table). The parameter  $\Sigma k_i[S_i]$  had values of the order  $10^5 \text{ s}^{-1}$ , while the stationary content of OH free radicals was varying in the limits  $1.30 \cdot 10^{-17} \text{ M} - 3.40 \cdot 10^{-17} \text{ M}$ . More intensively the processes of self-purification by radicals were taking place below the Dubasari barrage ( $\Sigma k_i[S_i] = 3,0 \cdot 10^5 \text{ s}^{-1}$ ), and least intensively at Mereseuca and Cosauti ( $\Sigma k_i[S_i] = 7.6 \cdot 10^5 \text{ s}^{-1}$  and  $8.10 \cdot 10^5 \text{ s}^{-1}$ ).

In June 2006 the waters of the segment Naslavcea – Cosauti were characterized by high purity since the values of the capacity of inhibition constituting  $3.20 \cdot 10^4 - 6.70 \cdot 10^4 \text{ s}^{-1}$ . The sector Bosernita – upper side of the Dubasari barrage was also considered favorable for the occurrence of intense self-purification processes. The values of the capacity of inhibition were in the limits of the order  $10^5 \text{ s}^{-1}$ .

In August 2006 the values of the capacity of inhibition constituted  $2.0 \cdot 10^5 \text{ s}^{-1}$  ( $1.50 \cdot 10^5 - 1.90 \cdot 10^5 \text{ s}^{-1}$ ) in all the sampling sites, except at Bosernita where  $\Sigma k_i[S_i] = 2.3 \cdot 10^5 \text{ s}^{-1}$ . This fact denotes that in August the values of the capacity of inhibition of Dniester waters indicated a normal occurrence of self-purification process with participation of free radicals.

The self-purification processes of Dniester waters occur with participation of OH free radicals and during the seasons with high solar activity this process occur in normal conditions and the observations prove that the capacity of inhibition of waters indicate a normal state of waters. The investigated segment of the river have shown the following correlation between redox agents (Table 4).

Table 4

The correlation equations and correlation coefficients of the redox parameters

Correlation parameters	Correlation equations	Correlation coefficients
<b>Naslavcea</b>		
$[H_2O_2] = f(rH)$	$[H_2O_2] = 1.45 \cdot 10^{-6} \cdot rH - 3.94 \cdot 10^{-5}$	$r = 0.7$
$[H_2O_2] = f(CBO)$	$[H_2O_2] = 6.68 \cdot 10^{-7} \cdot CBO - 6.24 \cdot 10^{-7}$	$r = 0.7$
$[H_2O_2] = f(\%O_2)$	$[H_2O_2] = 4.23 \cdot 10^{-8} \cdot (\%O_2) - 3.43 \cdot 10^{-6}$	$r = 0.4$
$rH = f[PO_4^{3-}]$	$rH = 1.20 \cdot [PO_4^{3-}] + 26.55$	$r = 0.4$
$rH = f(\%O_2)$	$rH = 0.01 \cdot (\%O_2) + 26.00$	$r = 0.6$
$[NO_2^-] = f[O_2]$	$[NO_2^-] = 0.002 \cdot [O_2] + 0.008$	$r = 0.3$
$CBO = f[O_2]$	$CBO = 0.259 \cdot [O_2] + 1.164$	$r = 0.6$
<b>Mereseuca</b>		
$CBO = f[O_2]$	$CBO = 0.49 \cdot [O_2] - 2.345$	$r = 0.7$
$[NO_2^-] = f[O_2]$	$[NO_2^-] = 0.003 \cdot [O_2] - 3.49 \cdot 10^{-6}$	$r = 0.4$
<b>Bosernita</b>		
$rH = f(\%O_2)$	$rH = 0.02 \cdot (\%O_2) + 26.09$	$r = 0.5$
$rH = f(pH)$	$rH = 1.76 \cdot pH + 14.17$	$r = 0.9$
$[H_2O_2] = f(\%O_2)$	$[H_2O_2] = 1.73 \cdot 10^{-8} \cdot (\%O_2) - 1.54 \cdot 10^{-6}$	$r = 0.8$
$[NO_2^-] = f[O_2]$	$[NO_2^-] = 0.002 \cdot [O_2] + 0.002$	$r = 0.5$
<b>Cosauti</b>		
$[H_2O_2] = f(CBO)$	$[H_2O_2] = 2.24 \cdot 10^{-7} \cdot CBO + 2.66 \cdot 10^{-7}$	$r = 0.5$
$[H_2O_2] = f(\%O_2)$	$[H_2O_2] = 9.13 \cdot 10^{-9} \cdot (\%O_2) - 1.39 \cdot 10^{-7}$	$r = 0.4$
$rH = f[NO_2^-]$	$rH = 9.99 \cdot [NO_2^-] + 27.75$	$r = 0.6$
$rH = f[O_2]$	$rH = 0.06 \cdot [O_2] + 27.72$	$r = 0.6$
$CBO = f[O_2]$	$CBO = 0.16 \cdot [O_2] + 1.26$	$r = 0.3$
<b>Dubasari, above the dam</b>		
$CBO = f[O_2]$	$CBO = 0.63 \cdot [O_2] - 2.303$	$r = 0.7$
$[NO_2^-] = f[O_2]$	$[NO_2^-] = 0.003 \cdot [O_2] - 0.0008$	$r = 0.3$
<b>Dubasari, below the dam</b>		
$rH = f(pH)$	$rH = 2.16 \cdot pH + 9.13$	$r = 0.5$
$rH = f[O_2]$	$rH = 0.38 \cdot [O_2] + 22.75$	$r = 0.4$

## Conclusions

The investigations carried out in the segment Naslavcea (below the barrage of the buffer reservoir) and Dubasari (below the barrage at) allowed the drawing of following conclusions.

The oxygen regime of Dniester was characterized by following peculiarities:

The content of dissolved oxygen in the waters of Naslavcea was always lower than in other sections of the river. The normal saturation of Dniester waters at this section line occurred only in spring, although in summer and in autumn the saturation of waters was permanently below the norms, constituting in average 70.5% in summer and 79.5% in autumn.

Lower at Naslavcea, most part of the year the concentrations of oxygen in water were close to normal saturation (95 – 110%), except in the cases when there was observed hypersaturation of waters of 158 -177% at Cosauti and Dubasari in 2005 and at the end of summer season of 2006 when there was observed a decrease of oxygen content at the Dubasari water reservoir.

According to the  $rH_2$  indicator the Dniester waters were instable both in seasonal and spatial aspects. The ratio of oxidants and reducers of the waters can be characterized as neutral at Naslavcea, at Cosauti in summer and in spring, at Bosernita and Dubasari in autumn and in spring. At Mereseuca and in the deep waters of Dubasari water reservoir this indicator was shifted most often towards the reducing processes.

Mineral forms of nitrogen and phosphorous were constantly present in the waters of the river. The content of ammonium ions was increasing from Naslavcea toward the lower pool of the Dubasari barrage from 0.015 – 0.021 till 0.136 mg  $NH_4$ /l. The seasonal variation was manifested by the increase of  $NH_4$  in autumn and its practical absence in spring.

The content of nitrites varied in the investigated segment of the Dniester in average from 0.027 – 0.058 mg  $NO_2$ /l. Its presence was permanent in all the section lines of the river. The absence of nitrites was observed only early in spring (March 2006) above and below the Dubasari barrage of the water reservoir.

The average content of phosphates varied in the section lines in the range 0.11 – 3.22 mg  $PO_4^{3-}$ /l. The maximal content of phosphates was observed in the summer of 2006 at Cosauti and Bosernita sites and constituted 3.22 and 1.37 mg  $PO_4^{3-}$ /l respectively. The increase in the content of phosphates occurred in spring in the segment of the river Naslavcea – Mereseuca, in summer - from Cosauti to Dubasari.

The amount of organic substances according to the BOD indicator constituted in average 3.1 – 3.3 mg  $O_2$ /l in the segment Naslavcea – Cosauti, and 3.6 -3.9 mg  $O_2$ /l at Dubasari water reservoir.

The Dniester waters are characterized by seasonal variation of the redox state. The general trend for the part of the year autumn – spring was toward the decrease of the concentration of hydrogen peroxide and the formation of an instable state or even of a quasy-reducing state of waters from the point of view of equilibrium of redox equivalents – of hydrogen peroxide and of reducers of peroxidazic type. The values of  $H_2O_2$  concentration were predominantly by order of  $10^{-7}M$ , a value that is insignificant for the occurrence of efficient chemical self-purification processes in water medium. The point characterized by continuous instable reducing state was the Bosernita site that is located in the proximity of the accumulation segment of the river above the Dubasari barrage. The last one was as well characterized repeatedly by instable state of the waters, since out of seven measurements of the redox state three have demonstrated an unfavorable state according to the content of hydrogen peroxide.

During the summer season, in the Dniester waters the chemical self-purification processes occur very effectively, that is why the negative impact of pollutants is partially diminished.

The degradation of the quality of water of Dniester river is influenced both by the elevated content of pollutants in tributary waters and discharges of wastewaters from municipalities located along the river above the Dubasari barrage.

## References:

- [1] Goreaceva, N. In Water resources in The state of the environment in the Republic of Moldova: Water Resources, 1999. p. 28-45.
- [2] Goreaceva, N.; Gladchi, V. In Intellectus: The ecological state of surface waters in the Republic of Moldova, 1999. p. 68-71.
- [3] Goreaceva, N.; Duca, Gh. Гидрохимия малых рек Республики Молдова: CE USM, 2004. 288 p.
- [4] Goreaceva, N. In Proceedings of the Symposium on Ecological Chemistry, Chişinău, 1- 4 october, 1995: Small rivers in the conditions of antropogenic stress. 1995, p. 15.
- [5] Bepalov, I.; Goreaceva N. In The International Scientific and Applied Conference on Dniester problems: Днестровское водохранилище – один из факторов деградации экосистем ижнего Днестра /*The Dniestrovsc water reserve as a factor of Lower Dniester Ecosystem degradation*/. 2000. p. 52.
- [6] Rusev, I., Ruseva T., Ternova P., Ternovaia Iu. Внедрение экологических правил эксплуатации Днестровского гидроузла – важнейший инструмент устойчивого функционирования экосистемы дельты Днестра /*The introduction of ecologicaly sound rules for exploitation of Dniestrovsk hydropower complex*/. In: Integrated management of natural resources in the transboundatry Dnister river basin. Chisinau. Eco-TIRAS. 2004.p. 61.
- [7] Rusev, I.; Ruseva, T.; Ternova, P.; Ternovaia, Iu. In: Integrated management of natural resources in the transboundatry Dnister river basin: Внедрение экологических правил эксплуатации Днестровского гидроузла – важнейший инструмент устойчивого функционирования экосистемы дельты Днестра /*The introduction of ecologicaly sound rules for exploitation of Dniestrovsk hydropower complex*/. 2004. p. 82.
- [8] Duca, Gh.; Scurlatov, Iu.; Misiti, A.; Macoveanu, M.; Surpăţeanu, M. Chimie ecologică Matrix Rom: Bucureşti, 1999. 305 p.

- [9] Duca, Gh.; Scurlatov, Yu.; Sychev, A. Redox Catalysis and Ecological Chemistry. CE USM: Chişinău, 2002. p. 291-316.
- [10] Biodiversity Conservation of the Dniester River Basin. Kishinev, 1999. p. 89.
- [11] Gladchi, V.; Goreaceva, N.; Bunduchi, E.; Borodaev, R. In ECWATEC –2004: The problems of the trans-boundary Dniester River. Moscow, 2004. p. 125.
- [12] Duca, Gh. Goreaceva, N.; Romanchuk, L. In Water resources: Исследование самоочищающей способности природной воды в модельных условиях /*The Assessment of self-purification capacity of natural waters on model systems*/, 1996, t 23, Nr 6, pp 668-671.
- [13] Semeniak, L.; Scurlatov, Yu.; Shtamm, E. Сезонные изменения направленности внутриводоемных окислительно-восстановительных процессов и проблемы воспроизводства осетровых в Волго-Каспийском регионе /*The seasonal changes of the direction of aquatic oxidation and reduction processes and the problems of regeneration of sturgeon fisheries in Volga and Kaspik Region*/, 1996. p. 28-35.
- [14] Shtamm, E.; Purmal, A.; Scurlatov, Y. In The realizations in Chemistry: The role of hydrogen peroxide in the aquatic environment, Russia, 1991.
- [15] Romanciuc, L.; Goreaceva, N.; Duca, Gh. In Water Pollution-95, III-rd Int. Conf., 25-28 Apr., Porto-Carras: Modelling of self-purification processes of aquatic medium, 1995, pp 98.
- [16] Duca, Gh.; Romanciuc, L.; Goreacev, N.; Borodaev, R. In Metal Compounds in Environment and Life, VII-th Int., Hans Wolfgang Nurnberg Memorial Symp., 4-7 June 1997, Modena (Italy): Model of self-purification processing in natural water, 1997. pp 51.
- [17] Goreaceva, N; Gladchi, V. Методика определения кинетических показателей качества поверхностных (пресных) вод /*A method of determination of kinetic indicators of the quality of fresh waters*/; Guidance document. Hydrometeoizdat publisher: Moscow, 1990.
- [18] Duca, Gh.; Bunduchi, E. In Abstracts of The Second Int. Conf. on Ecological Chemistry, 11-12 Oct., 2002: Radical self-purification of Prut river waters in the period of summer 2002 mean water, Chişinău, 2002. pp 40-41.
- [19] Cutter, G. Ph.D. Dissertation, Old Dominion University. 1991.
- [20] Rue, E.; Smith, G.; Cutter, G.; Bruland, K. The response of trace element redox couples to subox conditions in the water column; Deep-See Res., 1997, Vol 44, pp113-134.
- [21] Bielski, H.; Cabelli, D.; Arud, R.L. Journal of Physical Chemistry. 1985.
- [22] Petasne, R.; Zika, R. Nature, 1987, Vol 325.
- [23] Borodaev, R. In The collection of Scien. Papers of MSU: Редокс условия нижнего Днестра и состояние растворенных форм железа и меди /*The redox conditions of Lower Dniester and of the state of dissolved forms of iron and copper*/, 2002. p. 165-168.
- [24] Duca, Gh. In Free Radicals in Biology and Environment: Free radicals in natural water; Dordrecht, 1997; pp 475-489.
- [25] Gladchi, V. Starea redox a apelor naturale și influența ei asupra proceselor naturale /*The redox state of natural waters and its influence on natural processes*/ . J. Intellectus, 2000. p. 21-26.
- [26] Sichev, A.; Duca, Gh. Aspecte fundamentale și aplicate ale catalizei omogene cu metalocompuși: Sisteme oxidice și peroxidice. CE USM: Chişinau, 2002; p. 42.
- [27] Sichev, A. *Aspecte fundamentale și aplicate ale catalizei omogene cu metalocompuși: Sisteme oxidice și peroxidice*. CE USM: Chişinău, 2002, p. 332.
- [28] Gladchi, V. In The Scientific Proceedings of Moldova State University: Chemical and Biological Sciences Series Procese de transformare chimică a poluanților și rolul substanțelor tiolice în mediul acvatic /*Processes of pollutants chemical transformation and the role of thiolic substances* /. Chişinău, 2000.
- [29] Gladchi, V. In The Proceedings of the didactic and scientific staff conference “Balance of scientific activity of the Moldova State University for 1998/1999 years: Transformările chimice ale unor substanțe tiolice în mediul acvatic /*Chemical transformation of thiolic substances in aquatic medium*/. Chişinău, 2000.
- [30] Duca, Gh.; Gladchi, V.; Goreacev, N. Chimia apelor naturale; CEP USM: Chişinău, 2007. 107 p.
- [31] [30] Klokov, D.; Jacob, P. Chemistry of Multiphases Atmospheric Systems. Springer: Berlin – Verlag, 1986. p. 125.
- [32] Skurlatov, Yu.; Shtamm, E. In “Self-Purification Processes in Natural Waters. Proceedings of the International Symposium on Ecological Chemistry: Aquatic cycling of hydrogen peroxide as a principal way of natural waters self-purification, Chisinau, Moldova. 1995. p. 135.
- [33] Duca, Gh.; Zanoagă, C.; Duca, M.; Gladchi V. Procese redox în mediul ambiant, CEP USM: Chişinău, 2001. 386 p.

## INFLUENCE OF IODINATED OIL AND MARGARINE ON THE THYROID SYSTEM OF RATS

Rodica A. Sturza<sup>a</sup>, Olga I. Deseatnicov<sup>a</sup>, Cristina M. Popovici<sup>a\*</sup>, Valentin S. Gudumac<sup>b</sup>,  
Ion Nastas<sup>b</sup>

<sup>a</sup> Technical University of Moldova, 168 Stefan cel Mare bldv., MD 2004 Chisinau, Moldova, tel.: 23-86-45, fax: 31 – 91 – 76,  
E-mail : cristina\_popovici@mail.md

<sup>b</sup> State Medical and Pharmaceutical University “Nicolae Testemitanu”, Moldova

**Abstract:** Iodine deficiency is the most prevalent micronutrient deficiency in the world today. Food fortification is an important complement to food-based approaches, and iodine fortification of foods as one of the strategies for the control of iodine deficiency. Manufacturing and consumption of sunflower oil fortified with iodine as well as derivative products on it basis is a perspective direction for elimination of alimentary dependent iodine deficiency disorders. The present work examines morphological changes in the thyroid system of rats at the experimental mercatholile-induced hypothyroidism. As well it determines the influence of iodinated oil and margarine on the thyroid system of rats. It specifies the safe value of iodinated oil and margarine for rats. In-vivo study demonstrated the efficacy of fortification of lipid products with iodine under iodine deficiency status.

**Key words:** Iodine deficiency, food fortification, sunflower oil, margarine, in vivo study.

### Introduction

The problem of iodine deficiency (ID) is one of the main problems of the world society, including Republic Moldova [1]. ID affects all population at all stages of life, from the intrauterine stage to old age [2, 3].

The environment of Republic Moldova is characterized by a reduced values of the iodine content: 4,5-5,3mg/kg soil, 40mg/l water and 0,03-0,22mg/kg of vegetation, on a dry content of substances. Approximate 85% of populations of Moldova live in iodine deficient regions [4].

Researches performed by WHO and UNICEF in the Republic of Moldova have demonstrated a 37% prevalence of endemic goiter among children and teenagers [ 5].

In order to eliminate the iodine deficiency disorders, the Government Decision nr. 585 “*Decision regarding the approving of national system of eradication of disorders caused by iodine deficit till the 2010*” was approved on 1 June 2007 as a way of addressing the problem of iodine deficiency disorders and was adopted as Law. It provides instructions for the fortification of foodstuffs with nutrients that have insufficient values in local region [6].

The most appropriate way of fighting the iodine deficiency is to produce foodstuff for functional purposes which contain stable forms of iodine [7].

Sunflower oil takes up the biggest specific weight among edible fats used in nutrition in the Republic Moldova. Iodine administration in products with a lipid origine represents a remarkable interest. First, this would allow the easy incorporation of the iodine in the food fatty products. Secondly, the daily intake of lipids being limited, would allow an easy regulation of the iodine consumption, this being complementary with that from the iodinated salt and other products.

The aim of the research consisted of examination of metabolic displacement in the organism of animals and correction of experimental and spontaneous thyroid pathology by means of iodinated food products (sunflower oil, margarine).

### Results and discussion

*The level of thyroid hormones of rats during the examination of iodinated sunflower oil and margarine.*

For getting of the model of artificial hypothyroidism mercazolile was used for blocking the thyroid gland function. Peroxidase catalyzes the oxidation reactions. It is known that the activity of oxidation ferments decreases on hypothyroidism and increases on hyperthyroid states [8].

Mercazolile depresses the ferment activity of iodineperoxidase – the ferment which provides the iodination of  $\alpha$  – thyroxine. It provokes hypothyroidism because iodine an obligatory ingredient of thyroxine [9].

Biological activity of examined iodinated products was evaluated according to indexes that reflect the functional state of animals’ thyroid gland. Pursuing this aim, the level of thyroid gland hormones such as total Triiodothyronine ( $T_3$ ), Thyroxine ( $T_4$ ) in the experimental rats’ blood serum was determined. The condition of the hypophysial-thyroid system was evaluated according to the content of serum Thyroid-stimulating hormone (TSH, Thyrotropin) [10-13]. Received data reflected in the Table 1.

Table 1

Content of thyroid hormones in the rats' serum

Group of rats	Total Triiodothyronine hormone (T <sub>3</sub> )	Thyroxine hormone (T <sub>4</sub> )	Thyroid-stimulating hormone (TSH, thyrotropin)
	ng/dl	nmol/l	muI/l
I	92,65±19,12	114.1±16.49	0.894±0.032
II	84,65±14,54	93.1±14.54	1.272±0.037
III	89,94±18,52	95.81±19.53	0.966±0.025
IV	90,26±13,39	107.42±15.02	0.856±0.099
V	91,15±16,76	119.37±14.43	0.814±0.034
VI	73,00±19,94	92.83±14.48	1,257±0.027

Data regarding blood serum immune-enzyme analysis witnesses the decrease of thyroid gland functional activity in rats that were in the condition of experimental hypothyroidism (II and III group). Introduction of mercasolile called experimental hypothyroidism condition that was accompanied by morphological functional displacement in the thyroid system, expressed in T<sub>4</sub> level decrease and TSH concentration increase in the controlled group (group I) (Figure 1).

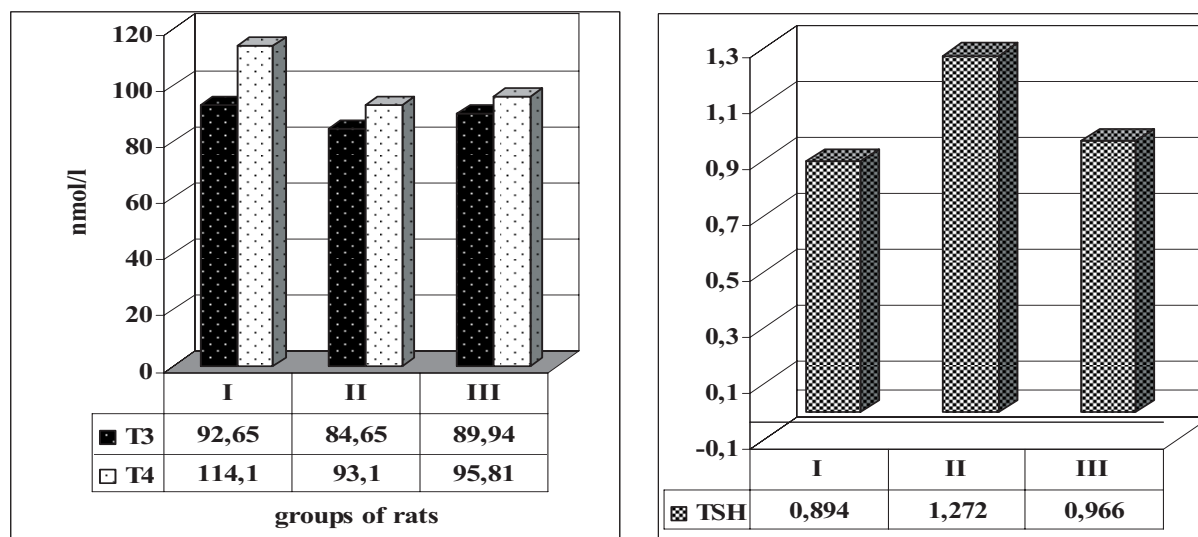
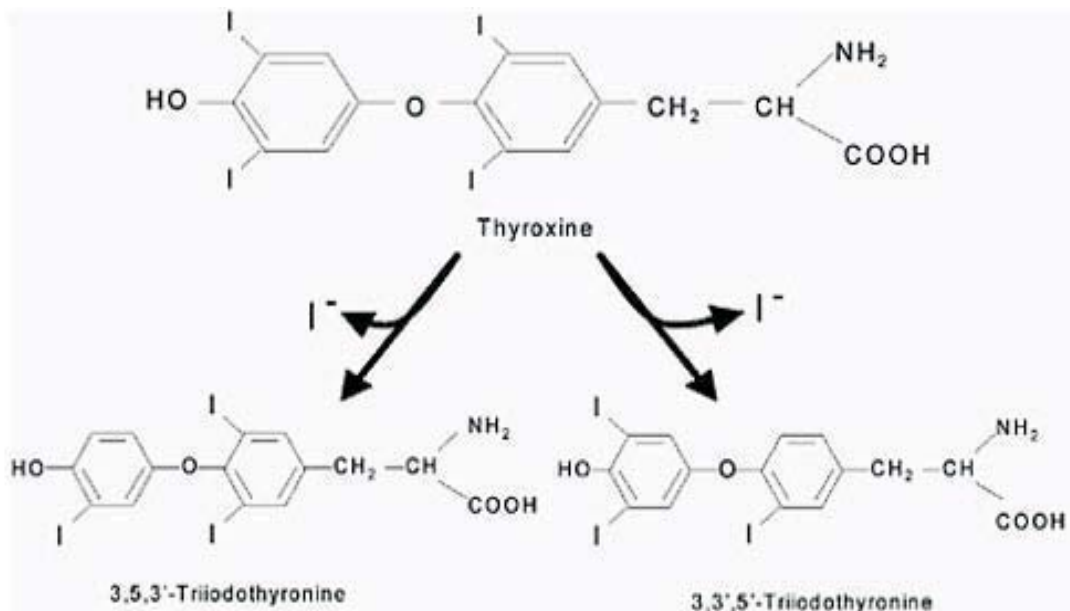


Fig. 1. Content of thyroid harmonious in the serum of rats belonging to I, II, III groups

Thus, T<sub>4</sub> concentration in the hypothyroid rats serum (IIInd group) decreased and become 93.1±14.54 nmol/l, in the IIIrd group – 95,81±19.53 nmol/l against 114.1±16.49 nmol/l of the controlled group. At the same time hypothyroidism contributes to the increase of thyrotrophic hormone (TSH) with 0.894±0.032 muI/l (controlled group) till 1.272±0.037 muI/l (IIInd group) and 0.966±0.025 muI/l (IIIrd group).

Thereby, experimental rats, introduced in the condition of mercasolile hypothyroidism, show expressed destructive-degenerative processes in the thyroid glands in comparison with the control group. In the thyroid grand the lack of colloid in follicles is the result of termination of thyreoglobulin thyrocotis synthesis.

All thyroxine (T<sub>4</sub>) and some triiodothyronine (T<sub>3</sub>) are produced by the thyroid gland, and their production there is stimulated by thyroid-stimulating hormone (TSH, thyrotropin), a product of the anterior pituitary gland. Some T<sub>4</sub> is converted to T<sub>3</sub> in other tissues, including the pituitary gland and the hypothalamus. T<sub>3</sub> inhibits pituitary secretion of TSH, and hypothalamic secretion of thyrotropin-releasing hormone (TRH), which stimulates TSH secretion. The interplay between T<sub>3</sub> and TSH maintains thyroid hormone production within a narrow range.



It is necessary to note, that the T<sub>3</sub> concentration at the hypothyroid rats (IIrd and IIIrd group) did not decrease significantly; that can be explained as activation of deiodination T<sub>3</sub> in T<sub>4</sub> processes:

The present regularity is observed as the account of protective-compensatory animal reaction in the condition of iodination blocking of remaining tyrosine as a component of thyroglobulin.

In the course of further research the evaluation of efficacy and safety of examined iodine complexes was performed in the five groups.

The analysis of the received data confirms that organically connected forms of iodine contributed to the increase of functional activity of thyroid gland. Thus, rats of IVth and Vth groups had significantly higher serum T<sub>4</sub> level than animals of IIrd and IIIrd group (Figure 2).

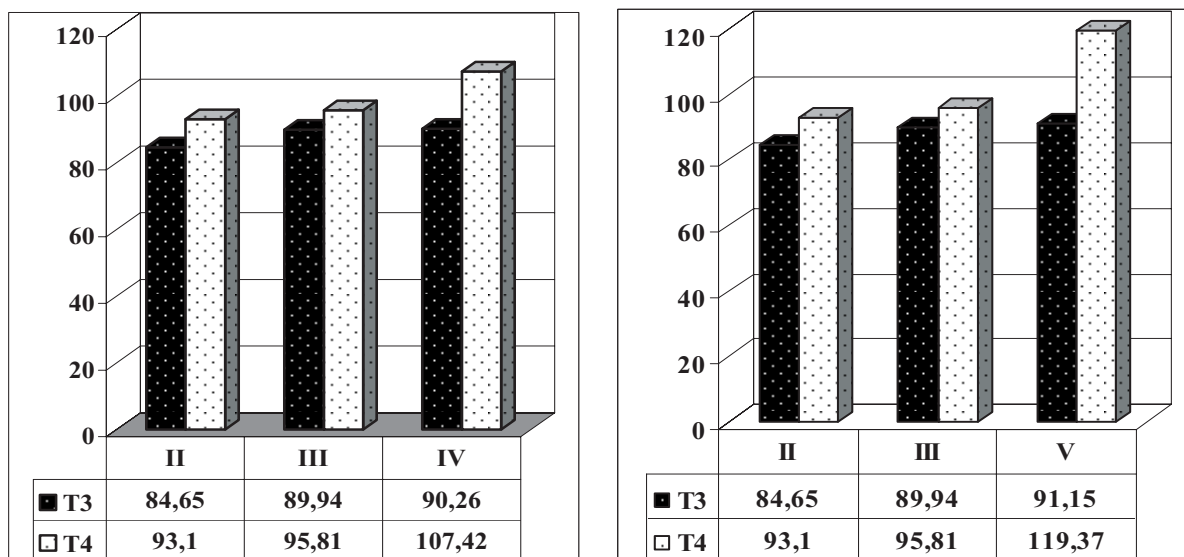


Fig. 2. Content of thyroid harmonious in the serum of rats belonging to II, III, IV и V groups

At the same time T<sub>4</sub> concentration in the IVth group made up 107-42±15-02 nmol/l, in the Vth one 119-37±14.43 nmol/l against 93.1±14.54 nmol/l in the IIrd one and 95.81±19.53 nmol/l in the IIIrd one. Concentration of T<sub>3</sub> in the compared groups does not differ in a significant way, remaining in limits of 90,26 ±13,39 ng/dl (IVth group) and 91,15±16,76 ng/dl (Vth group). The relatively high level of T<sub>3</sub> of the IIIrd group rats (98,94±18,52 ng/dl) is explained by the activation of T<sub>4</sub> deiodation processes in the condition of iodine deficit.

All animals who received additionally daily iodinated sunflower oil and margarine, showed increased level of T<sub>4</sub> secretion accompanied by rather low TSH level (Figure 3).

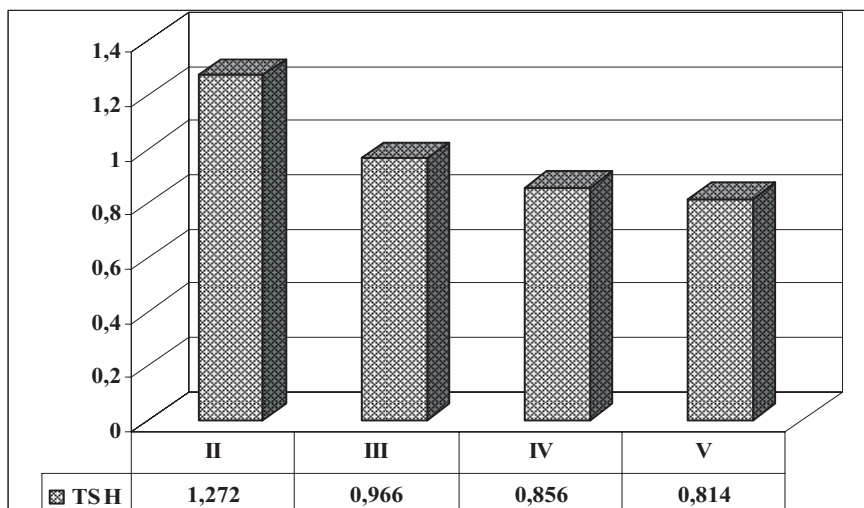


Fig. 3. Influence of iodinated food products over the rat thyroid-stimulating hormone synthesis

Hereby, if animals of the II<sup>nd</sup> and III<sup>rd</sup> group have TSH concentration of 1.272±0.037 μl/l and 0.966±0.025 μl/l correspondingly, in rats of the IV<sup>th</sup> and V<sup>th</sup> groups identical indexes reflected 0.856±0.099 μl/l and 0.814±0.034 μl/l. It is the evidence of stimulating influence of examining iodine products over the functional activity of rats' thyroid glands. Received data match with the research results reported by Kashin, Egorov, Fencenco, Gusakov [14-17].

Use of iodine sunflower oil and margarine in the rats' ration contributed to the gradual restoration of tyrocyte functional activity with the formation of colloid in follicles. All tested iodinated products have the homogeneous actions in the view of tyrocytes activity restoration.

When the main components of the tyroglobuline-iodine in the combination with fatty acids enter the organism, the synthesis of thyroid hormones in tyrocytes restarts. Consequently, regeneration possibilities and differentiation of thyroid glands tyrocytes are high and used substances assist in it. Positive activity of iodine products for the animals' organism are marked in the works of [14, 18].

Besides of that we carried out the research in evaluation of iodinated sunflower oil safety that included examination of chronic toxicity as well. The toxicity was tested on the animals (of IV<sup>th</sup> group) that received daily during the whole experiment period 10-fold iodine dose.

The value of tested iodine dose efficiency and safety over the rat organism held in two compared groups: IV – introduction of 1-fold iodine dose in iodine sunflower oil and VI group. The analysed data show that tested organic connected iodine form is not toxic for the experimental animals. Thus, the rats of VI group had the following T<sub>3</sub> and T<sub>4</sub> concentration level 73,00 ±19.94 ng/dl and 92,83±14.48 nmol/l against 90.26±13.39 ng/dl and 107.42±15.02 nmol/l in the IV group correspondingly. Meantime the TSH level of the rats from the VI<sup>th</sup> group increased and constituted 1.257±0.027 μl/l in comparison with TSH concentration of rats from IV group – 0.856±0.099 μl/l (Figure 4).

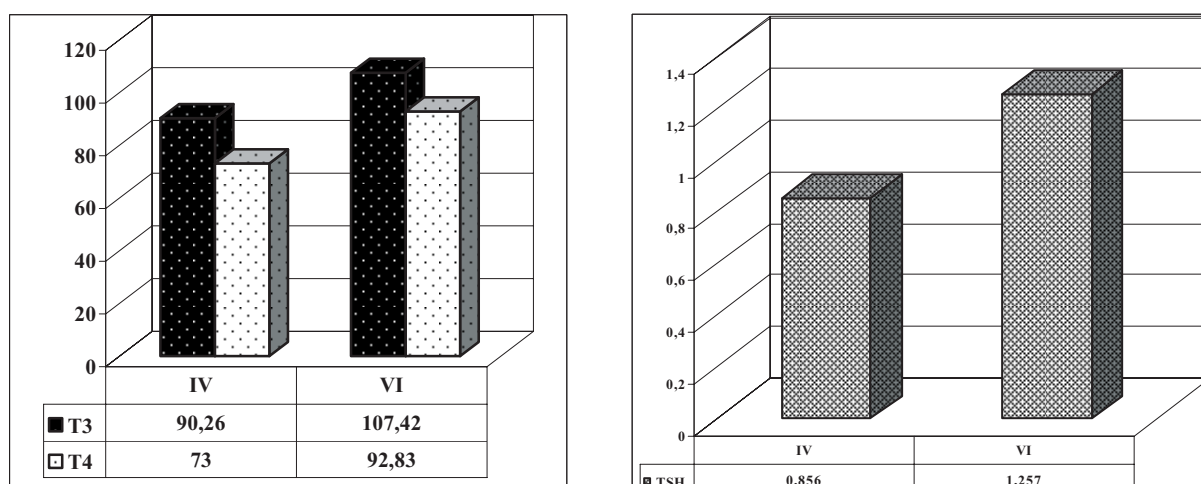


Fig. 4. Influence of 10-fold iodine dose in the structure of iodinated food products over the synthesis of rat thyroid hormones

Data received in the result of our research certify that the consumption of iodine in large quantities leads to decrease of  $T_3$  and  $T_4$  hormone secretion and increase of TSH concentration in comparison with the group of rats that received 1-fold iodine dose. It can be explained by decrease of thyroid gland ability to accumulate iodine and large quantities of iodine removed from the organism through kidneys.

It is necessary to mark, that iodinated sunflower oil and margarine contributed to better use of feedstuff for rats. Received data coincide with the messages of Alioshin, Bataev, Georgievskii [8, 19, 20].

#### *Effect of iodine intake on iodine content of thyroid gland.*

Iodine content in thyroid glands characterizes the intensity and direction of iodine metabolism of animals. Our investigations on iodine accumulation in thyroid glands confirmed the positive influence of optimal iodine level (3  $\mu\text{g}/\text{rat}$ ) on organism of experimental animals. Our data on investigation of iodine content in thyroid glands agree with the works of Baranov and Seleatitskaia [10, 21].

Feeding of experimental animals with optimal iodine level (3  $\mu\text{g}/\text{rat}$ ) increased the functional activity of thyroid gland and iodine concentration in it (table 2). The obtained data are congruent with the investigation results of Fenchenco and Kashin [16, 14].

Table 2

Effect of iodine intake on iodine content of thyroid gland

Group of rats	Iodine content of diet	Weight of thyroid gland	Thyroid iodine
	$\mu\text{g}/\text{rat}$	mg	mg%
I	$0,4 \pm 0,1$	$25,8 \pm 1,5$	$4,8 \pm 0,9$
II	$0,4 \pm 0,1$	$34,2 \pm 1,7$	$1,2 \pm 0,7$
III	$0,6 \pm 0,2$	$18,2 \pm 0,9$	$1,1 \pm 0,6$
IV	$3,5 \pm 0,8$	$24,8 \pm 2,2$	$5,4 \pm 0,7$
V	$3,6 \pm 0,7$	$31,4 \pm 3,8$	$13,0 \pm 1,5$
VI	$30 \pm 1,9$	$39,4 \pm 5,7$	$28,0 \pm 1,9$

\*average daily quantity of feed for rats–  $12 \pm 4$  g

The investigation data indicate that iodinated fats influence on metabolism results leading to the accumulation of the iodine by animals, as a result of more effective digestion and assimilability of iodine from present connections.

In summary our investigations, based on estimation of iodine content in the thyroid glands of experimental animals, proved that in experimental hypothyroidism the iodine content of rats decreased from 4,8 to 1,2 mg% (groups I and II), and on addition of iodinated fats with iodine content (3  $\mu\text{g}/\text{rat}$ ) the iodine quantity in thyroid gland increased from 5,4 to 13,0 mg% (groups III and IV).

On addition of considerable quantities of iodine (30  $\mu\text{g}/\text{rat}$ ) the iodine content also increased, but the capacity of thyroid gland for iodine accumulation is decreased (figure 5).

Analysis of iodine content in thyroid glands, which was obtained from rats after correction of iodine-critical state, at the expense of introduction in their ration of iodinated fats gives the possibility to underline the improvement of functioning and the capacity of iodine accumulation by thyroid gland.

Literature data and the results of proper research on laboratory animals lets us conclude concerning the safety, bioavailability and simplicity of use of organically connected iodine forms as iodinated fats (vegetable oil, margarine).

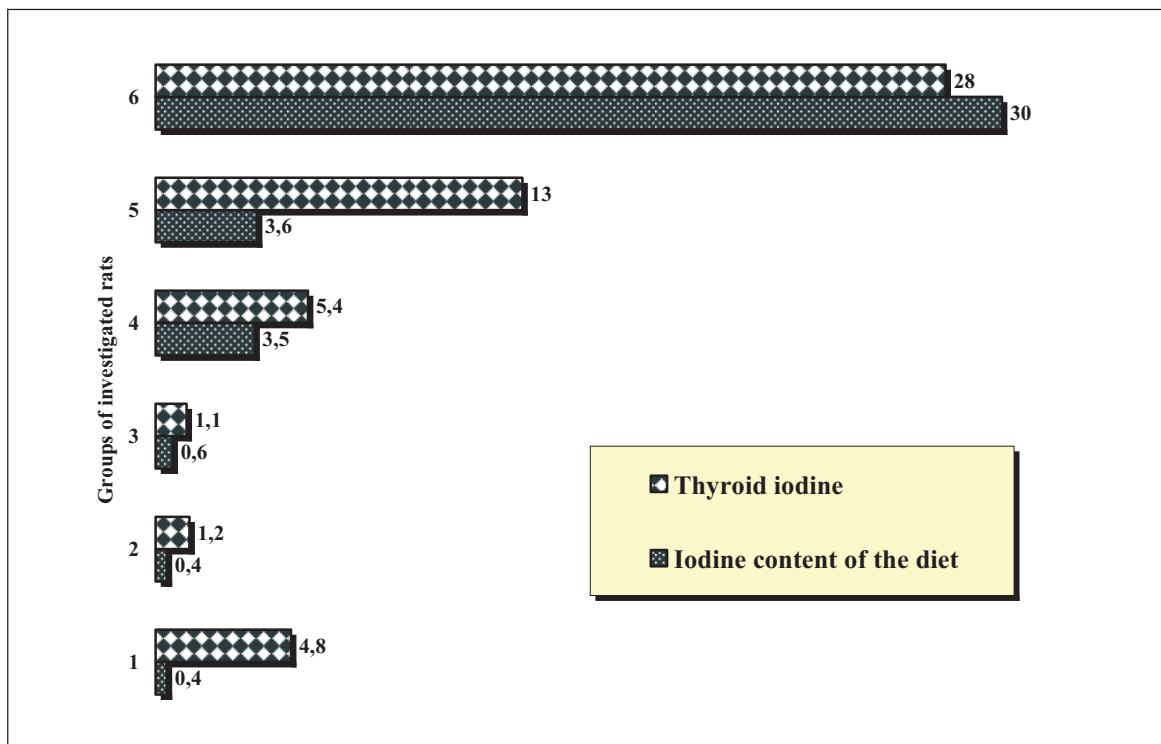


Fig. 5. Influence of consumption by animals of iodinated fats on the process of its metabolism and the accumulation capacity by thyroid gland

## Conclusions

1. Banding of iodine and vegetable oil gave the fixed organic connection with increased biological value, which is available for obtaining and does not require creation of additional technologies.

2. After introduction of iodinated fat products in the ration of hypothyroid animals, they manifest biological activity. Iodinated fat products contribute to restoration of such thyroid hormones levels as  $T_3$ ,  $T_4$  and TSH, i.e. functional activity of thyroid glands.

3. Investigational data indicate that iodinated fats influence on metabolism processes and contribute to the accumulation of the iodine by animal organism, as a result of more effective digestion and assimilability of iodine from present connections.

4. Application of iodinated fats supplies the lack of iodine in organism, does not have side effects and can be used in prevention of diseases, provoked by iodine deficiency.

## Experimental

### ➤ Sun flower oil fortification with iodine

In this study, doubly refined and deodorized oil was used (purchased from local stores) [STAS – 1129-93] [22].

To obtain the iodinated sunflower oil, chemically pure, crystalline iodine ( $I_2$ ) [STAS – 4159-79] [23] was added. After the establishment of the equilibrium, iodinated oil was used as sample for the present study.

### ➤ Manufacturing of iodinated margarine

In proposed iodinated margarine, a part of sun-flower oil was replaced by iodinated doubly refined and deodorized sun-flower oil with an iodine content of  $10\mu\text{g I}/\text{cm}^3$ .

### ➤ Investigations in vivo

For the purpose of elucidation of the influence of food regimes with different content of iodine on bioavailability of iodine from fortified lipidic products and the dynamics of evolution of experimental hypothyroidism, two series of experiments were performed.

The experiment was realized with the lot of white rats of the Wistar line with masses in the range 180 – 210 g. The feed was a standard ration with free access to water. Duration of the experiment was of 42 days. The animals were kept in individual cages, 5 animals in every cage.

The experiment had 2 stages:

Stage I – experimental reproduction of hypothyroidism with the help of mercazolil for blocking of thyroid gland function [24]. Daily (for 14 days) the rats were given water to drink with mercazole added. At the same time they were fed by bread without addition of iodinated salt (produced in the laboratory of Technical University of Moldova), with the purpose to exhaust the reserves of iodine of the organism.

Stage II – feed of animals with experimental hypothyroidism (28 days) by standard ration, without addition of iodine (group II); with additive of sunflower non-iodinated oil (group III); with addition of iodinated oil with iodine content 3 µg/rat (group IV); with addition of iodinated margarine with iodine content 3 µg/rat (group V); with addition of iodinated oil with iodine content 30 µg/rat (group VI).

Scheme of experimental work with white laboratory rats is presented as Figure 6.

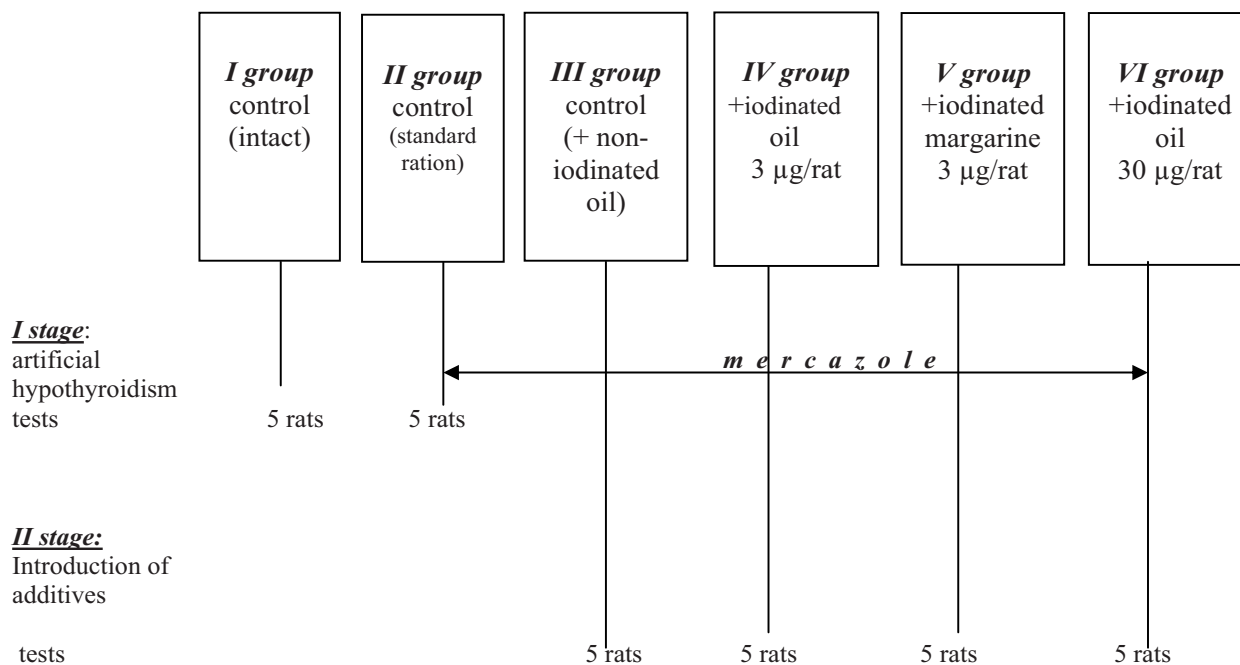


Fig 6. Scheme of experimental work with white laboratory rats

All the six groups of rats during the experiment received the following foodsuffs: whole-grain wheat porridge prepared on meat broth, so they got the lipid products. The porridge was given daily, for dinner, on the assumption of daily consumption of 12g product/rat.

➤ *Analysis of Total Triiodothyronine hormone ( $T_3$ ) in the serum of investigated rats*

The procedure follows the basic principle of enzyme immunoassay where there is competition between an unlabeled antigen and an enzyme-labeled antigen for a fixed number of antibody binding sites. The amount of enzyme-labeled antigen bound to the antibody is inversely proportional to the concentration of the unlabeled analyte present. Unbound materials are removed by decanting and washing the wells. The absorbance measured is inversely proportional to the concentration of  $T_3$  present in the serum. A set of  $T_3$  Standards is used to plot a standard curve of absorbance versus  $T_3$  concentration from which the  $T_3$  concentrations in the unknowns was calculated.

➤ *Analysis of the Thyroxine hormone ( $T_4$ ) in the serum of investigated rats*

The principle of the Thyroxine ( $T_4$ ) analysis in the serum of investigated rats is the same. A set of  $T_4$  Standards is used to plot a standard curve of absorbance versus  $T_4$  concentration from which the  $T_4$  concentrations in the unknowns was calculated.

➤ *Analysis of the Thyroid-stimulating hormone (TSH, thyrotropin) in the serum of investigated rats*

The TSH analysis is an enzymatically amplified “one-step” sandwich-type immunoassay. In the assay, standards, controls and unknown serum samples are incubated in microtitration wells which have been coated with anti-hTSH antibody in the presence of another anti-hTSH detection antibody labeled with the enzyme horseradish peroxidase

(HRP). After incubation and washing, the wells are incubated with the substrate tetramethylbenzidine (TMB). An acidic stopping solution is then added and the degree of enzymatic turnover of the substrate is determined by dual wavelength absorbance measurement at 450 and 620 nm. The absorbance measured is directly proportional to the concentration of TSH in the sample. A set of TSH standards was used to plot a standard curve of absorbance versus TSH concentration from which the TSH concentrations in the unknown samples were calculated.

➤ *Analysis of iodine content in thyroid glands of investigated rats*

For analysis of iodine content in thyroid glands of investigated rats was used a spectrophotometric method of iodine determination. The Method consists in mineralization of the sample with the following extraction of iodine with carbon tetrachloride in presence of sodium nitrite in acidic medium, measurement of absorption of reaction products on wavelength 514 nm. Relative error of average result consists  $\pm 2,05\%$  [25].

➤ *Determinations of errors and statistical analysis of obtained results*

Investigations realized in triplication and processed statistically by the method of those small squares with application of coefficient Student and determination of interval of investigation [26-28].

## References

- [1] Delange F et. al. Risks of iodine-induced hyperthyroidism following correction of iodine deficiency by iodized salt; *Thyroid*, 1999; 9:545-556.
- [2] Hetzel BS. Iodine deficiency disorders (IDD) and their eradication; *Lancet*, 1983; 2:1126-1129.
- [3] Stanbury JB et al. Iodine-induced hyperthyroidism: occurrence and epidemiology; *Thyroid*, 1998; 8:83-100.
- [4] World Health Organization, United Nations Children's Fund, and International Council for Control of Iodine Deficiency Disorders. Geneva ; World Health Organization. (WHO/NUT 94.6.), 1996.
- [5] Raportul UNICEF. Alimentația și nutriția umană în R. Moldova. Biroul pentru Moldova. 2002; p. 38.
- [6] Hotarire cu privire la aprobarea programului national de eradicare a tulburarilor prin deficit de iod pina in anul 2010. Monitorul oficial al RM, 1 iunie 2007.
- [7] Hurrell RF. Mineral fortification of food; England: Leatherhead Food Research Association, 1999.
- [8] Alioshin B.V. O necotoryh spornyh voprosah v patofiziologhii shitovidnoi jelezy.Uspehi sovremennoi biologhii. 1982; Vyp.1.s.121-138.
- [9] Dedov I.I., G. A. Gerasimov, N.I. Sviridenco, A.A. Shishkina, N.M. Maiorova. Ispolizovanie tabletirovannyh preparatov ioda dlia profilactiki endemiceskogo zoba; *Probl. Endokrin.* 1998; Vyp.1.s.24-27.
- [10] Baranov V.G., E.A. Loskutova, M.V. Pronin. O mehanizme podavlenia funkzii shitovidnoi jelezy tireoidnymi garmonami; *Probl.Endokrin*, 1970; Vyp.1.-s.43-46.
- [11] Starcova IG. Farmacoterapia v endocrinologii; M: Medicina, 1989.
- [12] Medvedev VV. Kliniceskaia laboratornaia diagnostiva; SPb: Gipocrat, 1997.
- [13] Lewis G. The nature of trace element problems; delineating the field problem; *Anim. Prod. Vet. Practice.* Edinbergh, 1983; Vol. 7.
- [14] Kashina V.K. Effektivnosti primeneniia ioda v jivotnovodstve. Microelementy v biologii I ih primeneniev s.-h. I medicine;Smarkand, 1990; s.367-369.
- [15] Egorov ID. Naucinye aspekty pitania ptuzy; Ptizevodstvo, 2002.
- [16] Fencenko N.G. Biologiceski aktivnyye veshstva v pitanii jivotnyh;Ufa, 2003;199 s.
- [17] Gusacov VK. Vlianie iodosoderjashih preparatov na pokazateli krovi jivotnyh; *Veterinaria*, 2004; 1, 54-55.
- [18] Newton GL. Iodine toxicity: physiological effects of elevated dietary iodine in animals; *G. Anim. Sci.*, 1974; Vol.39, 879.
- [19] Bataev AP. Biodostupnostiioda dlia jivotnyh; Borobsc, 1991.
- [20] Georgievskii BI. Mineralinoe pitanie ptizy; M: Kolos, 1970.
- [21] Seliatickaia V.G. Funkcionalinoe sostoianie shitovidnoi jelezy krys, poluciavshih kolicestva ioda s pitievoi vodoi; *Voprosy pitania.* 1994; №9. s.50-53.
- [22] STAS - 1129 – 93. Ulei de floarea soarelui. Condiții tehnice.
- [23] STAS – 4159- 79. Iod Cristalin. Conditii tehnice.
- [24] Teppermen D. i Teppermen H. Fiziolodhia obmena veshstv i endocrinnoi sistemy; *Vvodnyi curs : Per. s angl.-M.:Mir*, 1989; s. 302-308.
- [25] ACTES du seminaire d'animation regionale (Region Europe Centrale et Occidentale) SAR-2004 (Agence Universitaire de la Francophonie, Réseau "Génie des Procédés Qppliqué à l'Agro-Alimentaire", Université Techniqué de Moldavie ; Ch.:Tehnica - Info, 2004; 380 p.
- [26] Snedecor G.W. and Cochran C.V. *Statistical methods* Ams; IA, 1989.
- [27] Lakin GF. *Biometria*; M.:Vysshiaia shkola, 1990.
- [28] Kuziahmetov GG. *Metody izuceniia pocvennyh vodoroslei*; Ufa: Bashkirsk, 2001.

# SPECTROPHOTOMETRIC STUDIES OF SANGUINARINE- $\beta$ -CYCLODEXTRIN COMPLEX FORMATION

Veaceslav Boldescu,<sup>a,\*</sup> Irina Kacso,<sup>b</sup> Ioan Bratu<sup>b</sup> and Gheorghe Duca<sup>a</sup>

<sup>a</sup>Department of Industrial and Ecological Chemistry, State University of Moldova, 60, Mateevici str., MD 2009, Chisinau, Republic of Moldova

\* tel. (+373 79) 454062, fax (+373 22) 244248, e-mail: sboldescu@yahoo.com

<sup>b</sup>National Institute for Research and Development of Isotopic and Molecular Technologies, 71-103, Donath str., P.O. Box 700, RO-400293, Cluj-Napoca, Romania

**Abstract.** The main aim of this study was to investigate the influence of pH and the presence of hydrophilic polymer polyvinylpyrrolidone on the formation of sanguinarine- $\beta$ -cyclodextrin (SANG- $\beta$ -CD) inclusion complex. Spectrophotometric studies of the SANG- $\beta$ -CD systems in the presence and without 0.1 % PVP at the pH 5.0 did not show any evidence of the complex formation. However, the same systems showed several obvious evidences at the pH 8.0: the hyperchromic and the hypochromic effects and the presence of the isosbestic point in the region of 200 – 210 nm. The association constants calculated by three linear methods: Benesi-Hildebrand, Scott and Scatchard, were two times higher for the systems with addition of 0.1% PVP than for the systems without it.

**Keywords:** sanguinarine,  $\beta$ -cyclodextrin, inclusion complex, UV-vis spectrophotometry, association constant

## Introduction

Sanguinarine (SANG) is a quaternary benzo[c]phenanthridine alkaloid derived from the plants of *Papaveraceae* and *Fummaraceae* families (*Macleya cordata*, *Sanguinaria canadensis*, *Chelidonium majus*). It has been found to be a potent antimicrobial, anti-inflammatory, antioxidant agent [1, 2]. Moreover, recent studies have shown its *in vitro* and *in vivo* antiproliferative activity toward skin and prostate cancer cells [3-5].

Among the main obstacles of the pharmaceutical application of SANG are low solubility in water-based liquids at the physiological pH and possible mucosal and skin irritation. The low solubility is caused by the prevalence of SANG “pseudobase” form in the neutral and weak alkaline media (Figure 1). However, namely this form of SANG is supposed to penetrate membranes of the target cells.

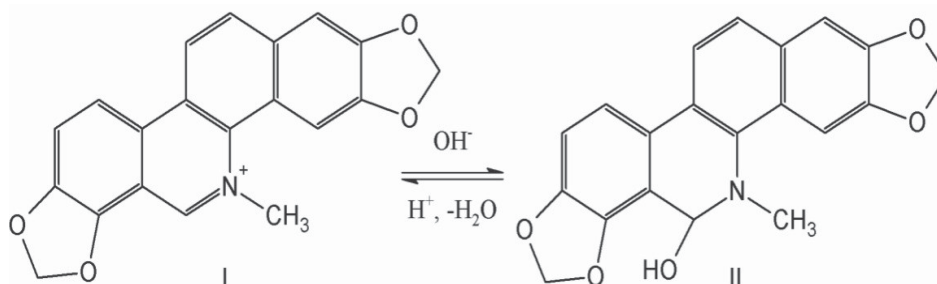


Figure 1. Sanguinarine iminium (I) and “pseudobase” forms (II)

One of the methods that can be used to enhance the water solubility and to reduce the irritating properties of different drugs, is formation of drug-cyclodextrin inclusion complexes.

Cyclodextrins (CDs) are cyclic oligosaccharides with a shape of truncated cone with a somewhat hydrophobic cavity and hydrophilic outside surface.  $\alpha$ -,  $\beta$  and  $\gamma$ -CDs, with six, seven and eight,  $\alpha$ -1,4-linked glucose residues respectively, are the most widely used. Inside of their cavity CDs can accommodate a wide range of lipophilic drug molecules. The process of drug-cyclodextrin inclusion complexes formation depends on several factors: type of cyclodextrin used ( $\alpha$ -,  $\beta$ - or  $\gamma$ -CD), chemical and physical properties of the drug molecule, the complexation medium properties [6, 7].

In order to influence the efficiency of the complexation process different methods have been used: controlled change of pH of the complexation media [8, 9]; addition of different co-complexing agents to it: hydrophilic polymers (polyvinylpyrrolidone, sodium carboxymethylcellulose, hydroxypropyl methylcellulose, polyethylene glycol) [10, 11], hydroxyacids [12], amino acids [13]; treatment of the complexation media with microwaves [14].

The aim of this study is to evaluate the effect of the pH control and addition of hydrophilic polymer polyvinylpyrrolidone on the complexation efficiency of  $\beta$ -CD with SANG.

## Experimental

### Preparation of the SANG- $\beta$ -CD systems for the spectrophotometric studies

The studied systems of SANG at constant concentration 0.03 mM and  $\beta$ CD at increasing concentrations 0.03, 0.06, 0.10, 0.30, 0.50, 0.80, 1.00, 1.30, 1.50, 1.80, 2.00 mM have been prepared with and without addition of 0.1% (w/v) PVP in phosphate buffer-alcoholic solution (95:5 v/v) at different pH. The obtained solutions were mixed for 2 hours at 35 °C wrapped in the aluminium foil to protect them from the direct light and then left for 24-hour equilibration.

**UV-vis spectrophotometry.** UV-vis absorption spectra were recorded on a Jasco UV/VIS spectrophotometer, model V-550 equipped with a quartz cells with 1.0 cm optical path length.

### Results and discussions

The spectrophotometric studies of the SANG- $\beta$ -CD systems with and without addition of 0.1% (w/v) PVP at pH 5.0 did not show any evidence of stable complex formation. These results can be explained by the prevalence of iminium form (Figure 1) of SANG in the studied systems at this level of pH. The iminium form is charged and is more hydrophilic than 'pseudobase' form, therefore, it can not be included into the hydrophobic cavity of the  $\beta$ -CD.

At the pH 8.0, close to physiological levels, SANG- $\beta$ -CD systems with and without addition of 0.1% (w/v) PVP showed several significant evidences of the inclusion complex formation: the hyperchromic and the hypochromic effects and the presence of the isosbestic point in the region of 200 – 210 nm (Figure 2. (a) and (b)).

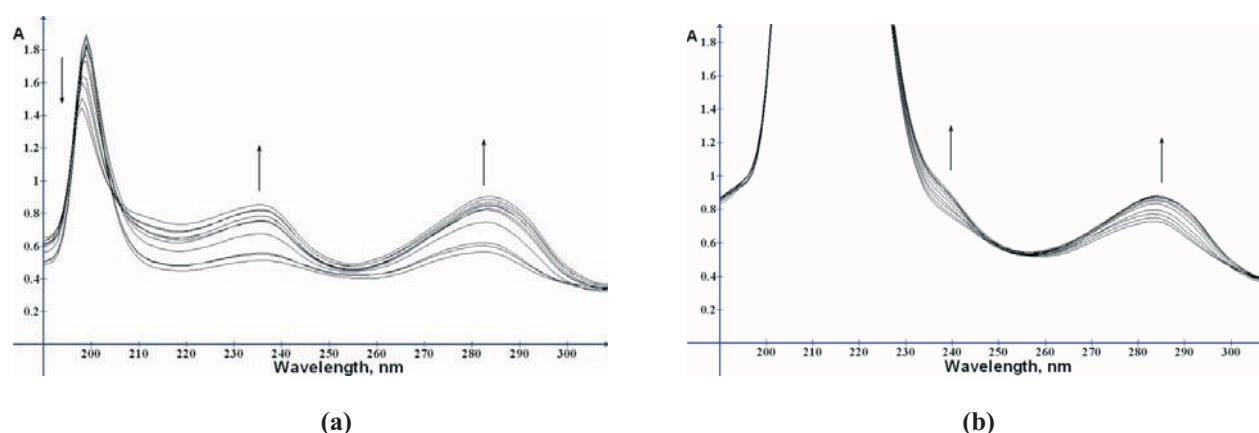
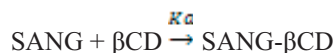


Figure 2. **(a)** UV-VIS absorption spectra of 0.03 mM SANG at different concentrations of  $\beta$ CD: 0.03, 0.06, 0.10, 0.30, 0.50, 0.80, 1.00, 1.30, 1.50, 1.80, 2.00 mM, in phosphate buffer-alcoholic solution (95:5 v/v), pH 8.0; **(b)** UV-VIS absorption spectra of 0.03 mM SANG at different concentrations of  $\beta$ CD: 0.03, 0.06, 0.10, 0.30, 0.50, 0.80, 1.00, 1.30, 1.50, 1.80, 2.00 mM in the presence of 0.1% PVP, in phosphate buffer-alcoholic solution (95:5 v/v), pH 8.0

The simulated curves of the spectrophotometric titration (at 283 nm) of 0.03 mM SANG with  $\beta$ CD in phosphate buffer-alcoholic solution (95:5 v/v) with and without addition of 0.1% PVP, at pH 8.0, are shown in the Figure 3. (a) and (b). The hyperbolic character of the obtained curves is one of the indicators of the 1:1 stoichiometric ratio in the inclusion complex formation between the host ( $\beta$ CD) and the guest molecule (SANG), according to the reaction shown in Scheme 1.



The curves resulted from the spectrophotometric titration of SANG with  $\beta$ CD (at 283 nm) were processed to obtain the values of the association constant  $K_a$  of SANG- $\beta$ CD systems, in the presence and without of 0.1% PVP. The constants were calculated using different linear methods: Benesi-Hildebrand, Scott, Scatchard [15]. The plots of these three methods for the studied host-guest complexes at pH 8.0, are shown in the Figures 4, 5 and 6. Among them, the Scott method showed the highest levels of the correlation coefficients of the obtained results, ranging in the values 0.98 – 0.99. The correlation coefficients for the Benesi-Hildebrand and the Scatchard methods were in the limits of 0.96 – 0.98 and 0.93 – 0.94 respectively.

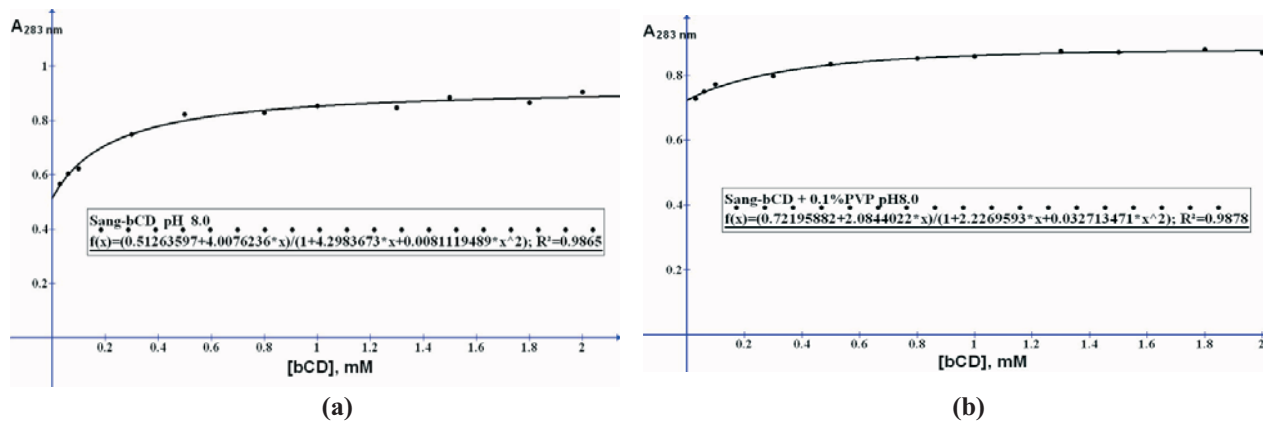


Figure 3. (a) Simulated curve of the spectrophotometric titration (at 283 nm) of 0.03 mM SANG with  $\beta\text{CD}$  in phosphate buffer-alcoholic solution (95:5 v/v) pH 8.0; (b) simulated curve of the spectrophotometric titration (at 283 nm) of 0.03 mM SANG with  $\beta\text{CD}$  in presence of 0.1% PVP, in phosphate buffer-alcoholic solution (95:5 v/v), pH 8.0

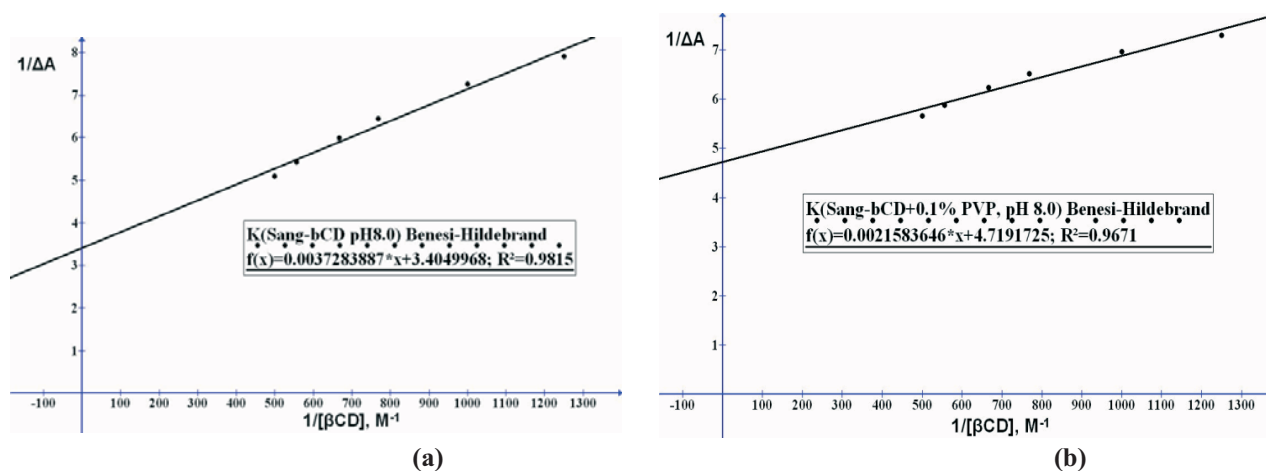


Figure 4. Benesi-Hildebrand plots for the SANG- $\beta\text{CD}$  systems in the presence of 0.1 % PVP (b) and without it (a), pH 8.0

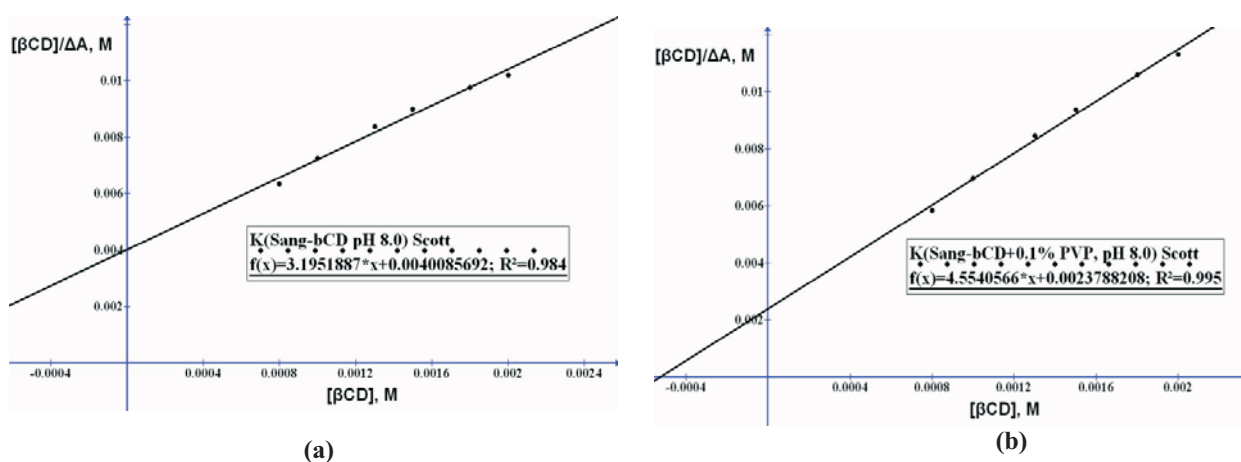


Figure 5. Scott plots for the SANG- $\beta\text{CD}$  systems in the presence of 0.1% PVP (b) and without it (a), pH 8.0

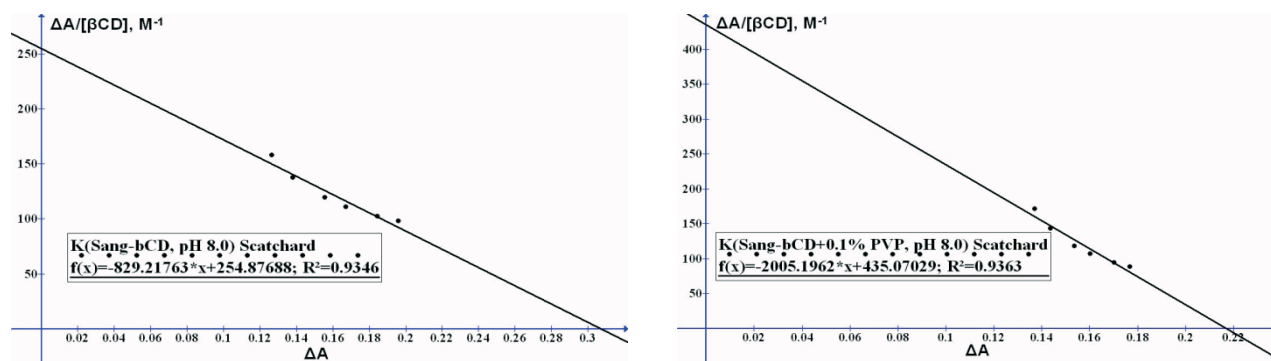


Figure 6. Scatchard plots for the SANG- $\beta$ CD systems in the presence of 0.1 % PVP (b) and without it (a), pH 8.0

The values of the association constants calculated by the three methods (Table 1) differ from each other not more than by their errors. This fact suggests a satisfactory level of correlation between the obtained results.

The main conclusion based on the analysis of the obtained values is a two fold increase of the association constant of SANG- $\beta$ CD complex in the presence of 0.1% PVP at the pH 8.0. This fact can be explained by the prevalence of the pseudobasic form of SANG (Figure 1) at this level of pH. This form is more lipophilic and, thus, it can be easier included inside of the hydrophobic cavity of the  $\beta$ CD.

Table 1

Association constants of complexation of SANG with  $\beta$ CD - without and in the presence of 0.1% PVP - in phosphate buffer-alcoholic solution (95:5 v/v), pH 8.0

Method of binding constant calculation	$K_a$ (SANG- $\beta$ CD), $M^{-1}$ [PVP] = 0 %	$K_a$ (SANG- $\beta$ CD), $M^{-1}$ [PVP] = 0.1 %
Benesi-Hildebrand	903 $\pm$ 58	2164 $\pm$ 132
Scott	798 $\pm$ 43	1919 $\pm$ 100
Scatchard	829 $\pm$ 47	2005 $\pm$ 111

## Conclusions

The obtained results suggest that pharmaceutical formulations containing sanguinarine and  $\beta$ -cyclodextrin should be prepared in the weak alkaline media. Moreover, in order to improve the complexation efficiency of the cyclodextrin a small amount ( $\sim$ 0.1%) of hydrophilic polymer (polyvinylpyrrolidone) should be added.

## Acknowledgements

The research described in this publication was made possible in part by Award No. MTFP-012/05 Follow-On Award of the Moldovan Research and Development Association (MRDA) and the U.S. Civilian Research & Development Foundation (CRDF).

## References

- [1] Walterová D., Ulrichová J., Válka I., Vičar J. Acta Univ. Palacki. Olomuc. Fac. Med. 1995, 139, 7–16;
- [2] Ding Z., Tang S.-C., Weerasinghe P., Yang X., Pater A., Liepins A. Biochem. Pharmacol. 2002, 63, 1415–1421;
- [3] Ahmad N., Gupta S., Husain M. M., Heiskanen K. M., Mukhtar H. Clin. Cancer Res. 2000, 6, 1524–1528;
- [4] Adhami V. M., Aziz M.H., Mukhtar H. J., Ahmad N. Clin. Ancer Res. 2003, 9, 3176 - 3182;
- [5] Adhami V. M., Aziz M.H., Regan-Shaw S., Nihal M., Mukhtar H., Ahmad N. Mol. Cancer Therap. 2004, 8, 933-940;
- [6] Loftsson T., Masso M. Int. J. Pharm. 2001, 225, 15–30;
- [7] Szejtli J. Pure Appl. Chem. 2004, 76, 1825-1845;
- [8] Ling P., Tabibi S.E., Yalkowsky S.H. J. Pharm. Sci. 1998, 87, 1535-1537;
- [9] McCandless R., Yalkowsky S.H. 1998, 87, 1639-1642;
- [10] Ribeiro L., Loftsson T., Ferreira D., Veiga F. Chem. Pharm. Bull. 2003, 51, 914–922;
- [11] Mura P., Faucci M. T., Bettinetti G.P. Eur. J. Pharm. Sci. 2001, 113, 187–194;
- [12] Mura P., Faucci M. T., Manderioli A., Bramanti G. J. Incl. Phen. 2001, 39, 131–138;
- [13] Mura P., Maestrelli F., Cirri M. Int. J. Pharm. 2003, 260, 293–302;
- [14] Atwater J.A. Carbohydr. Res. 2000, 327, 219 – 221;
- [15] Schneider H.-J., Yatsimirsky A. Principles and Methods in Supramolecular Chemistry; John-Wiley&Sons, New-York, 1999, pp 137-220.

# STEROIDAL SAPONINS FROM THE SEEDS OF *HYOSCYAMUS NIGER L.*

Irina Lunga<sup>a\*</sup>, Pavel Kintia<sup>a</sup>, Stepan Shvets<sup>a</sup>, Carla Bassarello<sup>b</sup>, Sonia Piacente<sup>b</sup>, Cosimo Pizza<sup>b</sup>

<sup>a</sup> Institute of Genetics and Physiology of Plants, Academy of Sciences of Moldova, Padurii 20, 2004, Chisinau, Moldova  
\*lunga\_irina@yahoo.com, tel. 373 22 555259, fax 373 22 556180

<sup>b</sup> Department of Pharmaceutical Sciences, University of Salerno, Ponte Don Melillo, 84084, Fisciano, Salerno, Italy

**Abstract:** Ten steroidal saponins have been isolated from the seeds of *Hyoscyamus niger L.* for the first time and their structures have been elucidated. Seven saponins belong to spirostane series, two are furostane-type and one is pregnane glycoside. Hyoscyamosides **B**, **C** and **C<sub>2</sub>** are new steroidal saponins, which have never been reported before in literature. Complete assignments of the <sup>1</sup>H and <sup>13</sup>C NMR chemical shifts for all these glycosides were achieved by means of one- and two-dimensional NMR techniques, including 1H–1H COSY, HSQC, HMBC and ROESY spectra.

**Keywords:** *Hyoscyamus niger L.*, steroidal saponins.

## Introduction

Steroidal saponins and pregnanes have established themselves as an important class of biologically active compounds. Pharmacological studies in recent years have shown that these compounds possess antitumor [1-3], bone resorbing [4] and antifungal activities [5]. A number of such compounds have been isolated from the plants, especially the Solonaceae family [6].

*Hyoscyamus niger L.* (Solonaceae) is a plant native to Europe and Asia and its leaves and seeds have been used in traditional medicine for the treatment of nervous and convulsive diseases. Previous works have been focused only to the alkaloid constituents of this plant and it has never been reported about its steroidal saponins. This fact and our interest in secondary metabolites of Solonaceae family prompted us to perform the phytochemical investigation of the seeds of *Hyoscyamus niger L.* Our investigation yielded three new steroidal saponins for which we propose the names hyoscyamosides **B** (**1**), **C** (**2**) and **C<sub>2</sub>** (**3**) and seven known compounds - hyoscyamosides **A** (**4**), **B<sub>1</sub>** (**5**), **B<sub>2</sub>** (**6**), **B<sub>3</sub>** (**7**), **C1** (**8**), **E** (**9**) and **F1** (**10**).

## Results and discussion

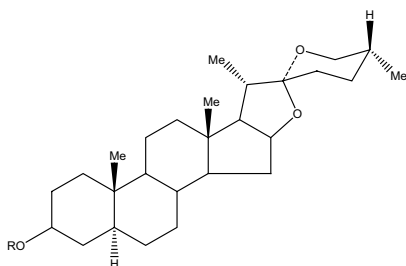
The buthanol extract, containing steroidal saponins was chromatographed on silica gel column and also using prep. HPLC to afford ten compounds, **1-10**. Among them, compounds **4-10** were identified as 3-*O*-β-D-galactopyranoside-(25*R*)-5α-spirostan-3β-ol (**4**) [7], 3-*O*-β-D-glucopyranosyl-(1→4)-β-D-galactopyranoside-(25*R*)-5α-spirostan-3β-ol (**5**) [7], 3-*O*-α-L-rhamnopyranosyl-(1→2)-β-D-glucopyranoside-(25*R*)-5α-spirostan-3β-ol (**6**) [8], 3-*O*-α-L-rhamnopyranosyl-(1→2)-β-D-glucopyranoside-(25*R*)-spirost-5-en-3β-ol (**7**) [8], 3-*O*-β-D-glucopyranosyl-(1→2)-β-D-glucopyranosyl-(1→4)-*O*-β-D-galactopyranoside-(25*R*)-5α-spirostan-3β-ol (**8**) [9], 3-*O*-β-D-glucopyranosyl-(1→4)-*O*-β-D-galactopyranoside-(25*R*)-26-*O*-β-D-glucopyranosyl-5α-furostan-3β,22α,26-triol (**9**) [10], 3-*O*-β-D-glucopyranosyl-(1→2)-β-D-glucopyranosyl-(1→4)-*O*-β-D-galactopyranoside-(25*R*)-26-*O*-β-D-glucopyranosyl-5α-furostan-3β,22α,26-triol (**10**) [10], on the basis of their spectroscopic data by comparison with literature data.

The <sup>1</sup>H NMR spectrum of **1** showed signals for four steroidal methyl groups at δ 0.82 (3H, s, Me-18), 0.89 (3H, s, Me-19), 1.00 (3H, d, Me-21), 1.12 (3H, d, Me-27), two methine proton signals at δ 3.68 (1H, m, H-3) and 4.41 (1H, m, H-16) indicative of secondary alcoholic functions and two anomeric protons at δ 4.38 (1H, d, *J* = 7.5 Hz), 4.53 (1H, d, *J* = 7.5 Hz), giving correlations with carbon signals at δ 103.5 and 105.0, respectively. The chemical shifts of all the individual protons of this sugar unit were ascertained from a combination of 1D-TOCSY and DQF-COSY spectral analysis, and the <sup>13</sup>C chemical shifts of their relative carbons could be assigned unambiguously from the HSQC spectrum. These data showed the presence of two sugars - β-D-galactose and β-D-glucose. The HMBC spectrum showed key correlation peaks between the proton signal at δ 4.38 (H-1<sub>gal</sub>) and the carbon resonance at δ 78.9 (C-3 of the aglycon) and at δ 4.53 (H-1<sub>glc</sub>) and the carbon resonance at δ 80.7 (C-3<sub>gal</sub>). On the basis of the above results the structure of **1** was determined as 3-*O*-β-D-glucopyranosyl-(1→3)-β-D-galactopyranoside-(25*R*)-5α-spirostan-3β-ol and was named by us hyoscyamoside **B**.

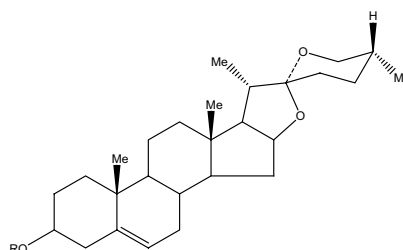
The <sup>1</sup>H NMR spectrum of **2** showed identical aglycon moiety of compound **1** -(25*R*)-5α-spirostan-3β-ol. One primary alcoholic function at δ 67.7 (C-26) suggested the occurrence of a glycoside spirostanol skeleton. The <sup>1</sup>H NMR spectrum showed signals for three anomeric protons at δ 4.39 (1H, d, *J* = 7.5 Hz), 4.56 (1H, d, *J* = 7.5 Hz), and 4.69 (1H, d, *J* = 7.5 Hz). 1D-TOCSY and DQF-COSY spectral analysis of the sugar moiety revealed the presence of one β-galactopyranosyl unit (δ 4.39) and two β-glucopyranosyl units (δ 4.56 and 4.69). The HMBC spectrum showed

key correlation peaks between the proton signal at  $\delta$  4.39 (H-1<sub>gal</sub>) and the carbon resonance at  $\delta$  79.1 (C-3 of the aglycon), the proton signal at  $\delta$  4.56 (H-1<sub>glc</sub>) and the carbon resonance at  $\delta$  78.1 (C-2<sub>gal</sub>), the proton signal at  $\delta$  4.69 (H-1<sub>glc</sub>) and the carbon resonance at  $\delta$  82.5 (C-3<sub>gal</sub>). Thus, the structure of compound **2** was deduced as 3-O- $\{[\beta$ -D-glucopyranosyl-(1 $\rightarrow$ 2)]- $\}[\beta$ -D-glucopyranosyl-(1 $\rightarrow$ 3)]- $\}$ - $\beta$ -D-galactopyranoside $\}$ -(25-R)-5 $\alpha$ -spirostan-3 $\beta$ -ol, which we named hyoscyamoside **C**.

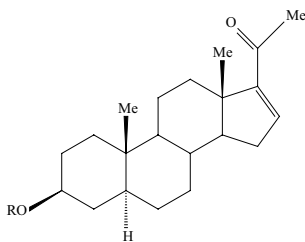
<sup>1</sup>H NMR spectrum of compound **3** displayed signals for three tertiary methyl groups at  $\delta$  0.90 (3H, s, Me-19), 0.91 (3H, s, Me-18) and 2.28 (3H, s, Me-21), one olefinic proton at  $\delta$  6.91 (1H, m, H-16) together with three anomeric protons (1H, d,  $\delta$  4.40; 1H, d,  $\delta$  4.56; 1H, d,  $\delta$  4.69). On the other hand, the <sup>13</sup>C-NMR signals due to a total of 21 carbon signals originating from the sapogenol were composed of three methyl groups at  $\delta$  12.2, 15.7, and 26.8, one oxygen-bearing methine carbon at  $\delta$  79.1 (C-3), one carbonyl group at  $\delta$  199.3 (C-20), two quaternary carbons at  $\delta$  35.7 and 47.2, four methine carbons at  $\delta$  34.7, 45.9, 56.1 and 57.3, eight methylene carbons at  $\delta$  21.3, 29.5, 30.0, 32.8, 32.9, 35.0, 35.7 and 37.9, and two olefinic carbons at  $\delta$  147.0 and 156.4. The HMBC disclosed the connectivities of the above functional carbons to form a pregnane skeleton. Using 1D-TOCSY, COSY, HSQC and HMBC spectra the sugar chain were characterized as  $\beta$ -D-galactose, two  $\beta$ -D-glucose. HMBC spectrum showed key correlation picks between sugars anomeric protons and attached carbons at  $\delta$  4.40 (H-1<sub>gal</sub>) and 79.1 (C-3 agl),  $\delta$  4.56 (H-1<sub>glc</sub>) and 80.2 (C-4<sub>gal</sub>),  $\delta$  4.69 (H-1<sub>glc</sub>) and 84.7 (C-2<sub>glc</sub>). Thus, compound **3** was elucidated as 3-O $\beta$ -D-glucopyranosyl (1 $\rightarrow$ 2)- $\beta$ -D-glucopyranosyl (1 $\rightarrow$ 4)- $\beta$ -D-galactopyranosyl-5 $\alpha$ -pregn-16-en-20-one-3 $\beta$ -ol, for which we proposed the name hyoscyamoside **C**<sub>2</sub>.



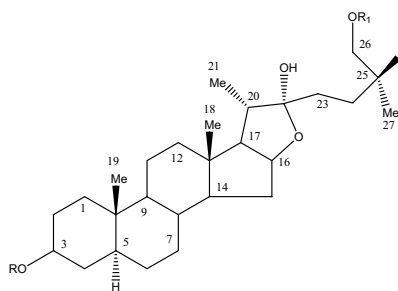
- 1: R=Glc(1-3)Gal  
 2: R=[Glc(1-3)][Glc(1-2)]Gal  
 4: R=Gal  
 5: R=Glc(1-4)Gal  
 6: R=Rha(1-2)Glc  
 8: R=Glc(1-2)Glc(1-4)Gal



- 7: R=Rha(1-2)Glc



- 3: R=Glc(1-2)Glc(1-4)Gal



- 9: R=Glc(1-4)Gal  
 R<sub>1</sub>=Glc  
 10: R=Glc(1-2)Glc(1-4)Gal  
 R<sub>1</sub>=Glc

Table 1

<sup>13</sup>C NMR spectral data (150 MHz, CD<sub>3</sub>OD) of saponins (1-3)

Carbon	1	2	3
1	37.9	37.9	37.9
2	30.4	30.2	30.0
3	78.9	79.1	79.1
4	34.9	35.1	35.0
5	45.8	45.8	45.9
6	32.9	32.9	29.5
7	34.6	34.6	32.9
8	36.0	36.0	34.7
9	55.2	55.2	56.1
10	36.5	36.4	35.7
11	21.5	21.5	21.3
12	40.5	40.5	35.7
13	41.8	41.8	47.2
14	57.5	57.5	57.3
15	32.3	32.3	32.9
16	82.1	82.2	147.0
17	63.7	63.7	156.4
18	16.7	16.7	15.7
19	12.5	12.6	12.2
20	42.6	42.6	199.3
21	14.2	14.2	26.8
22	110.5	110.5	
23	32.2	32.1	
24	29.1	29.1	
25	31.2	31.2	
26	67.7	67.7	
27	16.7	16.7	
1'	103,5	103,2	102.9
2'	72,9	78,1	72.9
3'	80,7	82.5	75.3
4'	70,5	71,7	80.2
5'	75,6	75,4	77.8
6'	60,3	60,1	60.4
1''	105,0	104,9	104.5
2''	75,5	75,5	84.7
3''	78,3	78,0	77.8
4''	71,2	71,2	71.4
5''	78,9	78,9	78.6
6''	63,1	62,9	62.5
1'''		105,1	105.1
2'''		75,5	75.5
3'''		78,3	78.2
4'''		71,7	71.3
5'''		78,1	78.9
6'''		63,1	63.1

## Experimental

The seeds of *Hyoscyamus niger* L. has been collected in the scientific research field of Institute of Scientific Researches and Technological Constructions for Tobacco and Tobacco Products of Moldova in November 2001 year. The voucher specimen has been deposited in Laboratory of selection under direction of Doctor in Biology Kalkei E.D.

Dry powdered seeds (500 g) were extracted three times in 50°C with n-buthanol saturated with water. The received n-buthanol-water extract was evaporated and then purified with chloroform. After purification it was crystallised in acetone. The residue was dried in vacuum at 40°C and the sum of steroidal saponins has been obtained as yellow powder in 3.7% yield. 3g of extract has been chromatographed on silica gel column (30-500mm, 60-100µm,

Merck). The column was eluted with system chloroform-methanol-water (8:2:0→20:10:1) and 4ml fractions were collected. Fractions showing identical characteristics [TLC, silica gel, chloroform-methanol (4:1)] were combined. Two subfractions, (A) and (B) were obtained, which were further separated on a C<sub>18</sub> column (7,8x300mm, LiChroprep RP18, 25-40µm, XTerra Waters) using a H<sub>2</sub>O/MeOH (60-80% MeOH) isocratic. Ten single compounds were isolated.

NMR experiments were performed on a Bruker DRX-600 spectrometer (Bruker BioSpin GmbH, Rheinstetten, Germany) at 300 K dissolving all the samples in CD<sub>3</sub>OD (Carlo Erba, 99.8 %). The standard pulse sequence and phase cycling were used for DQF-COSY, HSQC and HMBC spectra. The NMR data were processed using UXNMR software.

ESI-MS in the positive ion mode was performed using a Finnigan LCQ Deca ion trap instrument from Thermo Finnigan (San Jose, CA) equipped with Xcalibur software.

HPLC separations were carried out on a Waters 590 system equipped with a Waters R401 refractive index detector, a Waters XTerra Prep MSC<sub>18</sub> column (300 x 7.8 mm i.d.) and a Rheodyne injector.

Column chromatography was performed over Silica gel (0.1-0.06 mm, Merck). TLC was performed on silica gel plates (Merck precoated silica gel 60 F<sub>254</sub>). All solvents for chromatographic separation were of analytical grade from Carlo Erba (Rodano, Italy). HPLC grade water (18 mΩ) was prepared using a Millipore Milli-Q purification system (Millipore Corp., Bedford, MA).

**1.** HRMS *m/z* 741.452 [calculated for C<sub>39</sub>H<sub>64</sub>O<sub>13</sub> (M)<sup>+</sup>]; 579.3 [M-162]<sup>+</sup>; <sup>1</sup>H NMR (aglycon) δ 4.41 (1H, m, H-16), 3.68 (1H, m, H-3), 3.46 (1H, m, H-26a), 3.33 (1H, m, H-26b), 0.88 (3H, s, Me-19), 0.81 (3H, s, Me-18), 0.98 (3H, d, Me-21), 1.10 (3H, d, Me-27). (sugars) δ 4.38 (d, *J*=7.4 Hz, H-1Gal), 3.51 (dd, *J*=7.4 and 9.0 Hz, H-2Gal), 3.76 (dd, *J*=4.0 and 9.0 Hz, H-3Gal), 3.85 (dd, *J*=2.5 and 4.0 Hz, H-4Gal), 3.58 (ddd, *J*=2.5, 2.5 and 4.5 Hz, H-5Gal), 3.63 (dd, *J*=4.5 and 12.0 Hz, H-6aGal), 3.90 (dd, *J*=2.5 and 12.0 Hz, H-6bGal), 4.53 (d, *J*=7.5 Hz, H-1Glc), 3.29 (dd, *J*=7.5 and 9.0 Hz, H-2Glc), 3.39 (dd, *J*=9.0 and 9.0 Hz, H-3Glc), 3.24 (dd, *J*=9.0 and 9.0 Hz, H-4Glc), 3.31 (ddd, *J*=2.5, 4.5 and 9.0 Hz, H-5Glc), 3.62 (dd, *J*=4.5 and 11.5 Hz, H-6aGlc), 3.93 (dd, *J*=2.5 and 11.5 Hz, H-6bGlc). For <sup>13</sup>C NMR see Table 1.

**2.** HRMS, *m/z* 903.443 [calculated for C<sub>45</sub>H<sub>74</sub>O<sub>18</sub> (M)<sup>+</sup>]; 741.6 [M-162]<sup>+</sup>; 579 [M-2x162]<sup>+</sup>; <sup>1</sup>H NMR (aglycon) δ 4.40 (1H, m, H-16), 3.69 (1H, m, H-3), 3.47 (1H, m, H-26a), 3.34 (1H, m, H-26b), 0.89 (3H, s, Me-19), 0.82 (3H, s, Me-18), 0.99 (3H, d, Me-21), 1.27 (3H, d, Me-27). (sugars) δ 4.39 (d, *J*=7.4 Hz, H-1Gal), 3.84 (dd, *J*=7.4 and 9.0 Hz, H-2Gal), 3.78 (dd, *J*=4.0 and 9.0 Hz, H-3Gal), 4.02 (dd, *J*=2.5 and 4.0 Hz, H-4Gal), 3.69 (ddd, *J*=2.5, 2.5 and 4.5 Hz, H-5Gal), 3.62 (dd, *J*=4.5 and 12.0 Hz, H-6aGal), 3.95 (dd, *J*=2.5 and 12.0 Hz, H-6bGal), 4.56 (d, *J*=7.5 Hz, H-1Glc), 3.30 (dd, *J*=7.5 and 9.0 Hz, H-2Glc), 3.60 (dd, *J*=9.0 and 9.0 Hz, H-3Glc), 3.35 (dd, *J*=9.0 and 9.0 Hz, H-4Glc), 3.25 (ddd, *J*=2.5, 4.5 and 9.0 Hz, H-5Glc), 3.60 (dd, *J*=4.5 and 11.5 Hz, H-6aGlc), 3.93 (dd, *J*=2.5 and 11.5 Hz, H-6bGlc), 4.69 (d, *J*=7.5 Hz, H-1GlcI), 3.29 (dd, *J*=7.5 and 9.0 Hz, H-2GlcI), 3.36 (dd, *J*=9.0 and 9.0 Hz, H-3GlcI), 3.40 (dd, *J*=9.0 and 9.0 Hz, H-4GlcI), 3.42 (ddd, *J*=2.5, 4.5 and 9.0 Hz, H-5GlcI), 3.69 (dd, *J*=4.5 and 11.5 Hz, H-6aGlcI), 3.82 (dd, *J*=2.5 and 11.5 Hz, H-6bGlcI). For <sup>13</sup>C NMR see Table 1.

**3.** HRMS, *m/z* [calculated for C<sub>39</sub>H<sub>50</sub>O<sub>20</sub> (M)<sup>+</sup>]; 676.8 [M-162]<sup>+</sup>; <sup>1</sup>H NMR (aglycon) δ 6.91 (1H, m, H-16), 3.69 (1H, m, H-3), 0.90 (3H, s, Me-19), 0.91 (3H, s, Me-18), 2.28 (3H, d, H-21). (sugars) δ 4.40 (d, *J*=7.4 Hz, H-1Gal), 3.61 (dd, *J*=7.4 and 9.0 Hz, H-2Gal), 3.54 (dd, *J*=4.0 and 9.0 Hz, H-3Gal), 4.03 (dd, *J*=2.5 and 4.0 Hz, H-4Gal), 3.60 (ddd, *J*=2.5, 2.5 and 4.5 Hz, H-5Gal), 3.58 (dd, *J*=4.5 and 12.0 Hz, H-6aGal), 3.93 (dd, *J*=2.5 and 12.0 Hz, H-6bGal), 4.56 (d, *J*=7.5 Hz, H-1Glc), 3.59 (dd, *J*=7.5 and 9.0 Hz, H-2Glc), 3.61 (dd, *J*=9.0 and 9.0 Hz, H-3Glc), 3.36 (dd, *J*=9.0 and 9.0 Hz, H-4Glc), 3.26 (ddd, *J*=2.5, 4.5 and 9.0 Hz, H-5Glc), 3.61 (dd, *J*=4.5 and 11.5 Hz, H-6aGlc), 3.94 (dd, *J*=2.5 and 11.5 Hz, H-6bGlc), 4.69 (d, *J*=7.5 Hz, H-1GlcI), 3.29 (dd, *J*=7.5 and 9.0 Hz, H-2GlcI), 3.37 (dd, *J*=9.0 and 9.0 Hz, H-3GlcI), 3.41 (dd, *J*=9.0 and 9.0 Hz, H-4GlcI), 3.41 (ddd, *J*=2.5, 4.5 and 9.0 Hz, H-5GlcI), 3.83 (dd, *J*=4.5 and 11.5 Hz, H-6aGlcI), 3.69 (dd, *J*=2.5 and 11.5 Hz, H-6bGlcI). For <sup>13</sup>C NMR see Table 1.

## Conclusion

Three new compounds, hyoscyamosides **B (1)**, **C (2)** and **C<sub>2</sub> (3)**, together with seven known steroidal saponins (**4-10**) have been isolated from the seeds of *Hyoscyamus niger L.* for the first time. The structures of hyoscyamosides **B (1)**, **C (2)** and **C<sub>2</sub> (3)** were elucidated as 3-*O*-β-D-glucopyranosyl- (1→3) - β-D- galactopyranoside - (25 R)-5α-spirostan - 3β-ol, 3-*O*-{[β-D-glucopyranosyl-(1→2)]-[β-D- glucopyranosyl-(1→3)]-β-D-galactopyranoside}-(25-R)-5α-spirostan-3β-ol and 3-*O*-β-D-glucopyranosyl (1→2)- β-D-glucopyranosyl-(1→4)- β-D-galactopyranosyl-5α-pregn-16-en-20-one-3β-ol, respectively by means of physico-chemical methods.

## Acknowledgments

Thanks are due to the financial support from INTAS (The **I**nternational **A**ssociation for the **P**romotion of **C**o-operation with **S**cientists from the **N**ew **I**ndependent **S**tates). Also the authors are grateful to Dr. Assunta Napolitana from the Department of Pharmaceutical Sciences, University of Salerno for MS measurements.

## References

- [1] Zhang, R. S.; Ye, Y. P.; Shen, Y. M.; Liang, H. L. *Tetrahedron* 2000, **56**, 3875–3879.
- [2] Mellado, G. G.; Zubia, E.; Ortega, M. J.; Lopez-Gonzalez, P. J. *Steroids* 2004, **69**, 291–299.
- [3] Halaweish, F. T.; Huntimer, E.; Khalil, A. T. *Phytochem. Anal.* 2004, **15**, 189–194.
- [4] Yin, J.; Kouda, K.; Tezuka, Y.; Tran, Q. L.; Miyahara, T.; Chen, Y. J.; Kadota, S. J. *Nat. Prod.* 2003, **66**, 646–650.
- [5] Liu, H. W.; Xiong, Z.; Li, F.; Qu, G. X.; Kobayashi, H.; Yao, X. S. *Chem. Pharm. Bull.* 2003, **51**, 1089–1091.
- [6] Deepak, D.; Srivastav, S.; Khare, A. In Herz, W., Kirby, G. W., Moore, R. E., Strglic, W., Tamm, Ch., Eds.; *Progress in the chemistry of organic natural products*; Springer: New York, 1997, **71**, pp 169–325.
- [7] Gutsu, E.V.; Kintya, P.K.; Lazur'evskii, G.V. *Khimiya Prirodnikh Soedinenii* 1987, **2**, 242-246.
- [8] Imai, S.; Fujioka, S.; Murata, E.; Goto, M.; Kawasaki, T.; Yamauchi, T. *Takeda Kenkyusho Nenpo* 1967, **26**, 76-83.
- [9] Murakami, K.; Saijo, R.; Nohara, T.; Tomimatsu, T. *Yakugaku Zasshi* 1981, **101** (3), 275-279.
- [10] Shvets, S. A.; Naibi, A. M.; Kintya, P. K. *Khimiya Prirodnikh Soedinenii* 1995, **2**, 247-252.

## TOXICOPHORES AND QUANTITATIVE STRUCTURE -TOXICITY RELATIONSHIPS FOR SOME ENVIRONMENTAL POLLUTANTS

N. N. Gorinchoy<sup>a</sup>, I. Ya. Ogurtsov<sup>a</sup>, A. Tihonovschij<sup>a</sup>, I. Balan<sup>a</sup>, I. B. Bersuker<sup>a,b</sup>,  
A. Marenich<sup>b</sup> and J. Boggs<sup>b</sup>

<sup>a</sup>Institute of Chemistry, Academy of Sciences of Moldova, Academiei str. 3, MD 2028 Kishinev, Republic of Moldova

<sup>b</sup>Department of Chemistry & Biochemistry, University of Texas at Austin, USA

\*E-mail: ngorinchoy@yahoo.com; Phone 373 22 739649

**Abstract:** The electron-conformational (EC) method is employed to reveal the toxicophore and to predict aquatic toxicity quantitatively using as a training set a series of 51 compounds that have aquatic toxicity to fish. By performing conformational analysis (optimization of geometries of the low-energy conformers by the PM3 method) and electronic structure calculations (by *ab initio* method corrected within the SM54/PM3 solvation model), the Electron-Conformational Matrix of Congruity (ECMC) was constructed for each conformation of these compounds. The toxicophore defined as the EC sub-matrix of activity (ECSA), a sub-matrix with matrix elements common to all the active compounds under consideration within minimal tolerances, is determined by an iterative procedure of comparison of their ECMC's, gradually minimizing the tolerances. Starting with only the four most toxic compounds, their ECSA (toxicophore) was found to consist of a 4x4 matrix (four sites with certain electronic and topologic characteristics) which was shown to be present in 17 most active compounds. A structure-toxicity correlation between three toxicophore parameters and the activities of these 17 compounds with  $R^2=0.94$  was found. It is shown that the same toxicophore with larger tolerances satisfies the compounds with less activity, thus explicitly demonstrating how the activity is controlled by the tolerances quantitatively and which atoms (sites) are most flexible in this respect. This allows for getting slightly different toxicophores for different levels of activity. For some active compounds that have no toxicophore a bimolecular mechanism of activity is suggested. Distinguished from other QSAR methods, no arbitrary descriptors and no statistics are involved in this EC structure-activity investigation.

**Keywords:** aquatic toxicity, electron-conformational method, QSAR

**Abbreviations:** Tph – toxicophore  
EC – electron-conformational  
ECMC – electron-conformational matrix of congruity  
ECSA – electron-conformational sub-matrix of activity  
QSAR – quantitative structure-activity relationships

### Introduction

Many chemicals (organic environmental pollutants) and drugs, in addition to their useful properties, possess different types of toxicity to environmental living organisms. The QSAR methodology is usually used to reveal relationships between the chemical structure of the compound and the toxicity under consideration in order to predict the latter in new chemicals. The main problem in this approach is to choose the molecular features (descriptors) that properly represent the possible interaction of the toxicant with the bioreceptor to produce the toxicity, and to correlate the descriptors with the toxicity by means of some regression relationships. There are many monographs, review articles and original works devoted to this problem (see e.g. [1-3] and references therein). One of the latest versions of the QSAR approach to this problem is the so-called support vector machine (SVM) model [4, 5] in which the hypersurface in multi-dimensional space of the descriptors separates two classes of chemicals, toxic and not toxic. A rule to classify chemicals into four classes was proposed by Verhaar *et al.* [6].

In all these approaches to QSAR problems there is a common shortcoming: the choice of descriptors is not directly based on first principles, meaning it is arbitrary, and their weight is evaluated by means of statistical comparison with the activities. Since such a set of descriptors is necessarily incomplete and they are non-orthogonal to each other with unknown overlap, the comparison with activities may lead to chance correlations, some (or all) descriptors being thus artifacts with no physical meaning implied in their initial choice (see also [7]).

In the present paper we explore some problems of chemical toxicity, more precisely aquatic toxicity to fish, using the electron-conformational (EC) method of pharmacophore identification and quantitative bioactivity predictions which is free from the above shortcomings (see the reviews of this method in [8], and also in [1], p. 455; an earlier less accurate qualitative version of this method was reviewed in [9]). Distinguished from the traditional QSAR approaches, the EC method does not employ arbitrary descriptors and statistics in its evaluation. Instead one (a unique) descriptor based on first principles is used, the electronic structure and topology of the molecule, calculated by means of quantum-chemical methods and presented in computer friendly digital-matrix form (see below). The comparison of these matrices with the

activities allows us to reveal a group of matrix elements that are common to the active compounds under consideration and represent the numerical picture of pharmacophore, the necessary condition of activity (no statistics is involved in this process). This approach has been applied successfully to study several types of biological activities (see, e.g., [10-14]).

There are at least two recent publications where some approaches for prediction of aquatic toxicity were proposed. A rule-based system to classify chemicals into four classes was proposed by Verhaar *et al* [6]. Using this approach it is possible to calculate the toxicity of chemicals belonging to one of those four classes based on the octanol-water partition coefficient ( $P$ ) of the compound. The other approach applies CODESSA descriptors to correlate with toxicity through the use of regression relationships [15]. The latter publication is based on a data set comprising 293 diverse chemicals with toxicity to *Poecilia reticulata* (guppy). A significant contribution of HYBOT descriptors in modeling polar and non-polar narcosis was reported earlier [16]. These publications represent important progress in the field of construction of structure-ecotoxicity models. Nevertheless the creation of stable predictive models of ecotoxicological properties of organic chemicals is still a long way from realization.

In this paper we intend to construct an alternative (to [15, 16]) approach for the toxicity to *Poecilia reticulata* (guppy) based on the EC method (ECM). We apply the ECM only to one of four groups (Class 3) discussed in [15, 16], which consist of 51 compounds (Table 1, numbers 212-262 in [15, 16]).

Table 1

Name and experimental toxicity $-\log(LC_{50}^{\text{exp}})$ of the compounds in the data set					
No	Name	$-\log LC_{50}^{\text{exp}}$	No	Name	$-\log LC_{50}^{\text{exp}}$
1	4-Dinitrobenzylbromide	0.30	27	1,3-Butadienediepoxyde	-1.49
2	Hexachlorobutadiene	0.20	28	Benzaldehyde	-1.57
3	1-Chloro-2,4-dinitrobenzene	0.19	29	1,2,7,8-Diepoxyoctane	-1.67
4	1,4-Dichloro-2-butene	0.16	30	Styrene oxide	-1.77
5	$\alpha,\alpha'$ -Dichloro-m-xylene	0.16	31	Octanal	-1.79
6	2,4, $\alpha$ -Trichlorotoluene	-0.08	32	1-Chloro-2-butene	-1.82
7	2-sec-Butyl-4,6-dinitrophenol	-0.17	33	3-Chloro-1-butene	-1.85
8	Pentachlorophenol	-0.22	34	2-Ethylbutenal	-1.89
9	Benzyl chloride	-0.49	35	Heptanal	-1.89
10	2,3,4,6-Tetrachlorophenol	-0.67	36	1,2-Epoxyoctane	-1.91
11	Epibromhydrin	-0.77	37	Cyclohexanecarboxaldehyde	-1.91
12	1,2-Epoxydodecane	-0.78	38	Hexanal	-1.99
13	Epichlorohydrin	-0.85	39	2-Furaldehyde	-2.04
14	Chloroacetone	-0.88	40	Pentanal	-2.18
15	2-Butenal	-0.90	41	3-Methylbutanal	-2.19
16	1,3-Dichloropropene	-0.98	42	1,2-Epoxyhexane	-2.27
17	2,5-Dinitrophenol	-1.00	43	Butanal	-2.28
18	3,4,5,6-Tetrachloro-2-hydroxyphenol	-1.00	44	Propanal	-2.41
19	2,3-Dichloropropene	-1.01	45	2,2-Dichlorodiethyl ether	-2.54
20	3-Cyclohexene-1-carboxaldehyde	-1.01	46	2-Methylpropanal	-2.57
21	3,4,5-Trichloro-2-methoxyphenol	-1.03	47	1,2-Epoxybutane	-2.66
22	3,4,5-Trichloro-2,6-dimethoxyphenol	-1.12	48	Propylene Oxide	-2.74
23	Allyl chloride	-1.20	49	Glycidol	-2.83
24	Decanal	-1.31	50	Acetaldehyde	-2.90
25	1,2-Epoxydecane	-1.32	51	Methanal	-2.96
26	4,5- Dichloro-2-methoxyphenol	-1.40			

### Application of the Electron-Conformational Method

The electron-conformational method in its general form consists of the following consecutive steps [8]:

- 1) Evaluation of the low-energy conformations of the compounds in the training set.
- 2) Electronic structure calculation of all conformers.
- 3) Construction of ECMC for each conformation.
- 4) Identification of the ECSA, the toxicophore, by multiple comparisons of the ECMC of the active compounds.
- 5) Estimation of the influence of pharmacophore flexibility, anti-toxicophore shielding groups, and other out-of-toxicophore groups by means of a proper parameterization and least-squares regression analysis.
- 6) Use of the obtained toxicophore and out-of-toxicophore influence parameters for screening new potentially active compounds and prediction of their activity.

These steps were consecutively realized for the training set of 51 compounds.

**Step 1.** Using the methods of molecular mechanics with the Merck force field [17] and the Monte-Carlo randomized search method the low-energy conformers were determined for all compounds in Table 1.

**Step 2.** The energies of the conformers were calculated including the aqueous solvation effect by means of the SM5.4/P model [18].

Conformational analysis and electronic structure calculations were performed using the SPARTAN package [19]. The geometries of conformers were optimized with the semi-empirical PM3 method [20]. For optimized geometries single-point calculations of the total energies were carried out using the *ab initio* method in Restricted Hartree-Fock-Roothaan approximation with the 6-31G\* basis sets. Only conformers with the lowest total energy within 1 kcal/mole were kept for further consideration.

**Step 3.** Computation of electron-conformational matrices of congruity (ECMC)

The results of single-point calculations of the conformer's electronic structure (molecular orbital population analysis, Mulliken atomic charges, and bond orders) were used for construction of the ECMC for all the compounds in Table 1. In the ECMC the diagonal elements are atomic interaction indices (*II*) [8], a measure of electron-donor properties of the corresponding atoms in the molecule (numerical coefficients are chosen to compensate dimensionalities):

$$II^A = g^A \exp\left(-R_0 \sqrt{2 \text{VOIP}^A}\right), \quad (1)$$

where  $g^A$  is the Mulliken electron population of the outermost orbital of the atom *A* (for *np*-elements the  $g^A$  is equal to a third of the total occupancy of valence p-orbitals,  $p_x$ ,  $p_y$ , and  $p_z$ , of the atom), and  $\text{VOIP}^A$  in Hartree units refers to the valence orbital ionization potential of this atom-in-molecule orbital calculated as a function of the Mulliken charge and the electronic configuration of the atom using the reference data [21]. The value of  $R_0 = 1.51$  Bohr radii (0.8 Å) is conventional. It is approximately equal to the distance between the points of the maximum electronic density ( $R_1$ ) of the outermost orbital of the atom in the molecule and of the maximum overlap ( $R_2$ ) of this atomic orbital with the wave function of an arbitrary target atom [11]. The value  $R_2 - R_1 \sim 0.8$  Å for C, N, O, or S can be obtained directly from the values of the van der Waals radii [22] for  $R_2$  and Slater atomic radii [23] for  $R_1$ . Off-diagonal matrix elements represent Mulliken bond orders for chemically bonded atoms and interatomic distances for non-bonded pairs.

Figure 1 illustrates an example of the ECMC calculated for the lowest energy conformation of the compound **1**. For simplicity, the hydrogen atoms are excluded from consideration hereafter.

	C1	C2	C3	C4	C5	C6	C7	Br	N1	N2	O1	O2	O3	O4
C1	0,22	1,42	2,43	2,81	2,43	1,41	0,94	2,72	4,31	2,55	3,48	3,04	5,01	5,01
C2		0,19	1,40	2,42	2,79	2,41	2,54	3,52	3,80	0,73	2,34	2,35	4,19	4,76
C3			0,29	1,43	2,41	2,78	3,81	4,65	2,51	2,48	2,91	3,41	2,80	3,59
C4				0,20	1,41	2,40	4,28	5,11	0,77	3,77	4,26	4,63	2,34	2,34
C5					0,29	1,44	3,75	4,60	2,51	4,30	4,98	5,01	3,59	2,80
C6						0,32	2,46	3,45	3,78	3,82	4,66	4,36	4,75	4,18
C7							0,41	0,96	5,79	3,04	3,97	3,11	6,48	6,44
Br								0,42	6,52	3,84	4,28	4,22	7,22	7,11
N1									0,14	4,99	5,28	5,87	1,50	1,50
N2										0,14	1,52	1,48	5,10	6,06
O1											0,44	2,12	5,22	6,40
O2												0,45	5,98	6,93
O3													0,45	2,12
O4														0,45

Fig.1. The electron-conformational matrix of congruity for molecule **1**. The diagonal elements refer to the atomic ( $C_5$  in the picture) interaction indices calculated by eq 1, while the off-diagonal elements reproduce Mulliken bond orders for chemically bonded pairs of atoms ( $N_1$ - $O_3$ ) and interatomic distances for non-bonded pairs ( $C_5$ - $O_4$ )

**Step 4. Identification of the toxicophore (Tph)**

The ECSA sub-matrix that represents the Tph was obtained by comparing the ECMC's of the first four most toxic compounds in the training set. Applying the procedure described earlier [8] assuming reasonable tolerances we got the following common 4x4 submatrix of activity:

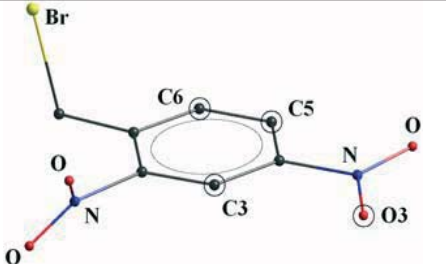
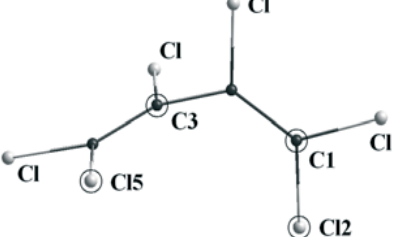
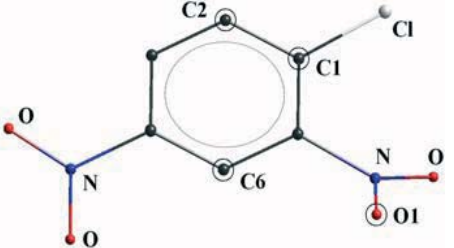
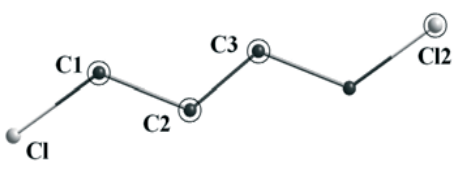
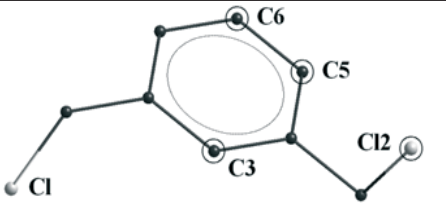
$$\begin{matrix} O3 \\ C6 \\ C5 \\ C3 \end{matrix} \begin{pmatrix} 0.457 & 4.753 & 3.598 & 2.804 \\ & 0.328 & 1.448 & 2.780 \\ & & 0.295 & 2.418 \\ & & & 0.296 \end{pmatrix} \quad (2)$$

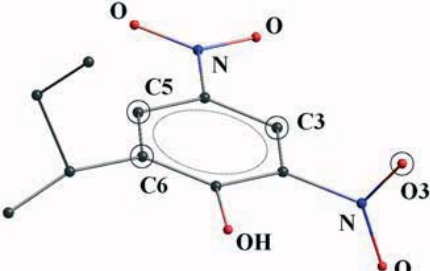
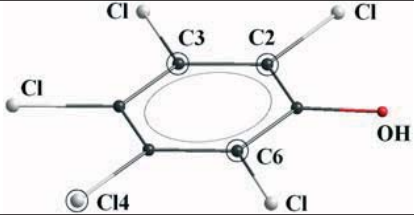
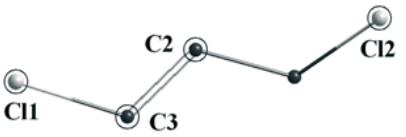
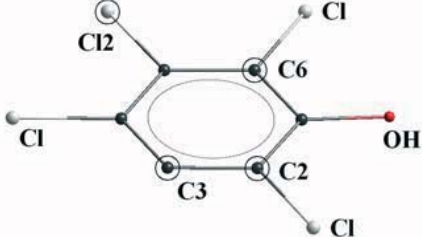
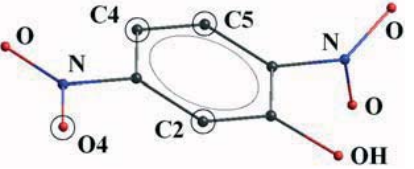
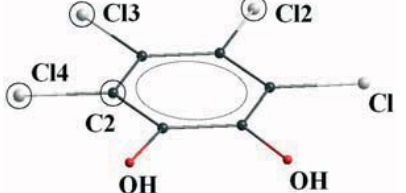
Analyzing the ECMC of the active compounds in the training set we found that the same ECSA obtained from the four most active compounds satisfies the next 17 compounds in some conformation assuming some reasonable tolerances for the matrix elements (see below). These compounds and their corresponding ECSA are shown in Table 2 with the circled four toxicophore atoms corresponding to these 4x4 matrices.

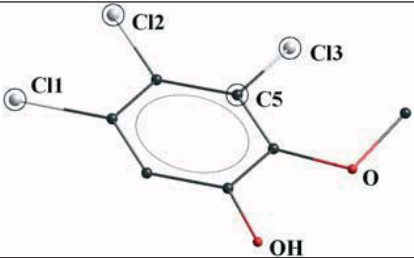
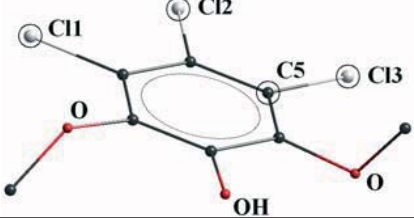
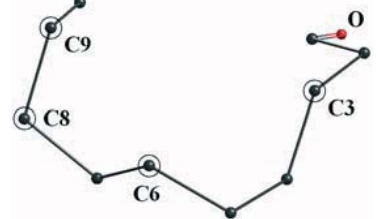
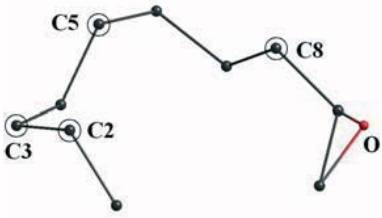
Table 2

The electron-conformational submatrices of toxicity and molecular structures for 17 compounds containing the Tph.

The four toxicophore atoms are marked by circles.

1		$\begin{matrix} O3 \\ C6 \\ C5 \\ C3 \end{matrix} \begin{pmatrix} 0.458 & 4.753 & 3.598 & 2.804 \\ & 0.328 & 1.448 & 2.780 \\ & & 0.295 & 2.418 \\ & & & 0.296 \end{pmatrix}$
2		$\begin{matrix} Cl15 \\ Cl2 \\ C1 \\ C3 \end{matrix} \begin{pmatrix} 0.332 & 4.299 & 3.788 & 2.657 \\ & 0.332 & 1.059 & 3.075 \\ & & 0.307 & 2.471 \\ & & & 0.281 \end{pmatrix}$
3		$\begin{matrix} O1 \\ C2 \\ C1 \\ C6 \end{matrix} \begin{pmatrix} 0.452 & 4.724 & 3.560 & 2.835 \\ & 0.321 & 1.388 & 2.788 \\ & & 0.278 & 2.423 \\ & & & 0.294 \end{pmatrix}$
4		$\begin{matrix} Cl2 \\ C1 \\ C2 \\ C3 \end{matrix} \begin{pmatrix} 0.401 & 4.951 & 3.762 & 2.653 \\ & 0.396 & 0.965 & 2.469 \\ & & 0.295 & 1.943 \\ & & & 0.295 \end{pmatrix}$
5		$\begin{matrix} Cl2 \\ C6 \\ C5 \\ C3 \end{matrix} \begin{pmatrix} 0.399 & 4.647 & 3.467 & 3.437 \\ & 0.314 & 1.451 & 2.784 \\ & & 0.318 & 2.415 \\ & & & 0.320 \end{pmatrix}$

6		$\begin{matrix} Cl1 \\ C4 \\ C3 \\ C2 \end{matrix} \begin{pmatrix} 0.396 & 4.948 & 3.838 & 3.069 \\ & 0.304 & 1.404 & 2.790 \\ & & 0.299 & 2.408 \\ & & & 0.307 \end{pmatrix}$
7		$\begin{matrix} O3 \\ C5 \\ C6 \\ C3 \end{matrix} \begin{pmatrix} 0.452 & 4.992 & 4.513 & 3.208 \\ & 0.305 & 1.426 & 2.425 \\ & & 0.253 & 2.822 \\ & & & 0.296 \end{pmatrix}$
8		$\begin{matrix} Cl4 \\ C2 \\ C3 \\ C6 \end{matrix} \begin{pmatrix} 0.333 & 4.467 & 3.953 & 2.657 \\ & 0.321 & 1.368 & 2.433 \\ & & 0.278 & 2.802 \\ & & & 0.312 \end{pmatrix}$
9		$\begin{matrix} Cl1 \\ C4 \\ C5 \\ C2 \end{matrix} \begin{pmatrix} 0.400 & 5.129 & 4.638 & 3.454 \\ & 0.316 & 1.450 & 2.410 \\ & & 0.315 & 2.783 \\ & & & 0.318 \end{pmatrix}$
10		$\begin{matrix} Cl2 \\ Cl1 \\ C3 \\ C2 \end{matrix} \begin{pmatrix} 0.397 & 5.096 & 3.749 & 2.652 \\ & 0.3687 & 1.011 & 2.626 \\ & & 0.347 & 1.903 \\ & & & 0.282 \end{pmatrix}$
11		$\begin{matrix} Cl2 \\ C2 \\ C3 \\ C6 \end{matrix} \begin{pmatrix} 0.336 & 4.461 & 3.957 & 2.658 \\ & 0.321 & 1.405 & 2.431 \\ & & 0.295 & 2.808 \\ & & & 0.310 \end{pmatrix}$
17		$\begin{matrix} O4 \\ C5 \\ C4 \\ C2 \end{matrix} \begin{pmatrix} 0.459 & 4.764 & 3.603 & 2.791 \\ & 0.303 & 1.428 & 2.800 \\ & & 0.319 & 2.423 \\ & & & 0.348 \end{pmatrix}$
18		$\begin{matrix} Cl2 \\ Cl4 \\ C2 \\ Cl3 \end{matrix} \begin{pmatrix} 0.338 & 5.308 & 3.961 & 3.066 \\ & 0.335 & 1.119 & 3.048 \\ & & 0.309 & 2.661 \\ & & & 0.338 \end{pmatrix}$

21		$  \begin{matrix}  C11 \\  C13 \\  C5 \\  C12  \end{matrix}  \begin{pmatrix}  0.347 & 5.304 & 3.956 & 3.060 \\  & 0.340 & 1.098 & 3.053 \\  & & 0.296 & 2.663 \\  & & & 0.342  \end{pmatrix}  $
22		$  \begin{matrix}  C11 \\  C13 \\  C5 \\  C12  \end{matrix}  \begin{pmatrix}  0.341 & 5.295 & 3.956 & 3.048 \\  & 0.340 & 1.107 & 3.044 \\  & & 0.302 & 2.663 \\  & & & 0.341  \end{pmatrix}  $
24		$  \begin{matrix}  C3 \\  C8 \\  C9 \\  C6  \end{matrix}  \begin{pmatrix}  0.365 & 4.726 & 4.407 & 3.050 \\  & 0.349 & 0.962 & 2.522 \\  & & 0.351 & 3.059 \\  & & & 0.355  \end{pmatrix}  $
25		$  \begin{matrix}  C8 \\  C3 \\  C2 \\  C5  \end{matrix}  \begin{pmatrix}  0.369 & 4.716 & 4.388 & 3.050 \\  & 0.349 & 0.963 & 2.522 \\  & & 0.361 & 3.060 \\  & & & 0.355  \end{pmatrix}  $

Averaging the corresponding matrix elements in these 17 sub-matrices we obtained the following averaged matrix of toxicity  $\hat{T}_{av}$  :

$$\hat{T}_{av} = \begin{matrix} T1 \\ T2 \\ T3 \\ T4 \end{matrix} \begin{pmatrix} 0.395 & 4.803 & 4.053 & 3.053 \\ & 0.350 & 1.207 & 2.743 \\ & & 0.302 & 2.481 \\ & & & 0.318 \end{pmatrix} \quad (3)$$

with the matrix of tolerances (in relative values of the matrix elements):

$$\Delta \hat{T}_{rel} = \begin{pmatrix} 0.162 & 0.105 & 0.144 & 0.131 \\ & 0.133 & 0.202 & 0.121 \\ & & 0.160 & 0.233 \\ & & & 0.116 \end{pmatrix} \quad (4)$$

resulting in following ECSA, the digital toxicophore for the 17 compounds with the toxicity in interval  $-1.32 < -\log LC_{50} < 0.30$ :

$$T = \begin{pmatrix} 0.395 \pm 0.064 & 4.803 \pm 0.504 & 4.053 \pm 0.585 & 3.053 \pm 0.401 \\ & 0.350 \pm 0.046 & 1.207 \pm 0.244 & 2.743 \pm 0.332 \\ & & 0.302 \pm 0.049 & 2.481 \pm 0.578 \\ & & & 0.318 \pm 0.037 \end{pmatrix} \quad (5)$$

Moving to the compounds with lower activity one may find out that this ECSA (revealed for the most active compounds) does not work for them, but they can be accommodated within this ECSA by allowing larger tolerances. In this way one can get slightly different ECSA's and hence *pharmacophores/toxicophores for different levels of activity*. The activity is thus quantitatively a function of the tolerances. The dynamics of change of the tolerances of different atoms when moving from more active to less active compounds reveals also the role of their flexibility in the change of activity.

Let us illustrate this important feature by an example. The compound **benzaldehyde** with  $\log LC_{50} = 1.57$  has the following ECSA:

$$\begin{pmatrix} O1 & 0.51 & 4.79 & 5.06 & 2.89 \\ C3 & & 0.35 & 1.45 & 2.79 \\ C4 & & & 0.31 & 2.41 \\ C6 & & & & 0.31 \end{pmatrix} \quad (6)$$

We see that although this matrix does not fit to the above ECSA for the most active compounds (5), it fails just by some increase of the tolerances, mainly in the distance 5.06 Å between the oxygen atom and the carbon C4, which is out of the limits of the corresponding distance  $4.05 \pm 0.58$  in the most active compounds. This feature comprises the next 7 less active compounds with toxicities  $1.9 > \log LC_{50} > 1.4$ . It demonstrates the important role of the most active heteroatom (chlorine, oxygen, etc.) in the toxicity. The falling toxicity with the increase of the distance of this active atom to the main skeleton of the molecule may be due to either its out of the limits of efficient docking to the bioreceptor or its poor bonding and hence decay through the metabolic processes. The dependence of the quantitative activity on the tolerances is of general importance in the EC method, and it is used to estimate the activity quantitatively (see below).

As mentioned above, this picture of activity presented by ECSA as the pharmacophore or toxicophore and the dependence of the quantitative activity on the tolerances may be complicated by the presence of out-of-pharmacophore groups that influence the activity either by shielding or competing with the pharmacophore in its interaction with the bioreceptor [8]. Therefore the presence of the pharmacophore should be considered as just a *necessary condition of activity*, but not a sufficient one. Since it is based on first principles (quantum-chemical calculations) and not involving statistics, the prediction of the pharmacophore in the EC method has a potential of the same reliability as that of the experimental data of the training set, meaning 100% reliability if based on experimental data of highest accuracy. The latter are thus most important in getting the absolutely reliable pharmacophore.

Another important feature that influences the pharmacophore in the EC method is the diversity of the training set. The ECSA (the pharmacophore/ toxicophore) is valid for levels of activity and classes of molecules the ECMC of which were used in its calculation. For the same mechanism of substrate-receptor interaction different classes of compounds should have the same pharmacophore, but if the latter is obtained from one (or a limited number) of classes with active compounds, it may happen that it includes more active sites (atoms) than the minimal necessary, which thus may be absent in active molecules from other classes.

To screen new compounds for the activity under consideration, their ECMC should be calculated, and then the presence of the ECSA should be checked taking into account the above class and activity level limits. If only very active compounds are looked for, the ECSA (5) of the highly active ones should be tried, while for less active compounds another ECSA (with enlarged tolerances) should be involved. We thus have a very flexible system of searching for leads of active compounds. Presently these procedures of matrix comparison are very fast.

The high reliability of pharmacophore identification by the EC method may serve as a basis for revealing novel knowledge [7]. Indeed, if the pharmacophore is a necessary condition of activity, it should be present in all the active compounds. What if there are active compounds that have no pharmacophore (as in some of the above compounds in Table 1)? If the structure of the molecules, as well as the experimental measurement of activity are beyond doubt and the compound under consideration is within the diversity of the training set, the situation calls for a special investigation. The first time we encountered such a case was in the search for the pharmacophore in musk odorant activity [24]. The pharmacophore that was present in several hundred compounds with musk odor from a variety of rather different classes failed in the case of a patented musk tibeten (a benzene derivative). The solution of this controversy was found in the suggestion that this molecule exhibits its odor properties in the form of a dimer formed by two stacking substituted benzene rings; the dimer has the pharmacophore.

In fact bimolecular activity does not require a priori dimerization before the interaction with the bioreceptor. Indeed, it is widely accepted that the drug-receptor interaction, like any other substrate(S)-enzyme(E) interaction, follows the Michaelis-Menten mechanism [25] with pre-equilibrium in the formation of the complex SE before the transformation to the product P:



This mechanism can be extended to the simultaneous action of two molecules. Indeed, if the first molecule S has no pharmacophore, there will not be transformation to the product. Then the equilibrium (Boltzman distribution) allows for the second molecule to enter the intermediate complex:



If two molecules in a bimolecular docking to the receptor possess the pharmacophore, they may produce the necessary action that triggers the drug activity, albeit with lower probability than a single molecule with the pharmacophore. In the problem of aquatic toxicity to fish under consideration, for instance, the molecule allyl chloride (**II**) with  $\log LC_{50} = 1.20$  has no pharmacophore, while a 1,4-dichloro-2-butene (**I**) with  $\log LC_{50} = -0.16$  has the pharmacophore. The structure of these two molecules in Fig. 2 shows how two molecules of **II** produce the structure **III** which is similar to **I** and has the pharmacophore; hence the activity of **II** can be explained in this way.

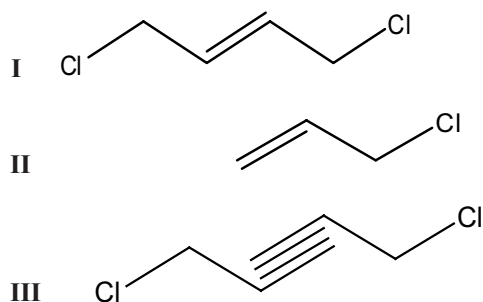


Fig. 2. Illustration of bimolecular activity: two active molecules of allyl chloride (**II**), which separately have no pharmacophore, by stacking along the double bond produce a bimolecular structure (**III**) which is similar to 1,4-dichloro-2-butene (**I**) and has the pharmacophore.

**Step 6.** In accordance with the EC method techniques [8], the presence of toxicophore is only a necessary condition of activity; the evaluation of activity quantitatively involves the regression analysis mentioned above. For the 17 most active molecules the following relations for biological activity was employed [7, 8]:

$$\log(LC_{50})_i = \log(LC_{50})_{ref} - 2.30259 \left\{ \frac{E_i - E_{ref}}{kT} + S_i[R] \right\} \quad (9)$$

where  $(LC_{50})_i$ , and  $(LC_{50})_{ref}$  stand for numerical values of activity of the  $i$ -th compound and the reference compound, respectively,  $E_i$  is the relative energy of the lowest energy conformer of the  $i$ -th compound that contains toxicophore, and  $S_i[R]$  is a function of the electronic and geometric parameters of the substrate molecule.

The parameters in the function  $S_i[R]$  in Eq. (9) should be obtained from the condition of minimum difference between the calculated toxicity  $(LC_{50})_i$  and the experimental values  $(LC_{50})_i^{exp}$ . The regression analysis was performed over the 17 toxicophore-containing molecules and the correlation coefficient as good as  $R^2 = 0.94$  and  $R^2 = 0.92$  in a cross-validated procedure was obtained with just three parameters of their electronic structure:

$$S_i[R] = k_1 (II_{max}^i - II_{max}^{ref}) + k_2 (q^i - q^{ref}) + k_3 (C_{13}^i - C_{13}^{ref}), \quad (10)$$

where  $II_{max}^i$  is the largest "interaction index"  $II$  in  $i$ -th molecule,  $q^i$  is a Mulliken charge of the most electron-negative atom near to the toxicophore atom  $T2^i$  (within the radius of  $R < 2\text{\AA}$  of the typical chemical bond length) and  $C_{13}^i$  is the matrix element of the ECSA corresponding to the distance (in  $\text{\AA}$ ) between the toxicophore atoms  $T1^i$  and  $T3^i$ ;  $T1$ ,  $T2$ ,  $T3$ , and  $T4$  denote consecutively the four atoms in their ECSA (see eq. 3). The following values of the coefficients minimize the expression (10):

$$k_1 = 7.58; \quad k_2 = -14.74; \quad k_3 = 1.36. \quad (11)$$

The theoretical values of toxicities calculated with this set of coefficients and those received in the leave-one-out cross-validation procedure are given in Table 3. The correlation between the experimental and calculated values of  $-\log(LC_{50})$  is presented graphically in Fig. 3.

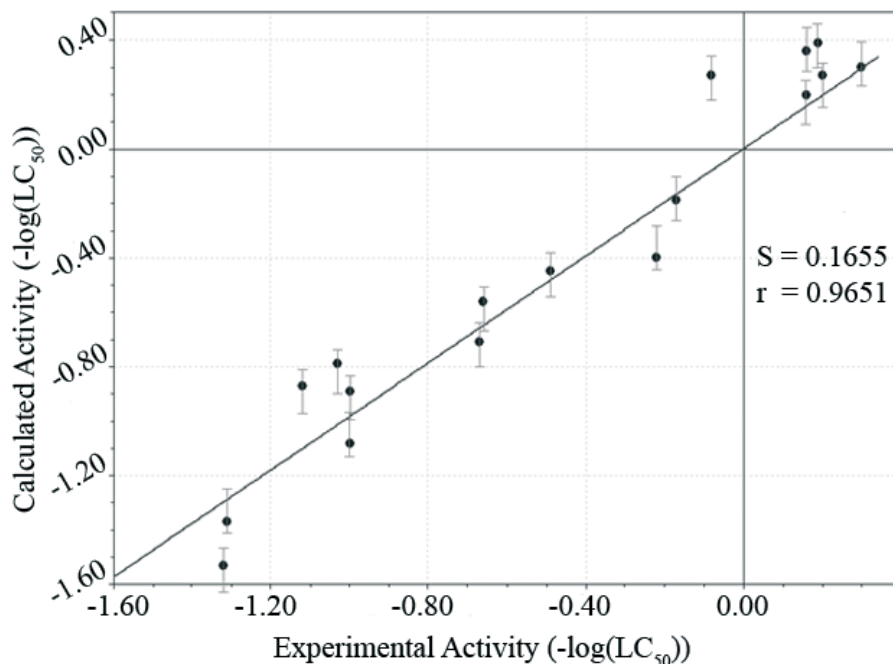
Fig. 3. Calculated vs. experimental  $-\log(LC_{50})$  ratio for 17 most active compounds of the training set

Table 3

Calculated with and without cross-validation (C-V) and experimental values of  $-\log(LC_{50})$  of 17 most active compounds

	$-\log(LC_{50})^{\text{exp}}$	$-\log(LC_{50})^{\text{calc}}$	
		Without C-V	With C-V
1(REFER)	0.30	0.30	
2	0.20	0.27	0.28
3	0.19	0.39	0.39
4	0.16	0.36	0.37
5	0.16	0.21	0.21
6	-0.08	0.28	0.29
7	-0.17	-0.20	-0.23
8	-0.22	-0.40	-0.43
9	-0.49	-0.45	-0.42
10	-0.66	-0.56	-0.53
11	-0.67	-0.71	-0.72
17	-1.00	-0.89	-0.85
18	-1.00	-1.08	-1.10
21	-1.03	-0.79	-0.75
22	-1.12	-0.87	-0.83
24	-1.31	-1.38	-1.41
25	-1.32	-1.53	-1.62

With the parameters of the weakly active compounds included a quantitative relationships between the toxicophore parameters and the toxicity can be obtained from a regression calculation that yields the following new correlation formula:

$$\log(LC_{50})_i = a_0 + a_1 H_{\text{max}}^i + a_2 q_{\text{max}}^i + a_3 C_{13}^i + a_4 C_{12}^i \quad (12)$$

where  $a_i$  are the fitting coefficients,  $H_{\text{max}}^i$  and  $q_{\text{max}}^i$  are the largest values of the ECSA atomic interaction index and atomic charge, respectively, and  $C_{1j}^i$  are the corresponding first row matrix elements of the ECSA in Table 2 (the distance between the most active atom and another one in the toxicophore).

The results are presented in Table 4: **I** and **II** are the fittings obtained over the 17 most active compounds with three and five regression parameters, respectively, and **III** is a fitting received over 21 compounds that include the weakly active ones. While correlation **II** is somewhat better than **I** due to the additional two parameters, correlation **III** allows one to screen and predict also weak toxicities with  $\log LC_{50} > 1.4$ . For strong toxicity with  $\log LC_{50} < 1.4$  correlation **I** is quite reasonable. This indicates the significance of the parameters of the active atom **1** in reducing the toxicity.

Table 4

Regression coefficients for three types of correlation (eqs. 10, 12)

Regression	$a_0$	$a_1$	$a_2$	$a_3$	$a_4$	$R^2$
<b>I</b>	-	7.58	14.74	1.36	-	0.94
<b>II</b>	5.18	2.83	5.82	0.39	0.31	0.97
<b>III</b>	1.6	3.29	6.49	0.46	0.54	0.86

## Conclusions

Using the electron-conformational method we have shown that aquatic toxicity to fish is due to a special functional group, the toxicophore, a combination of four atomic sites with special electronic and topology characteristics represented numerically as the sub-matrix of activity, ECSA. An important feature of the latter is the set of tolerances in the values of the matrix elements which control the quantitative value of activity. It was shown that by varying the tolerances one can obtain different toxicophores for different levels of activity. A distinguished feature of this approach is that it does not employ arbitrary descriptors and statistics at the level of toxicophore identification, thus making the latter void of artifacts and chance correlations and fully reliable (at the level of reliability of the experimental data in the training set). This led us to suggest a bimolecular mechanism of activity for allyl chloride. The toxicophore for 17 most active compounds yields a good correlation ( $R^2 = 0.94$ ) with the experimental activities using only three electronic structure parameters.

## References

- [1] Guner O.F. Ed. Pharmacophore Perception, Development, and Use in Drug Design, International University Line: La Jolla, 2000.
- [2] Kubinyi, H.; Folkers, G.; Martin, Y. C. 3D QSAR in Drug Design. Volume 3, Recent Advances; Kluwer Academic Publishers: New York, 2002.
- [3] Marshall G.R. In: Wolff M.E., Ed. Burger's medicinal chemistry and drug discovery: principles and practice. 5th ed. Vol. 1. New York: John Wiley, 1995, 573-659.
- [4] O. Ivanciuc, Internet Electron. J. Mol. Design, **2**, 195-208 (2003).
- [5] Zhong-Sheng Yi, Shu-Shen Liu, Internet Electron. J. Mol. Design, **4**, 835-849 (2005).
- [6] Verhaar, H.J.M., Leeuwen, C.J., Hemmiens. J.L.M., Chemosphere, **25**, 471-491(1992).
- [7] I. B. Bersuker, J. Comp.-Aid. Mol. Des., submitted for publication.
- [8] I. B. Bersuker. Current Pharmaceutical Design., **9**, 1575-1606 (2003).
- [9] Bersuker I. B., Dimoglo A. S., In Reviews in Computational Chemistry; Lipkowitz K.B., Boyd D.B. Eds.; VCH: New York, 1991; vol.2, pp.423-60.
- [10] Bersuker, I. B.; Bahceci, S.; Boggs, J. E.; Pearlman, R. S., J. Computer-aided Mol. Design **13**, 419-434 (1999).
- [11] Bersuker, I. B.; Bahceci, S.; Boggs, J. E., J. Chem. Inf. Comput. Sci., **40** (2000)1363-1376.
- [12] Rosines, E.; Bersuker, I. B.; Boggs, J. E., Quan. Struct.-Act. Relat. **2001**, *20*, 327-334.
- [13] A. H. Makkouk, I. B. Bersuker and J. E. Boggs, Int. J. Pharm. Med., **18**, 81-89 (2004).
- [14] A.V. Marenich, Pei-Han Yong, I. B. Bersuker and J. E. Boggs, J. Chem. Inf. Mod., submitted.
- [15] Katritzky, A.R., Tatham, D.B. and Maran U., J. Chem. Inf. Comput. Sci., **41**, 1162-1176 (2001).
- [16] Dearden. J.C. and Raevsky, O.A., SAR and QSAR in Environm. Research, **15**, 433-448 (2004).
- [17] Halgren T. A., J. Comp. Chem. **1996**, *17*, 490-519.
- [18] Chambers, C. C.; Hawkins, G. D.; Cramer, C. J.; Truhlar, D. G. J. Phys. Chem. **1996**, *100*, 16385-16398.
- [19] *Spartan'02*; Wavefunction, Inc.: Irvin, CA. Except for molecular mechanics and semi-empirical models, the calculation methods used in Spartan'02 have been documented in: Kong, J.; White, C. A.; Krylov, A. I.; Sherrill, D.; Adamson, R. D.; Furlani, T. R.; Lee, M. S.; Lee, A. M.; Gwaltney, S. R.; Adams, T. R.; Ochsenfeld, C.; Gilbert, A. T. B.; Kedziora, G. S.; Rassolov, V. A.; Maurice, D. R.; Nair, N.; Shao, Y.; Besley, N. A.; Maslen, P. E.; Dombroski, J. P.; Daschel, H.; Zhang, W.; Korambath, P. P.; Baker, H.; Byrd, E. F. C.; Voorhis, T. V.; Oumi,

- M.; Hirata, S.; Hsu, C.-P.; Ishikawa, N.; Florian, J.; Warshel, A.; Johnson, B. G.; Gill, P. M. W.; Head-Gordon, M.; Pople, J. A. Q-Chem 2.0: A High-Performance Ab Initio Electronic Structure Program Package. *J. Comput. Chem.* 2000, 21, 1532–1548.
- [20] Stewart, J. J. P., *J. Comp. Chem.* **1989**, 10, 209–220.
- [21] Basch, H.; Viste, A.; Gray, H. B., *Theoret. chim. Acta (Berl.)* **1965**, 3, 458–464.
- [22] Bondi, A., *J. Phys. Chem.* **1964**, 68, 441–451).
- [23] Slater, J. C., *J. Chem. Phys.* **1964**, 41, 3199–3204).
- [24] Bersuker I.B., Dimoglo A.S., Gorbachov M.Yu., Vlad P.F., Pesaro M. *New J. Chem.*, **15**, 307-20 (1991).
- [25] Metzler, D. E. *Biochemistry: The Chemical Reactions of Living Cells*; Academic Press: New York, 1977.

# VIBRONIC ORIGIN OF THE “SKEWED” ANTICLINE CONFIGURATION OF THE HYDROGEN PEROXIDE MOLECULE

N. N. Gorinchoy\*, I. Ya. Ogurtsov and Ion Arsene

*Institute of Chemistry, Academy of Sciences of Moldova, Academiei str. 3, MD 2028 Kishinev, Republic of Moldova*

\*E-mail: ngorinchoy@yahoo.com; Phone 373 22 739649

**Abstract:** The vibronic origin of instability of the symmetrical forms ( $D_{\infty h}$ ,  $C_{2h}$  and  $C_{2v}$ ) of the hydrogen peroxide molecule  $H_2O_2$  was revealed using *ab initio* calculations of the electronic structure and the adiabatic potential energy curves. The vibronic constants in this approach were estimated by fitting of the *ab initio* calculated adiabatic potential in the vicinity of the high-symmetry nuclear configurations to its analytical expression. It was shown that the equilibrium “skewed” anticline shape of the  $C_2$  symmetry can be realized in two ways:  $D_{\infty h} \rightarrow C_{2v} \rightarrow C_2$  or  $D_{\infty h} \rightarrow C_{2h} \rightarrow C_2$  with the decreasing of the adiabatic potential energy at every step.

**Keywords:** hydrogen peroxide, electronic structure, pseudo Jahn-Teller effect.

## Introduction

It is known that molecules of the type ABBA have a different geometry in gaseous phase: acetylene HCCH is a linear molecule ( $D_{\infty h}$ ), HNNH has a bent form with the  $C_{2h}$  symmetry and hydrogen peroxide  $H_2O_2$  adopts a “skewed” anticline shape with  $\angle HOO=94.8^\circ$  and dihedral angle  $\varphi_{HOOH}=111.5^\circ$  [1]. In general, the problem of molecular geometry can be determined experimentally or by numerical calculations of its equilibrium (lowest in total energy) conformation. There are many modern computer program packages that perform such geometry optimization at least for the ground state, the results being strongly dependent on the method of calculation and on the type of the used basis set. However, such studies of the molecular geometry give no physical explanation of the origin of the shape of molecule. Very often the symmetry of the nuclear configuration at the minimum is lower than the possible high-symmetry one. It was proved (see in [2]) and confirmed by numerical calculations [3-7] that the only reason of instability and distortions of high-symmetry configurations of systems in non-degenerated electronic states is the pseudo Jahn-Teller effect (PJTE).

Quantum chemical calculations of the hydrogen peroxide molecule available in literature (see, for example, [8-10] and references therein) are devoted mainly to determination of the equilibrium geometrical parameters and the barriers (*cis*-, *trans*-) to internal rotation. The analysis of the whole adiabatic potential energy surface (APES) of the  $H_2O_2$  molecule and of the reasons causing its low-symmetry equilibrium nuclear configuration were not considered as yet.

In the present paper, distinguished from other works, we started the calculations of the hydrogen peroxide molecule from the highest possible  $D_{\infty h}$  symmetry, analyzed its distortion towards planar bent *cis*- ( $C_{2v}$ ) and *trans*- ( $C_{2h}$ ) transition states, and then to the equilibrium “skewed” ( $C_2$ ) shape, and demonstrated that at every step the distortion of the molecule, accompanied by lowering of the symmetry of the nuclear configuration, is due to the pseudo Jahn-Teller effect.

## General theory

According to the PJTE theory [2] the adiabatic potential (AP) surface  $\varepsilon_0(q_{\bar{\Gamma}})$  in the space of small displacements  $q_{\bar{\Gamma}}$  (read off from  $\varepsilon=0$ ) may be written as follows:

$$\varepsilon_0(q_{\bar{\Gamma}}) = \frac{1}{2} (K_{0\bar{\Gamma}}^{\Gamma} + K_{v\bar{\Gamma}}^{\Gamma}) \cdot q_{\bar{\Gamma}}^2, \quad (1)$$

where the bare (nonvibronic) force constant  $K_{0\bar{\Gamma}}^{\Gamma}$ ,

$$K_{0\bar{\Gamma}}^{\Gamma} = \left\langle \Gamma \left| \partial^2 \hat{H}(r, q_{\bar{\Gamma}}) / \partial q_{\bar{\Gamma}}^2 \right|_0 \right\rangle, \quad (2)$$

describes the contribution of the fixed ground state electron distribution to the force constant, while the second term,  $K_{v\bar{\Gamma}}^{\Gamma}$  (which is always negative),

$$K_{\nu\bar{\Gamma}}^{\Gamma} = -2 \sum_{\Gamma'} \left| F_{\bar{\Gamma}}^{\Gamma\Gamma'} \right|^2 / (E_{\Gamma'} - E_{\Gamma}). \quad (3)$$

is the vibronic coupling contribution to the curvature of the AP arising from the mixing of the ground ( $\Gamma$ ) with the excited ( $\Gamma'$ ) states in the second order perturbation theory, and

$$F_{\bar{\Gamma}}^{\Gamma\Gamma'} = \left\langle \Gamma \left| (\partial \hat{H}(r, q_{\bar{\Gamma}}) / \partial q_{\bar{\Gamma}})_0 \right| \Gamma' \right\rangle, \quad (4)$$

is the constant of vibronic coupling between the mixing states. In eqs. (2)-(4)  $\hat{H}$  is the electronic Hamiltonian of the system, and  $E_{\Gamma}$  and  $E_{\Gamma'}$  are the total energies of the ground and excited states respectively. Derivatives in these equations are taken in the reference configuration at  $q_{\bar{\Gamma}}=0$ . Note that the vibronic constants  $F_{\bar{\Gamma}}^{\Gamma\Gamma'}$ , and therefore the vibronic contribution  $K_{\nu\bar{\Gamma}}^{\Gamma}$  to the curvature of the AP, are nonzero only if  $\Gamma \otimes \Gamma'$  contains  $\bar{\Gamma}$ .

It was proved analytically and confirmed by a series of numerical calculations [2-7] that for any molecular system the contribution to the curvature of AP of the ground state is always positive,

$$K_{0\bar{\Gamma}}^{\Gamma} \geq 0. \quad (5)$$

This means that structural instabilities and distortions of high-symmetry configurations of any polyatomic system in non-degenerate states are due to, and only to the PJTE, the mixing of the electronic state under consideration with higher in energy (excited) states under the nuclear displacements in the direction of distortion. The instability takes

place if the inequality  $\left| K_{\nu\bar{\Gamma}}^{\Gamma} \right| \geq K_{0\bar{\Gamma}}^{\Gamma}$  holds, i.e. when the vibronic coupling is strong enough and/or the energy gap between the mixing states is relatively small. To answer the questions whether the system in the reference nuclear configuration is stable or not with respect to any low-symmetry coordinate  $q_{\bar{\Gamma}}$ , the wave functions, energy gaps  $E_{\Gamma'}$ -

$E_{\Gamma}$ , and the matrix elements  $F_{\bar{\Gamma}}^{\Gamma\Gamma'}$  and  $K_{0\bar{\Gamma}}^{\Gamma}$  should be calculated for the states that are mixed under the displacement under consideration.

### Coordinates of instability

Investigation of the possible spatial structures of the system should be started with its highest possible symmetry. In the case of the  $\text{H}_2\text{O}_2$  molecule the linear configuration of  $D_{\infty h}$  symmetry is the reference one. In this configuration the four-atom molecular system  $\text{H}_2\text{O}_2$  has seven vibrational degrees of freedom, which transform according to the irreducible representations  $2\sigma_g^+ + \sigma_u^+ + \pi_g + \pi_u$ . Two modes,  $\pi_u$  and  $\pi_g$ , correspond to the bending of the molecule and transform the linear nuclear configuration into the *cis*- ( $C_{2v}$ ) and *trans*- ( $C_{2h}$ ) transition states, leaving them, however, planar. Schematic illustration of these two modes is shown in Fig.1, a,b.

After separating of the center of masses we come to the following symmetrized displacements of the  $\pi$  type, describing the internal motions of the atoms under the bending distortion:

$$\begin{aligned} q_{\pi_g x} &= \sqrt{\frac{m}{2(M+m)}}(x_{O_1} - x_{O_2}) - \sqrt{\frac{M}{2(M+m)}}(x_1 - x_2), \\ q_{\pi_g y} &= \sqrt{\frac{m}{2(M+m)}}(y_{O_1} - y_{O_2}) - \sqrt{\frac{M}{2(M+m)}}(y_1 - y_2), \\ q_{\pi_u x} &= \sqrt{\frac{m}{2(M+m)}}(x_{O_1} + x_{O_2}) - \sqrt{\frac{M}{2(M+m)}}(x_1 + x_2), \\ q_{\pi_u y} &= \sqrt{\frac{m}{2(M+m)}}(y_{O_1} + y_{O_2}) - \sqrt{\frac{M}{2(M+m)}}(y_1 + y_2), \end{aligned} \quad (6)$$

Here the index  $\gamma = x, y$  of  $q_{\pi\gamma}$  labels the lines of the degenerate representations of the  $\pi$  type,  $x_{O_i}, y_{O_i}, x_j$  and  $y_j$  are the Cartesian displacements of the atoms of oxygen and hydrogen respectively.

In the optimized planar  $C_{2v}$  and  $C_{2h}$  geometries there are out-of-plane vibrations ( $a_2$  type in configuration of the  $C_{2v}$  symmetry and  $a_u$  type in the  $C_{2h}$  one) which lead to the final “skewed” anticline shape of the  $C_2$  symmetry (Fig.1, c, d). Corresponding symmetrized coordinates are:

$$q_{a_2} = \frac{1}{\sqrt{2}}(y_1 - y_2), \quad q_{a_u} = \frac{1}{\sqrt{2}}(y_1 + y_2). \quad (7)$$

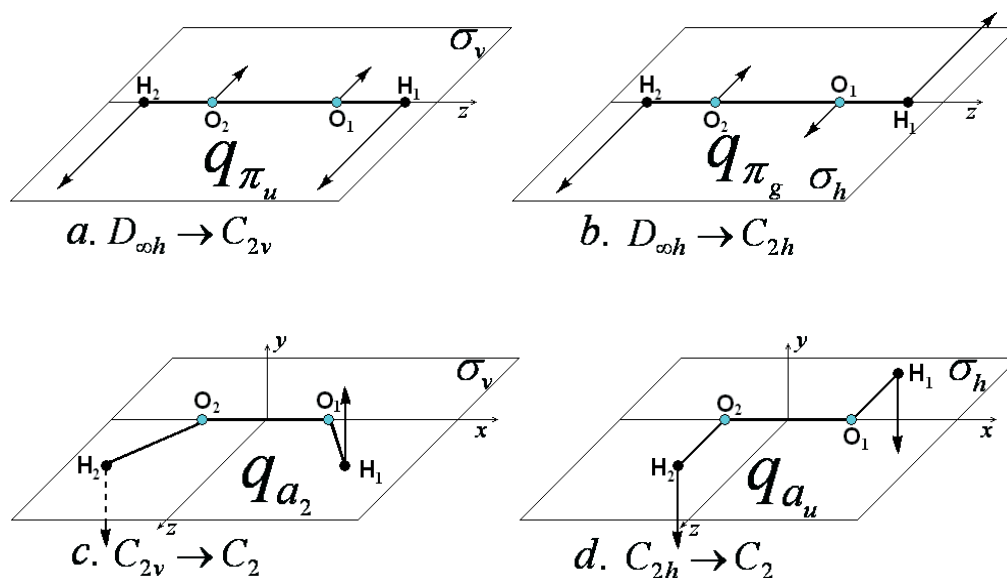


Fig.1. The coordinate axes and atomic numeration for the  $H_2O_2$  molecule. The arrows schematically show the displacements active in the PJTE:  $\pi_u$  (a) and  $\pi_g$  (b) types in the  $D_{\infty h}$  configuration, and  $a_2$  (c) and  $a_u$  (d) modes in the  $C_{2v}$  and  $C_{2h}$  symmetries respectively

In accordance with the remark in Section 2, the vibronic contribution to the curvature of AP that can lead to the instability of the high-symmetry nuclear configurations come from the vibronic mixing of only those many-electronic states, ground  $\Gamma$  and excited  $\Gamma'$ , for which  $\Gamma \otimes \Gamma'$  contains  $\Pi_u$  or  $\Pi_g$  representations of the  $D_{\infty h}$  point symmetry group (linear geometry), and  $A_2$  ( $C_{2v}$ ) and  $A_u$  ( $C_{2h}$ ) representations in corresponding bending configurations.

### Electronic structure of hydrogen peroxide $H_2O_2$

The geometry parameters of the hydrogen peroxide  $H_2O_2$  in the linear ( $D_{\infty h}$ ), planar bent ( $C_{2h}$  and  $C_{2v}$ ) and “skewed” anticline ( $C_2$ ) nuclear configurations were optimized by *ab initio* SCF method in the RHF approximation with the use of the extended basis set of the TZV type augmented by polarization d- and f-functions on the oxygen atoms and p-functions on the hydrogen ones. Further the electronic energetic spectrum of the  $H_2O_2$  molecule in all the optimized symmetrical geometries was calculated using the configuration interaction (CI) approximation. The active space of CI included seven occupied and three lower unoccupied molecular orbitals. All calculations were performed using the PC GAMESS version [11] of the GAMESS (US) QC package [12].

Calculated parameters of the geometrical structure for all considered symmetrical configurations of the  $H_2O_2$  molecule and the values of the total and relative energies of the states are presented in Table 1.

Note that in all the cases not all obtained excited states are listed in Table 1, but only those that give the predominant contribution to the pseudo Jahn–Teller instability (negative force constant) of the ground state.

Table 1

Optimized geometries (Å), total energies (hartree), relative energies (eV) and electronic configurations of the ground and low-lying excited states for symmetry nuclear configurations

Symmetry	Geometry	State	Total energy	Relative energy	Electronic configuration
$D_{\infty h}$	$R_{O-O}=1.30$ $R_{O-H}=0.94$	$\Sigma_g^+$	-150.6219	0	$[\dots(\pi_u)^4(\pi_g)^4(\sigma_u)^0(\sigma_g)^0]$
		$\Pi_u$	-150.4905	3.57	$[\dots(\pi_u)^4(\pi_g)^3(\sigma_u)^1(\sigma_g)^0]$
		$\Pi_g$	-150.3415	7.63	$[\dots(\pi_u)^4(\pi_g)^3(\sigma_u)^0(\sigma_g)^1]$
$C_{2h}$	$R_{O-O}=1.39$ $R_{O-H}=0.94$ $\angle HOO=101.6^\circ$	$A_g$	-150.8533	0	$[\dots(a_g)^2(b_g)^2(b_u)^0(a_u)^0]$
		$A_u$	-150.5966	6.98	$[\dots(a_g)^2(b_g)^1(b_u)^1(a_u)^0]$
$C_{2v}$	$R_{O-O}=1.39$ $R_{O-H}=0.94$ $\angle HOO=107.3^\circ$	$A_1$	-150.8496	0	$[\dots(b_2)^2(a_2)^2(a_1)^0(b_1)^0]$
		$A_2$	-150.5872	7.14	$[\dots(b_2)^2(a_2)^1(a_1)^1(b_1)^0]$
$C_2^a$	$R_{O-O}=1.39$ $R_{O-H}=0.94$ $\angle HOO=103.2^\circ$ $\varphi_{dihedral}=110.2^\circ$	$A$	-150.8595	0	$[\dots(a)^2(b)^2(a)^0(b)^0]$

<sup>a</sup> Experimental values of the angles:  $\angle HOO=94.8^\circ$ ,  $\varphi_{HOOH}=111.5^\circ$  [1].

The scheme of the electronic terms is shown in Fig. 2, where the dashed lines indicate the alteration of the states under the vibronically stabilized distortions. It is seen that in the high-symmetry linear ( $D_{\infty h}$ ) nuclear configuration the system has a nondegenerate ground state  $^1\Sigma_g^+$ , and two low-lying two-fold degenerate  $^1\Pi_u$  and  $^1\Pi_g$  excited electronic states.

As was mentioned in the previous Section, only the vibronic constants of the type  $F_{\pi_u} = \langle \Sigma_g^+ | (\partial \hat{H}(r, q) / \partial q_{\pi_u})_0 | \Pi_u \rangle$

and  $F_{\pi_g} = \langle \Sigma_g^+ | (\partial \hat{H}(r, q) / \partial q_{\pi_g})_0 | \Pi_g \rangle$ , and hence only the vibronic contribution to the curvature of the adiabatic

potential  $K_{\pi_u}^v$  and  $K_{\pi_g}^v$  are nonzero. If these values are large enough, the linear configuration is unstable with respect to  $\pi_u$  and  $\pi_g$  types nuclear displacements, and the system passes to more stable *cis*- ( $C_{2v}$ ) or *trans*- ( $C_{2h}$ ) nuclear configurations. In their turn due to the pseudo JT coupling of the ground  $^1A_g$  ( $C_{2h}$ ) or  $^1A_1$  ( $C_{2v}$ ) and excited  $^1A_u$  (or  $^1A_2$ )

electronic states (i.e. non-zero  $F_{a_u} = \langle A_g | (\partial \hat{H}(r, q) / \partial q_{a_u})_0 | A_u \rangle$  and  $F_{a_2} = \langle A_1 | (\partial \hat{H}(r, q) / \partial q_{a_2})_0 | A_2 \rangle$  vibronic constants) these bent shapes become unstable with respect to the out-of-plane ( $a_u$  or  $a_2$  type) displacements of the hydrogen atoms resulting in the equilibrium “skewed” antiplane configuration of the  $C_2$  symmetry.

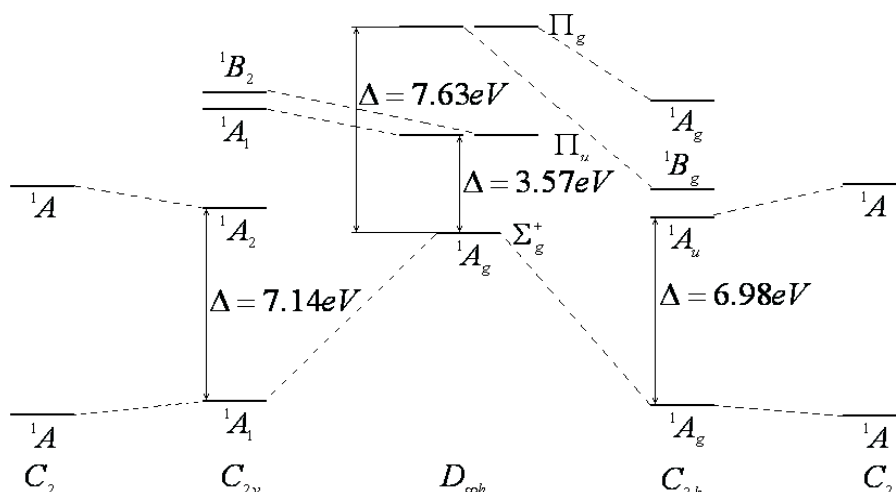


Fig. 2. Electronic terms of the  $H_2O_2$  molecule in four symmetry configurations

Consider in more detail the nature of the mixing states. In the linear configuration the first excited  $\Pi_u$  term arises from the excitation of one electron from the fully occupied  $\pi_g$  molecular orbital (formed almost solely from the  $2p_\pi$  AOs of the oxygen atoms) to the unoccupied  $\sigma_u$  MO which is an antisymmetrical linear combination of the  $2p_\sigma$  AOs of the oxygen atoms and  $1s$  AOs of hydrogens. The second excited  $\Pi_g$  state is formed by one-electron excitation from the same occupied  $\pi_g$  MO to the virtual  $\sigma_g$  one which is a symmetrized linear combination of the  $2p_\sigma$  AOs of the O atoms and  $1s$  AOs of the H atoms (Table 1 and Fig. 3). Thus the determinants in the CI wavefunctions of the ground  $\Sigma_g^+$  and corresponding excited  $\Pi_u$  and  $\Pi_g$  electronic states differ by one spin-orbital only. Taking into account that the Hamiltonian  $H$  in eq. 4 is a sum of one-particle operators, the vibronic constants  $F_{\pi_u}$  and  $F_{\pi_g}$  can be calculated as

one-electron matrix elements of the type  $\langle \pi_g x | (\partial \hat{H}(r, q) / \partial q_{\pi_u x})_0 | \sigma_u \rangle$  and  $\langle \pi_g x | (\partial \hat{H} / \partial q_{\pi_g x})_0 | \sigma_g \rangle$ . For the planar bent  $C_{2h}$  and  $C_{2v}$  configurations corresponding vibronic constants  $F_{a_u} = \langle A_g | (\partial \hat{H}(r, q) / \partial q_{a_u})_0 | A_u \rangle$  and  $F_{a_2} = \langle A_1 | (\partial \hat{H}(r, q) / \partial q_{a_2})_0 | A_2 \rangle$  are reduced to the matrix elements  $\langle b_g | (\partial \hat{H}(r, q) / \partial q_{a_u})_0 | b_u \rangle$  and  $\langle a_2 | (\partial \hat{H}(r, q) / \partial q_{a_2})_0 | a_1 \rangle$  respectively.

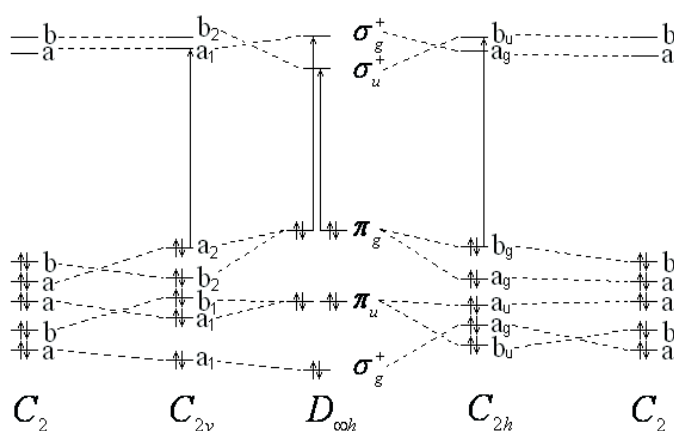


Fig. 3. MO energy level scheme for the  $H_2O_2$  molecule in linear ( $D_{\infty h}$ ), bent ( $cis-C_{2v}$  and  $trans-C_{2h}$ ) and equilibrium “skewed” anticline ( $C_2$ ) nuclear configurations

The large values of the vibronic constants are due to the nature of the mixing MOs determining the essential changes of the binding by the distortion. Indeed, for example, in the linear configuration the overlap of the occupied  $\pi_g$  and unoccupied  $\sigma_u$  ( $\sigma_g$ ) orbitals is zero by symmetry restrictions (Fig. 4), and hence these orbitals do not contribute to oxygen-hydrogen bonding. Under the  $\pi_g$  ( $\pi_u$ ) type nuclear displacements the  $\pi_g$  MO split and one of its component become of the same symmetry as the respective admixing virtual orbital. Now their overlap is nonzero resulting in the additional bonding of the  $2p_\pi$  AOs of the oxygen atoms with the orbital of the nearest hydrogen atom.



Fig. 4. Schematic illustration to the covalence origin of the vibronic instability of the linear configuration of  $H_2O_2$ : (a)  $\pi_g \otimes \sigma_u$ , (b)  $\pi_g \otimes \sigma_g$ . The overlap integral between the vibronically mixing molecular orbitals (white areas) is zero in the linear  $D_{\infty h}$  configuration and becomes nonzero by  $\pi_g$  ( $\pi_u$ ) distortions bending the  $H_2O_2$  molecule towards to the  $cis-C_{2v}$  (a) and  $trans-C_{2h}$  (b) transition states

## Numerical calculations of the adiabatic potential

Potential energy curves of the  $\text{H}_2\text{O}_2$  for all considered displacements  $q_{\bar{\Gamma}}$  ( $\bar{\Gamma} = \pi_g, \pi_u, a_u, a_2$ ) (Fig. 1) were calculated with the *ab initio* SCF CI method described in Section 3. Fig. 5 show corresponding cross sections of the APES along the coordinates  $q_{\bar{\Gamma}}$ . In the starting linear ( $D_{\infty h}$ ) nuclear configuration ( $q_{\pi_g} = 0, q_{\pi_u} = 0$ ), as mentioned above, the electronic ground state is  $^1\Sigma_g^+$ , and there are two double-degenerate  $^1\Pi_u$  (at 3.57 eV above the ground state) and  $^1\pi_g$  (at 7.63 eV) excited electronic states. Along  $q_{\pi_g} \neq 0$  (Fig.5, a) or  $q_{\pi_u} \neq 0$  (Fig.5, b) the  $D_{\infty h}$  symmetry is reduced to  $C_{2h}$  ( $C_{2v}$ ), the  $\Pi_g$  ( $\Pi_u$ ) doublets split and one of their components ( $A_g$  in  $C_{2h}$  and  $A_1$  in  $C_{2v}$  configuration) has the strong vibronic admixture to the ground state (due to the relatively large vibronic constants) resulting in the instability of the later with respect to *trans*- and *cis*- bending.

Planes (c) and (d) in Fig. 5 represent the cross sections of the APES along the out-of-plane displacements of the hydrogen atoms ( $a_u$  or  $a_2$  type) when starting from the  $C_{2h}$  or  $C_{2v}$  configurations. In these cases due to the pseudo JT admixture of the excited  $^1A_u$  ( $C_{2h}$ ) or  $^1A_2$  ( $C_{2v}$ ) terms (Fig.2) the ground electronic  $^1A_g$  (or  $^1A_1$ ) states become unstable with respect to these out-of-plane displacements of the hydrogen atoms. The energies of stabilization are equal to 0.17 kcal/mole in the case of  $C_{2h} \rightarrow C_2$  distortion and 0.27 kcal/mole in the  $C_{2v} \rightarrow C_2$  case.

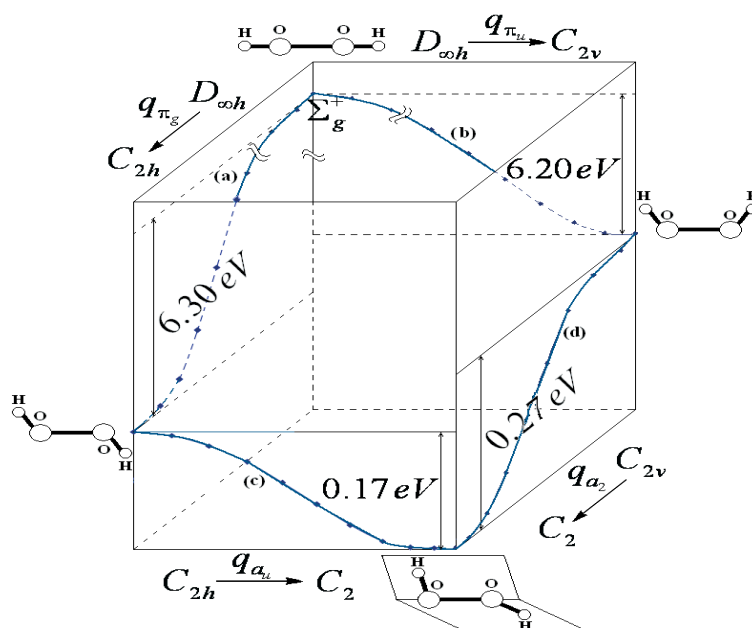


Fig.5. Four cross-sections of the APES of the hydrogen peroxide along:  $q_{\pi_u}$  ( $D_{\infty h} \rightarrow C_{2v}$ ),  $q_{\pi_g}$  ( $D_{\infty h} \rightarrow C_{2h}$ ),  $q_{a_2}$  ( $C_{2v} \rightarrow C_2$ ) and  $q_{a_u}$  ( $C_{2h} \rightarrow C_2$ ) coordinates

We used eq. (1) to estimate the parameters of the vibronic coupling by fitting *ab initio* data for the APES to the general formulas. The values of parameters of the PJTE,  $K_0$ ,  $V$  and  $K$ , obtained in this way are presented in Table 2.

Table 2

Values of the parameters of the PJT coupling,  $K_0$ ,  $V$  and  $K$

$q_{\bar{\Gamma}}$	$\Delta_{\bar{\Gamma}}$ (eV)	$\Delta E_{\text{PJTE}}$ (eV)	$K_0^{\bar{\Gamma}}$ (eV/Å <sup>2</sup> )	$V_{\bar{\Gamma}}$ (eV/Å)	$K_{\bar{\Gamma}}$ (eV/Å <sup>2</sup> )
$q_{\pi_g}$ ( $D_{\infty h} \rightarrow C_{2h}$ )	7.63	6.30	3.05	6.83	-9.18
$q_{\pi_u}$ ( $D_{\infty h} \rightarrow C_{2v}$ )	3.57	6.20	2.28	6.29	-19.88
$q_{a_u}$ ( $C_{2h} \rightarrow C_2$ )	6.98	0.17	4.09	4.25	-1.09
$q_{a_2}$ ( $C_{2v} \rightarrow C_2$ )	7.14	0.27	4.26	4.43	-1.24

It is seen from the Table 2, that the values of  $K_r = K_0^r - 2V_r^2/\Delta_r$  (the curvature of the adiabatic potential) in all these geometries are negative. This confirms that all symmetrical forms ( $D_{\infty h}$ ,  $C_{2h}$  and  $C_{2v}$ ) of the hydrogen peroxide molecule  $H_2O_2$  are energetically unstable due to the PJT effect. Both transition paths from the  $D_{\infty h}$  to  $C_2$  ( $D_{\infty h} \rightarrow C_{2h} \rightarrow C_2$  and  $D_{\infty h} \rightarrow C_{2v} \rightarrow C_2$ ) have the same energetic effect:  $\sim 6.47$  eV.

Note, that the energy gaps between the mixing ground and excited electronic states are rather large in all the cases. However, the vibronic coupling is much larger producing at first one of the planar bent configurations and then the stable “skewed” anticline shape of the hydrogen peroxide. Note also that more sophisticated methods of calculations can give more precise values of the total energies, but they do not change the qualitative details of the rearrangement of molecular orbitals and the formation of new covalent bonds in the system by distortion.

## Conclusion

On the base of the *ab initio* calculations of the electronic structure and the potential energy surfaces it was shown that the  $H_2O_2$  molecule is unstable in both the linear nuclear configuration of the  $D_{\infty h}$  symmetry and planar bent *cis*- ( $C_{2v}$ ) or *trans*- ( $C_{2h}$ ) shapes. By fitting of the equation (1) obtained from the vibronic theory to the *ab initio* calculated hydrogen peroxide APES it is shown that the origin of the instability of these configurations is the pseudo Jahn-Teller effect. The equilibrium “skewed” anticline shape of the  $C_2$  symmetry can be realized in two ways:  $D_{\infty h} \rightarrow C_{2v} \rightarrow C_2$  or  $D_{\infty h} \rightarrow C_{2h} \rightarrow C_2$  with decreasing adiabatic potential energy at every step.

## References

- [1] Koput J., J. Mol. Spectrosc., 1986, **115**, 438-441.
- [2] I. B. Bersuker, The Jahn-Teller Effect, Cambridge University Press, Cambridge, England, 2006.
- [3] I. B. Bersuker, N.N.Gorinchoi, V.Z.Polinger, Theor. Chim. Acta, 1984, **66**, 161.
- [4] V.Z.Polinger, N.N.Gorinchoi and I.B.Bersuker, Chem. Phys., 1992, **159**, 75-87.
- [5] N.N.Gorinchoi, F.Cimpoesu, I.B.Bersuker, J. Mol. Struct. (Theochem), 2001, **530**, 281–290.
- [6] I.Ogurtsov, N.Gorinchoy, I.Balan, J. Mol. Struct., 2007, **838**, 107–111.
- [7] I. B. Bersuker, N. B. Balabanov, D. M. Pekker, J. E. Boggs, J. Chem. Phys., 2002, 117, 10478-86.
- [8] J.E.Carpenter and F.Weinhold, J. Phys. Chem., 1988, **92**, 4295-4306.
- [9] R.Block and L.Jansen, J. Chem. Phys., 1985, **82**, 3322-3328.
- [10] T.H.Dunning, Jr., N.W.Winter, J. Chem. Phys., 1975, **63**, 1847-1855.
- [11] Alex A. Granovsky, www <http://classic.chem.msu.su/gran/gamess/index.html>.
- [12] M.W.Schmidt, K.K.Baldrige, J.A.Boatz, S.T.Elbert, M.S.Gordon, J.H.Jensen, S.Koseki, N.Matsunaga, K.A.Nguyen, S.Su, T.L.Windus, M.Dupuis, J.A.Montgomery, J.Comput.Chem., 1993, **14**, 1347-1363.

## **AB INITIO ANALYSIS OF EXCHANGE INTERACTIONS IN [V<sub>2</sub>O(bipy)<sub>4</sub>Cl<sub>2</sub>]<sup>2+</sup> COMPLEX**

Ivan Ogurtsov\*, Andrei Tihonovschi

*Institute of Chemistry, Academy of Sciences of Moldova, Republic of Moldova, Chisinau, Academiei str., 3.*

\* *io\_quant@yahoo.com, +373 22 739675*

**Abstract:** In this work an *ab initio* analysis of the binuclear vanadium complex [V<sub>2</sub>O(bipy)<sub>4</sub>Cl<sub>2</sub>]<sup>2+</sup> electronic structure is performed. The ground state was calculated to be a quintet, which means a ferromagnetic interaction between centers. The orbitals participating in exchange interaction according to ROHF+CI calculations are two molecular orbitals consisting of vanadium d-orbitals and two molecular orbitals with main contributions from p-orbitals of bipyridine ligands perpendicular to V-V axis, vanadium d- and p-orbitals and μ-oxygen p-orbital. Calculated energy values of the multielectronic states are placed in accordance with Lande rule. The value of magnetic moment at 293K calculated for the complex in vacuum taking into consideration the Boltzmann distribution and the energies of the excited states is 3.95BM which is in accordance with experimental value of 3.99BM (for complex in acetone).

**Keywords:** binuclear vanadium complex, binuclear μ-oxo-bridged complex, exchange interactions, magnetic properties, theoretical *ab initio* study.

### Introduction

Polynuclear compounds of vanadium as well as of other transitional metals are of great interest not only from the theoretical point of view. They can be used as models of metalloproteins of natural enzymatic systems (especially iron complexes) [1]. Moreover they can serve as model systems in studies and development of new molecular magnetic materials [2]. Natural enzymatic systems containing paramagnetic ions have been characterized by their magnetic properties [3] too.

Numerous magneto-structural correlations have been established for the polynuclear complexes (see, for instance [4-8] and references therein). In order to describe these correlations the Heisenberg-Dirac-Van Vleck model of the exchange interactions between metal centers is usually used. Detailed studies of the electronic structure and related properties are not performed. Meanwhile the knowledge of the interactions origin is needed to work out the well-founded theoretical models of the polynuclear magnetic materials and to predict new systems with the wanted properties.

The relatively simple binuclear oxygen bridged compounds can be useful for the elaboration of the magnetic interactions models based on their electronic structure. There are known some theoretical attempts to give the interpretation of the exchange parameters dependence from the Metal-Oxygen-Metal angle values in these compounds [9]. However the suggested in [9] interpretation is based on the crystal-field theory or on the Angular Overlap Model which both are only approximate models of the compounds electronic structure and do not give the base for the adequate exchange interaction theory.

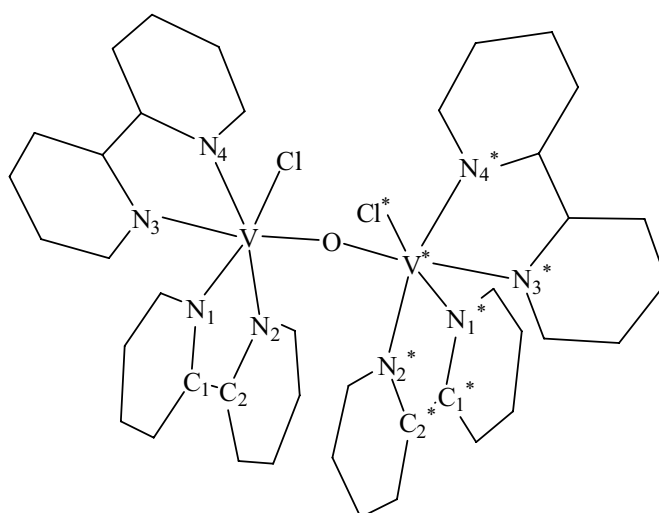


Fig. 1. The system [V<sub>2</sub>O(bipy)<sub>4</sub>Cl<sub>2</sub>]<sup>2+</sup> and atom numbering

For such a task binuclear systems with equivalent magnetic centers can represent a good choice. The simplest case is  $d^1-d^1$  systems but for these complexes the only question that arises is which state is the ground from two possible – singlet or triplet. Much more interesting are  $d^2-d^2$  systems. There can be singlet, triplet and quintet states for these complexes and it is interesting not only which state is the ground one but also what is the order of states and which are their energies and energy gaps between them. From the other point of view these systems are relative simple and easy to study.

The binuclear complex  $[V_2O(bipy)_4Cl_2]^{2+}$  (Fig. 1) was chosen for study in this work. First of all it is a representative of the  $d^2-d^2$  family and there are available experimental magnetic data for this complex to compare results with.

This work goals are the study of the  $[V_2O(bipy)_4Cl_2]^{2+}$  binuclear complex electronic structure and the interpretation of its magnetic properties using the *ab initio* approach.

### Geometry optimization

The  $[V_2O(bipy)_4Cl_2]^{2+}$  complex theoretically may have three different geometrical configurations with the mirror analogues. However only one geometrical configuration given in Fig. 1 was observed in experimental works [10]. In this work this system configuration was initially built and optimized using MM+ methods. In the next step of the optimization the gradient methods realized in PC GAMESS [11] program package was used. Total energy calculations were performed in the ROHF (Restricted Open Hartree - Fock) and UHF (Unrestricted Hartree – Fock) approximations. Geometry optimizations using ROHF method have been carried out for three different spin states ( $S = 2, 1, 0$ ). Process of the optimization using UHF method was converged only for the state with  $S=2$ . For further electronic structure studies there were selected two optimized geometries with lowest energies: one obtained in the UHF optimization and one in the ROHF (both optimized in the states with  $S=2$  and with approximately coincided values of the total energy: -4833.76627647 Hartree (ROHF) and -4833.7689578 Hartree (UHF)).

List of significant parameters both calculated and observed experimentally is given in Table 1. It is seen that geometry obtained after ROHF optimization is satisfactorily good in distances and angles between different parts of molecule. However the dihedral angle  $Cl-V^*-Cl^*$  was calculated to be about  $113^\circ$  while reported experimental value is about  $62^\circ$  [10]. The geometry parameters obtained by the UHF optimization are sufficiently close to that given by X-ray data. Therefore below this conformation will be used in study of the  $[V_2O(bipy)_4Cl_2]^{2+}$  electronic structure.

Table 1

Experimental and calculated values of the geometry parameters

Parameter	$[V_2O(bipy)_4Cl_2]^{2+}$ (ROHF)	$[V_2O(bipy)_4Cl_2]^{2+}$ (UHF)	$[V_2O(bipy)_4Cl_2]^{2+}$ (experimental [10])
$r_{VO}, \text{\AA}$	1.661	1.664	1.787
$r_{VCl}$	2.263	2.150	2.381
$r_{VN_1}$	1.954	1.970	2.126
$r_{VN_2}$	1.924	1.935	2.140
$r_{VN_3}$	2.139	2.142	2.178
$r_{VN_4}$	2.089	2.079	2.106
$r_{VV}$	3.301	3.315	3.568
$\varphi_{VOV^*}, \text{deg}$	166.8	170.2	173.5
$\varphi_{ClVV^*Cl^*}, \text{deg}$	113.4	65.5	61.6
$\varphi_{OVCl}, \text{deg}$	94.0	98.6	100.2

### Electronic structure calculations

Electronic structure studies were performed both using the ROHF method with further taking into consideration CI (Configuration Interaction) and the UHF method. The basis set STO-6G (Slater Type Orbital approximated by 6 Gauss-type orbitals) was used for all calculations. The calculations were carried out for geometry configuration obtained using ROHF as well as for geometry configuration obtained using UHF.

All the UHF calculations were performed for states with spin values equal to  $S=2, 1, 0$ . When the ROHF+CI method was used the active space was selected according to reasons described below.

**One-electron energy levels and molecular orbitals**

Molecular orbitals close to HOMO orbital are given in Table 2. Orbitals below 206 and above 211 are of ligand nature and (or) are placed far away from HOMO orbital.

Table 2

One-electron states considered as active in CI calculations			
No	Sym	Energy	Composition
211	a	-0.0575	<i>Ligand(bipy)</i>
210(LUMO)	b	-0.0581	$-0.11(d_{xy}^V + d_{xy}^{V*}) + \text{Ligand}(bipy)$
209(HOMO)	a	-0.1819	$-0.11(p_x^V - p_x^{V*}) - 0.09p_z^O + \Phi^{bipy} - \Phi^{bipy*}$
208	b	-0.1822	$0.14(d_{xz}^V + d_{xz}^{V*}) - 0.12(p_x^V + p_x^{V*}) + \Phi^{bipy} + \Phi^{bipy*}$
207	b	-0.2292	$-0.40(d_{x^2-y^2}^V - d_{x^2-y^2}^{V*}) + 0.67(d_{z^2}^V - d_{z^2}^{V*}) + 0.25(d_{yz}^V - d_{yz}^{V*})$
206	a	-0.2296	$-0.40(d_{x^2-y^2}^V + d_{x^2-y^2}^{V*}) + 0.67(d_{z^2}^V + d_{z^2}^{V*}) + 0.25(d_{yz}^V - d_{yz}^{V*})$
205	a	-0.4177	<i>Ligand(bipy)</i>

$\Phi^{bipy}$  and  $\Phi^{bipy*}$  in the Table 2 are linear combinations of p-orbitals located on nitrogen and carbon atoms of the bipyridine ligands laying perpendicularly to V-V axis:

$$\Phi^{bipy} = -0.29p_x^{N_1} - 0.28p_x^{N_2} + 0.33p_x^{C_1} + 0.31p_x^{C_2} + \dots$$

$$\Phi^{bipy*} = -0.29p_x^{N_1*} - 0.28p_x^{N_2*} + 0.33p_x^{C_1*} + 0.31p_x^{C_2*} + \dots$$

$C_1$  and  $C_2$  ( $C_1^*$  and  $C_2^*$ ) are two carbon atoms connecting pyridine cycles in the bipyridine molecule (Fig. 1).

In the state with the total spin value equal to  $S=2$  four electronic orbitals beginning with 206 are populated by one electron each. It is seen that two of these molecular orbitals (206 and 207) are composed from the vanadium d-orbitals and two MO (208 and 209) are the combinations of the vanadium p- and d-orbitals as well as of the  $\mu$ -oxygen  $p_z$ -orbital and  $p_x$ -orbitals of the bipyridine ligands perpendicular to V-V axis. In the Fig. 2 these four states are given in picture form.

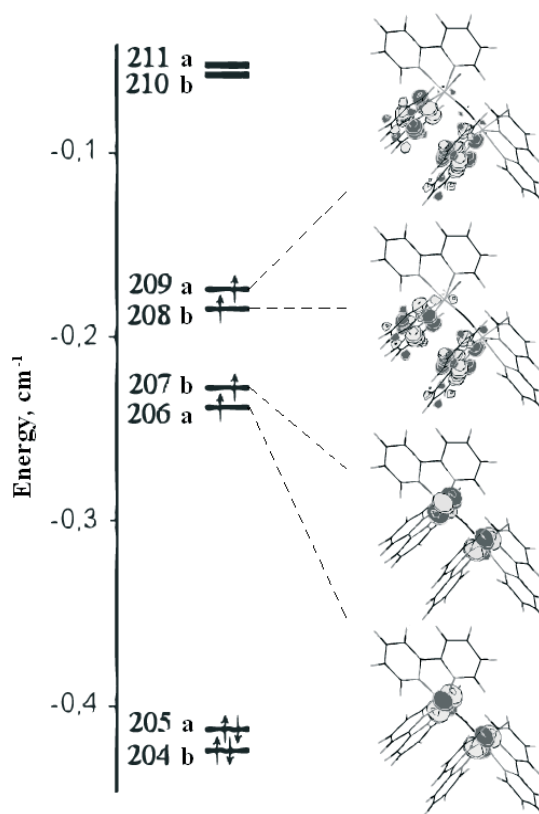


Fig. 2. ROHF one-electron states

### Multielectronic states

According to above discussion only 7 orbitals (from 205 to 211) can be introduced in the active space for the ROHF+CI calculations. In this approximation 7 multielectronic configurations with full spin value  $S=3$ , 140 configurations with  $S=2$ , 588 configurations with  $S=1$  and 490 configurations with  $S=0$  form a basis for the CI calculations.

From our calculations we have obtained ten multielectronic states and lowest of them are given in Fig. 3. The formulas for these multielectronic states are given in Table 3. As it was mentioned above only four one-electron states are participating in forming of the ground and first two excited states.

Table 3

Composition of the lowest multielectronic states in the CI. approximation

State	Term	Formula
2 <sup>nd</sup> excited	<sup>1</sup> A	$0.5\{[206a^2 208b^2] - [207b^2 208b^2] + [207b^2 209a^2] - [206a^2 209a^2]\}$
1 <sup>st</sup> excited	<sup>3</sup> B	$0.5\{[206a^2 208b^{\uparrow} 209a^{\uparrow}] - [207b^2 208b^{\uparrow} 209a^{\uparrow}] + [206a^{\uparrow} 207b^{\uparrow} 208b^2] - [206a^{\uparrow} 207b^{\uparrow} 209a^2]\}$
Ground	<sup>5</sup> A	$[206a^{\uparrow} 207b^{\uparrow} 208b^{\uparrow} 209a^{\uparrow}]$

From the Table 3 and Fig. 3 it is seen that the ground state is the multielectronic state <sup>5</sup>A consisting of one electronic configuration in which two electrons are placed on mainly metal d-orbitals (206 and 207) and two on the hybrid  $dp\Phi^{bipy}$  orbitals (208 and 209). The wave functions of the excited multielectronic states <sup>3</sup>B and <sup>1</sup>A are the linear combinations of different configurations obtained by the respective populations of the same orbitals. It follows that we can imagine the scheme of formation of the molecular orbitals participating in exchange interactions from four localized magnetic orbitals as it is shown in Fig. 4.

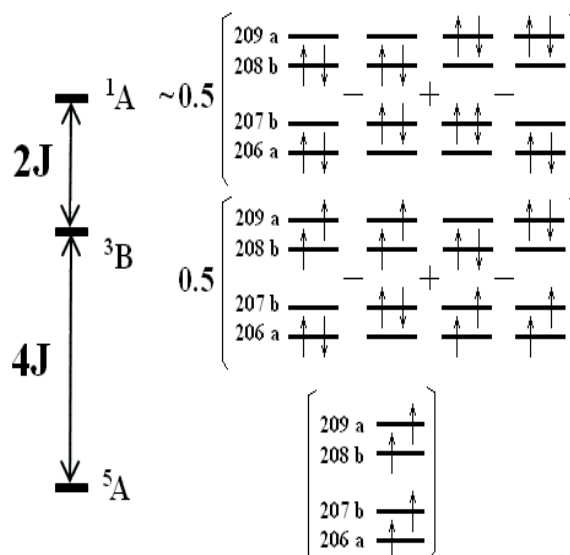


Fig. 3. Multielectronic states schemes (State symmetries are given according to  $C_2$  molecular symmetry group). One-electron states are given beginning with the MO № 206

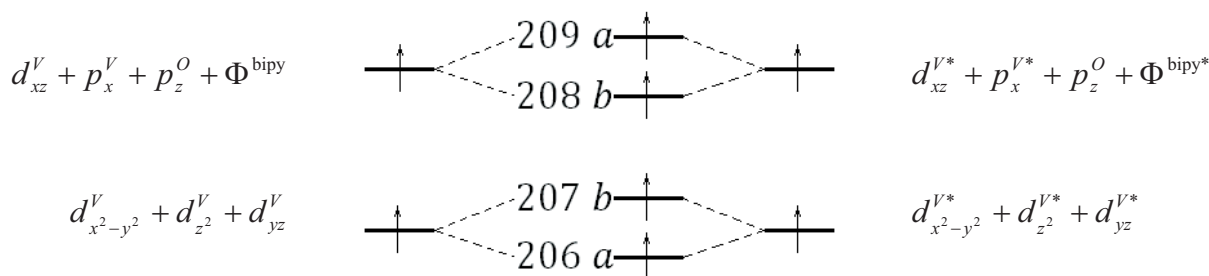


Fig. 4. Localized magnetic orbitals contributing to 206-209 MOs

The exchange interaction in this case is due to superexchange between the electron pairs localized on the vanadium centers through the hybridized metal d- and p-orbitals with the bipyridine and oxygen p-orbitals. This interpretation differs qualitatively from the  $d^2 - d^2$  model served as base for the Heisenberg interpretation of magnetic properties of binuclear systems. ROHF+CI calculation give the order of states with different spin values (Fig. 5) similar to the Heisenberg model (Fig. 5 inserted picture) and even the energy differences between first excited and ground states and second excited and first excited states ratio 4:2 is preserved (according to Lande rule). When carrying out calculations using UHF method it was obtained that ground state is a state with  $S=2$  too but the other UHF calculations results does not coincide with ROHF calculations and Heisenberg model.

Thus in spite of the qualitative difference in interpretation of the exchange interaction origin the intervals between the energy levels satisfy the Lande rule in both approaches and correspond to ferromagnetic interaction of two localized spins ( $S_1=S_2=1$ ). This conclusion confirms the applicability of the Heisenberg model for the magnetic properties interpretation in the considered case.

For the system under consideration the reported experimental value of the exchange parameter [9]  $J$  is less than  $-400\text{cm}^{-1}$  and the ground state is quintet one with total spin value  $S=2$ .

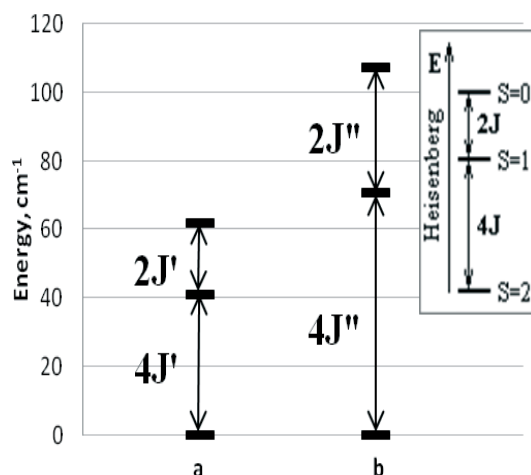


Fig. 5. Multielectronic states spectra obtained in different approximations: a) ROHF+CI, optimized in UHF,  $J' = 10.3 \text{ cm}^{-1}$ ; b) ROHF+CI, optimized in ROHF,  $J'' = 18.0 \text{ cm}^{-1}$

For the calculated values of energies of the ground and excited states (ROHF) we have built plots of dependence of magnetic moment  $\mu_{\text{eff}}$  from temperature  $T$  (Fig. 6). These plots were constructed using well-known formulas (see [7] for instance).

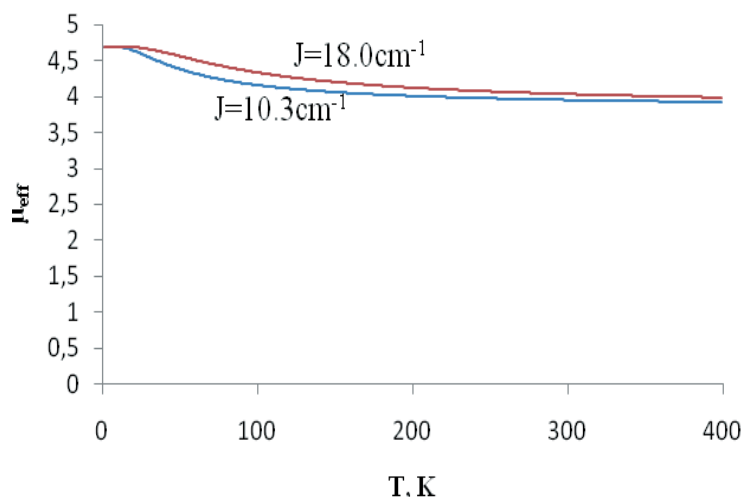


Fig. 6. Calculated dependence of the magnetic moment value from the temperature.  $g=1.915$  [12]

The magnetic moment values for T=293K (room temperature) are  $\mu_J = 3.95\text{BM}$ ;  $\mu_{J,S} = 4.04\text{BM}$ . This is in a good accordance with experimental data for the complex in acetone  $\mu_{\text{eff}, 293} = 3.99\text{BM}$  (2.82BM per vanadium atom) [13]. However calculated plot differ from straight horizontal at  $\mu_{\text{eff}} = 4.48\text{BM}$  (3.17BM per vanadium atom) obtained in [10]. The difference may be because of the solid state effect (measurements in [10] were carried out for the powder form) and/or temperature independent paramagnetism. The value of 4.48BM obtained in [10] is lower than 4.7BM needed for the ground state with S=2 to be the only populated state. This means that the excited state(s) are populated at room temperature too.

### Conclusions

It follows from our calculations that the exchange interaction in the  $[\text{V}_2\text{O}(\text{bipy})_4\text{Cl}_2]^{2+}$  can be envisaged as the superexchange of the V atoms electronic pairs localized on the magnetic orbitals of d- type metal orbitals and of the d- type metal orbitals hybridized with p- orbitals of the bridge oxygen and bipyridine molecules laying perpendicularly to V-V axis. In our calculations we have obtained results which are in accordance with experiment - in studied complex there is a ferromagnetic interaction between centers. The magnetic moment value is predicted with a good adequacy. The *ab initio* study have confirmed the keeping of the Lande rule in energy spectrum of the  $[\text{V}_2\text{O}(\text{bipy})_4\text{Cl}_2]^{2+}$  too.

### References

- [1] Armstrong W.H., Spool A., Papaefthymion G.C., Frenkel R.B., Lippard S.J. *J. Am. Chem. Soc.* 1984, Vol. 106, p. 3653.
- [2] Gatteschi, D. *Adv. Mat.* 1994, Vol. 6, p. 635.
- [3] Dawson J., Gray H.B., Hoenig H.E., Rossmann G.R., Schredder J.M., Wang R-H. *Biochemistry.* 1972, Vol. 1, 3, p. 461.
- [4] Crawford V.H., Richardson H.W., Wassen J.R., Hodgson D.J., Hatfield W.E. *Inorg. Chem.* 1976, Vol. 9, p. 2107.
- [5] Glerup J., Hodgson D.J., Pedersen E. *Acta Chem. Scand.* 1983, Vol. A37, p. 161.
- [6] Weihe H., Güdel H.U. *J. Am. Chem. Soc.* 1997, Vol. 119, p. 6539.
- [7] Kahn, O. *Molecular magnetism*. N.Y. : VCH Publishers Inc., 1993.
- [8] Tsukerblat, B. S. *Group Theory in Chemistry and Spectroscopy. A Simple Guide to advanced Usage*. London : Academic Press, 1994.
- [9] Weihe H., Güdel H.U. *J. Am. Chem. Soc.* 1998, Vol. 120, p. 2870.
- [10] Brand S.G., Edelstein N., Hawkins C.J., Shalimoff G., Snow M.R., Tiekink E.R.T. *Inorg. Chem.* 1990, Vol. 29, pp. 434-438.
- [11] Granovsky, A. PC GAMESS version 7.0. [Online] <http://classic.chem.msu.su/gran/gamess/index.html>.
- [12] Abragam A., Bleaney B. *Electron paramagnetic resonance of transition ions*. Moscow : Mir, 1972. Vol. I.
- [13] Toma H.E., Santos P.S., Lellis F.T.P. *J. Coord. Chem.* 1988, Vol. 18, pp. 307-316.

## ESTABLISHMENT OF THE ANTIOXIDANT/ANTIRADICAL ACTIVITY OF THE INHIBITORS USING THE DPPH – RADICAL

Maria Gonta<sup>a\*</sup>, Gheorghe Duca<sup>b</sup>, Diana Porubin<sup>a</sup>

<sup>a</sup> State University of Moldova, 60 Mateevici str., Chisinau, Republic of Moldova

<sup>b</sup> The Academy of Sciences of Moldova, 1 Stefan cel Mare blvd., Chisinau, Republic of Moldova

\* Corresponding author: Phone: (373 22) 57-75-53, Email: mvgonta@yahoo.com

**Abstract.** This research paper presents the results of the investigation of antioxidant activities of various inhibitors, which are constituents of winery products: quercetin, rezveratrol, dihydroxyfumaric acid. Also, the antioxidant activity of tartaric and dihydroxyfumaric (DFH<sub>4</sub>) acids derivatives has been determined: sodium dihydroxyfumarate, dimethylic ester of DFH<sub>4</sub> and dimethylic ester of tartaric acid. The enotannin extracts obtained from grape seeds have been evaluated: the non-oxidized enotannin extract *Eneox* and the oxidized one *-Enoxil*. For the determination of the antioxidant/antiradical activity the 2,2-diphenil-1-picrylhidrazil (DPPH) radical was used, which has the absorption maxima at 517 nm. The efficient concentration EC<sub>50</sub>, the stoichiometric value of the antioxidant and the free radical, the antiradical power (1/EC<sub>50</sub>) and the number of moles of DPPH-radical reduced by one mole of inhibitor have been calculated for all investigated inhibitors. It was found that catechin, quercetin and DFH<sub>4</sub> exhibit the highest inhibition rate.

**Keywords:** antioxidant activity, DPPH radical, inhibition rate, natural inhibitors from secondary winery materials

### Overview

Numerous practical and epidemiological studies have confirmed that the micronutrients, thus the antioxidants existing in aliments, are able to inhibit the cancerigenesis through their influence on the molecular level, during the initiation, promotion and progression stages.

In recent times, the most studied compounds were the polyphenols, which are constituents of the plants.

The antioxidant activity of the polyphenols is controlled by the presence of the hydroxylic groups in the B ring in 3' and 4' positions and in a lesser degree, by the presence of the hydroxylic group from the C ring in 4' position.

The flavonols, especially catechin, quercetin, kaempherol and their glucosides are elements of the black and green teas [5] and red wine [5]. The diets rich in vegetables and fruits, especially in grapes, protect against heart diseases, various forms of cancer [7, 8], methemoglobinemy, and display anti-inflammatory, as well as antimutagenic effects [9]. These protective upshots were attributed, in a great measure, to the antioxidants that include flavonoids as well as carotenoids and vitamins C and B.

The majority of the polyphenolic constituents from products (flavonols – like quercetine and kaempherol, flavones – like luteolin, flavonones – like catechin, anthocyanidin, for example, cyanidin and malvidin and their glycosides) presents high efficiency, in comparison to the nutrient antioxidants: vitamins C, E, β-carotene, that are easily adsorbed in the intestines [10].

The grapes and the wine contain high concentrations of antioxidants. Based on the study of the overall antioxidant activity of the red wine, we concluded that 54,76% is determined by the contribution of catechin and epicatechin, that form approximately 63,54% of the phenolic constituents (191 and 82 mg/l, correspondingly) [10].

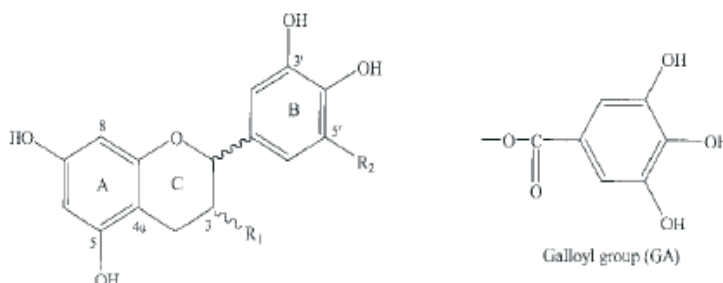


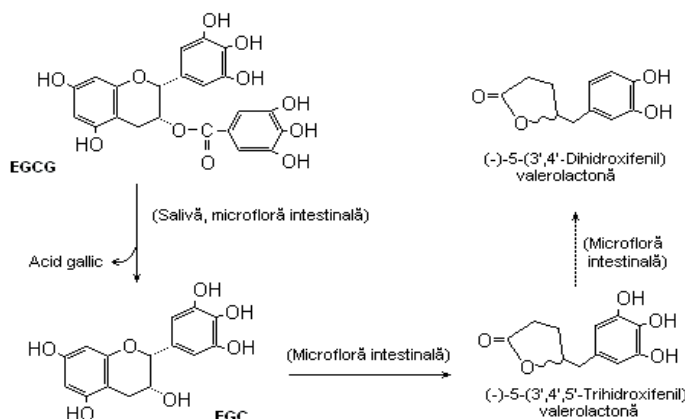
Fig.1. Chemical structure of the catechins present in tea and wine [5]. Catechin-(R<sub>1</sub> - OH, R<sub>2</sub> - H), gallocatechin-(R<sub>1</sub> - OH, R<sub>2</sub> - OH), catechingallate (R<sub>1</sub> - GA, R<sub>2</sub> - H), gallocatechingallate (R<sub>1</sub> - GA, R<sub>2</sub> - OH)

The presence of the orto-dihydroxylic groups in B ring pointed to catechins capacity to scavenge the radicals [1]. Addition of the gallate-grouping in the 3<sup>rd</sup> position of C ring of the catechins increases the scavenging effect of the radicals. The major metabolites of (-)-epicatechin (EC) and of (+)-catechin, spotted within plasma after the oral administration are (-)-epicatechin-5-o- $\beta$ -glucuronide and (+)-catechin-5-o- $\beta$ -glucuronide [2]. These joined conjugated glucuronides showed a scavenging effect of the radicals, similar to initial substances, since the orto-dihydroxylic grouping in the 3'- and 4'- positions from B ring were not substituted. And on the contrary, metylation in 3'- position of the hydroxyl group of B ring, with the formation of 3'-o-metyl(-)-epicatechin-5-o- $\beta$ -glucuronide and 3'-o-metyl(+)-catechin-5-o- $\beta$ -glucuronide led to the decrease of super oxides' scavenging activity.

Epigallocatechin-gallate metabolites (EGCG) exercise antioxidant effects, similar to their non-conjugated compounds and which are determined by the presence of di- or trihydroxyl groups in B ring or the component gallate group. The metabolites isolated and found out in urine, (-)-5-(3',4',5'-trihydroxyphenyl)- $\gamma$ -valerolacton and (-)-5-(3',4'-dihydroxyphenyl)- $\gamma$ -valerolacton possess anti-oxidant properties [3]:

Catechins and polyphenols are efficient scavengers of the free radicals in various in vitro systems. The capacity of the compounds to scavenge the radicals is partially determined by the reduction potential of one electron, which is a measure of antioxidants reactivity, as donors of hydrogen or oxygen [4]. A low reduction potential proves the fact that less energy is squandered in order to donate hydrogen or electron and is an influencing factor in the antioxidant activity.

Based on table 1, we concluded that EGCG (0,43 V) and EGC (0,43 V) have [17] a lower potential than



vitamin E (0,48 V), fact suggesting that they are donors of electrons, more active than vitamin E [5]. However, vitamin C displayed a significantly lower potential of reduction (0,28 V) than all the polyphenols.

Additionally to the hydrogen or in the electron donation activity, the efficiency of the antioxidants is determined, as well by the speed of their interaction with the free radicals that are introduced into the system (constant of scavenging speed) and the stability of the formed antioxidant radical.

Taking into account the study of pulse radiolysis, which allows the comparison of the reactivity of a series of flavonoids with hydroxyl radical ( $\cdot$ OH), super-oxide anion ( $\cdot$ O<sub>2</sub><sup>-</sup>) and azid radical ( $\cdot$ N<sub>3</sub>), Bors and Michel [6] conclude that the catechins are superior agents of radicals scavenging, in comparison with the monomeric flavonols and flavones, representing the most essential anti-oxidants of the red wine and tea.

Table 1

Reduction Potential and Antioxidant Activity of the Inhibitors

Antioxidant	Reduction Potential (pH 7, 20°C)	Antioxidant Activity, mM TEAC
(-)-Epicatechin	0,57	2,4 ± 0,02
(-)-EGC	0,43	3,8 ± 0,06
(-)-ECG	0,53	4,9 ± 0,02
(-)-EGCG	0,43	4,8 ± 0,02
TeaFlavin	0,51	2,9 ± 0,08
TeaFlavin digallate	0,54	6,2 ± 0,43
Green tea (1 ppm)	-	3,8 ± 0,03
Black tea	-	3,5 ± 0,03
Vitamin E	0,48	1,0 ± 0,03
Vitamin C	0,28	1,0 ± 0,02

Therefore, the degree of polymerization that increases together with galloylation has a great influence upon the inhibitory features of the polyphenols. The polyphenolic fractions extracted from the grapes with various degrees of polymerization had a different antioxidant/antiradical and antiproliferative effect [6]. The polyphenol solutions extracted from grapes were divided with RP-HPLC into two fractions having different degrees of polymerization. The antioxidant/antiradical activity determined via DPPH test was higher for the polyphenolic fraction from grapes, composed of small monomers and oligomers, if compared to the fraction that included flavonols and procyanidin oligomers, having a great molecular mass.

The grasping activity of catechin radicals from tea was tested for different in vitro systems. The study of catechin antiradical activity setting via spectrometric method (RES) proved the efficiency of scavenging the singlet oxygen ( $^1O_2$ ),  $O_2^{\cdot-}$ ,  $\cdot OH$  and the peroxy radical  $HO_2^{\cdot}$  [7,9].

Through the radiolytic generation of species of reactive oxygen, in presence of various catechins, which are active constituents of the tea, we spotted that DNA damage, produced by these reactive particles, decreases predominantly in presence of EGCG [11]. Hence, 66% from the antioxidant activity of the green tea is determined by epigallocatechin and epigallocatechin-gallate, fact that is in compliance with the content of these compounds from the green tea (20,44% out of 26,71% of overall polyphenols). In a great part of the analyzed systems, EGCG was a better radical grasper than ECG, EGC or EC, for the reason that the trihydroxyl group from B ring and gallate component in the 3<sup>rd</sup> position of C ring amplifies the catechins antioxidant activity in various systems.

The watery extracts from *Peumus boldus* leaves contain catechin and alkaloids in a proportion of 37:1 and are used in hepatic infections. The antioxidant activity of these extracts is determined via DPPH $\cdot$  test and is due to the catechins content [28], which is much higher than the alkaloids content.

Additionally, there were investigated the extracts obtained from aromatic and medicinal plants (sage, lavender, calendula, echinacea, etc.) through the application of DPPH $\cdot$  test and ABTS [29]. These extracts, especially *Salvia officinalis*, have a very high free radicals scavenging activity. We noticed the correlation between extracts anti-radical activity and the total content of phenolic compounds.

Stable radicals, such as 1,1-diphenyl-2-picryl-hydrazyl (DPPH $\cdot$ ) radical and ABTS $^{+\cdot}$  cation-radical (2,2-azino-bis-3-ethylbenzthiazoline-6-sulphonic acid) are used for the assessment of flavonoids in vitro antioxidant activity. The use of the Trolox equivalent antioxidant activity test (TEAA) demonstrated that the catechin and TeaFlavin are more efficient in ABTS $^{+\cdot}$  cation-radical reduction than vitamins E and C [10]. Rice-Evans and others [10] studied the total antioxidant activity (TAA) and Trolox equivalent antioxidant activity (TEAA) for the polyphenols that are contained in the green and black tea and in the red wine.

TEAA measures the concentration of Trolox solution (mM) with an antioxidant potential, equivalent to a standard concentration of the compound under study.

The authors stated that the antioxidant activity of the polyphenolic constituents of the green tea (**Fig.1**), in correlation with their content in the consecutiveness of antioxidant activity diminution is as follows: epigallocatechin (34%)  $\approx$  epigallocatechingallate (32%)  $\gg$  epicatechingallate (7%)  $\approx$  epicatechin (6%)  $>$  catechin (1%) [10].

The catechins were more efficient in the scavenging of the DPPH radical, according to the series: EGCG $\approx$ ECG $>$ EGC $>$ EC [7,8]. Thus, we conclude that we obtained similar results via both methods (test with radical DPPH $\cdot$  and cation-radical ABTS $^{+\cdot}$ ).

The overproduction of nitrogen oxide (II) and of peroxynitryl (ONOO $\cdot$ ), result of the swift interaction between  $O_2^{\cdot-}$  and  $\cdot ON$ , is well-associated with severe inflammations and might be related with the etiology and pathology of chronic diseases.

The researches carried out in vitro outlined the antioxidant potential of the polyphenols as a parameter that determines the scavenging capacity of the free radicals, as for example, super oxides radicals ( $O_2^{\cdot-}$ ), the singlet oxygen ( $^1O_2$ ), the hydroxyl radical ( $\cdot OH$ ), peroxy radical ( $HO_2^{\cdot}$ ), nitrogen monoxide ( $\cdot ON$ ) and peroxynitrite (ONOO $\cdot$ ), which in their turn, are the causes of various pathologies. The chemical structures that contribute to polyphenols antioxidant activity, including the dihydroxy- or trihydroxy-neighbouring structure, can chelate the ions of metal, forming the complexes and preventing the creation of free radicals. This structure also allows the delocalization of the electrons, offering a higher reactivity of free radicals destruction.

There has been proved that the flavonoids, including the catechins, are efficient in scavenging  $\cdot NO$  in vitro [11]. The green and black teas displayed the property of scavenging  $\cdot NO$  in vitro, although the green tea was five times stronger than the black one [12]. The inhibition of tyrosine nitroization was searched as a pattern of ONOO $\cdot$  scavenging activity by flavonoids. In this test, the catechins of the tea were much more effective than vitamin E. EGCG, ECG and

the gallic acid manifested equal properties of inhibition during the process of tyrosine nitroization, but which were higher than EGC and EC, thus implying that the gallate component was the crucial structure in the interaction with ONOO<sup>-</sup>. Additionally, EGCG manifested stronger inhibitory properties in the formation of 8-OHdG, which is the product of the interaction between the active species of nitrogen (ONOO<sup>-</sup>) and DNA, than vitamin C and glutathione [13]. The exact mechanism of the inhibitory activity is unknown, but it seems that several structures are crucial in the establishment of this activity. All the catechins have the dihydroxylic group (o-3',4'-OH) in B ring that participate in the delocalization of the electron and the fixing of the radical form [14]. The gallo catechins (EGC and EGCG) have the trihydroxylic group in B ring (3',4',5'-OH), while the catechingallates (EGC and EGCG) have the gallate component esterified in the 3<sup>rd</sup> position of C ring and 3 hydroxyl groupings. The gallate component, together with the 3 hydroxyl groupings (3', 4', 5'-OH) is associated with the augmentation of the antioxidant activity [7]. The researches made in the domain of products oxidation with peroxy radical (HO<sub>2</sub><sup>·</sup>) in presence of gallo catechins stated that 3',4',5'-OH grouping from B ring is the principal position in the antioxidant property of EGC and EGCG [15,16].

In different systems, the free radicals can be formed as a result of hydrogen peroxide decay in presence of various metals: Fe<sup>2+</sup>, Cu<sup>2+</sup>, Cr<sup>3+</sup>, etc. As a consequence of H<sub>2</sub>O<sub>2</sub> reduction through Fenton reaction in presence of Cr<sup>3+</sup> (which is toxic and causes genotoxicity), OH<sup>·</sup> radical is being formed:



The hydroxyl radical formed in vivo starts DNA oxidative damage with the formation of 8-hydroxy-2-deoxyguanosine (8-OH-dG), which serves as a biomarker in this process [12].

In the result of the study, Silvia Lopez-Burillo et al. [12] concluded that the antioxidants inhibit DNA oxidative processes. Among the studied polyphenols [12], the highest inhibitory effect belongs to (-)-epigallocatechin-3-gallate (EGCG) in a concentration of 1 μM and more, and which reduces the formation of 8-OH-dG. The catechins of the tea can form stable complexes with Cu(II) and Cr(III) and as a result, there occurs the formation of OH<sup>·</sup> radicals [13]. It was established that in the case of EGCG, OH<sup>·</sup> radicals are separated from gallate grouping existing in complex and therefore, the pro-oxidant effect of this compound is not displayed [14].

The green and black teas are able to inhibit the oxidation of the lipoproteins induced by Cu<sup>2+</sup> [13], contributing to the prevention of arteriosclerosis and other heart diseases. The inhibition of this process is determined by the fact that the polyphenols can chelate metals, decreasing the concentration of the active forms of the oxygen, which in its turn takes part in the proteins oxidation.

Anthocyanidins and catechins have been tested in vitro for the inhibitory activity on cyclooxygenase enzymes (COX) that enhance the augmentation of the carcinogen cells and influence upon the proliferation of human cancer cells [5]. It was established that cyanidin (having 3',4'-dihydroxylic groupings in B ring) has the greatest inhibitory effect among COX. The inhibitory activity decreased for delphinidin and pelargonidin, both having 3',4',5'-trihydroxylic and 4'-hydroxylic groupings in B ring. From the point of view of the link between structure and activity, the number and the position of the hydroxylic groupings within B ring of anthocyanidins influence the inhibitory activity of these compounds. For catechin, cis-, trans-isomerism and epimerization did not influence significantly the inhibitory activity of COX enzymes, but the presence of galloyl groupings in the structure of the catechins influenced their inhibitory activity on COX enzymes. Based on the results obtained during the inhibition of cancer cells proliferation under the influence of anthocyanidins and catechins, there was set that the degree of inhibition is higher for galloyl derivations of catechins [5] (gallo catechin – 95%, epigallocatechin – 100% and gallo catechingallate – 97%), while for anthocyanidins it is approximately 75%.

Certain natural colorants can be important nutritional antioxidants and their presence in the food can also reduce the risk of cancer and heart diseases [19-21]. Several researches were based on the study of such natural colorants as carotenoids, anthocyanidins and curcuminoids, that displayed antioxidant, anti-inflammatory, anti-viral, anti-cancerous properties and anti-tumour effects [22,23]. Betalains are essential natural colorants to be found in the red beet. The latest studies [24, 25] demonstrated that betalains from the beet have higher antiradical effect and antioxidant activity than carotenoids. The inhibitory concentration IC<sub>50</sub> of the betanine for proteins oxidation with a lower density is superior to that of the catechin, i.e. the betanine has a higher antioxidant activity than (+)-catechin.

Although the betalains (betanine, betaxantine, iso-betain, amarantine) are not flavonoids, they contain o-diphenol-monoglicosidic group and amino-grouping, manifesting very well the electro-donor properties [25]. Betalain molecules are very good electrons donors, because they contain hydroxyl (-OH) groups, amino-groupings (=NH) and tiolic (-SH) groups.

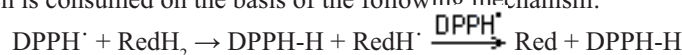
The antioxidant/antiradical activity for various betalains depends on the chemical structure and augments

together with the number of hydroxyl groups and amino-groups from molecule, while the glycosylation reduces their antiradical activity [26].

The uric acid is a grasper of free radicals within biological systems [27].

### Assessment methods of antioxidant/antiradical activity of the inhibitors via DPPH<sup>•</sup> test

There was studied the antioxidant/antiradical activity of various inhibitors: quercitine (Qu), resveratrol (Resv), dihydroxyfumaric acid (DFH<sub>4</sub>), dimethyl ester of dihydroxyfumaric acid (EDMD) and extracts of grapes seeds (Eneox – enotainin non-oxidized extract, ENXIL and ENX – oxidized extracts). In this regard, we studied DPPH<sup>•</sup> test, which includes the establishment of the variation of the DPPH<sup>•</sup> radical concentration, as a result of its interaction with antioxidant components. The application of DPPH<sup>•</sup>-radical (2,2-diphenyl-1-picryl-hydrazyl) (**Fig.1**) allows to determine the antioxidant/antiradical activity of pure compounds and of extracts from vegetal products according to the variation of DPPH<sup>•</sup> concentration, which is consumed on the basis of the following mechanism:



The ability of the compound to scavenge radicals is governed by their property to yield electrons or hydrogen, thus, it depends upon the potential of reduction of the antioxidants. The lower the reduction potential, the more active the antioxidant (Tab.1).

During the research, we determined the antiradical activity of the antioxidants, based on the DPPH<sup>•</sup> concentration variation in alcoholic solution (75%). The absorbance decrease was determined at  $\lambda=517$  nm, at 1, 5, 10 min, during two hours. Almost in all the cases, we could obtain zero kinetic curve (without antioxidant), fact underlining DPPH<sup>•</sup> concentration variation in time. We studied DPPH<sup>•</sup> radical concentration variation for every antioxidant, depending on the reducer's concentration. Afterwards, we calculated DPPH<sup>•</sup> residual concentration (%) depending on time and we elaborated the kinetic curves. The outcomes of the kinetic behaviour of the reducer are presented in Fig.2.

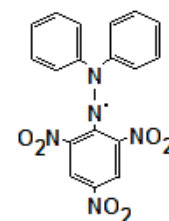
The evolution of the kinetic reactions depends on the nature of tested antioxidants. In this context, there are three types of behaviour [18]: (i) swift kinetic behaviour, in which the reaction time,  $t < 1$  min, (ii) intermediary kinetic behaviour ( $5 < t < 30$  min), (iii) slow kinetic behaviour, when the reaction takes place from 1 h to 6 h and more. Fig.2 shows the kinetic curves according to DPPH<sup>•</sup> percentage variation in time. We consider that Resv (a) interacts quickly. The reaction finishes within a minute, passing into a stationary state. Therefore, the resveratrol can be classified as an antioxidant that participates in reaction with the radicals, according to a swift kinetic behaviour. Other inhibitors can be classified as belonging to the intermediary kinetic behaviour type.

According to the method used in [18] the anti-radical activity was assessed based on the percentage of remained DPPH<sup>•</sup>, at the stage when the kinetic curve does not vary in time any longer. The antiradical activity (ARA) was defined as the quantity of antioxidant necessary for the decrease of DPPH<sup>•</sup> initial concentration with 50% and was called efficient concentration CE<sub>50</sub> (mol/L antiox./mol/L DPPH<sup>•</sup>).

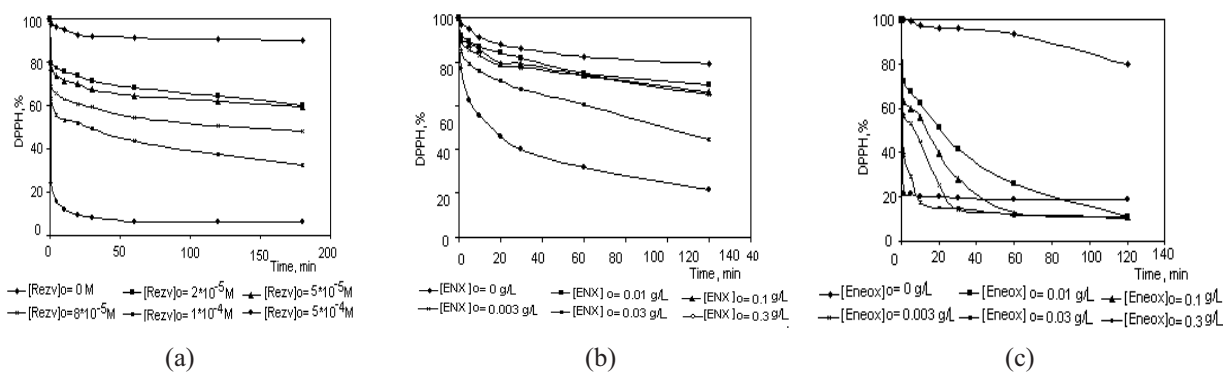
### Findings and Debates

#### The practical study of the antioxidant/antiradical activity via DPPH<sup>•</sup> - radical test

Based on the investigational data (Fig.2) we fixed that the concentration of DPPH<sup>•</sup> is stable for all antioxidants, when setting  $t=120$  min. Thus, taking into account all these data, we issued the diagram of concentration dependence (%) on DPPH<sup>•</sup> at 120 min, in correlation with the molar report of the antioxidant and DPPH<sup>•</sup> (Fig.3)



The chemical structure of the DPPH radical



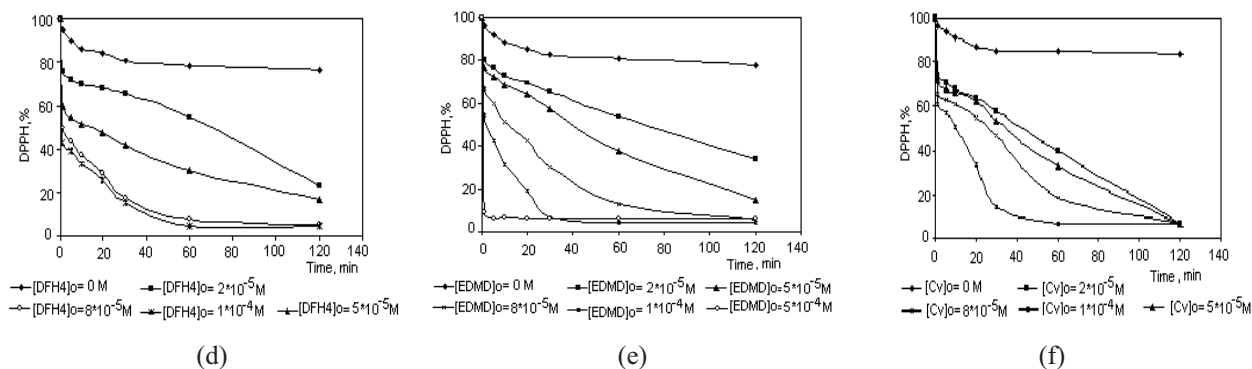


Fig. 2. The kinetic curves of DPPH<sup>·</sup> consumption at the interaction with: (a)-Resv; (b)-ENOXIL; (c)-Eneox; (d)- DFH<sub>4</sub>; (e)-EDMD; (f)-Qu; in alcoholic solutions of 75%; [DPPH<sup>·</sup>]=5·10<sup>-5</sup> M

The data obtained for CE<sub>50</sub> are presented in Tab.2. Based on the empirical results, we noticed that the lowest CE<sub>50</sub> was characteristic for Eneox (CE<sub>50</sub><sup>Eneox</sup>=0,14) while the highest - for Resv (CE<sub>50</sub><sup>Resv</sup>=1,7). Another more distinctive peculiarity of the antiradical activity of the reducers is the antiradical power (ARP), which is to be determined as the opposite mass of CE<sub>50</sub> (1/CE<sub>50</sub>). According to the data displayed in Tab. 2, ARP vary between 2,0 – 12,5, for the studied antioxidants. The lowest ARP was established for Resv (2,0), and the highest is peculiar for Eneox (12,5). ENX extract has an ARP<sub>Enx</sub> equal to 6,7.

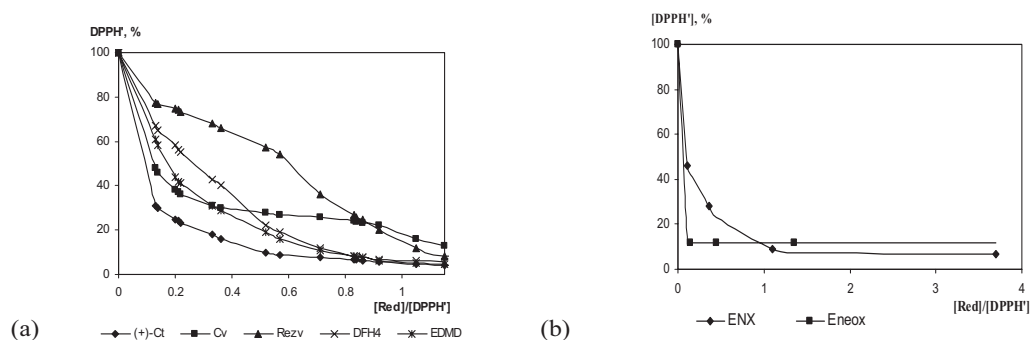


Fig.3. DPPH<sup>·</sup> Concentration Dependence (%) on the molar report [Red]/[DPPH<sup>·</sup>]: (a) (+)-Ct, Qu, Resv, DFH<sub>4</sub>, EDMD; (b) ENX, Eneox

The stoichiometric value equal to CE<sub>100</sub>, determined via CE<sub>50</sub> multiplication by two, forms the efficient concentration needed to reduce one 100% of DPPH<sup>·</sup>. In this case, the classification of the antiradical efficiency will be incorrect, for the compounds that have a slow kinetic behaviour, because the reaction might not reach the end.

The stoichiometric value that varies within 0.2-1.0 limits is presented in Tab.2 for all the studied reducers. We also calculated the opposite amount of CE<sub>100</sub> (1/CE<sub>100</sub>), that determines the number of DPPH<sup>·</sup> mols from which 1 mol of reducer can be cut.

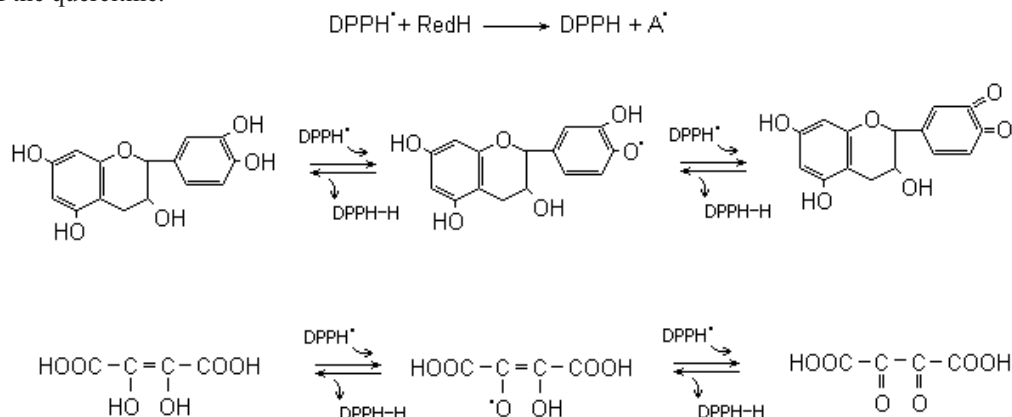
Table 2

Classification of the antiradical efficiency, in compliance with the kinetic behaviour

Kinetic Behaviour	Compounds	Efficient CE <sub>50</sub> Concentration	CE <sub>50</sub> x2 Stoichiometric Value	ARP (1/CE <sub>50</sub> )	Nr. of mols DPPH <sup>·</sup> reduced (1/CE <sub>100</sub> )
Fast Kinetic Behaviour (1 min)	Resveratrol	0,5	1,0	2,0	1,0
Intermediary Kinetic Behaviour (5-30 min)	ENX	0,15	0,3	6,7	3,3
	Eneox	0,08	0,16	12,5	6,25
Slow Kinetic Behaviour	Quercitine	0,1	0,2	10,0	5,0
	(+)-Catechin	0,1	0,2	10,0	5,0
	DFH <sub>4</sub>	0,1	0,2	10,0	5,0
	EDMD	0,15	0,3	6,7	3,3

According to the data obtained in Tab.2 for the compounds that have an intermediary kinetic behaviour,  $1/CE_{100}$  coincides with the number of hydrogens or hydroxyl groups, available for donation. For quercetin, (+)-catechin,  $1/CE_{100}$  is approximately 2; thus, a molecule of (+)-catechin reduces 2 molecules of DPPH $\cdot$ , fact that corresponds to the number of hydroxyl groups participating in the reduction process, shown in the scheme below.

We calculated  $1/CE_{100}$  for resveratrol, and we established that three molecules of Resv reduce one molecule of DPPH $\cdot$ . Taking into consideration the structure formula of the Resv, we might state that dihydroxy-grouping is lacking, i.e. there are no neighbouring dihydroxylic groups. Hence, in this case, the mechanism of radicals' removal is different from the compound that contains dihydroxylic or trihydroxylic groups. The antiradical activity of (+)-catechin is lower than that of the quercetine.



The stoichiometric value calculated for DFH $_4$  is 0,8, while the number of DPPH $\cdot$  mols reduced by a molecule of DFH $_4$  is equal to 1,25, though the number of hydroxylic groupings is two.

We established the degree of inhibition (%) of DPPH $\cdot$  - radical, according to the formula [29]:  $ID = [A_{control} - A_{test}] \cdot 100 / A_{control}$ , where  $A_{control}$  - is control absorbance (solution of DPPH $\cdot$  without reducer) and  $A_{test}$  - is the absorbance of the tested sample (solution of DPPH $\cdot$  and reducer).

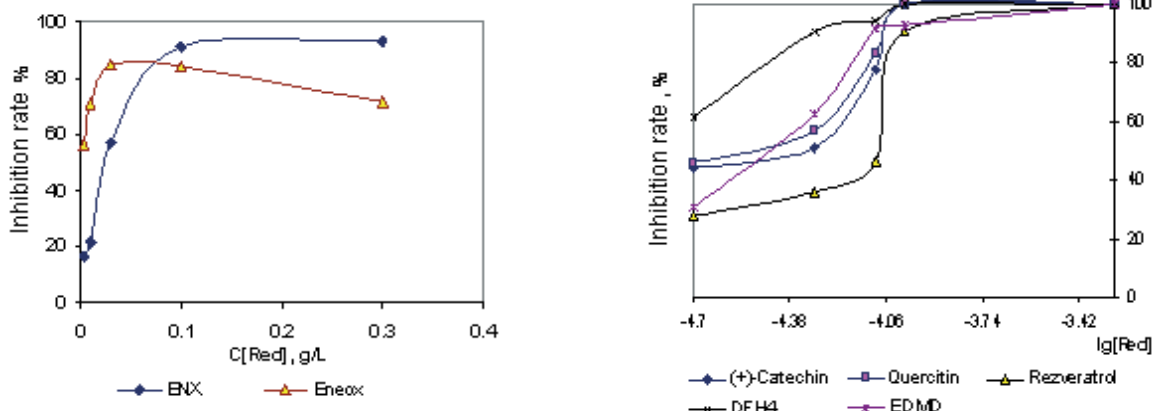


Fig. 4. ID at  $t=30$  min depending on the concentration of the studied inhibitors

We found out that the inhibition degree (ID) increases together with the augmentation of the reducers' concentration within the interval of  $2 \cdot 10^{-5} - 5 \cdot 10^{-4}$  M.

In case of the interaction between DPPH $\cdot$  radical and DFH $_4$ , Qu, (+)-Ct, for the interval of concentrations  $2 \cdot 10^{-5} - 1 \cdot 10^{-4}$  M, there is a higher variation of the ID (~30-90%), and when  $[Red]_0$  increases  $> 1 \cdot 10^{-4}$  M, the ID varies insignificantly.

Dimethyl ester of dihydroxyfumaric acid and ENX (enotanin oxidized extract of grapes seeds) interacts slower with DPPH $\cdot$  and ID varies from ~20% to ~70% for the interval  $2 \cdot 10^{-5} - 1 \cdot 10^{-4}$  M, and due to ongoing increase of  $[Red]_0$  to  $5 \cdot 10^{-4}$  M, ID reaches ~90% in respect to the control. For resveratrol, the augmentation of ID during the first interval of concentrations of Red, is the most insignificant (~20-35%), and further on at  $5 \cdot 10^{-4}$  M reaches 90%. In the case of Eneox (enotanin non-oxidized extract from grapes seeds), DPPH $\cdot$  radical, in small quantities is wasted most rapidly. For  $C_{red} = 2 \cdot 10^{-5}$  M there is an ID=50%. ID correlates positively with  $1/CE_{100}$  calculated for these reducers (Tab. 2).

The greatest number of DPPH molecules is reduced by Eneox (6.25), further on Qu (+)-Ct, DFH $_4$  has  $1/CE_{100}$  equal to 5, EDMD and ENX - 3.3, and Resv reduces the smallest number of DPPF molecules (1,0).

Comparing the ID of the reducers (Fig.5) for  $[\text{Red}]_0 = 1 \cdot 10^{-4} \text{ M}$ , we find out that  $\text{DFH}_4$  has the greatest ID (94%), while Resv, the lowest - (46%).

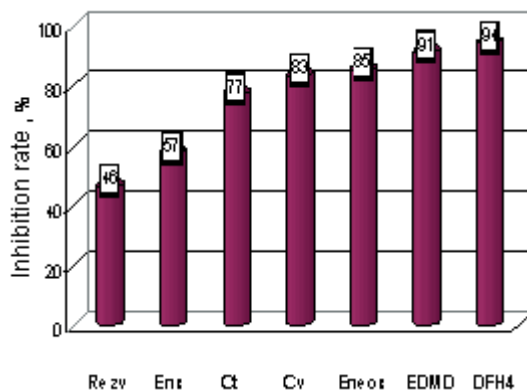
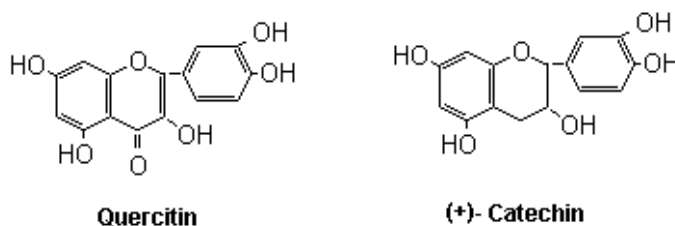


Fig. 5. ID in f (Red), for  $[\text{Red}]_0 = 1 \cdot 10^{-4} \text{ M}$

Resveratrol has a lower inhibitory activity because it is a monofenol, i.e. does not contain o-dyfenol grouping. The position of the second or third hydroxylic group is essential [30]. Those compounds, in which the second hydroxylic group is in orto- or para-position, have a higher activity than in meta-position [18].

Hence, we established that (+)-Ct, Qu have a higher grasping activity of the radicals, if compared to resveratrol, since (+)-Ct and Qu contain dihydroxylic group. Eneox extract, which contains galocatechin, has the trihydroxylic group, that is why, its anti-radical activity is higher ( $\text{EC}_{50} = 0.08$ ).

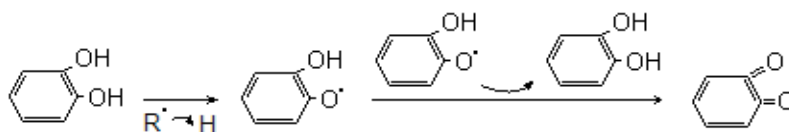
If we compare (Fig.5) the antiradical activities of (+)-Ct and Qu, we notice that ID is higher for Qu (83%). The difference of the chemical structure between Qu molecule and (+)-Ct is determined by the double liaison 2,3 in conjugation with 4-oxo in C ring, responsible for the delocalization of the electrons from B ring. Similarly, groups 3 and 5-OH from A ring, together with 4-oxo group from C ring, increase the antiradical activity of Qu, if compared to that of (+)-Ct [33].



These structural aspects of flavonols (Qu) due to which they differ from flavonones (Ct), assures a higher antiradical activity.

On one hand, the efficiency of orto- and para-diphenols is connected with aryl-oxyl radical fixation by the hydrogen link or the regeneration of a diphenol molecule [30]:

Cuvelier [30] and Shahidi [31] studied the influence of the orto-metoxi substitution and deduced that ariloxy radical is made stable through electron donation [32] and consequently, the antioxidant/antiradical efficiency increases.



Based on the experimental data presented in Fig.5, we presume that for Eneox ID is the highest, in the case of small concentrations, and together with the increase of  $C_{\text{Eneox}} > 1 \cdot 10^{-4} \text{ M}$ , ID decreases.

Bors [33] suggested the idea that sometimes the stability of the flavonoid ariloxy radical is doubtful and might produce pro-oxidant effects. This effect could be explained by the formation of arbitrary liaisons that are unexpected in the case of antioxidants concentration augmentation, which in its turn decrease inhibitor's ID.

We obtained the highest degree of inhibition for  $\text{DFH}_4$  at  $C_{\text{DFH}_4} = 1 \cdot 10^{-4} \text{ M}$ . The presence of the  $-\text{C}(\text{OH})=\text{C}(\text{OH})-$  group assures a higher donation capacity of hydrogen and afterwards, the stability of the created radical. The reducing potentials of the inhibitors are inversely proportional to the donation power of electrons. The carboxyl group has a greater impact on the electrophile features.

## References

- [1] Nanjo F., Mori M., Goto K., and Hara Y., Radical scavenging activity of tea catechins and their related compounds, *Biosci. Biotechnol. Biochem.*, 1999; 63:1621–1623.
- [2] Harada M., Kan Y., Naoki H., et al., Identification of the major antioxidative metabolites in biological fluids of the rat with ingested (+)-catechin and (-)-epicatechin, *Biosci. Biotechnol. Biochem.*, 1999; 63:973–977.
- [3] Li C., Lee M. J., Sheng S., et al., Structural identification of two metabolites of catechins and their kinetics in human urine and blood after tea ingestion, *Chem. Res. Toxicol.*, 2000; 13:177–184.
- [4] Halliwell B. and Gutteridge J. M. C., *Free Radicals in Biology and Medicine*, 3rd ed., New York: Oxford University Press, 1999.
- [5] Jovanovic S. V., Steenken S., and Simic M. G., Reduction potentials of flavonoid and model phenoxyl radicals, *J. Chem. Soc. Perkins Trans.*, 1996; 2:2497–2503.
- [6] Bors W., and Michel C., Antioxidant capacity of flavanols and gallate esters: pulse radiolysis studies, *Free Radic. Biol. Med.*, 1999; 27:1413–1426.
- [7] Nanjo F., Mori M., Goto K., and Hara Y., Radical scavenging activity of tea catechins and their related compounds, *Biosci. Biotechnol. Biochem.*, 1999; 63:1621–1623.
- [8] Guo Q., Zhao B., Shen S., Hou J., Hu J., and Xin W., ESR study on the structure-antioxidant activity relationship of tea catechins and their epimers, *Biochim. Biophys. Acta*, 1999; 1427:13–23.
- [9] Zhao B., Guo Q., and Xin W., Free radical scavenging by green tea polyphenols, *Methods Enzymol.*, 2001; 335:217–231.
- [10] Rice-Evans C. A., Miller N. J., and G. P., Antioxidant properties of phenolic compounds, *Trends Plant Sci.*, 1997; 2:152–159.
- [11] Haenen G. R. and Bast A., Nitric oxide radical scavenging of flavonoids, *Methods Enzymol.*, 1999; 30 :490–503.
- [12] Paquay J. B., Haenen G. R., Stender G., Wiseman S. A., Tijburg L. B., and Bast A., Protection against nitric oxide toxicity by tea, *J. Agric. Food Chem.*, 2000; 48:5768–5772.
- [13] Fiala E. S., Sodum R. S., Bhattacharya M., and Li H., (-)-Epigallocatechin gallate, a polyphenolic tea antioxidant, inhibits peroxynitrite-mediated formation of 8-oxodeoxyguanosine and 3-nitrotyrosine, *Experientia*, 1996; 52:922–926.
- [14] Rice-Evans C. A., Miller N. J., and Paganga G., Structure- antioxidant activity relationships of flavonoids and phenolic acids, *Free Radic. Biol. Med.*, 1996; 20:933–956.
- [15] Valcic S., Muders A., Jacobsen N. E., Liebler D. C., and Timmermann B. N., Antioxidant chemistry of green tea catechins. Identification of products of the reaction of (-)-epigallocatechin gallate with peroxyl radicals, *Chem. Res. Toxicol.*, 1999; 12:382–386.
- [16] Valcic S., Burr J. A., Timmermann B. N., and Liebler D. C., Antioxidant chemistry of green tea catechins. New oxidation products of (-)-epigallocatechin gallate and (-)-epigallocatechin from their reactions with peroxyl radicals, *Chem. Res. Toxicol.*, 2000; 13:801–810.
- [17] Jane V. Higdon and Balz Frei, *Tea Catechins and Polyphenols: Health Effects, Metabolism, and Antioxidant Functions*. Linus Pauling Institute, Oregon State University, Corvallis, OR 97331.
- [18] W. Brand-Williams, M. E. Cuvelier and C. Berset, Use of a free radical method to evaluate antioxidant activity. *Lebensm, u, Technol*, 28, 25-30(1995).
- [19] Pszczola, D. E. Natural colors: pigments of imagination. *Food Technol.* 1998, 52, 70-76.
- [20] Kritchevsky, S. B. /3-Carotene, carotenoids and the prevention of coronary heart disease. *J. Nutr.* 1999, 129, 5-8.
- [21] Mazza, G. Health aspects of natural colors. In *Natural Food Colorants Science and Technology*, Lauro, G. J., Francis, F. J., Eds.; Marcel Dekker: New York, 2000; pp 289-314.
- [22] Wang, H.; Nair, M. G.; Strasburg, G. M.; Chang, Y. C.; Booren, A. M.; Gray, J. I.; DeWitt, D. L. Antioxidant and antiinflammatory activities of anthocyanins and their aglycon, cyanidin, from tart cherries. *J. Nat. Prod.* 1999, 62, 294-296.
- [23] Espin, C. J.; Soler-Rivas, C.; Wichers, H. J.; Garcia-Viguera, J. Anthocyanin-based natural colorants: a new source of antiradical activity for foodstuffs. *J. Agric. Food Chem.* 2000, 48, 1588- 1592.
- [24] Pedreno, M. A.; Escribano, J. Studying the oxidation and the antiradical activity of betalain from beetroot../. *Biol. Ediic.* 2000, 35, 49-51.
- [25] Kanner, K.; Harel, S.; Granit, R. Betalains—A new class of dietary cationized antioxidants. *J. Agric. Food Chem.* 2001, 49, 5178-5185.
- [26] Yizhong Cai, Mei Sun and Harold Corke, Antioxidant activity of Betalains from Plants of the Amaranthaceae.
- [27] E. Abuin, E. Lissi, P. Ortiz and C. Henriquez Uric Acid Rreaction With DPPH Radicals at the micellar interface.
- [28] G. Schmeda, J.A. Rodriguez, C. Theoduloz, S.L. Astudillo, G.E., Feresin and A. Tapia, Free- radical Scavengers and Antioxidants from Peums boldus Mol., *Free-radical research*, 2003, Vol 37(4), pp. 447-452.
- [29] Son, S.; Lewis, B. A. Free radical scavenging and antioxidative activity of caffeic acid amide and ester analogues: Structure-activity relationship. *J. Agric. Food Chem.* 2002, 50, 468-472.

# DIHYDROXYFUMARIC ACID TRANSFORMATION

Secara Natalia

*Institute of Chemistry, 3, Academy st., Chisinau, Republic of Moldova*

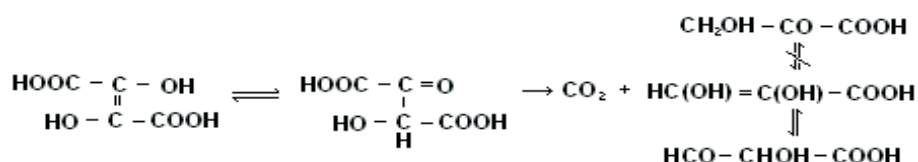
*Email: natalia\_secara@yahoo.com, Phone: (+373 22) 72 97 61*

**Abstract:** This short communication presents several preliminary results obtained during kinetic investigation of dihydroxyfumaric acid decarboxylation. The reaction order towards the hydrogen ions concentration has been established, the correlation between the decarboxylation velocity and temperature has been found, the Arrhenius equation for the decarboxylation constant has been drawn.

**Keywords:** dihydroxyfumaric acid, decarboxylation, activation energy

## Introduction

The papers [1, 2] have demonstrated that in solid form, the dihydroxyfumaric acid (DFH<sub>4</sub>) has the structure of the tautomeric ketonic form. Researches conducted by *Souchay et al.* [3] have shown that in solution this equilibrium is greatly influenced by the pH value of the medium, i.e., the equilibrium is totally shifted towards the ketonic form at pH < 0,5 and at pH > 12 – towards the enolic form. *Fleury* [4] has shown that dihydroxyfumaric acid decarboxylation can only take place through the formation of the ketonic form – oxaloglycolic acid, transparent for spectrometric measurements ( $\lambda > 200$  nm). The mechanism proposed in [4] for the primary decarboxylation is shown below:



## Experimental

The following reagents were used during the research: dihydroxyfumaric acid hydrate 98% purchased from Aldrich, sodium hydroxide, hydrochloric acid, EDTA – titration standards. All solutions were prepared using bidistilled water. Freshly prepared dihydroxyfumaric acid solution was used in each experiment. The investigated solution contained:  $[\text{DFH}_4]_0 = 1 \cdot 10^{-4}$  M,  $[\text{EDTA}] = 5 \cdot 10^{-3}$  M. The anaerobic medium was created by purging argon through the solution. Spectrometric measurements have been made using a Perkin Elmer Lambda 25 Spectrometer at  $\lambda = 290$  nm, the established value of dihydroxyfumaric acid absorption maximum.

## Results

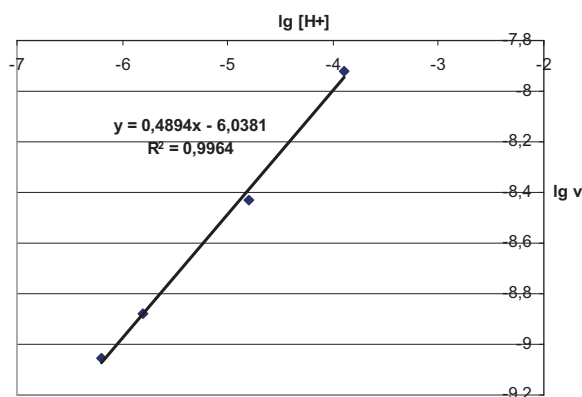


Fig. 1. The decarboxylation velocity of the dihydroxyfumaric acid, as function of the pH value of the solution,  $t = 30^\circ\text{C}$

According to [4], for values of pH > 3, the rate of decrease of the enolic form concentration is equivalent with the velocity of decarboxylation of the dihydroxyfumaric acid, therefore making it possible to investigate the decarboxylation reaction by the decrease in absorbance at 290 nm.

Investigations allowed finding the dependence of the decarboxylation velocity on the pH value of the solution (for  $\text{pH} > 3$ ), the decarboxylation velocity and the rate constant which describe this reaction have been calculated (Table 1 and Figure 1). It was found that the reaction order towards  $[\text{H}^+]$  equals to 0,49.

Table 1

The decarboxylation velocity of the dihydroxyfumaric acid, as function of the pH value of the solution,  $t=30^\circ\text{C}$

pH	$v_p, \text{mol/l}\cdot\text{s}$
3,9	$1,2\cdot 10^{-8}$
4,8	$3,71\cdot 10^{-9}$
5,8	$1,33\cdot 10^{-9}$
6,2	$8,79\cdot 10^{-10}$

During current investigations, the influence of temperature on the rate of the decarboxylation process was established. The decarboxylation rates and the rate constants have been calculated for the temperature range  $20^\circ\text{C} - 60^\circ\text{C}$ . The obtained results are shown in Table 2.

Table 2

The decarboxylation rate of the dihydroxyfumaric acid, as function of the temperature of the solution at pH 4,8

$t, ^\circ\text{C}$	$v_p, \text{mol/l}\cdot\text{s}$	$k_p, \text{s}^{-1}$
20	$5,43\cdot 10^{-10}$	0,0004606
30	$3,71\cdot 10^{-9}$	0,0020727
40	$4,29\cdot 10^{-9}$	0,0027636
50	$1,15\cdot 10^{-8}$	0,0076
60	$1,68\cdot 10^{-8}$	0,011515

Figure 2 illustrates how the rate constant of the decarboxylation reaction depends on the temperature of the investigated solution.

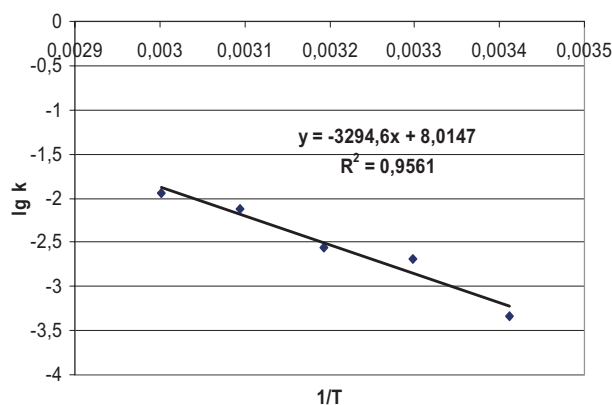


Fig. 2. The rate constant of the decarboxylation, as function of the temperature of the solution at pH 4,8

Using the graphical method, the activation energy and the pre-exponential factor have been determined. There were obtained the following values: for the pre-exponential factor –  $1,034\cdot 10^8$ , for the activation energy calculated by the graphical method – 63,08 kJ/mol, and by the analytical method – 65,3 kJ/mol.

Therefore, we propose the Arrhenius equation which describes the variation of the rate constant with temperature, of the following form:

$$k = 1.034 \cdot 10^8 \cdot e^{-7.58 \cdot 10^3 / T}$$

**Acknowledgements:** I would like to express my sincere gratitude to my scientific adviser, Acad. Gh. Duca, who helped and guided me through the entire work, and Prof. Maria Gonta, who encouraged me from the beginning.

#### References:

- [1]. Syciov A., Scutaru Yu., Duca Gh., Journal of structural chemistry (Russia), 1986, Vol. 27, nr. 5, pp. 142.
- [2] Duca Gh., *Catalysis of oxidation of tartaric and Dihydroxyfumaric acids*, PhD thesis, Chisinau, 1979.
- [3]. Souchay P., Fleury D., Fleury M., C.R. Acad. Sci. Paris, 1967, Vol. 264, pp.2130.
- [4]. Fleury D., Bull. de la Soc. Chimique de France, 1970, Nr.1, pp.370.

## HIS LIFE WAS A LEGEND

Antonie Ablov  
(1905-1978)



What does a character mean, how could we embrace a definition of that called a temperament, how courage and longing for culminations of human perfection become apparent? What does it mean to have visions and live imagination of ideas in a world of platitude, ignorance and of a common viewpoint? What does it mean to be an effective creative spirit, possessor of a permanently incentive potential? What does it mean to have vocation of a master? How does a person manifest himself, a personality labelled with the sign of creativity and of exactness, of passion and patience?

Questions, questions... Where originate these rare accomplishments, exceptional accomplishments of a human being? I have read 10-15 years ago a statement of two American notorious physicians, who stated by their research that a human, in a proportion of 70 percent, is a product of genetic factors, and only 30 percent - of education. If this is so, the time registers and selects, rewards everybody according to his deserts. With everything endowed by the Lord. Genetic inheritance has worked in the case of my master Antonie Ablov, who had been more than a guider - a supporter and a parent. When I search an answer to my questions above, I wake up surrounded by remembrances of the former times and his steady and unforgettable image appears to me.

Through his effort and endeavor I achieved to model my character, to integrate myself as a human, to free my temperament, to mature a courage, maybe to accomplish a crumb of dreams that came into my mind in that incomparable village of my childhood and, in the end, to join the ant hill of chemists of contemporaneity. How could I be grateful forever as it should be and how the Lord teaches us to observe the order of things. We are born to die in turn and to deplore all of these losses. However those most deserving remain in the world of remembrance for their achievements of physical and spiritual value. We shall not consign to oblivion the deeds of predecessors and the memory about them.

It is a duty to outline the portrait of my master Antonie Ablov, whose supervision, support and spiritual protection I fully benefited for many years and whom I remember with the greatest faith and devotion, as a parent of soul and suffering deserves. His shadow beyond us today is a light. My gesture is also directed to the light, to which he devoted the purpose of his life. Like a scrupulous painter decomposes the daylight in those seven colours of the rainbow, so as later with its points to make a picture, I would like to unwind the clew of memories and from the thread I am spinning for more than half a century to weave a small portrait, using the features of his character as warp, and his fruitful research - as weft.

### Childhood and adolescence which led him to the broad world

It was to be that from the Abla the real adventure and story of Abloven life begin. Antonie Ablov enjoyed an exceptional genetic code which endowed him with most distinguished accomplishments which have fully manifested themselves, often simultaneously, as it will be seen below. His grandfather, who was by origin a Greek from Constantinople and beared the name of Abla (which in translation means «brother-in-law»), married a Romanian who made him to settle on our land for whole his life. Out of his marriage the farther of our scientist will be born, with the first name Vasile. The spelling of the last name was transformed into Ablov, after the Russian model, moreover, the patronymic Ivan was added officially, for the unknown reasons. This Vasile Ablov has taken as a spouse a Russian from Odessa, called Eudochia. It seems that it was a lucky marriage because from this love match on August 3/16, 1905 in Odessa a son was born our protagonist Antonie. This genealogical Greek-Romanian-Russian amalgam seems to imprint to the descendent from Abla origin firmness and dignity and, without doubt, helped to face with temerity all vicissitudes of life and to run with honesty and scrupulosity the difficult way of cognition and achievements.

He spent his childhood and adolescence and thereafter lived his whole prodigious life in sweet Moldova, the destiny bestowed him to know and breathe the air of two political regimes, with all their specific features and shortcomings,

which he knew how to appreciate with wisdom. He attends the gymnasium from Cetatea Alba, taking his bachelor degree (1923) graduates from the Physical-Chemical Faculty of Iassy University (1923-1927) and Chemical-Technological Institute of Iassy (1925-1931), then works as a research assistant for the Department of Inorganic Chemistry (1927-1940) at Iassy University and chemistry engineer at «Astra Romana» of Ploiesti (1939-1940).

In 1940 the Chisinau period of his life begins, which lasted till the painful year 1978, May 18, when he had gone into the world of shadows and into the space beyond the suffering and pain. The life will offer and will bring him different challenges. He will be by turn the Head of Chemistry Department at Agricultural Institute, today the State Agrarian University (1940-1946), Head of the Department of Inorganic Chemistry of the State University of Moldova (1946-1959), Head of Chemistry Division (1955-1957), afterwards Head of Inorganic Chemistry Division (1957-1959) and Director of the Chemistry Institute (1959-1961) of the Moldovan Branch of the Academy of Sciences of the former USSR, Academician Coordinator of the Division of Natural and Technical Sciences of the Academy of Sciences of Moldova (1961-1964), at the same time Head of Inorganic Chemistry Laboratory (1959-1978), since 1975 renamed as the Laboratory of Coordination Compounds Chemistry, etc. He was awarded the title of doctor (1932) and doctor habilitat (1944) in chemistry, university professor (1945), academician of the Academy of Sciences of Moldova (1961). He was distinguished with many prizes and medals. He was a Laureate of State Award of Moldova (1983, post-mortem).

The image of master Antonie Ablov. His aspect was of an ideal or almost ideal distinction. He was of special bearing, a tall man, well looking, with dark brown hair, in the long run turned into grey, but permanently fresh cut, tastefully dressed, vivid and seemingly excited, to which one should add a sharp sight, imperative gesture, proper to a character who sometimes used to become infuriated. Furthermore, his sonorous voice, hard in his way, as if destined not only to explain, but also to command, without giving the interlocutor the time and possibility to respond, as if he did not wish to admit the retort. I think these features suit him - namely him - perfectly. We, those who surrounded him, always knew that beyond these asperities a heart of kindness beats equal to the mind keenness and to the force of his character, the kindness always abused by each of us - those 10 doctors habilitat and 65 doctors in science, guided and urged by him, as well as those more than 1 700 of students who attended lectures of the impressive professor and scientist, to whom tens of thousands of those who knew him and enjoyed his long-standing friendship could be added.

I shall emphasize once again that through his glasses which he worn with great accuracy his permanently laughing hazel eyes glistened, penetrating and a bit ironic. I think that this irony, mostly inoffensive, helped him to remain ever spiritual, full of wisdom, intelligent, kidding and making good cheer even in most serious situation.

The elation with which he rushed into the research work and science organization, his robust and exuberant temperament, amazing power of work, persistent will, irreproachable punctuality, talent and ingenuity of experimenter, erudition and basis of scientific information, valuable contribution to elucidate numerous problems of an obvious actuality in chemistry, ranks the Antonie Ablov's personality as a Patriarch of native science, positioning him in space and time among the distinct names of our nation, makers of history and civilization.

The novel charm of his personality consisted in irreproachable moral and physical behavior, due to his uplifting mind and clean soul, perfect humanity and common kindness, immeasurable honesty and unlimited devotion, his formidable punctuality and love to work, his complex preoccupations and his uninterrupted strive for self-perfection, etc.

All these wonderful human qualities collected together in a temper of an eventful destiny, made his aureole name a legend.

### **Years of professorate**

Each academic year at the Faculty of Chemistry of the State University of Moldova started off with an opening introductory hour held by the erudite professor Antonie Ablov. This lesson looked as a praise brought to chemistry and chemical technology with its latest achievements and discoveries. The audience could always enjoy the novelty arisen from a creative, ingenious and emotional spirit thanks to a charismatic power with which he was endowed loving people and life.

During my years of post-graduate studies (1952-1956) I attended very conscientiously all lessons of my deep and severe scientific master. Thus it happened to attend for some years the same course of chemistry drafted with skillfulness that always changed. And I was convincing myself more and more that my severe professor, due to his consciousness and special attitude to himself and to the discipline to which he was devoted, each year introduced into his course of inorganic chemistry something new and interesting, making us to feel completely a significance of this area, which can provoke explosion and destruction, but at the same time provide people with the light and heat, food and clothes, etc. In one word, the magical professor was amazing us, amusing, awoke the curiosity, made us to polemic through multiple and fascinating demonstrative experiments made by a virtuoso experimental chemist, as if we were present at a wonderful performance.

Due to his firm and precise gesture, intonation and multiple modulations of the voice - authoritative and bearing a lot of information - he knew how to make you to see and to understand even the most insensible molecular architectonics with their spatial settings, those subtle bonds between atoms which create phantasmagorical designs, determining admiration and great interest of some happy students attracted by the vocation and passion for chemistry who, fortunately, were present in the hall led by a wise persons in this area.

His introductive hour opening each academic year of the master course was unrolling in the atmosphere of beautiful solemnity, was a true holiday. I think it came from the tradition of the Iassy school with its great professors. Several minutes before the beginning of the lesson the first line of the spacious hall was engaged by lecturers, assistants, doctors, sometimes university professors from other institutions. The professor seemed to be an inexhaustible fountain of information. It was easy for him to transmit data and information, unusual details, etc., being himself a prodigious creator of science, destined with a double vocation: those to disseminate the science and those for increase the wealth.

I am thinking now, after many years, after more than half a century, how deeply the great chemist understood the spirit and objectives of chemistry and how viable his concepts related to this area remain until now. His lessons remain alive, because they had the concept and features appropriate only for genuine creator of science.

### **Researcher and inventor**

No doubt, in the portrait of the Patriarch we distinguish a multitude of colours, which reflect a contradictory and mysterious character, an incomparable professor, a good organizer and creator of research and education institutions, etc. But most lively the colours glisten which surround the man of science, who brought to life thousands of new chemical compounds, watching them during half a century, nicknaming them with long but exact names, as if using a magic wand to reveal their mystery. He is one who discerned new crystalline structures, elucidated new mechanisms, discovered new phenomena, tested new antiviral and anticarcinogenic properties, experimented with new plant and animal growth simulators, elaborated new methods of intensification of fabric dyes, etc., exerting himself permanently to follow and apply the triad Education - Research - Production.

A coincidence, both occasional and amazing, is permanently turning in my mind - Antonie Ablov was born in 1905, just in the year when Lev Chugaev discovered the famous reaction of the nickel with dimethylglyoxim, the phenomenal coincidence in the science history, which like a miracle marked the newborn, determining his preoccupation for his life: devotion with his body and soul to study of dioximines of transition metals, which occurred to be splendid models of different biological systems. Thus, Antonie Ablov and his assistants have fully demonstrated trans-configuration of Chugaev dioximines; as a result of numerous syntheses of new octahedral compounds they collected, like glass beads on a thread, coordinated ligands according to their capacity to exert influence in transposition; they revealed a new type of isomers, so called «of half-opened book»; elucidated the physiological proprieties and catalytic activity of this important class of substances; synthesized series of dioximines, absolutely unknown before, which totally differ from those of Chugaev's, presenting a new type of binuclear structures with cis-configuration, and which entered into the patrimony of the world science under the name of Ablov's dioximines.

Intuiting the calls of time, approaching the problems of the most acute up-to-dateness, Antonie Ablov orientated his research, especially on some polynuclear compounds with atoms or bridge groups closely associated with an aggregate of identical atoms named cluster. Abundant stereochemistry and fantastic conformance of these compounds generate specific spectroscopic and thermodynamic properties important for understanding of life processes which condition the considerable role of these compounds in superconductivity and semi-conductivity, of magnetic memory of high density, as well as for resolving the fundamental problem of managing the reactivity and synthesizing new compounds with desired properties.

### **Ablovianian school**

Antonie Ablov was a scientist and person who, due to his prestige, the deep knowledge he possessed, was able to create, to manage and to educate the prestigious Scientific School in the area of Coordination Chemistry. The fact is remarkable that our grandmaster takes his origin from the environs of the creator of coordination chemistry, legendary professor of Polytechnical University at Zurich Alfred Werner (1866-1919), laureate of Nobel Prize (1913). In these laboratories his scientific supervisor, Professor at the «Al. I. Cuza» University at Iassy, Nicolae Costachescu (1876-1939) was educated. Antonie Ablov, in his turn, has elaborated under the supervision of Nicolae Costachescu and defended on the date of February 20, 1932, the doctorate thesis in Chemistry on the theme «Effect of substituents in bases and in anions on coordination number of a metal», and on July 25, 1944, he defended the habilitation doctor thesis in Chemistry «Contribution to the nature of bonds and stereochemistry of coordination compounds» in front of the Scientific Council of Kazan University. As a consequence, it can be summarized, than we, who are considered to be the followers of Antonie Ablov, are representing the fourth generation of chemists-researchers, while our disciples who

currently represent the Ablovian School of Coordination Chemistry are the fifth generation of researchers starting from Alfred Werner.

We can certainly affirm today that the Ablovian School is a long-living one, it will be lasted for ages; and the principal component of this veritable school is manifested through the formative virtue. It can be compared with the fireworks, when each sparkle exploded in the sky generates a shaft of sparkling lights, which in the case of professor Antonie Ablov are the research schools with his followers and followers, which have exceeded the borders of the Republic of Moldova making roots in other centers of coordination chemistry throughout the world.

Antonie Ablov published more than 760 peer-reviewed papers, he has educated 75 doctors and habilitation doctors, among them heads of leading research schools in the new areas of coordination chemistry, such as crystallochemistry, quantum chemistry, magnetochemistry, radiospectroscopy, biotechnology, super-molecular chemistry, polynuclear systems, etc. He has promoted an interdisciplinary research, thus exceeding the borders between chemistry, biology, physics and mathematics, which had a significant impact on medicine, agriculture and technology. In his research Antonie Ablov have synthesized fantastic molecular designs, as it could be done by an architect in coordination compounds. Due to the immense imagination, which he proved to have, he has discovered splendid objects of study and knowledge, unique in their way, having applied the latest research methods in the area of physics and mathematics, having adapted, improved them, sometimes elaborating new laboratory methods and techniques.

Antonie Ablov made a marked input in the contemporary coordination chemistry. Through his activity and creativity as a scientist, professor and public figure, he has contributed to our science, economy and spirituality with the prestigious achievements recognized and appreciated throughout the world.

### **Leaving for eternity**

With all he had foreseen and created, inexhaustible Ablov remains to be a scientist whose heritage still has to be discovered.

Our Grandmaster was an unsurpassed leader due to his knowledge, skills, ingenuity, initiative and deeds. His name has always been associated with the word «the first»: the first Head of the Department of Inorganic Chemistry, the first Dean of Chemical Faculty, the first Director of the Institute of Chemistry, the first Academician coordinating the appropriate section, etc. To be the first was his lifestyle, this was an essence of his existence. And if today we have the prosperous Faculty of Chemistry and Chemical Technology, the recognized Institute of Chemistry and the School of Coordination Chemistry - we owe all this to him, the unique Antonie Ablov.

Academician Antonie Ablov was not only a great chemist, but a spirit whose soul was always occupied with the spiritual values - he was an expert in music, fine arts, subtle and knowledgeable theater-lover, passionate book lover and book collector, the thinker deeply involved into the problems of philosophy and universal history, burning popularizer of science.

Great people never die, they go to immortality to illuminate the way of living people. The death brings with it, along with the infinite pain, also the hour of blooming, when all the misery and vanity of everyday life is forgotten, and only that remains belonging to eternity. The dead are no more dead if living people revive them in their heart, their soul, their spirit, via their noble deeds which add the light.

On the date of September 13, 2004, the memorial plate «To Academician Antonie Ablov» was inaugurated at the Institute of Chemistry of the Academy of Sciences of Moldova. At the unveiling of this memorial, I had the sense that our grandmaster, Antonie Ablov, appeared and was among us, and I could not help telling him, in the presence of the audience, with the greatest emotion: «Welcome home, in the House which you have built, to the Institute of Chemistry, our dear preceptor!».

At this very time, the President of the Academy of Sciences of Moldova set up the honorary stipend named after Academician Antonie Ablov, in the sum of ten thousands lei (830 USD), which is granted annually to the best doctorand (post graduate student) in chemistry.

Love and respect of people, concern for people full of tact, delicacy and charm, lucidity of mind and sense of justice, courageous behavior, absolute honesty and great passion to chemistry which was hand down to us by Academician Antonie Ablov are carried today as a torch illuminating the thoughts of the followers.

Such a person was Antonie Ablov, the man who have presented us with the essence of his soul, towards him we are directing today our grateful thoughts, being always thrilled and touched by the Shakespearean question: «And when will the other come, alike himself?».

Dumitru BATÎR  
Dr. hab. in chemistry University professor  
State Prize Laureat

CHEMISTRY JOURNAL OF MOLDOVA.  
General, Industrial and Ecological Chemistry

Instructions for authors

Please follow these instructions carefully to ensure that the review and publication of your paper are as swift and efficient as possible. These notes may be copied freely.

**Journal policy**

“Chemistry Journal of Moldova. General, Industrial and Ecological chemistry” seeks to publish experimental or theoretical research results of outstanding significance and timeliness in all fields of Chemistry, including Industrial and Ecological Chemistry. The main goal of this edition is strengthening the Chemical Society of Moldova, following development of research in Moldovan chemical institutions and promotion of their collaboration with international chemical community. Publications may be in the form of *Short Communications*, *Full Papers* and *Review Papers*.

The contents of papers are the sole responsibility of the authors, and publication shall not imply the concurrence of the Editors or Publisher.

*Short Communications* should describe preliminary results of an investigation and for their significance are due to rapid communication. For this kind of publications, experimental confirmation is required only for the final conclusion of the communication. Maximum allowed length – 2 pages.

*Full Papers* should describe original research in chemistry of high quality and timeliness. Experimental work should be accompanied by full experimental details. Priority will be given to those contributions describing scientific work having as broad appeal as possible to the diverse readership. Maximum allowed length – 6 pages.

*Review Papers* are specially commissioned reviews of research results of topical importance. Maximum allowed length – 20 pages.

The language of submission is English, articles in other languages will not be considered. Papers are submitted on the understanding that the subject matter has not been previously published and is not being submitted elsewhere. Authors must accept full responsibility for the factual accuracy of the data presented and should obtain any authorization necessary for publication. All papers are sent to referees who advise the Editor on the matter of acceptance in accordance with the high standards required.

Referees' names are not disclosed, but their views are forwarded by the Editor to the authors for consideration. Authors are strongly encouraged to suggest the names and addresses of suitable referees.

**Journal conventions**

*Nomenclature*: Authors will find the following reference books and websites useful for recommended nomenclature. It is the responsibility of the author to provide correct chemical nomenclature.

- IUPAC Nomenclature of Organic Chemistry; Rigaudy, J.; Klesney, S. P., Eds; Pergamon: Oxford, 1979.
- A Guide to IUPAC Nomenclature of Organic Compounds (Recommendations 1993); Panico, R.; Powell, W. H.; Richer, J. C., Eds; Blackwell Publishing: Oxford, 1993.
- <http://www.acdlabs.com/iupac/nomenclature>
- <http://www.chem.qmul.ac.uk/iupac/>

*X-ray crystallographic data*: Prior to submission of the manuscript, the author should deposit crystallographic data for organic and metal-organic structures with the Cambridge Crystallographic Data Centre. The data, without structure factors, should be sent by e-mail to: [deposit@ccdc.cam.ac.uk](mailto:deposit@ccdc.cam.ac.uk), as an ASCII file, preferably in the CIF format. Hard copy

data should be sent to CCDC, 12 Union Road, Cambridge CB2 1EZ, UK. A checklist of data items for deposition can be obtained from the CCDC Home Page on the World Wide Web (<http://www.ccdc.cam.ac.uk/>) or by e-mail to: [fileserv@ccdc.cam.ac.uk](mailto:fileserv@ccdc.cam.ac.uk), with the one-line message, send me checklist. The data will be acknowledged, within three working days, with one CCDC deposition number per structure deposited. These numbers should be included with the following standard text in the manuscript: Crystallographic data (excluding structure factors) for the structures in this paper have been deposited with the Cambridge Crystallographic Data Centre as supplementary publication numbers CCDC ... . Copies of the data can be obtained, free of charge, on application to CCDC, 12 Union Road, Cambridge CB2 1EZ, UK [fax: 144-(0)1223-336033 or e-mail: [deposit@ccdc.cam.ac.uk](mailto:deposit@ccdc.cam.ac.uk)]. Deposited data may be accessed by the journal and checked as part of the refereeing process. If data are revised prior to publication, a replacement file should be sent to CCDC.

*Experimental:* Authors should be as concise as possible in experimental descriptions. The Experimental section must contain all the information necessary to guarantee reproducibility. An introductory paragraph containing information concerning solvents, sources of less common starting materials, special equipment, etc. should be provided. The procedures should be written in the past tense and include the weight, mmol, volume, etc. in brackets after the names of the substances or solvents. General reaction conditions should be given only once. The title of an experiment should include the chemical name and compound number of the product prepared: subsequently, these compounds should be identified by their number. Details of the work up procedure must be included. An experimental procedure is not normally required for known compounds prepared by a literature procedure; in such cases, the reference will suffice. For known compounds prepared by a novel procedure, comparative data together with the literature reference are required (e.g. m.p. and published m.p. with a reference to the latter).

*Characterization of new compounds:* All new compounds should be fully characterized with relevant physical and spectroscopic data, normally including compound description, m.p./b.p. if appropriate, IR, NMR, MS and  $[\alpha]_D$  values for enantiopure compounds. In addition, microanalyses should be included whenever possible (normally  $\pm 0.4\%$ ). Under appropriate circumstances, and at the Editor's discretion, high resolution mass data (normally to  $\pm 5$  ppm) may serve in lieu of microanalyses; in this case a statement must be included regarding the purity of the products and how this was determined [e.g. all new compounds were determined to be  $>95\%$  pure by HPLC (or GLC or  $^1\text{H}$  NMR spectroscopy)]. For compound libraries prepared by combinatorial methods, a significant number of diverse examples must be fully characterized (normally half of the members for libraries up to 40 compounds, 20 representative examples for bigger libraries). Resin-bound intermediates do not have to be fully characterized if acceptable characterization of released products is provided. No supplementary data are accepted in addition to the basic material.

## **Manuscript preparation**

Please follow these guidelines for manuscript preparation. An example of manuscript formatting is provided after the descriptive part of the document.

*General requirements:* Manuscripts will be accepted only in electronic form in A4 format, one column layout, single-spaced, margins 2.5 cm on top and bottom and 2 cm on left and right sides (see the sample formatting page). Pages must be numbered. The corresponding author's full mailing address, plus phone and fax numbers and e-mail address should be included. The manuscript should be compiled in the order depending on the paper type.

A theoretical or physicochemical paper normally contains the *Title, Authors, Affiliations, Abstract, Keywords*, a brief *Introduction* and formulation of the problem, an *Experimental Section* (or methodical part), *Results and Discussion, Conclusion*, followed by *Acknowledgments and References*.

A paper devoted to synthesis contains the *Title, Authors, Affiliations, Abstract, Keywords, Introduction, Results and Discussion, Conclusion, Experimental, Acknowledgments and References*.

*Graphical Abstracts:* Authors must supply a graphical abstract at the time the paper is first submitted. It will include the article title and authors with the same formatting as in the article. The abstract body should summarize the contents of the paper in a concise, pictorial form designed to capture the attention of a wide readership and for compilation of databases. Carefully drawn chemical structures are desired that serve to illustrate the theme of the paper. Authors may also provide appropriate text, not exceeding 50 words. The whole graphical abstract should be kept within an area of 5cm by 17cm. Authors must supply the graphical abstract on a separate page integrated in the article file. The graphics which is a part of the graphical abstract should be sent separately in its original format.

*Title:* The title should be brief, specific and rich in informative words; it should not contain any literature references or compound numbers. The title is in size 14 pt Bold (all capital letters).

*Authors and affiliations:* Where possible, supply given names, middle initials and family names for complete identification. Indicate all the authors in order of their affiliation and provide affiliation address after the author's names. Addresses should be as detailed as possible and must include the country name. The corresponding author should be indicated with an asterisk, and contact details (fax, e-mail) should be placed after nomination of the authors. There should be only one corresponding author. The names of the authors are in size 12 pt Normal and the name of the organization and its address are in size 9 pt Italic.

*Abstract:* Authors must include a short abstract of approximately four to six lines that states briefly the purpose of the research, the principal results and major conclusions. References and compound numbers should not be mentioned in the abstract unless full details are given. The abstract body is 9 pt in size with the heading in bold.

*Keywords:* Authors are expected to provide maximum 5 keywords using 10 pt font size with the heading in bold.

*Text:* Text should be subdivided in the simplest possible way consistent with clarity. Headings should reflect the relative importance of the sections. Ensure that all tables, figures and schemes are cited in the text in numerical order. The graphics and artworks should be integrated in the paper. Trade names should have an initial capital letter, and trademark protection should be acknowledged in the standard fashion, using the superscripted characters TM and ® for trademarks and registered trademarks respectively (although not for words which have entered common usage, e.g. pyrex). All measurements and data should be given in SI units where possible. Abbreviations should be used consistently throughout the text, and all nonstandard abbreviations should be defined on first usage. Authors are requested to draw attention to hazardous materials or procedures by adding the word CAUTION followed by a brief descriptive phrase and literature references if appropriate. The experimental information should be as concise as possible, while containing all the information necessary to guarantee reproducibility. The text body is 10 pt in size with the heading in bold.

*Acknowledgments:* This is an optional section. The authors have to decide acknowledgement of certain collaborators, funds or programs who contributed in a way to the research described in the paper.

*References:* In the text, references should be indicated by Arabic numerals taken in square brackets, which run consecutively through the paper and appear before any punctuation; ensure that all references are cited in the text and vice versa. The reference list should preferably contain only literature references; other information (e.g. experimental details) should be placed within the body of the text. Preferably, each reference should contain only one literature citation. Authors are expected to check the original source reference for accuracy. Journal titles should be abbreviated according to American Chemical Society guidelines (The ACS Style Guide; Dodd, J. S., Ed.: American Chemical Society: Washington, DC, 1997). Inclusive pagination is strongly recommended. Book references [2,3] should cite author(s), chapter title (if applicable), editor(s), book title, edition/volume, publisher name, publisher location, date and pages. Examples, including a thesis citation, 4 are shown below.

- [1] Barton, D. H. R.; Yadav-Bhatnagar, N.; Finet, J.-P.; Khamisi, J. *Tetrahedron Lett.* 1987, 28, 3111–3114.
- [2] Katritzky, A. R. *Handbook of Organic Chemistry*; Pergamon: Oxford, 1985; pp 53–86.
- [3] Smith, D. H.; Masinter, L. M.; Sridharan, N. S. In *Heuristic DENDRAL: Analysis of Molecular Structure*;
- [4] Wipke, W. T.; Heller, S. R.; Feldmann, R. J.; Hyde, E., Eds. *Computer representation and manipulation of chemical information*. John Wiley: New York, 1974; pp 287–298.
- [5] Cato, S. J. Ph.D. Thesis, University of Florida, 1987.

*Footnotes:* Footnotes should appear at the bottom of the appropriate page and be indicated by the following symbols: \*, †, ‡, §, ¶, k.

*Tables:* All tables should be cited in the text, and numbered in order of appearance with Arabic numerals. All table columns should have a brief explanatory heading and where appropriate, units of measurement. Vertical lines should not be used. Footnotes to tables should be typed below the table, each on a separate line, and should be referred to by superscript letters.

*Artwork:* Only black and white artwork will be accepted. Figures, schemes and equations must be cited in the text and numbered in order of appearance with Arabic numerals; other graphics should be placed at a particular position in the text but not specifically referenced. All graphics (including chemical structures) must be supplied in digital format integrated into the paper. If graphics are created using ChemDraw the preferred settings is RSC-1997.cds set

(File/Apply settings/RSC-1997.cds): font 7 pt Arial, chain angle 120°, bond spacing 20% of length, fixed length 0.43 cm, bold width 0.056 cm, line width 0.016 cm, margin width 0.044 cm and hash spacing 0.062 cm. Compound numbers should be in bold face. Computer-generated illustrations, halftones and line/tones should also be provided where possible. The following points should be taken into consideration when preparing electronic graphic files:

Preferred graphics programs: ChemDraw, CorelDraw 6 and 7, Photoshop

Restricted use: ChemWindow, ISIS-Draw

Unusable: \*.doc files, Excel graphics, C-Design, Origin, ClarisDraw, ChemIntosh, MacDraw Pro

Acceptable formats of all graphics programs: TIFF, WMF, BMP, CDX, CDR.

Files of scanned line graphics can be accepted at a minimum resolution of 1000 dpi, for scanned halftones, 300 dpi, and scanned line/tones.

### **Copyright guidelines**

Upon acceptance of an article, Authors will be asked to transfer copyright. This transfer will ensure the widest possible dissemination of information. A letter will be sent to the corresponding Author confirming receipt of the manuscript. A form facilitating transfer of copyright will be provided. If excerpts from other copyrighted works are included, the Author(s) must obtain written permission from the copyright owners and credit the source(s) in the article. Authors will be provided preprinted forms for use by Authors in these cases.

### **Submission of manuscripts**

Please send your contribution as an e-mail attachment to:

Journal Editor, Academician Gheorghe DUCA  
e-mail: chemjm@cc.acad.md

using Microsoft Word (Office 97 or higher for PCs) word processing soft.

Please prepare a single file (allowed formats: \*.doc or \*.rtf) containing on a separate page a short accompanying letter to the Editor, justifying why your article should appear in "Chemistry Journal of Moldova. General, Industrial and Ecological Chemistry", followed by the article body with all schemes, figures, tables integrated in the text (though not crystallographic CIF files). On the last page of this file please provide the Graphical Abstract. Submission of figures and artwork in separate files is mandatory in their native formats.

**Authors should indicate the field of chemistry of their paper (see below) as well as the nature of contribution (Short Communication, Full Paper or Review Article) in their accompanying letters, along with their mailing address, daytime phone number and fax if available.** Authors will be notified by email if their contribution is received and accepted.

### **Editorial office:**

Institute of Chemistry, Academy of Sciences of Moldova, Str. Academiei, 3, MD-2028, Chisinau, Republic of Moldova.  
e-mail: chemjm@cc.acad.md  
Fax: +373 22 739954  
Tel: + 373 22 725490

*Proofs:* Proofs will be dispatched via e-mail and should be returned to the publisher with corrections as quickly as possible, normally within 48 hours of receipt.

### **Fields of research:**

1. Analytical chemistry
2. Ecological chemistry
3. Food chemistry
4. Industrial chemistry
5. Inorganic and coordination chemistry
6. Natural product chemistry and synthesis
7. Organic chemistry
8. Physical chemistry and chemical physics
9. Supramolecular chemistry

**A CONTRIBUTION TO “CHEMISTRY JOURNAL OF MOLDOVA.  
GENERAL, INDUSTRIAL AND ECOLOGICAL CHEMISTRY” (14 pt  
Bold, All CAPITALS)**

First Author<sup>a</sup>, Second Author<sup>a\*</sup>, and Third Author<sup>b</sup> (12 pt Normal) (no titles please)

<sup>a</sup>*First Organization, First Address (9 pt, Italic)*

<sup>b</sup>*Second Organization; Second Address (9 pt, Italic)*

\* *E-mail, phone and fax numbers of the corresponding author*

**Abstract:** This document is an example of a contribution to be submitted to “Chemistry Journal of Moldova. General Industrial and Ecological Chemistry”. This is the abstract in font size: 9 pt with the heading in bold. Please use the Times New Roman font. The title is in size 14 pt Bold (all capital letters), the names of the authors are in size 12 pt Normal and the name of the organization and its address are in size 9 pt Italic. The rest of the text is in single-space, typed in a one column layout and font size 10 pt.

**Keywords:** Insert a maximum of 5 keywords that will facilitate database searching.

### **1. Introduction (Headings - 10 pt Bold)**

Contributions should comprise an even number of pages. There are no limits to the contribution size. Authors are also kindly requested to adhere to the formatting instructions for font size and layout.

### **2. How to prepare your paper**

In MS Word, under the *File* menu, choose *Page setup* and set the *Top, Bottom, Left & Right Margins* as 2.5 cm, the *Gutter* as 0 cm, and the *Header* and *Footer* to 1.2 cm and choose *Apply to: Whole Document*. Then select the “*Paper Size*” tab and set the *Paper Size: A4* and *Orientation: Portrait*.

### **3. Figures and Tables**

Figure and table titles must be typed in bold and should appear below the figures and above the tables.

### **4. Equations**

Please use *italics* for symbols, bold face for vectors and normal fonts for standard functions (i.e. log, In, exp) and subscripts (i.e. //<sub>app1</sub>).

### **5. Acknowledgments (optional)**

You can acknowledge certain collaborators, funds or programs who contributed in a way to the research described in the paper.

### **6. References**

References should be numbered in the text in the order they are cited [1]. Multiple consecutive references may be abbreviated as [2-5]. The following style must be used for all contributions:

- [1] Barton, D. H. R.; Yadav-Bhatnagar, N.; Finet, J.-P.; Khamsi, J. *Tetrahedron Lett.* 1987, 28, 3111–3114.
- [2] Katritzky, A. R. *Handbook of Organic Chemistry*; Pergamon: Oxford, 1985; pp 53–86.
- [3] Cato, S. J. Ph.D. Thesis, University of Florida, 1987.

### **7. Graphical Abstract**

Please, supply a graphical abstract that will include title, authors (with the same formatting as in the article) and graphical abstract body. The whole graphical abstract should be kept within an area of 5cm by 17cm. The graphical abstract must be on a separate page integrated in the article file.

### **8. How to submit your document**

Please send your contribution as an e-mail attachment to Journal Editor, Academician Gheorghe DUCA (e-mail: chemjm@cc.acad.md), using Microsoft Word (Office 97 or higher for PCs).

Please prepare a single file (allowed formats: \*.doc or \*.rtf) containing all schemes, figures, tables integrated in the text (though not crystallographic CIF files). In this file, please include on a separate page an accompanying letter justifying why your article should appear in “Chemistry Journal of Moldova. General, Industrial and Ecological Chemistry”. Submission of figures and artwork in separate files is mandatory in their native formats.

ISSN 1857-1727



No. 1, 2008

Volume 3